

https://dspace.org/

Numerical modelling of gold transport and deposition

James, Christophe Stephen

2015-06-29
http://hdl.handle.net/10539/18024

Downloaded from a DSpace repository. https://dspace.org/

NUMERICAL MODELLING OF GOLD TRANSPORT AND DEPOSITION

Christopher Stephen James

A thesis submitted to the Faculty of Engineering, University of the Witwatersrand, Johannesburg for the degree of Doctor of Philosophy.

Johannesburg, 1984

ABSTRACT

A pair of mathematical models are presented for simulating the hydraulic transport and deposition of gold in fluvial systems such as existed during the formation of Witwatersrand reefs. The first model describes the transverse distribution of suspended particles over plain areas adjacent to channels while the second describes the longitudinal distribution within a channel. These models enable the distribution patterns of gold deposits to be related deterministically to channel geometry and the hydraulic conditions prevailing during reef formation.

The gold now present in the reefs was transported mainly in suspension. This is confirmed by showing that the hydraulic conditions required to mobilize the largest quartz particles in a typical reef sample are easily capable of suspending typical gold particles. Deposition patterns of gold are therefore closely related to the distribution of gold particles in suspension, which can be described by the diffusion analogy.

The transverse movement of suspended particles from a channel over an adjacent inundated plain is described by a two-dimensional elliptic partial differential equation which accounts for transport by diffusion and convection in the vertical and transverse directions. This equation is solved in finite difference form for steady, longitudinally uniform flow conditions.

The transverse model is verified by comparing predicted and measured distributions of fine sand deposits in a laboratory flume with a compound section. The model is applied to hypothetical situations to determine which factors have the greatest influence on the extent and variation of plain deposits. Several gold distributions

observed in the reefs are successfully reproduced by the model using suitable combinations of flow parameters.

The longitudinal distribution of suspended particles in a channel is described by a parabolic partial differential equation which includes terms for diffusion and convection in the vertical, longitudinal and transverse directions. Prior evaluation of transverse transport rates by the transverse model enables the longitudinal distribution equation to be solved as a two-dimensional problem. The solution is obtained by a finite difference approach for steady, longitudinally uniform flow.

The longitudinal model is applied to a hypothetical channel to identify the factors which have the greatest influence on longitudinal distributions and to a hypothetical distributary channel system to illustrate its use and determine general relationships between system configuration and gold distribution.

The models provide a deterministic link between the deposition patterns of any particles transported in suspension and their causative events and should lead to a sounder understanding of reef formation and gold distribution.

I declare that this dissertation is my own, unaided work. It is being submitted for the degree of Doctor of Philosophy in the University of the Witwatersrand, Johannesburg. It has not been submitted before for any degree or examination in any other University.

C S Jones

_____ day of _____, 19__

ACKNOWLEDGEMENTS

I would like to express my gratitude and appreciation to those people who have contributed to the production of this thesis in various ways.

Professor David Stephenson, my supervisor, has been the source of much valuable advice and encouragement. His consideration in allocating my other duties and those of his secretarial staff in the Water Systems Research Programme during the latter stages is greatly appreciated.

The Chamber of Mines of South Africa initiated and funded the research leading to the thesis. Several members of the Chamber's staff were also involved on a technical level. In particular, I would like to thank Dr M Nami for his assistance in defining the problem and explaining sedimentological aspects and Dr J Napier for some helpful discussion of numerical methods.

Finally, I must thank my wife Sue for her support and encouragement.

Table of Contents

		Page
	Abstract	i
	Acknowledgements	iv
Chapter 1:	Introduction	1
	1.1 Background	1
	1.2 Existing Models	4
	1.3 Proposed Models	12
Chapter 2:	Mode of Transport of Gold Particles	16
Chapter 3:	The Transverse Transfer Equation	30
	3.1 Introduction	30
	3.2 Theory	33
	3.3 Finite Difference Formulations	36
	3.4 Numerical Solution	46
Chapter 4:	Transfer Components	52
	4.1 Introduction	52
	4.2 Turbulent Diffusivities for Sediment	52
	4.3 Shear Velocity	64
	4.4 Transverse Convection	67
	4.5 Calculation of Flow Velocities	70
Chapter 5:	Boundary Conditions	78
	5.1 Vertical Boundary Concentrations	78
	5.2 Probability of Deposition	82
Chapter 6:	Experimental Verification of the Transverse Distribution Model	89
	6.1 Introduction	89
	6.2 Description of Apparatus	89
	6.3 Experimental Procedure	93

Table of Contents (contd)

		Page
	6.4 Results	95
	6.5 Comparison of Measured and Simulated Distributions	102
Chapter 7:	Application of the Transverse Distribution Model	112
	7.1 Introduction	112
	7.2 Sensitivity Analysis	112
	7.3 Comparison with Observed Distributions	132
Chapter 8:	The Longitudinal Distribution Model	141
	8.1 Theory	141
	8.2 Finite Difference Solution	142
	8.3 Turbulent Diffusivities for Sediment	150
	8.4 Convective Transport Components	151
	8.5 Probability of Deposition	152
Chapter 9:	Application of the Longitudinal Distribution Model	155
	9.1 Introduction	155
	9.2 Sensitivity Analysis	156
	9.3 Hypothetical Distributary System	176
Chapter 10:	Conclusion	185
Appendix A:	Transverse Distribution Model PLAINDEP	194
	A.1 Description of Computer Program	194
	A.1.1 Main Program PLAINDEP	195
	A.1.2 Subroutine BCPROF	198
	A.1.3 Subroutine SHVEL	198
	A.1.4 Subroutine FLOVEL	198

Table of Contents (contd) Page

A.2 Users' Guide 199
A.3 List of Variables 204
A.3.1 Input 204
A.3.2 Main Program PLAINDEP 205
A.3.3 Subroutine BCPROF 209
A.3.4 Subroutine SHVEL 209
A.3.5 Subroutine FLOVEL 209
A.4 Program Listing 211
A.5 Example 223

Appendix B: Longitudinal Distribution Model LONGDIS 228
B.1 Description of Computer Program 228
B.2 Users' Guide 230
B.3 List of Variables 235
B.4 Program Listing 239
B.5 Example 246

References 252

1. INTRODUCTION

1.1 Background

The Witwatersrand Basin was filled with about 14 000 m of sediments and volcanics between 2 500 and 2 800 million years ago. The Basin is now considered to be the most important gold field in the world, having yielded about 55 percent of all gold ever mined. Mining operations have reached depths of 3 600 m and some stratigraphic horizons have been mined out for 70 kilometres along strike and for 8 kilometres down dip (Schumm (1975)).

The gold in the reefs is very nonuniformly distributed and because of the expense and technical difficulty of mining at great depths it is becoming increasingly important to be able to predict locations of relatively high and low gold concentration. This is important on a large scale for planning new mining ventures and on a much smaller scale for improving mining methods and operations.

Any attempts to predict the patterns of gold distribution within reefs must be founded on a thorough understanding of the processes involved in reef formation and the original transport and deposition of the gold particles. The objective of this study is to develop a quantitative description of the hydraulic processes associated with gold transport and deposition.

On a scale meaningful to mining the deposition environment can be described as a multiple channel fluvial system with relatively wide, flat plain areas between adjacent channels as shown in Figure 1.1. The channels are generally shallow with high width-depth ratios. Channels vary in size over a wide range in different parts of the reefs but are mostly less than about 0,7 m deep.



Fig. 1.1 Deposition environment

Samples taken from the Carbon Leader Reef show that the distribution of gold can be related to the features of this environment (Nami (1983)). Figure 1.2 shows a typical cross section observed in a reef with a channel clearly visible and a uniform pebble band overlying channel and plain. Gold is dispersed through the material within the bounds of the channel in an erratic and non-continuous manner, suggesting an active bed at the time of deposition; gold concentration is high in isolated patches but the mean value is low. Over the plain areas gold is concentrated at the base of the pebble band, which is often underlain by carbonaceous material. The concentration is relatively high and persistent, tending to decrease with distance from the channels (Nami (1982)).

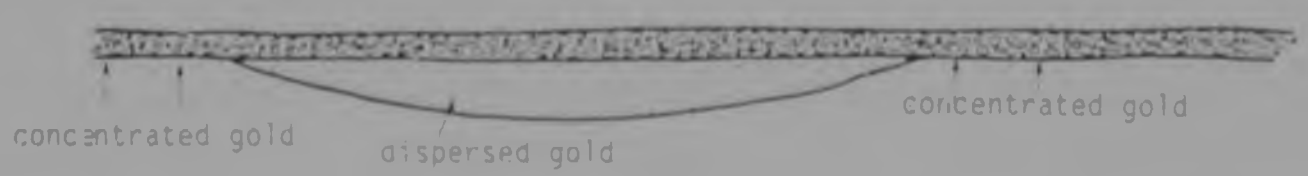


Fig. 1.2 Cross section through reef

It is apparent that gold was transported with the material now filling the channels. Within the channels gold would have been mixed with the bed material, bed load and suspended load and concentrated locally on a bedform scale by differential entrainment and deposition. This local sorting would have caused the high concentration patches observed in the reefs.

During periods of high flow the plain areas would be inundated as well as the channels. The strong interaction between the deep flow in the channels and the relatively shallow flow over the plains would have involved any suspended sediment as well as water. It is shown in Chapter 2 that gold particles could easily have been transported in suspension for the hydraulic conditions prevailing during reef formation. Flow in the channels would have been deeper and faster than flow over the plain areas and would therefore have had much greater capacity for transporting gold in suspension. The concentration of suspended gold would therefore have been much higher in the channels than over the plain areas. The resulting concentration gradient across the interaction zone would give rise to a transverse transport of gold analogous to diffusion, in addition to any transverse convection. Once over the plain the gold particles would tend to deposit because of the reduced capacity of the flow to maintain material in suspension. There would therefore have been continuous transfer and deposition of gold particles to the plain surface throughout periods of high flow. During long periods of high flow considerably more gold would have deposited on the plain than in the channels, resulting in the relatively high mean concentrations observed over plain areas.

Particles with lower densities than gold but with similar fall velocities would also have been transported to the plain. These particles would, however, have

...ver the gold ... as discussed ... in Chapter 2, would ... have deposited ... (mainly on the plain surface). The finer particles ... have been entrained and deposited much more easily by subsequent flow events. This differential ... and entrainment would have further concentrated the gold deposits close to the original plain ..., as observed on the reefs.

...quantitative explanation of the distributions observed on the reefs and general prediction of distributions ...requires a detailed knowledge of the deposition environment, the hydraulic conditions prevailing at the time of deposition and the mechanics of sediment transport. The geometry of the fluvial system is obviously not well known at the required scale. The results of this study will therefore become more useful as more information becomes available. Certain results may in fact be useful if applied in an inverse sense to infer geometric properties from reef samples. This approach is used to estimate prevailing hydraulic conditions from reef particle size data, as described in Chapter 4.

1.4 Existing models

A model for predicting the distribution of gold deposits must be able to describe the processes of transport and deposition as the transporting medium moves through the system being considered. The model must be sensitive to the distinguishing characteristics of gold and other sediments being transported so that sorting ... segregation during transport and deposition can be ...simulated. The level of detail of the model must be ...(e.g. ... the scale at which sorting ... of ...

... (1) ... the ... (2) ... is the result of

differential entrainment and [illegible] rates for different size and/or density particles as well as the movement of particles associated with the formation and movement of bed forms. The effect of these processes in concentrating heavy minerals has been demonstrated by Brady and Jobson (1973) but no successful mathematical description has been developed. The concentration of suspended sediment also varies over short distances in a vertical section. This variation can be adequately described, if not explained, by the diffusion analogy applied in one dimension (see Chapter 5.1 .

On a much larger scale, progressive sorting in a channel results from cumulative effects of local sorting and variations in the transport capacity of the flow. Rana, Simons and Mahmood (1973) developed a mathematical model to describe the variation in size of bed material with distance along an alluvial channel. The model is based on the assumptions of steady flow, a channel slope which decreases exponentially in the downstream direction, and a channel profile which is treated as an independent variable. The distribution of the median grain size is determined by assuming bed material characteristics, gradient and discharge at the beginning of the channel. The sediment transport rate is calculated at this position using Einstein's (1950) bed load function. It is assumed that the composition of the bed material discharge at this first position is the same as that of the bed material at a second position some distance downstream. The energy gradient at the second section required to ensure equality of water discharge and bed material discharge at the two sections is then determined. The distance between the two sections can then be calculated from an assumed equation describing the exponential decrease of gradient with distance. By considering new sections progressively the variation of median [illegible] distance can be described [illegible]

channel. The model would therefore enable the location of bed material with particular characteristics to be determined in a given channel and for a specified discharge.

The model described above cannot be used to determine the location of gold deposits in a channel for a number of reasons. Most important of these is that the results represent a situation in which the bed material is in equilibrium with the channel profile at all sections. Gold in the reefs was transported during relatively short events together with material different from that which determined the channel characteristics. The gold content in the transported material would have been very small and may have been equivalent to a wash load fraction, which cannot be treated by the model. The use of Einstein's bed load function precludes consideration of non-quartz material. Einstein's function incorporates empirical constants determined from data obtained for quartz particles. There are, however, sediment transport models which are not so restricted and one of these could be substituted. The model assumes a wide channel ignoring side effects with an exponentially decreasing slope. The gold distributions in the reefs have been seen to be closely related to compound cross section geometries and the longitudinal profile may have been completely different. A more general specification of channel geometry is required.

As hydraulic sorting takes place along a channel the size of bed material decreases in a downstream direction but must also increase with time at any section. The transport capacity of the flow therefore reduces with time and aggradation of the channel takes place. The Rana et al (1973) model does not account for the rate of aggradation and the resulting relationship between slope and grain size is somewhat unsatisfactory as the sediment load diminishes continuously with time.

Deigaard (1980) developed a longitudinal sorting model which accounts for the change of profile as aggradation occurs and can also be used to locate bed material with particular size characteristics along a river. In this model the channel is assumed to have an exponentially decreasing gradient and the same bed material along its entire length at time equal to zero. The sediment load at the beginning of the channel is assumed constant with time. A constant discharge is applied and the development of the longitudinal profile is described by a finite difference solution of the continuity equation for sediment. The change in composition of the bed material is calculated by solving the continuity equation for each of ten size fractions of the bed material.

In Deigaard's (1980) sorting model the rates of sediment transport are calculated according to the theory developed by Engelund and Fredsoe (1976). This theory is a development of ideas introduced by Bagnold (1954) and considers bed load and suspended load separately. The bed load equation is particularly suitable for use in sorting models because the motion of individual particles is considered. The rate of bed load discharge for a particular size fraction is calculated as the product of particle velocity, particle volume and the fraction of available particles that move (i.e. the probability of motion). Both particle velocity and probability of motion depend on the relationship between applied and critical shear stresses. These parameters are calculated using equations based on theory and experimental results obtained by Fernandez Luque and van Beek (1976). The critical shear stress concept is useful when particles with different characteristics are considered although Deigaard has not accounted for variations caused by shielding effects in mixtures with significantly different particle sizes.

Suspended load is calculated by Deigaard as the product of flow velocity and sediment concentration, integrated over the flow depth. The concentration at any depth is calculated by applying the diffusion analogy in one dimension as in Chapter 5.1 but assuming the distribution of eddy viscosity to be described by two straight lines rather than a parabola. The velocity profile is assumed to be logarithmic near the boundary and parabolic in the main body of the flow, instead of logarithmic throughout. These distributions of eddy viscosity and velocity enable the integration of the product of velocity and concentration to be performed explicitly rather than numerically as done by Einstein (1950).

Although an improvement on the model of Rana et al (1973), Deigaard's 1980) sorting model is still not suitable for locating concentrated deposits of gold. The distribution of particles of a particular size is closely related to the local gradient and the model can only be used to consider size fractions which are involved in determining the equilibrium channel profile. The quantities of gold being transported would have been insignificant in the channel forming process. Gold distributions must also be described on a somewhat smaller scale than considered by this model.

Diegaard (1980) also developed a model to describe the sorting of sediments in channel bends but this produces results in terms of mean diameters and would obviously not be suitable for analysing distributions of relatively small quantities of gold.

Models such as those of Rana et al (1973) and Deigaard (1980) which treat sediment sorting in conjunction with the morphological development of channels are clearly unsuitable for locating deposits of particles with low

concentrations in transport, such as gold. The principles underlying these models could, however, prove to be very useful for inferring prevailing hydraulic conditions from morphologic and sediment characteristics observed in the reefs. For locating concentrated gold deposits a model is required which will describe the movement of the particles through a system with arbitrary geometry at an appropriate time scale. Although the geometries of the ancient channel systems in the reefs are not known this approach should enable some general relationships between geometric properties and distribution patterns to be developed.

Various models have been developed for routing sediment through river reaches with specified geometric characteristics to study the responses of rivers to development. These models predict locations and quantities of erosion and deposition along the length of a river for given water and sediment discharge inputs. Both the time scale and distance scale are smaller than considered by the sorting models already discussed and therefore event-related, non-equilibrium deposition patterns can be dealt with. Sediment routing models describe the movement of sediment by a simultaneous solution of the equations of continuity for sediment and sediment-laden flow and the equation of motion for sediment-laden flow. The more simple models consider one-dimensional flow which enables only general patterns of river morphology to be considered in non-uniform systems. More detailed analyses can be performed by modifying the one-dimensional approach to accommodate multiple streams or compound channels. Alternatively two-dimensional models can be applied.

The various solution techniques for these three types of model are comprehensively reviewed by Chen (1979). Either a finite difference or a finite element approach can be adopted; a finite element solution will

generally give a better representation of irregular channel configurations but requires considerably more computational effort.

Four different types of numerical solution procedures are available. The complete solution technique is a simultaneous solution of the three basic equations and gives the best treatment of the continuous interaction of water and sediment transport. Under certain conditions simpler numerical solutions are suitable. If aggradation or degradation of the channel is slow an uncoupled unsteady solution technique can be used in which flow continuity and flow momentum are solved first and the solution is subsequently refined by applying continuity for sediment. A recent example of this approach is the one-dimensional model developed by Krishnappan (1981). In many cases changes in flow conditions at a section are slow compared with changes to the bed and the flow variation is known. In such cases the flow can be considered to be quasi-steady for sediment computations and the solution obtained by solving sediment continuity and flow momentum, the known discharge solution. If, in addition, the effects of changes to the bed are negligible within a time step an uncoupled steady solution can be used in which the flow momentum equation can be solved first to determine the water surface profile and the sediment continuity equation solved subsequently to determine sediment movement.

The shortcomings for predicting gold distribution patterns of the various sediment routing models available lie primarily in the purposes for which they were developed. The conventional application is to predict regions of erosion and deposition within rivers on a relatively large scale. In such cases it is not necessary to distinguish in detail between different particle sizes and often a sediment trans-

port model is used which calculates discharge rates in terms of a single size representative of the whole bed material. This is not a serious failing as any suitable sediment transport model could be substituted. The main drawbacks lie in the scale considered and the treatment of flow over flood plains. One-dimensional models are clearly inadequate for describing flood plain deposition, even if modified to account for multiple stream or compound channel configurations. A two-dimensional model, at least, is required. Existing two-dimensional models do not account for the interaction between channel and plain flow in sufficient detail to be useful for predicting gold deposits on the scale required. Weiss (1976), for example, developed a two-dimensional model which can be used to predict sediment deposits on flood plains. The sediment transport equation, however, is in terms of the median grain size and movement of sediment by convective transport only is considered. This is quite adequate for analysing bulk sediment deposits on a large scale but not if distinctive particles, such as gold, must be identified.

Particles in suspension are transferred from channel to plain by the turbulence associated with the interaction between the relatively fast and slow flows in addition to convective transport. This 'diffusive' transfer is negligible on the scale considered by established sediment routing models but the channel sizes associated with gold deposits in the reefs are generally small enough for it to be significant. This is corroborated by the nature of some distributions observed in the reefs. The diffusion transfer is a much smaller scale phenomenon than convective transport and if it were included in a general sediment routing program the small grid spacing required would lead to excessive computation times. In addition it would be necessary to describe the distribution of suspended material over

the depth and a third dimension to the finite difference grid would become necessary.

It is established in Chapter 2 that suspension was the dominant mode of transport of gold particles in the reefs. A model for gold distribution should therefore consider suspension in more detail than is done by most sediment routing models. Those models which do distinguish between suspended load and bed load use equilibrium concentration profiles for calculating suspended load which is not sufficient for describing the channel to plain transfer.

Various models have been developed on the basis of the diffusion analogy to describe the behaviour of suspended particles. Camp (1946) presented an analytical solution for the distribution of suspended sediment under the influences of turbulent diffusion and settling. This solution depends on the assumptions of a uniform velocity distribution and constant diffusivity. To account for the logarithmic distribution of velocity and the parabolic distribution of diffusivity, Sarikaya (1977) proposed a numerical solution of the diffusion-settling equation. Sarikaya's model can be used to describe the vertical and longitudinal distribution of suspended sediment in a channel but does not account for transverse diffusive transport or for bed conditions which are not totally absorbing.

There appears to be no existing model which could be used for predicting the distribution of gold deposits which accounts for all the relevant processes at the appropriate scale. A new approach is therefore developed which draws on applicable aspects of existing techniques.

1.3 Proposed Model

A pair of models are proposed for conjunctive use to

the depth and a third dimension to the finite difference grid would become necessary.

It is established in Chapter 2 that suspension was the dominant mode of transport of gold particles in the reefs. A model for gold distribution should therefore consider suspension in more detail than is done by most sediment routing models. Those models which do distinguish between suspended load and bed load use equilibrium concentration profiles for calculating suspended load which is not sufficient for describing the channel to plain transfer.

Various models have been developed on the basis of the diffusion analogy to describe the behaviour of suspended particles. Camp (1946) presented an analytical solution for the distribution of suspended sediment under the influences of turbulent diffusion and settling. This solution depends on the assumptions of a uniform velocity distribution and constant diffusivity. To account for the logarithmic distribution of velocity and the parabolic distribution of diffusivity, Sarikaya (1977) proposed a numerical solution of the diffusion-settling equation. Sarikaya's model can be used to describe the vertical and longitudinal distribution of suspended sediment in a channel but does not account for transverse diffusive transport or for bed conditions which are not totally absorbing.

There appears to be no existing model which could be used for predicting the distribution of gold deposits which accounts for all the relevant processes at the appropriate scale. A new approach is therefore developed which draws on applicable aspects of existing techniques.

1.3 Proposed Models

A pair of models are proposed for conjunctive use to

predict the distribution of gold deposits through a channel-plain system with any specified configuration and discharge.

Only suspended transport is considered because this has been shown to be the dominant mode and will determine the ultimate destinations of most particles. The movement of particles in suspension is assumed to be by diffusion-type processes and convection, including settling. These transport components are used to develop the continuity equation for sediment.

Although the scales of the variations of gold deposits transverse to a channel and along its length are significantly different, both are determined by the transfer of suspended gold from the channel to the plain and both depend on the vertical distribution of suspended particles. The distribution of deposits therefore depends on the distribution of suspended gold in three dimensions during transport. Because of the level of detail required to describe the transverse transfer, a three dimensional model capable of describing the relatively gradual longitudinal variations of deposits would be extremely large and computational effort would be prohibitive. The three-dimensional problem has therefore been decomposed and solved using two two-dimensional models. The first model describes the transverse transfer of suspended particles from channel to plain flow and the deposition of particles on the plain surface. The second model describes the longitudinal transport of suspended particles subject to deposition on the bed and transfer to the plain. The rates of transfer to the plain depend on concentration gradients which are determined by the first model and assumed to apply over a certain length of channel. The second model can therefore not be used without a preliminary application of the first.

Very little is known about the hydraulic conditions prevailing during deposition of gold in the reefs, particularly concerning the temporal characteristics of deposition events. Until more information becomes available there seems to be little motivation for taking account of unsteady flow in great detail. As presented, the models are used to describe gold distributions resulting from steady, longitudinally uniform flow conditions in straight channel reaches. This corresponds to the uncoupled steady solution approach discussed earlier, with Manning's equation used to describe the flow. Nonuniform conditions in the longitudinal direction could be accounted for by performing a preliminary nonuniform flow calculation for the channel and then applying the longitudinal distribution model to reaches short enough for the results of the transverse model to be representative. If reaches are sufficiently short a certain degree of time variation could be accounted for by quasi-steady treatment.

The continuity equation for sediment is solved using a finite difference approach. A finite element method would allow a better representation of irregular configurations but would be more difficult to set up and would require more computer time. The equations describing the transfer of sediment from channel to plain are based on empirical results and do not warrant a detailed geometric representation as could be afforded by a finite element method.

The models presented can be used to determine distribution patterns for any type of particle that would be transported mainly in suspension for the specified flow conditions and which is significantly smaller than the bed material on the plain. The size restriction arises from the deposition model described in Chapter 5.2. If larger particles are to be studied the equation for deposition probability in the transverse model should

be applicable to the criterion used for the longitudinal model.

The applicability of the longitudinal model will decrease as very wide channels are specified. This is because sediment is assumed to be uniformly distributed across the channel at all sections, implying complete mixing between sections. Transverse diffusion within a channel is considerably less than across the channel-plain interaction zone. If a significant portion of the channel is unaffected by the interaction transverse mixing will be poor and transfer to the plain will decrease rapidly with distance as sediment near the banks is depleted.

The proposed model assumes [illegible] gold distributions in the reefs to be dealt with in sufficient detail for general conclusions to be drawn concerning the relationship between sedimentation patterns and channel [illegible]

2. MODE OF TRANSPORT OF GOLD PARTICLES

There are three mechanisms by which sediment particles can be transported by flowing water. These are by rolling or sliding along the bed, by saltation, and in suspension. The first two mechanisms both result from surface traction and are usually considered as a combined mechanism; the sediment transported by this combined mechanism is known as bed load or contact load. Particles moving by saltation are ejected from the bed layer into the flow but are too heavy to remain in suspension and fall back to the bed. Transport is therefore by a series of jumps. The suspended load consists of particles which are kept within the body of the flow by the action of turbulence.

The physical processes involved in transport of sediment as bed load and suspended load are very different and the behaviour of particles in each of these transport modes is distinctive. The mode of transport depends on physical characteristics of the sediment particles and on prevailing hydraulic conditions. A certain particle may be transported as bed load under certain hydraulic conditions and as suspended load under other conditions. Knowledge of sediment characteristics and hydraulic conditions would enable the correct transport mode to be established and if the relevant physical processes are understood the distribution of deposits could be predicted. Using the same principles it should be possible to infer the prevailing hydraulic conditions from a knowledge of distribution patterns and sediment characteristics. Identifying the mode of transport is fundamental to the understanding and interpretation of the distribution of sediment deposits.

Small sediment particles are kept in suspension by turbulence in the flow. A criterion for determining whether a given particle will be kept in suspension or

be obtained by comparing the fall velocity of the particle with the root mean square of the vertical velocity fluctuations associated with the turbulence. This approach was first used by Lane and Kalinske (1939) to formulate the following criterion for particle suspension.

$$\frac{w}{u_*} \leq 1,0 \qquad (2.1)$$

in which w is the fall velocity of the particle and u_* is the shear velocity of the flow, defined by

$$u_* = \sqrt{\tau_0/\rho} \qquad (2.2)$$

in which τ_0 is the boundary shear stress and ρ is the fluid density.

Engelund (1973) considered the shear stress associated with grain roughness only, and not the combination of grain roughness and form resistance. He proposed that particles would be suspended if

$$\frac{w}{u_*'} < 0,8 \qquad (2.3)$$

in which u_*' is the shear velocity associated with grain roughness only.

This form of criterion has been confirmed by the diffusion theory of sediment suspension proposed by Ippen and Rouse and verified by Vanoni (1946). Vanoni found experimentally that there was very little, if any, suspended material for the condition $w/u_* = 1,0$. Further experimental verification was obtained by Francis (1973).

Middleton (1976) concluded that there is good theoretical and experimental justification for using this type of criterion for separating sediments transported by traction and suspension.

The form of the suspension criterion proposed by

Engelund was applied to gold particles assuming a representative size of 0,14mm. This required an estimate of the particle fall velocity.

The fall velocity of a particle in a fluid depends on both fluid and particle characteristics, the most important being fluid viscosity and the size, shape and density of the particle. Many theoretical and empirical formulas have been proposed for calculating fall velocities for spheres (see Fig. 2.1) and these have been well reviewed by Graf (1971) who also discusses the effects of the above-mentioned and other fluid and particle characteristics. None of the established formulas could be used to estimate the fall velocity of gold particles without verification because all were developed for spherical and/or relatively low density particles. Gold particles have highly irregular, generally flaky shapes and the specific gravity is about 19,3. It was therefore necessary to determine fall velocities for gold experimentally.

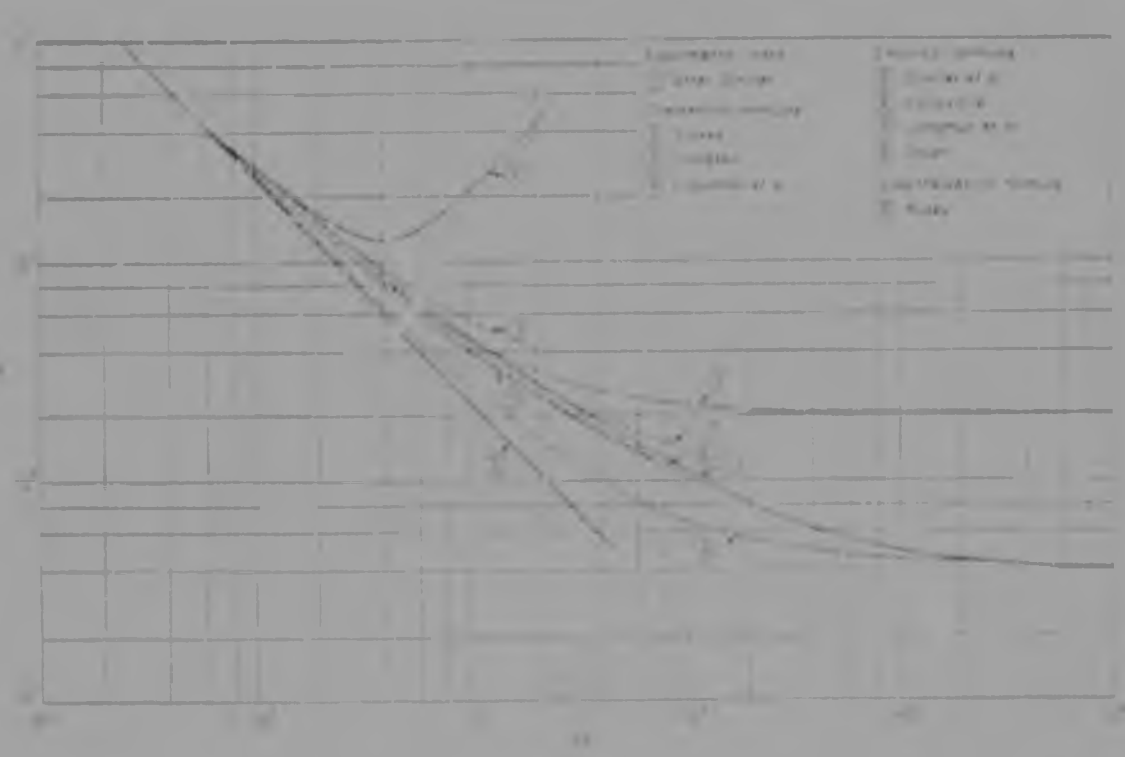


Fig. 2.1 Drag coefficient vs Reynolds number for spheres (Graf (1971)).

The Chamber of Mines supplied nine gold particles representing a range of sizes and masses for fall velocity measurements. Fall velocities were measured in water for all particles and in alcohol for three of them (Msutwana, 1982). Particle characteristics and measured fall velocities are listed in Table 2.1

Table 2.1 Characteristics of Gold Particles

Particle	Length(mm)	Width (mm)	Mass (mg)	Fall Velocity (m/s)	
				Water	Alcohol
1	1,185	0,444	0,794	0,160	0,167
2	0,815	0,630	0,397	0,105	-
3	0,889	0,407	0,209	0,093	0,103
4	0,704	0,444	0,227	0,095	0,108
5	0,630	0,370	0,136	0,091	-
6	0,630	0,296	0,077	0,064	-
7	0,704	0,222	0,109	0,080	-
8	0,519	0,370	0,048	0,052	-
9	0,148	0,111	0,180	0,105	-

These results were used to determine the Reynolds number and drag coefficient for each particle. Reynolds number is defined by

$$Re = \frac{wd}{\nu} \qquad (2.4)$$

in which d is a particle length dimension and ν is the kinematic viscosity which is $1,1 \times 10^{-6}$ m^2/s for water and $1,53 \times 10^{-6}$ m^2/s for alcohol. The length dimension d was assumed to be the diameter of a sphere with the same volume as the particle. This was calculated from the measured mass using a specific gravity of 19,3. In fact the fall velocity of particles with different shapes is well represented by this assumption in the laminar region as shown by previous workers.

The drag coefficient C_D is defined by the equation

$$F_D = \tfrac{1}{2} C_D \rho A w^2 \qquad (2.5)$$

in which F_D is the drag force which is equal to the submerged weight at terminal velocity and A is the projected area of the spherical particle.

The Chamber of Mines supplied nine gold particles representing a range of sizes and masses for fall velocity measurements. Fall velocities were measured in water for all particles and in alcohol for three of them (Msutwana, 1982). Particle characteristics and measured fall velocities are listed in Table 2.1

Table 2.1 Characteristics of Gold Particles

Particle	Length(mm)	Width (mm)	Mass (mg)	Fall Velocity (m/s)	
				Water	Alcohol
1	1,185	0,444	0,794	0,160	0,167
2	0,815	0,630	0,397	0,105	-
3	0,889	0,407	0,209	0,093	0,103
4	0,704	0,444	0,227	0,095	0,108
5	0,630	0,370	0,136	0,091	-
6	0,630	0,296	0,077	0,064	-
7	0,704	0,222	0,109	0,080	-
8	0,519	0,370	0,048	0,052	-
9	0.148	0,111	0,180	0,105	-

These results were used to determine the Reynolds number and drag coefficient for each particle. Reynolds number is defined by

$$Re = \frac{wd}{\nu} \qquad (2.4)$$

in which d is a particle length dimension and ν is the kinematic viscosity which is $1,1 \times 10^{-6}$ m^2/s for water and $1,53 \times 10^{-6}$ m^2/s for alcohol. The length dimension d was assumed to be the diameter of a sphere with the same volume as the particle. This was calculated from the measured mass using a specific gravity of 19,3. In fact the fall velocity of particles with different shapes is well represented by this assumption in the laminar region as shown by previous workers.

The drag coefficient C_D is defined by the equation

$$F_D = \tfrac{1}{2} C_D \rho A w^2 \qquad (2.5)$$

in which F_D is the drag force which is equal to the submerged weight at terminal velocity and A is the projected area of the spherical particle.

The Reynolds numbers and drag coefficients for all the gold particles are shown in Table 2.2

TABLE 2.2 Fall Velocity Data for Gold Particles

Particle	Equivalent D am.(mm)	Water w(m/s)	Re	C_D	Alcohol w(m/s)	Re	C_D
1	0,43	0,160	63	4,30	0,167	47	4,04
2	0,34	0,105	32	7,95	-	-	-
3	0,27	0,093	23	8,71	0,103	18	7,31
4	0,28	0,095	24	8,04	0,108	20	6,35
5	0,24	0,091	20	7,13	-	-	-
6	0,20	0,064	12	12,24	-	-	-
7	0,22	0,080	16	9,00	-	-	-
8	0,17	0,052	8	15,55	-	-	-
9	0,26	0,105	25	6,16	-	-	-

These results have been plotted on Fig. 2.2. This graph can be used in conjunction with equations (2.4) and (2.5) to determine the fall velocity of a gold particle with any required equivalent diameter. It is assumed that the fall velocities in turbulent flow are the same as in quiescent fluid, that the effective viscosity of the fluid is not affected by particles in suspension, and that particles do not interfere with one another, i.e. the concentration is low.

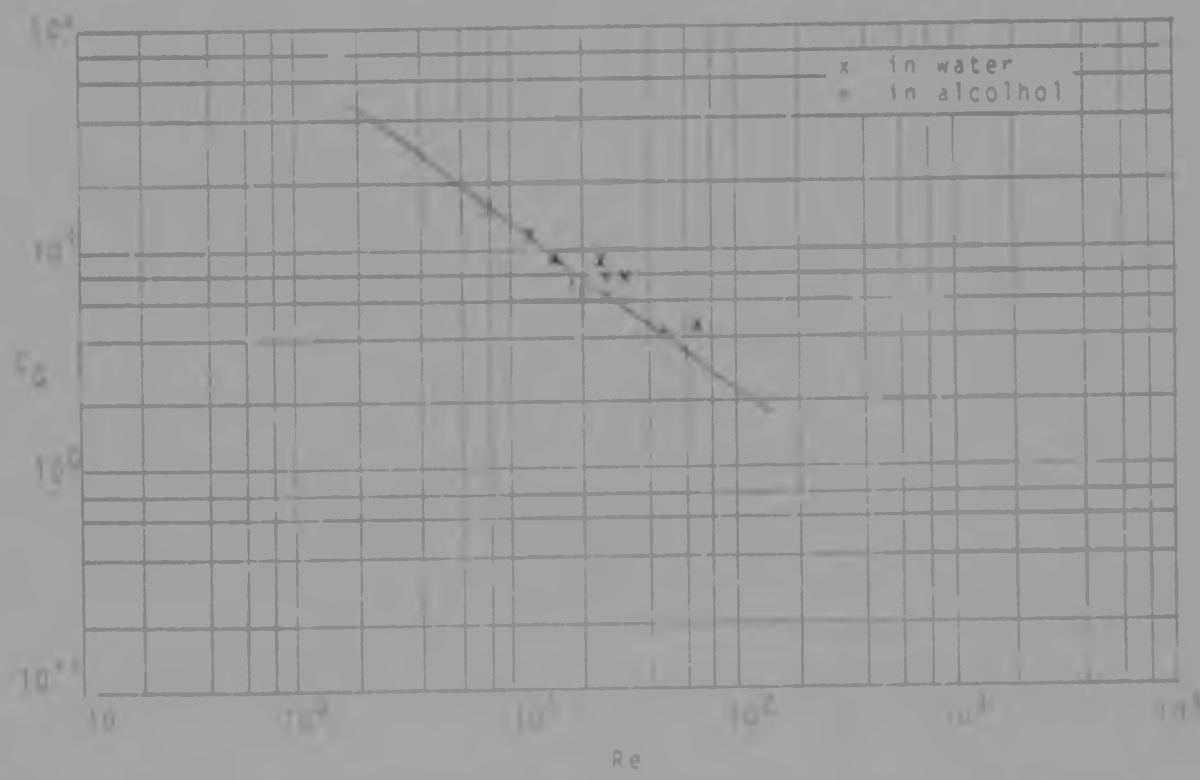


Fig. 2.2 Drag coefficient vs Reynolds number for gold particles

Using these results a gold particle with an equivalent diameter of 0,140 mm will have a fall velocity of 0,035 m/s. Using Fig. 2.3 it can be calculated that a spherical sand grain with a diameter of 0,3mm would have the same fall velocity. While in suspension, therefore, a gold particle with an equivalent diameter of 0,14mm would behave in very much the same way as a 0,3mm sand particle.

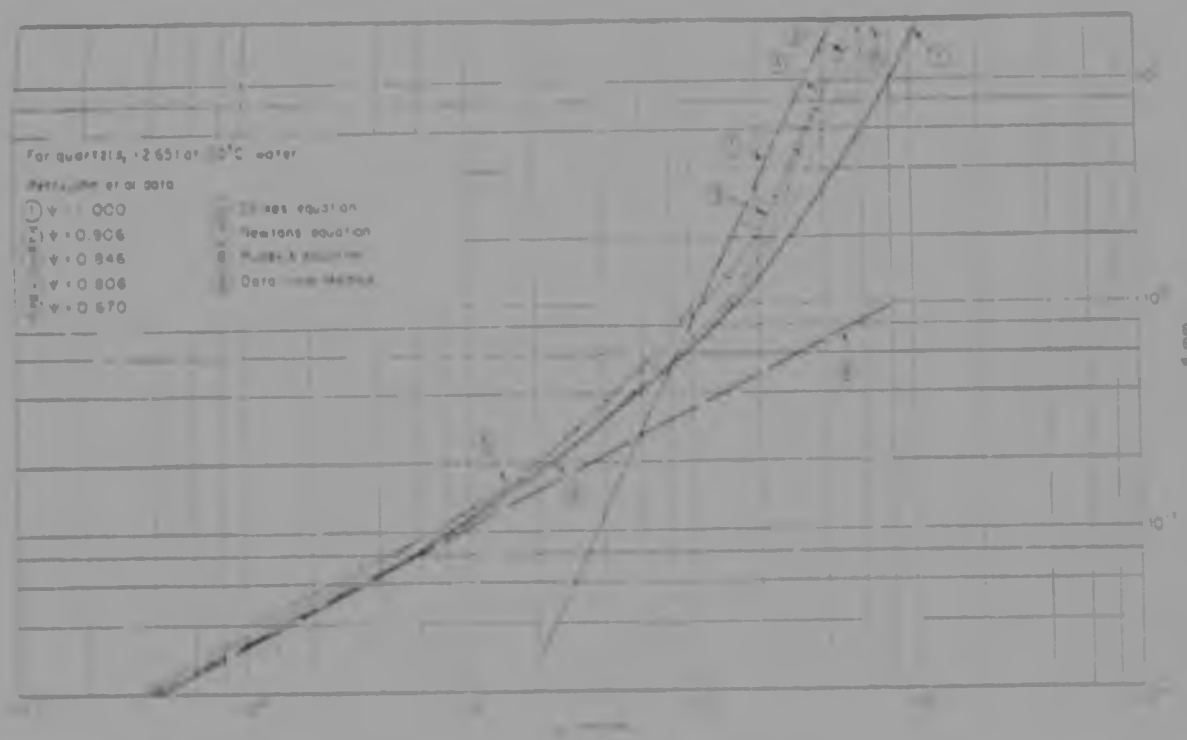


Fig. 2.3 Sediment velocity for quartz grains (Graf (1971))

The hydraulic conditions for suspension of gold with an equivalent particle size of 0,14mm and a fall velocity of 0,035 m/s were determined. Substituting this value of fall velocity into Engelund's criterion for suspension (equation (2.3)) indicates that gold will be in suspension if the shear velocity associated with grain roughness exceeds 0,044 m/s. If it is assumed that no bed forms are present and that the hydraulic radius can be approximated by the flow depth, then the suspension criterion can be expressed as a relationship between fall velocity, flow depth D and hydraulic gradient, i.e.

$$w < 0{,}8\sqrt{gDS} \qquad (2.6)$$

Using this relationship the minimum depths for which gold would be in suspension over a range of hydraulic gradients were calculated and plotted in Fig. 2.4. The criterion of Lane and Kalinske (equation (2.1) has been plotted in the same way.

The conditions for suspension of gold particles were confirmed for a smaller range of hydraulic gradients using Einstein's (1950) model for sediment transport. This model is valid only for quartz-density sediments and gold particles could not be analysed directly. The analysis was therefore done for sand grains with the same fall velocity as the gold particles. Because these sand particles are larger than the gold particles entrainment would not be modelled accurately, but the error should not be too great for this comparison. Using Einstein's model, the minimum flow depths required to produce a suspended load for the equivalent sand size were determined for different hydraulic gradients. These results are also plotted on Fig. 2.4 and agree closely with the other criteria.

Sumer (1974) identified two different conditions of suspension in flow over a smooth boundary. For certain flow conditions suspended particles would have significant interaction with the boundary, settling to the boundary periodically and then being re-entrained. For other conditions the particles would remain suspended within the fluid for practically all the time, rarely settling to the boundary. The criterion for a particle to be in suspension practically all the time is

$$\frac{w}{\kappa u_*} < A \qquad (2.7)$$

and $d > \delta$ (2.8)

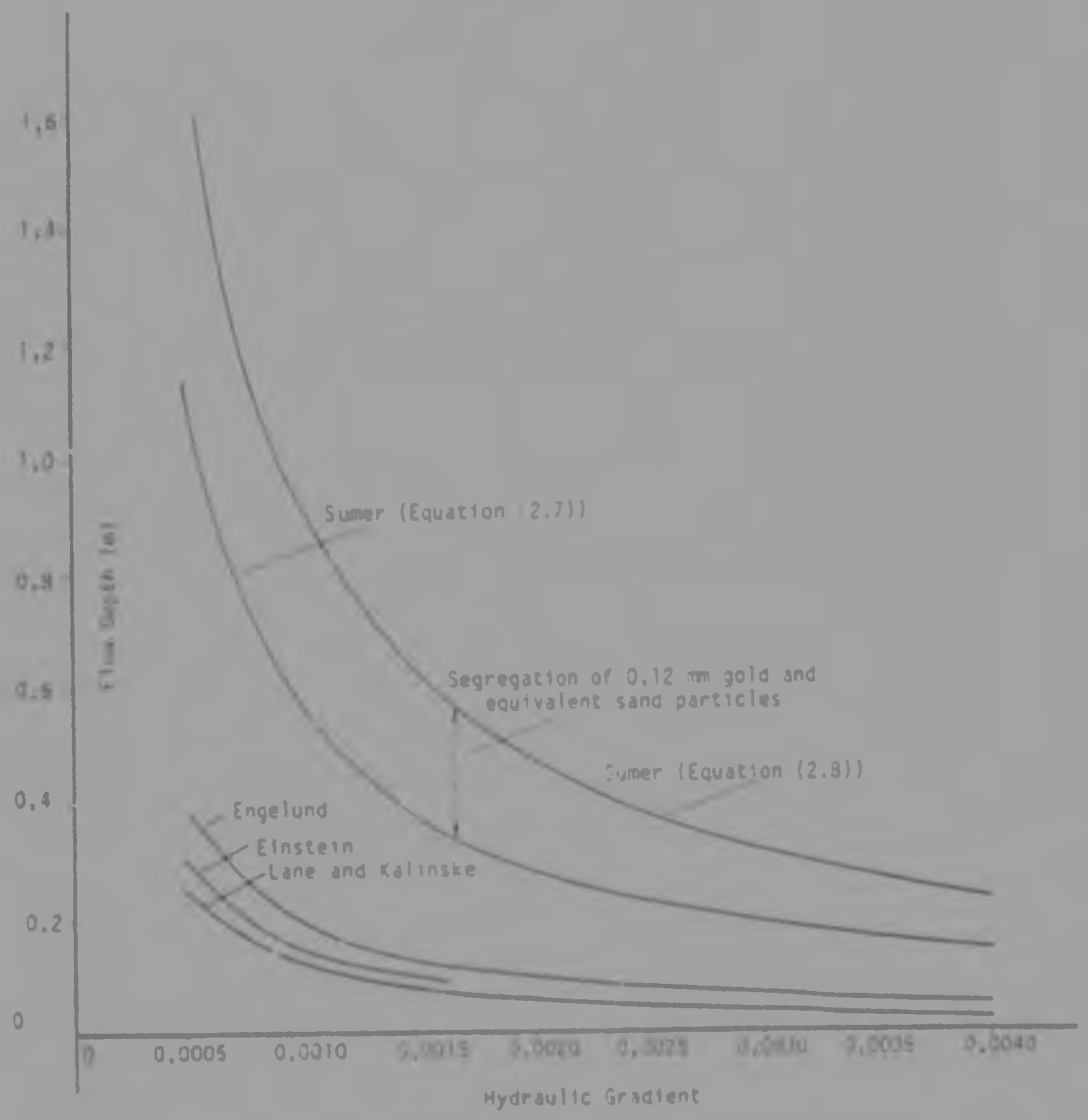


Fig. 2.4 Hydraulic conditions for suspension of gold particles

in which κ is Karman's constant (equal to 0,4 for clear water), A is a constant of order unity, and δ is the thickness of the laminar boundary sublayer which can be calculated from the expression

$$\delta = \frac{11,6}{u_*} \qquad (2.9)$$

The criterion represented by equation (2.7) was applied to the gold and equivalent sand particles with A equal to 1,0. This condition is also shown on Fig. 2.4.

The requirement of equation (2.8) has interesting implications. For certain conditions equation (2.7) could be satisfied by gold and equivalent sand particles while equation (2.8) is satisfied by the sand particle only. In such a case the sand would be in suspension practically all the time while the gold particles would be involved in interaction with the bed. It would therefore be possible for gold particles to be deposited but not sand particles. Likewise if bed material containing sand and gold were subjected to these conditions the sand particles could be permanently removed while gold remained in the bed. Segregation of this type would occur for gold particles smaller than about 0,14 mm. The range of conditions for segregation between 0,12 mm gold particles and equivalent (0,25 mm) sand is shown on Fig. 2.4. The positions of the curves vary with particle size and the range would become larger with decreasing particle size.

Although the conditions defined by equations (2.7) and (2.8) were developed for a smooth bed and obviously would not apply in real cases, the shielding effect afforded to small particles by larger particles on a poorly sorted bed would have the same sort of effect as the laminar sublayer. This effect might account for the concentration of small heavy mineral particles on a bedform scale.

The curves on Fig. 2.4 describing the conditions necessary for the suspension of gold particles represent particular values of shear velocity, or boundary shear stress which would be competent to move pebbles or sand particles of a particular size as bed load. The larger particles in the reef would have been transported to their final deposition locations as bed load. The shear

stress required to move material as bed load can be estimated and it is therefore possible to relate the conditions for suspension of gold to the sizes of other particles in the reef.

The Shields criterion (Fig. 2.5) is widely accepted for determining the hydraulic conditions for movement of sediment. Using this diagram and the shear velocity defined by the Engelund criterion for gold suspension the largest particle moving at the conditions necessary to suspend gold would be about 2,5mm. This implies that any deposit which contains quartz density particles larger than 2,5mm would have been laid under hydraulic conditions for which gold could be transported in suspension. It should be borne in mind that the presence of particular size fractions depends on the availability or supply of that fraction in addition to the competence of the flow to transport it. The absence of particles larger than 2,5mm would therefore not necessarily imply that gold was not in suspension.

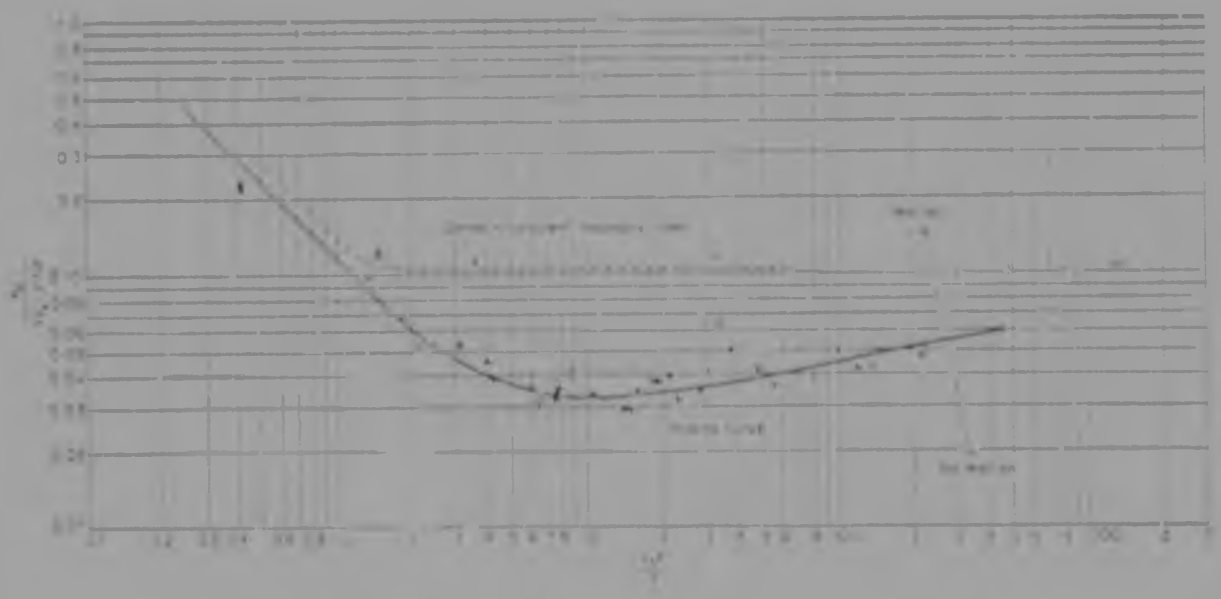
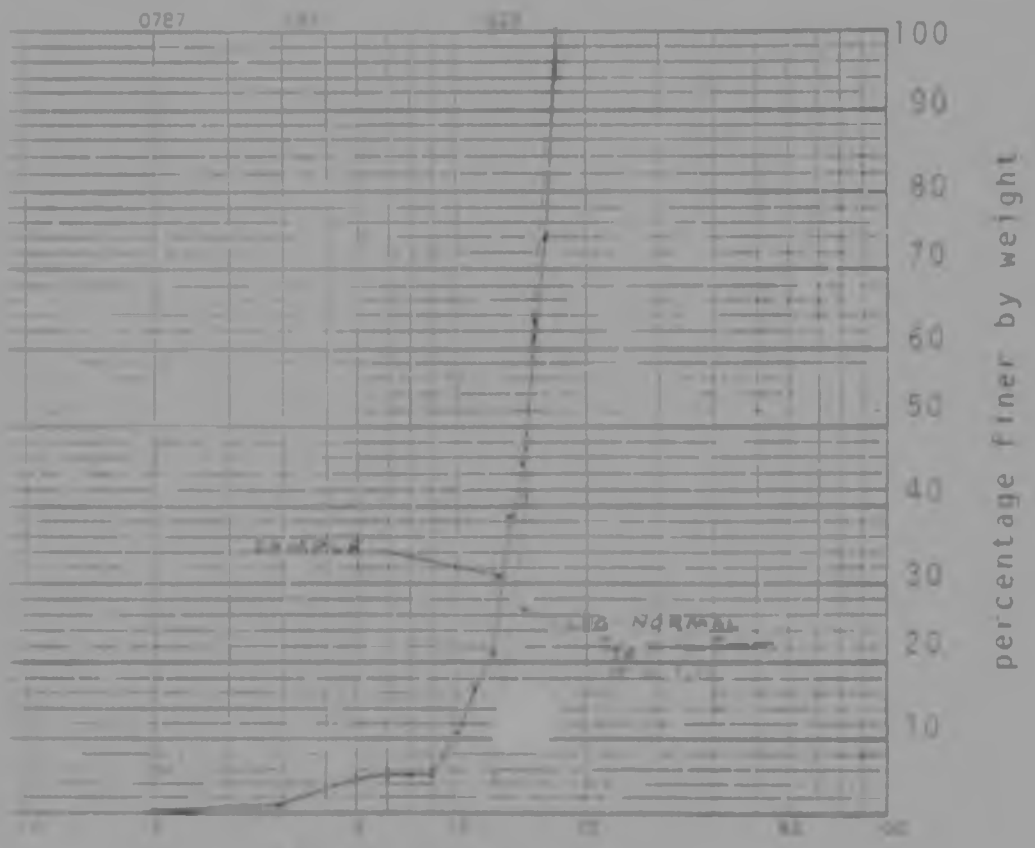


Fig. 2.5 The Shields criterion for sediment motion (Graf (1971))

The hydraulic conditions necessary to transport the material in the pebble layer of the reef have also been

...mation. A sample description was provided by the ...hamber of Mines, giving the number of particles in ...various size fractions at a particular location. This ...as converted to a cumulative weight distribution, which ...s shown in Fig. 2.6.



...ig. 2.6 Particle size distribution for pebble band

...This distribution may not be truly representative of the pebble material as it was determined by measuring and counting particles on a slice of rock sample which would exaggerate the content of the smaller size fractions. The sample was also too small to be representative; the number of particles in the larger fractions were small but constituted a large percentage by weight of the sample. The hydraulic interpretation considered only the largest sizes however, and is intended to give a rough indication only of the hydraulic conditions.

The ...required to move the largest particle ...about 7mm ...determined by the Shields criterion and ...corresponding flow depths and hydraulic gradients ...compared with the conditions for gold suspension in ...

The results were confirmed by applying the Meyer-Peter and Muller bed load equation,

$$\frac{\gamma R(k/k')^{3/2} S}{d} - 0{,}047(\gamma_s - \gamma) = 0{,}25\rho^{1/3} \left(\frac{g_s'}{d}\right)^m \qquad (2.10)$$

In this equation R is the hydraulic radius, S is the hydraulic gradient, the factor $(k/k')^{3/2}$ represents the proportion of total energy loss associated with grain roughness and g_s' is the sediment transport rate in terms of submerged weight. If the transport rate is set equal to zero, equation (2.10) reduces to a criterion for sediment movement very similar to the Shields criterion. The flow conditions necessary for movement of the pebble material according to the Meyer-Peter and Muller equation are also shown on Fig. (2.7).

Other sediment transport equations incorporating a critical condition for transport could be used in a similar manner and would give similar results. Transport models such as that of Einstein are inappropriate because no condition can be defined at which sediment motion begins. Einstein's model was actually run for the pebble material and the hydraulic conditions for transport showed a similar variation to those obtained by the other methods. The position of the curve would depend, however, on the magnitude of sediment transport used as a cut-off between motion and no motion which is very subjective.

Fig. 2.7 represents many combinations of flow depth and gradient required to suspend gold and move pebbles. No unique condition can be identified at present. Further information on flow depths or hydraulic gradients would enable the range of possible conditions to be reduced. Valuable information would be obtained by examining variations of sediment size distributions over long distances in isolated channels.

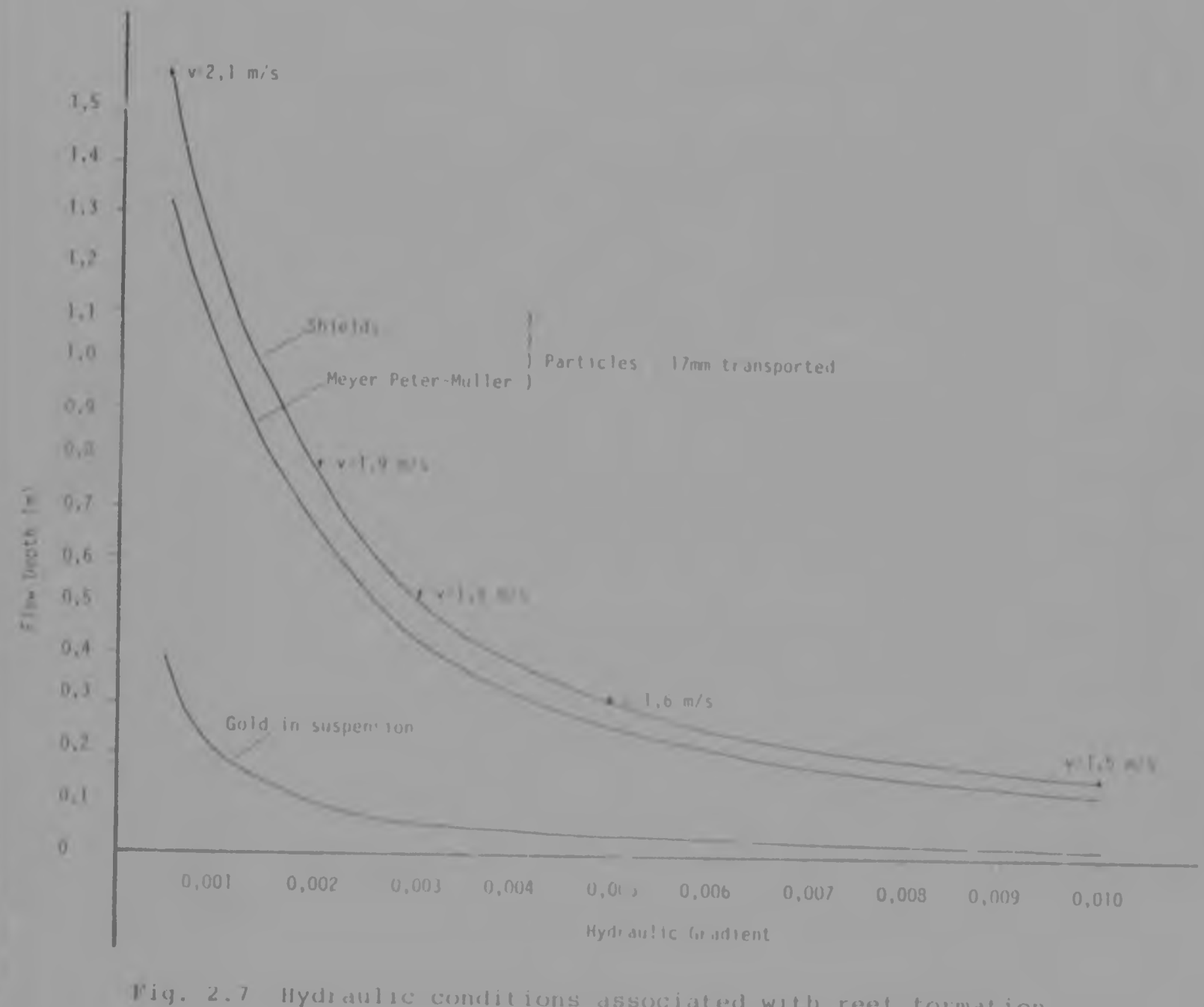


Fig. 2.7 Hydraulic conditions associated with reef formation

The comparison in Fig. 2.7 shows that flow conditions occurred during formation of the reef which were far in excess of those required to transport gold in suspension. The freedom of movement of suspended material is much greater than that of material moving as bed load and deposition patterns of gold should be closely related to the distribution of the suspended fraction in flow through the channel-plain configuration.

3. THE TRANSVERSE TRANSFER EQUATION

3.1 Introduction

It has been shown (Chapter 2) that suspension was probably the dominant mode of transport of gold particles now present in the reefs. The distribution of gold deposits must therefore be closely related to the distribution of suspended gold particles during transport. The models developed to predict gold distribution patterns are therefore based on descriptions of the behaviour of particles in suspension.

Prior to the mid 1930s the phenomenon of particle suspension by moving fluids was poorly understood. The importance of turbulence was appreciated but could not be explained physically or mathematically. Various theories have been proposed since then but understanding of all the associated processes is still incomplete.

The conventional model of turbulent flow explains velocity fluctuations as the result of the superposition of disturbances caused by eddies of different sizes. The size of the largest eddies, or the scale of macroturbulence, can be described by Prandtl's mixing length which is related to the distance from the boundary by the Karman constant. Yalin (1977) points out that vertical and horizontal velocity fluctuations are different. Eddies should therefore be considered to be elliptic rather than circular and associating a single mixing length to turbulent flow is not correct. The instability of large eddies generates smaller eddies, which in turn generate still smaller ones. In recent years the formation of eddies in turbulent flow has been explained in terms of the so-called burst-sweep cycle. According to this concept small scale turbulence develops within an inner layer of flow close to the bed and is periodically advected into an outer layer where burst or

'break-up' vortices occur, followed by accelerated downward sweep motions of fluid towards the bed. Leeder (1983) explains this process and reviews recent developments.

The most popular approach for describing suspended distributions is based on the assumption that the effect of turbulence in keeping particles in suspension can be described as a diffusion process. This implies that if a variation in concentration of suspended material exists, particles will move from regions of high concentration to regions of low concentration at a rate which is proportional to the concentration gradient. An equilibrium state of turbulent suspension can exist if this diffusive transport is balanced by a convective transport component in the opposite direction. For example, the distribution of suspended sediment in a vertical plane has been described by equating the rates of particle settling and upward diffusion (see Chapter 5.1). A general diffusion-convection equation can be derived by applying the principle of mass conservation to a control volume equation (5.1).

Application of the diffusion model requires estimates of diffusivities for sediment, which define the proportionality between concentration gradient and the rate of diffusive transport. Diffusivities for sediment are related to diffusion for fluid mass and momentum and depend on the turbulent structure of the flow. The turbulent shear stresses within the fluid can be related to the magnitudes of velocity fluctuations and, by using Prandtl's mixing length, to the velocity gradient. Shear stress and velocity gradient are related by momentum diffusivity and so by assuming distributions for shear stress and velocity an expression for momentum diffusivity can be derived (see Chapter 4.2).

The diffusional theory cannot explain the fact that a

statistically steady mass of suspended particles has an excess submerged weight that must be balanced by an upthrust exerted by the fluid. The energy approach, developed mainly by Bagnold (1966), reasons that the particles are supported by momentum transfer from other particles or fluid and that the particles must be lifted at the rate at which they settle under gravity. The work rate of suspended load can then be equated to the available power supply of the flow to determine the rate of suspended transport. This theory is based on the presence of a residual upward shear stress to support the suspended particles which implies that velocity fluctuations are larger in the upward direction than in the downward direction. To conserve momentum the mass of fast upward moving fluid must be smaller than that of the slower downward moving fluid. This can be reconciled with the modern concepts of turbulence with fast upward masses corresponding to burst motions and slow downward masses to sweep motions.

Although the energy approach for describing sediment suspension is more appealing physically than the diffusion theory it cannot easily be used to describe the distribution of suspended particles. The distribution is important for calculating the transfer of sediment from channels to flood plains because only the sediment suspended in a channel above the level of the plain surface is available for transfer. The diffusional approach has been found to predict distributions which agree reasonably well with experiment and should be adequate on the scale required for predicting gold distribution. The energy approach also does not enable particles with different characteristics to be distinguished during transport, and is therefore unsuitable if sorting between different particles is to be considered. Gold was transported in a mixture of other sediments, probably constituting only a very small fraction, and a model is therefore required which can consider gold

individually. The diffusional approach can be applied separately to different fractions and is therefore well suited to sediment sorting and gold distribution analysis. The shortcoming of a diffusion model that the magnitude of suspended load cannot be estimated without knowledge of absolute sediment concentration close to the bed is not restrictive because only relative concentrations are necessary to describe the distribution patterns. The models developed for gold distribution are therefore based on the diffusion analogy. Appropriate diffusion-convection equations are presented in the following section for the transverse distribution and in Chapter 8 for the longitudinal distribution.

3.2 Theory

The general three-dimensional equation for the transfer of a neutrally buoyant solute by diffusion and convection is

$$\frac{\partial C}{\partial t} + \sum_{i=1}^{3} u_i \frac{\partial C}{\partial x_i} = \sum_{i=1}^{3} \frac{\partial}{\partial x_i}\left(\epsilon_i \frac{\partial C}{\partial x_i}\right) \qquad (3.1)$$

in which C is concentration, t is time, x_i are the coordinate directions, u_i are the convective velocity components in the coordinate directions and ϵ_i are the diffusivities in the coordinate directions.

In the stream system being considered x, y and z represent the longitudinal, vertical and transverse directions respectively. For heavy particles the convective velocity in the vertical direction will be the particle fall velocity w, which is assumed to be positive downwards. Transverse convective effects resulting from secondary currents can be accounted for in the transverse diffusivity ϵ_z. For a channel which is straight and parallel to the steepest gradient of the plain there will be no additional transverse convection. If, however, the channel deviates from this direction

there will be a component of flow velocity normal to the channel above the plain level, giving rise to a transverse convection velocity component, u. When considering steady state conditions and flow which is uniform in the longitudinal direction the sediment concentration will not vary with respect to time or longitudinal distance over short distances, i.e. $\frac{\partial C}{\partial t}=0$ and $\frac{\partial C}{\partial x}=0$.

Therefore for steady, longitudinally uniform flow in a straight channel system, equation (3.1) can be simplified to

$$0 = \frac{\partial}{\partial y}(\varepsilon_y \frac{\partial C}{\partial y}) + \frac{\partial}{\partial z}(\varepsilon_z \frac{\partial C}{\partial z}) + w\frac{\partial C}{\partial z} - u\frac{\partial C}{\partial z} \qquad (3.2)$$

Equation (3.2) describes the variation of sediment concentration in the vertical and transverse directions across a flow section.

The method of solution of a two-dimensional second-order partial differential equation depends on its particular form and several distinct types of equation are recognized. Consider the general form of a partial differential equation,

$$a\frac{\partial^2 \phi}{\partial x^2} + b\frac{\partial^2 \phi}{\partial x \partial y} + c\frac{\partial^2 \phi}{\partial y^2} + d\frac{\partial \phi}{\partial x} + e\frac{\partial \phi}{\partial y} + f\phi + g = 0 \qquad (3.3)$$

where a, b, c, d, e, f and g may be functions of the independent variables x and y and of the dependent variable ϕ. Equation (3.3) is said to be elliptic when $b^2 - 4ac < 0$, parabolic when $b^2 - 4ac = 0$, and hyperbolic when $b^2 - 4ac > 0$.

Relating equation (3.2) to the general form of equation (3.3), the vertical diffusivity ε_y corresponds to a, the transverse diffusivity ε_z corresponds to c, the fall velocity w corresponds to d, and the transverse convective component u corresponds to e. The diffusivities will have positive values and there is no term in

there will be a component of flow velocity normal to the channel above the plain level, giving rise to a transverse convection velocity component, u. When considering steady state conditions and flow which is uniform in the longitudinal direction the sediment concentration will not vary with respect to time or longitudinal distance over short distances, i.e. $\frac{\partial C}{\partial t}=0$ and $\frac{\partial C}{\partial x}=0$.

Therefore for steady, longitudinally uniform flow in a straight channel system, equation (3.1) can be simplified to

$$0 = \frac{\partial}{\partial y}(\epsilon_y \frac{\partial C}{\partial y}) + \frac{\partial}{\partial z}(\epsilon_z \frac{\partial C}{\partial z}) + w\frac{\partial C}{\partial z} - u\frac{\partial C}{\partial z} \qquad (3.2)$$

Equation (3.2) describes the variation of sediment concentration in the vertical and transverse directions across a flow section.

The method of solution of a two-dimensional second-order partial differential equation depends on its particular form and several distinct types of equation are recognized. Consider the general form of a partial differential equation,

$$a\frac{\partial^2 \phi}{\partial x^2} + b\frac{\partial^2 \phi}{\partial x \partial y} + c\frac{\partial^2 \phi}{\partial y^2} + d\frac{\partial \phi}{\partial x} + e\frac{\partial \phi}{\partial y} + f\phi + g = 0 \qquad (3.3)$$

where a, b, c, d, e, f and g may be functions of the independent variables x and y and of the dependent variable ϕ. Equation (3.3) is said to be elliptic when $b^2 - 4ac < 0$, parabolic when $b^2 - 4ac = 0$, and hyperbolic when $b^2 - 4ac > 0$.

Relating equation (3.2) to the general form of equation (3.3), the vertical diffusivity ϵ_y corresponds to a, the transverse diffusivity ϵ_z corresponds to c, the fall velocity w corresponds to d, and the transverse convective component u corresponds to e. The diffusivities will have positive values and there is no term in

equation (3.2) corresponding to the second term of equation (3.3) so b is zero. The value of b^2-4ac is therefore negative and equation (3.2) is elliptic.

The domain of integration of a two-dimensional elliptic equation is always an area bounded by a closed curve. Boundary conditions must be specified for all points on the closed curve and may specify either function values or normal derivatives, or a combination of both.

The domain of integration for the transverse distribution problem is a rectangular flow area above the plain portion of the compound channel. This area is bounded by the plain surface at the bottom and the water surface at the top. The vertical side boundaries will be defined by adjacent channels as in Fig. 3.1 a or by a channel on one side and a solid vertical boundary on the other, as in Fig. 3.1 b. The double channel configuration applies to practical applications and the solid vertical boundary to laboratory conditions.

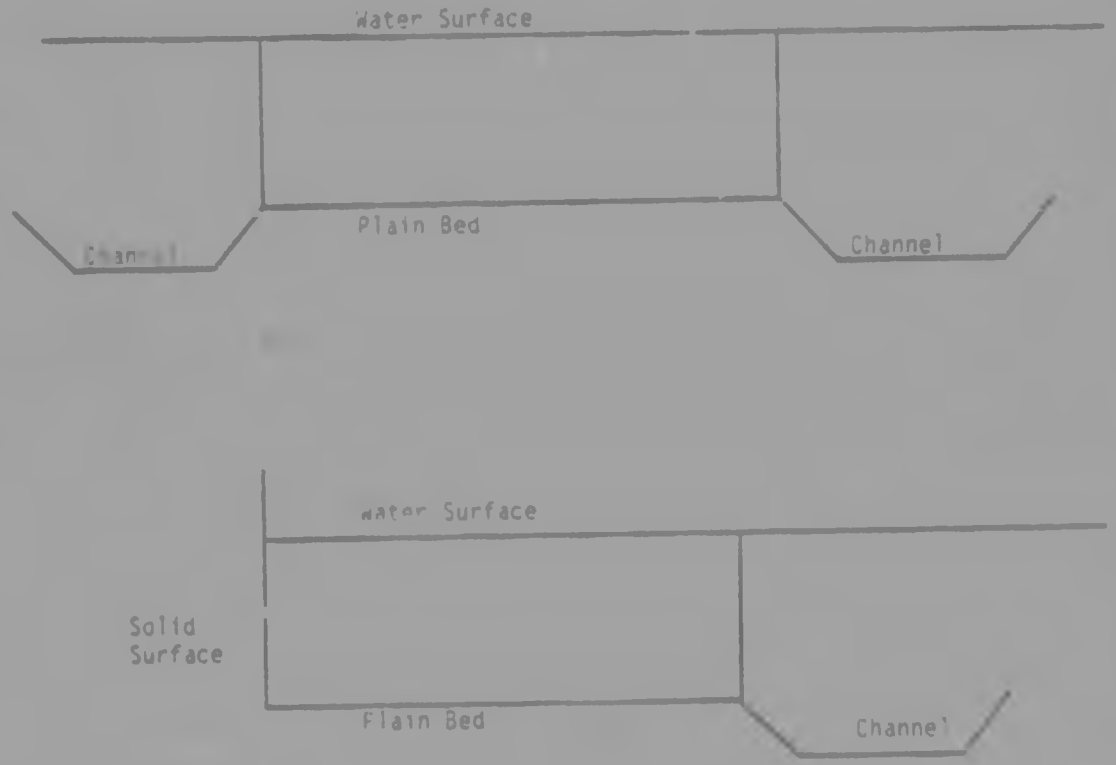


Fig. 3.1 Domain of integration

The boundary conditions at vertical surfaces defined by channels are specified in terms of concentration values which are generated from flow conditions in the channels. All other boundary conditions are of the derivative type. There can be no transport of suspended material across the water surface or the solid vertical boundary while at the plain surface the rate of transport across the boundary is defined by a specified probability that a particle reaching the surface will be deposited.

Boundary conditions are satisfied by applying appropriately formulated finite difference approximations to the transfer equation at all boundary points.

3.3 Finite Difference Formulations

The diffusion-settling equation is solved numerically by using a finite difference approach. The domain of integration is divided into N equal vertical increments

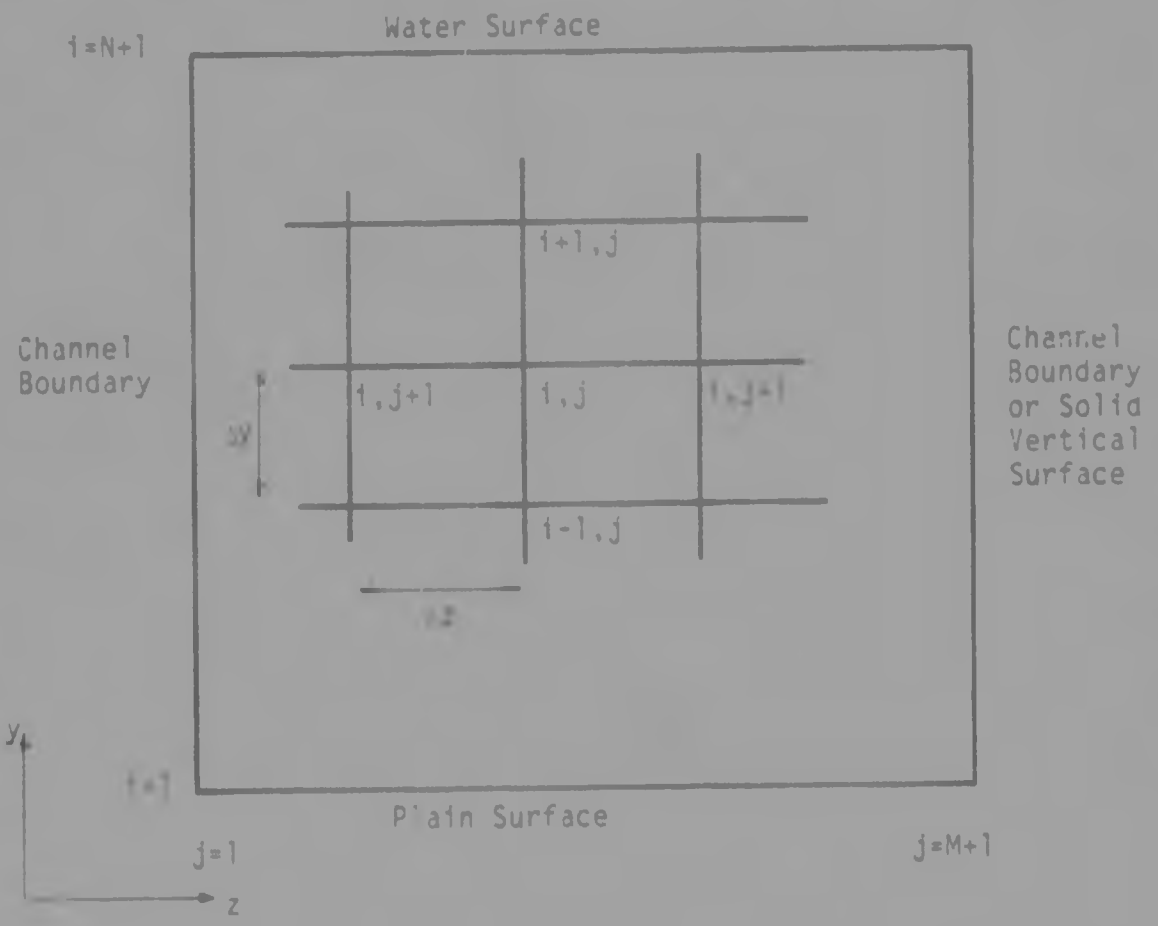


Fig. 3.2 Finite difference grid

and ∆ equal horizontal increments, as shown in Fig. [illegible] ncrement boundaries are numbered from I=1 on the plain surface to I=N+1 at the water surface and from J=1 at the first channel boundary to J=M+1 at either the second channel boundary or the solid vertical surface.

The following finite difference approximations are made

$$\frac{\partial C}{\partial y} \rightarrow \frac{C_{I+1,J} - C_{I,J}}{\Delta y} \tag{3.4}$$

$$\frac{\partial C}{\partial z} \rightarrow \frac{C_{I,J+1} - C_{I,J}}{\Delta z} \tag{3.5}$$

$$\frac{\partial}{\partial y}\left(\varepsilon_y \frac{\partial C}{\partial y}\right) \rightarrow \frac{1}{\Delta y}\left[\frac{\varepsilon_{I+1,J} + \varepsilon_{I,J}}{2}\left(\frac{C_{I+1,J} - C_{I,J}}{\Delta y}\right) - \frac{\varepsilon_{I,J} + \varepsilon_{I-1,J}}{2}\left(\frac{C_{I,J} - C_{I-1,J}}{\Delta y}\right)\right] \tag{3.6}$$

Equation [illegible] is reduced to

$$\frac{\partial}{\partial y}\left(\varepsilon_y \frac{\partial C}{\partial y}\right) \rightarrow \frac{E_{y\,I+1}C_{I+1,J} - [E_{y\,I+1} + E_{y\,I}]C_{I,J} + E_{y\,I}C_{I-1,J}}{\Delta y^2} \tag{3.7}$$

where

$$E_{y\,I} = \frac{\varepsilon_{I,J} + \varepsilon_{I-1,J}}{2} \tag{3.8}$$

and $E_{y\,I+1} = \frac{\varepsilon_{I+1,J} + \varepsilon_{I,J}}{2}$

Similarly

$$\frac{\partial}{\partial z}\left(\varepsilon_z \frac{\partial C}{\partial z}\right) \rightarrow \frac{E_{z\,J+1}C_{I,J+1} - [E_{z\,J+1} + E_{z\,J}]C_{I,J} + E_{z\,J}C_{I,J-1}}{\Delta z^2} \tag{3.9}$$

where

$$E_{z\,J} = \frac{\varepsilon_{I,J} + \varepsilon_{I,J-1}}{2} \tag{3.10}$$

and $E_{z\,J+1} = \frac{\varepsilon_{I,J+1} + \varepsilon_{I,J}}{2}$

For the transverse convection component the finite difference approximation is

$$\frac{\partial C}{\partial z} \rightarrow \frac{C_{i,j} - C_{i,j-1}}{\Delta z} \qquad 3.11$$

Using the above finite difference approximation the diffusion-settling equation (3.2) can be written as

$$\frac{1}{\Delta y^2}(E_y(i+1)C_{i+1,j} - [E_y(i+1)+E_y(i)]C_{i,j} + E_y(i)C_{i-1,j})$$
$$+\frac{1}{\Delta z^2}(E_z(j+1)C_{i,j+1} - [E_z(j+1)+E_z(j)]C_{i,j} + E_z(j)C_{i,j-1})$$
$$+\frac{w}{\Delta y}(C_{i+1,j} - C_{i,j}) + \frac{u}{\Delta z}(C_{i,j} - C_{i,j-1}) \qquad 3.12$$

or

$$[\frac{E_y(i+1)}{\Delta y^2} + \frac{w}{\Delta y}]C_{i+1,j} + \frac{E_z(j+1)}{\Delta z^2}C_{i,j+1} + [\frac{E_z(j)}{\Delta z^2}$$
$$+ [\frac{E_z(j)}{\Delta z^2} - \frac{u}{\Delta z}]C_{i,j-1} - [\frac{E_y(i+1)+E_y(i)}{\Delta y^2} + \frac{E_z(j+1)+E_z(j)}{\Delta z^2}$$
$$+ \frac{w}{\Delta y} + \frac{u}{\Delta z}]C_{i,j} = 0 \qquad 3.13$$

Equation (3.13) can also be derived by considering the mass balance of material entering and leaving a fluid element. Fig. 3.3 shows an element with sides Δy and Δz centred at grid point (i,j) and the diffusive and convective transport components across each boundary.

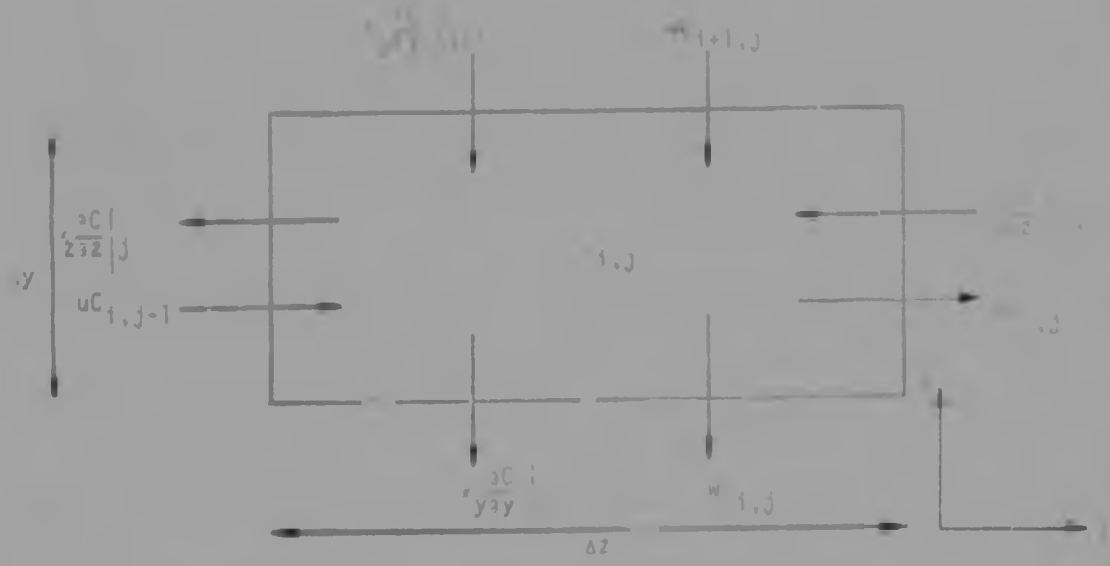


Fig. 3.3 Fluid element for an interior point

The material transported by diffusion across any boundary is equal to the product of the diffusivity in the relevant direction and the concentration gradient, both at the appropriate position. Material transported by convection is equal to the product of convective velocity and concentration.

The net mass of material entering the element in the y direction is given by

$$(\epsilon_y \frac{\partial C}{\partial y}|_{i+1} - \epsilon_y \frac{\partial C}{\partial y}|_i + wC_{i+1,j} - wC_{i,j})\Delta z \qquad (3.14)$$

and in the z direction by

$$(\epsilon_z \frac{\partial C}{\partial z}|_{j+1} - \epsilon_z \frac{\partial C}{\partial z}|_j + uC_{i,j-1} - uC_{i,j})\Delta y \qquad (3.15)$$

For a steady process the net mass entering the element from all directions must be zero, and therefore

$$[\epsilon_y \frac{\partial C}{\partial y}|_{i+1} - \epsilon_y \frac{\partial C}{\partial y}|_i + wC_{i+1,j} - wC_{i,j}]\Delta z$$

$$+[\epsilon_z \frac{\partial C}{\partial z}|_{j+1} - \epsilon_z \frac{\partial C}{\partial z}|_j + uC_{i,j-1} - uC_{i,j}]\Delta y = 0 \qquad (3.16)$$

By making the finite difference approximations of equations (3.4) and (3.5) and the substitutions of equations (3.8) and (3.10), equation (3.16) can be written as

$$[E_y(i+1)\frac{C_{i+1,j}-C_{i,j}}{\Delta y} - E_y(i)\frac{C_{i,j}-C_{i-1,j}}{\Delta y} + wC_{i+1,j} - wC_{i,j}]\Delta z$$

$$+ [E_z(j+1)\frac{C_{i,j+1}-C_{i,j}}{\Delta z} - E_z(j)\frac{C_{i,j}-C_{i,j-1}}{\Delta z} + uC_{i,j-1} - uC_{i,j}]$$

$$\Delta y = 0 \qquad (3.17)$$

Dividing by $\Delta y \Delta z$ and rearranging terms yields

$$[\frac{E_y(i+1)}{\Delta y^2}+\frac{w}{\Delta y}]C_{i+1,j} + [\frac{E_z(j+1)}{\Delta z^2}]C_{i,j-1}+[\frac{E_y(i)}{\Delta y^2}]C_{i-1,j}$$
$$+[\frac{E_z(i)}{\Delta z^2}+\frac{u}{\Delta x}]C_{i,j-1}$$
$$-[\frac{E_y(i+1)+E_y(i)}{\Delta y^2} + \frac{E_z(j+1)+E_z(j)}{\Delta z^2} + \frac{w}{\Delta y}+\frac{u}{\Delta x}]C_{i,j} = 0 \quad (3.18)$$

which is identical to equation (3.13).

The mass balance approach is used to derive finite difference approximations to the diffusion-settling equation while satisfying the boundary conditions at each surface of the domain of integration.

At the water surface (i=N+1) the fluid element associated with each grid point will have dimensions of $\Delta y/2$ and Δz in the vertical and transverse directions respectively, as shown in Fig. 3.4

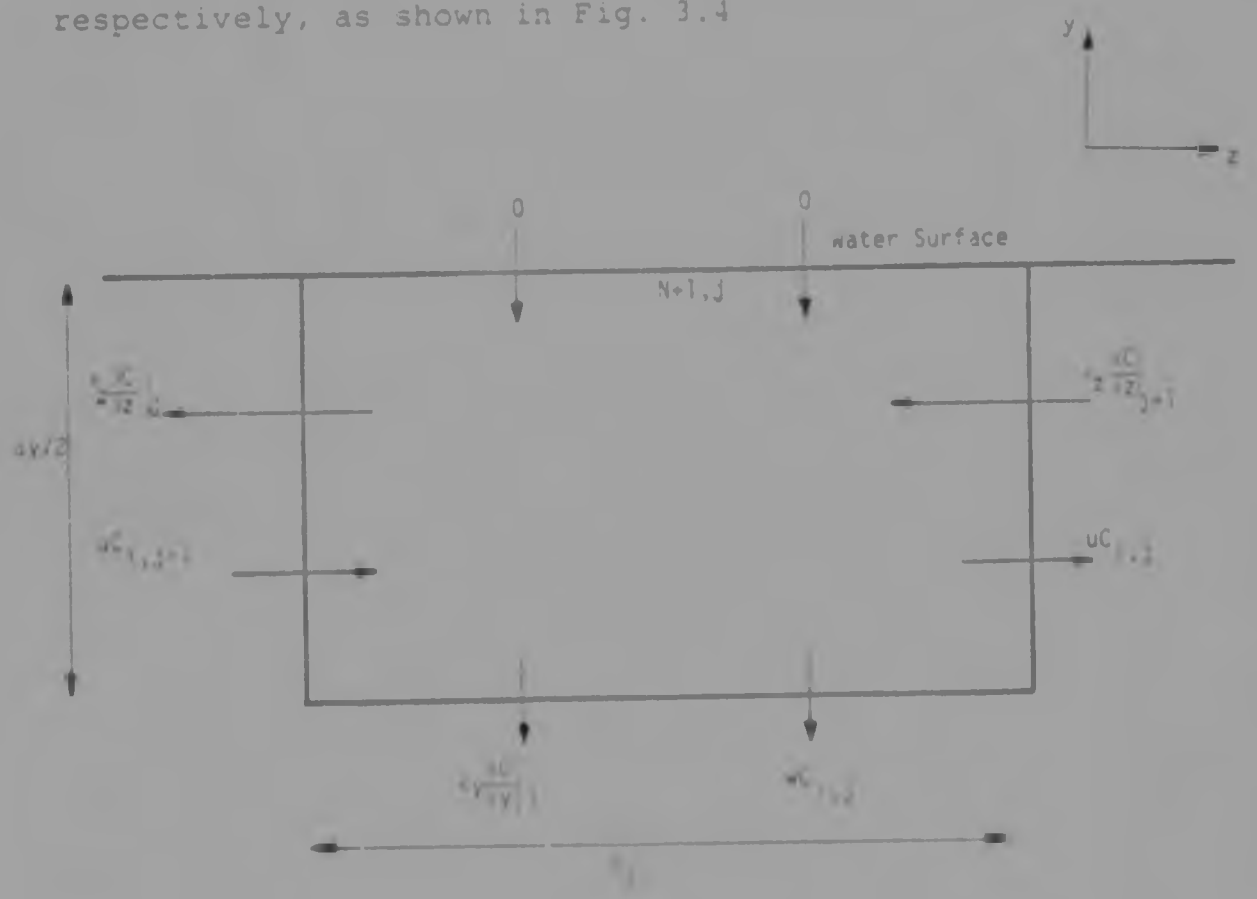


Fig. 3.4 Fluid element for points at water surface

The diffusion component at the water surface is zero because the vertical diffusivity decreases to zero at the surface. The convective term at the water surface is zero because there is no contribution of material from above the surface. By following the same mass balance approach as for interior points a finite difference equation for water surface points can be derived,

$$\left[\frac{E_z(j+1)}{2\Delta z^2}\right]C_{i,j+1} + \left[\frac{E_y(i)}{\Delta y^2}\right]C_{i-1,j} - \left[\frac{E_z(j)}{2\Delta z^2} + \frac{u}{2\Delta z}\right]C_{i,j-1}$$

$$- \left[\frac{E_y(i)}{\Delta y^2} + \frac{E_z(j+1)+E_z(j)}{2\Delta z^2} + \frac{w}{\Delta y} + \frac{u}{2\Delta z}\right]C_{i,j} = 0 \qquad (3.19)$$

At the plain bed boundary (i=1) the dimensions of the fluid element will again be $\Delta y/2$ and Δz in the vertical and transverse directions respectively, as shown in fig. 3.5.

The diffusion component across the boundary is again zero because the vertical diffusivity decreases to zero at the plain bed. In general, the amount of material crossing the boundary by convection will be less than the product of particle fall velocity and concentration because the rate of deposition of material reaching the boundary is determined by the nature of the bed surface and the hydraulic conditions near the bed. Some particles will deposit while others will immediately be re-entrained. The rate of deposition, or transport across the boundary, is therefore defined by a probability, p, that a particle at the bed will in fact be deposited. This can also be interpreted as the proportion of particles at the boundary which will be deposited. The probability, p, is calculated as a function of the plain surface characteristics, the settling particles and the flow conditions.

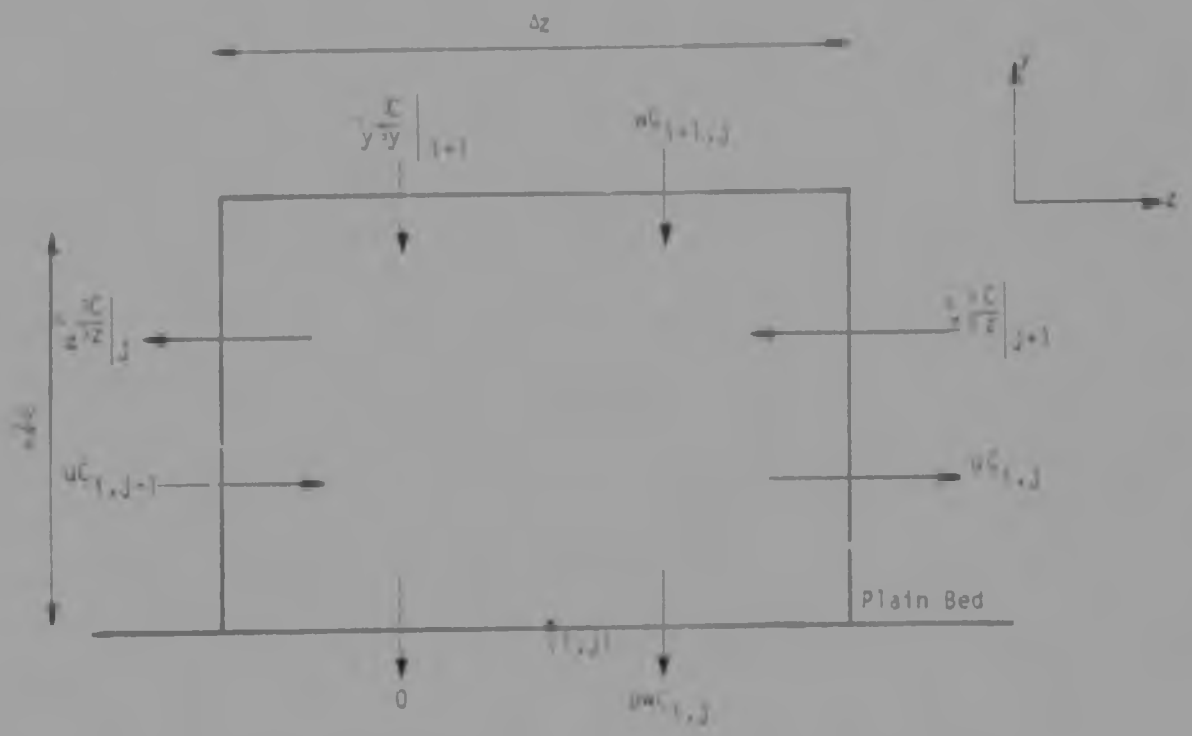


Fig. 3.5 Fluid element for points on the plain bed

Applying mass balance to the transport components shown in Fig. 3.5 leads to the following finite difference equation for points on the plain bed boundary.

$$[\frac{E_y(i+1)}{\Delta y^2} + \frac{w}{\Delta y}]C_{i+1,j} + [\frac{E_z(j+1)}{2\Delta z^2}]C_{i,j+1} + [\frac{E_z(j)}{2\Delta z^2} + \frac{u}{2\Delta z}]C_{i,j-1}$$

$$- [\frac{E_y(i+1)}{\Delta y^2} + \frac{E_z(j)+E_z(j+1)}{2\Delta z^2} + \frac{pw}{\Delta y} - \frac{u}{2\Delta z}]C_{i,j} = 0 \quad (3.20)$$

If the integration domain is bounded by channels on both sides, both vertical boundary conditions will be specified in terms of concentration values. If one vertical boundary is a solid surface then the boundary condition will be in derivative form and a finite difference equation must be derived for points on this boundary. In the case of a solid vertical boundary there can be no transverse flow component and the transverse convection term is not included in the formulations for this option. In this case the fluid element to be considered will have dimensions of Δy in the vertical direction and $\Delta z/2$ in the transverse

direction, as shown in Fig. 3.6

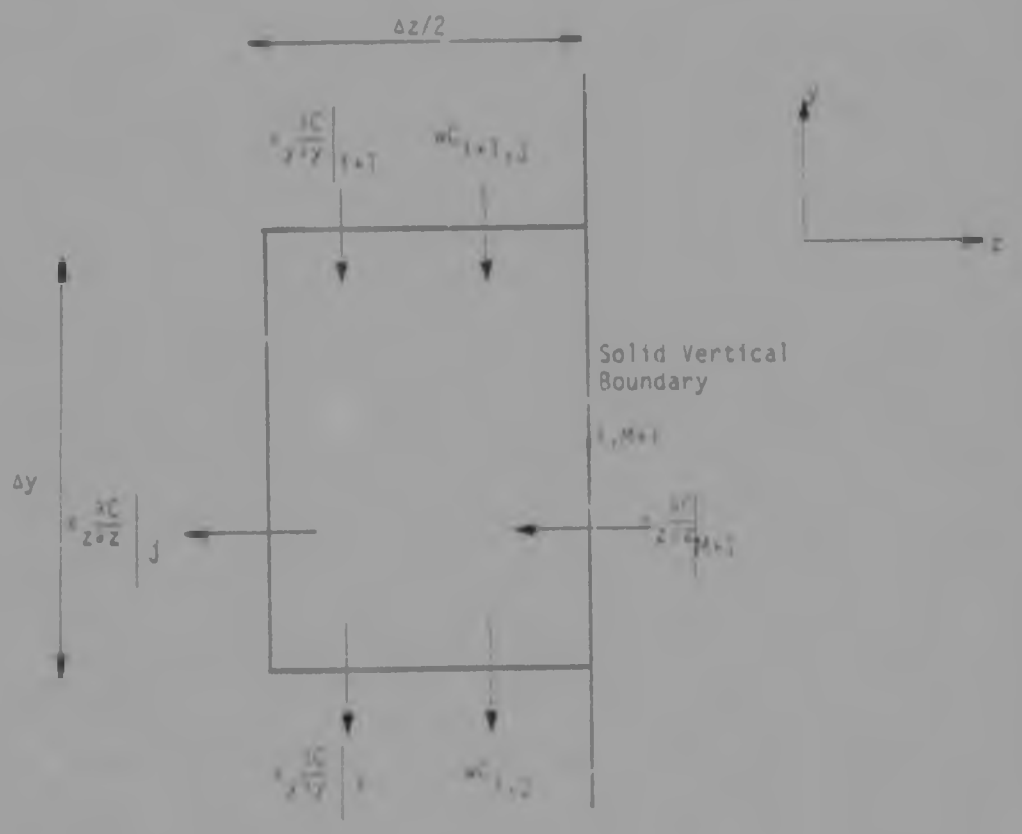


Fig. 3.6 Fluid element for points on solid vertical boundary

In this case the transverse diffusivity is not assumed to decrease to zero at the boundary and therefore the term for the diffusion component of transport across the boundary cannot be assumed to be zero in the mathematical formulation, although it is zero physically. An assumption of zero would imply a zero value for the concentration gradient over the element adjacent to the boundary, effectively preventing any diffusion between the last two grid points. The rate of diffusion is determined by the change in the term $\varepsilon \frac{\partial C}{\partial z}$ between adjacent points. For the finite difference formulation it is assumed that this change over the last grid space is the same as the change over the second last grid space, i.e.

$$\varepsilon_z \frac{\partial C}{\partial z}\Big|_{j=M+1} = \varepsilon_z \frac{\partial C}{\partial z}\Big|_{j=M} + \left[\varepsilon_z \frac{\partial C}{\partial z}\Big|_{j=M} - \varepsilon_z \frac{\partial C}{\partial z}\Big|_{j=M-1}\right] \quad (3.21)$$

By making the same approximations as before the right hand side of equation (3.21) can be expressed in finite difference form. So for j=M+1,

$$\varepsilon_z \frac{\partial C}{\partial z}\Big|_{j=M+1} = 2E_z(j)\frac{C_{i,j}-C_{i,j-1}}{\Delta z} - E_z(j-1)\frac{C_{i,j-1}-C_{i,j-2}}{\Delta z} \quad (3.22)$$

If this substitution is made while applying mass balance to the transport components shown in Fig. 3.6 the following finite difference equation is obtained for points on the solid vertical boundary

$$\left[\frac{E_y(i+1)}{2\Delta y^2} + \frac{w}{2\Delta y}\right]C_{i+1,j} + \left[\frac{E_y(i)}{2\Delta y^2}\right]C_{i-1,j} + \left[-\frac{E_z(j)+E_z(j-1)}{\Delta z^2}\right]C_{i,j-1}$$
$$+ \left[\frac{E_y(i+1)+E_y(i)}{2\Delta y^2} + \frac{E_z(j)}{\Delta z^2} + \frac{w}{2\Delta y}\right]C_{i,j} + \frac{E_z(j-1)}{\Delta z^2}C_{i,j-2} = 0 \quad (3.23)$$

Separate finite difference equations are also required for the grid points at the intersections of the boundaries which are specified in terms of derivatives.

At the intersection of the water surface and solid vertical boundaries the fluid element and trarsport components are as shown in Fig. 3.7

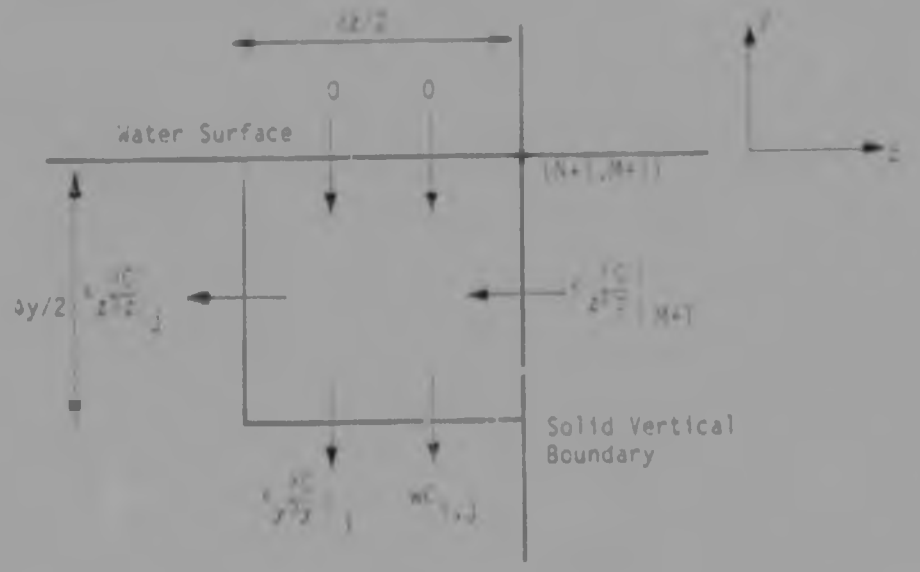


Fig. 3.7 Fluid element at the intersection of the water surface and the solid vertical boundary

The finite difference equation for point (N+1,M+1), obtained by applying mass balance to the transport components shown in Fig. 3.7 is

$$[\frac{E_y(i)}{\Delta y^2}]C_{i-1,j} + [-\frac{E_z(j)+E_z(j-1)}{\Delta z^2}]C_{i,j-1} + [-\frac{E_y(i)}{\Delta y^2} + \frac{w}{\Delta y} - \frac{E_z(j)}{\Delta z^2}]C_{i,j}$$

$$+ \frac{E_z(j-1)}{\Delta z^2} C_{i,j-2} = 0 \qquad (3.24)$$

The fluid element and transport components at the intersection of the plain bed and the solid vertical boundary are shown in Fig. 3.8

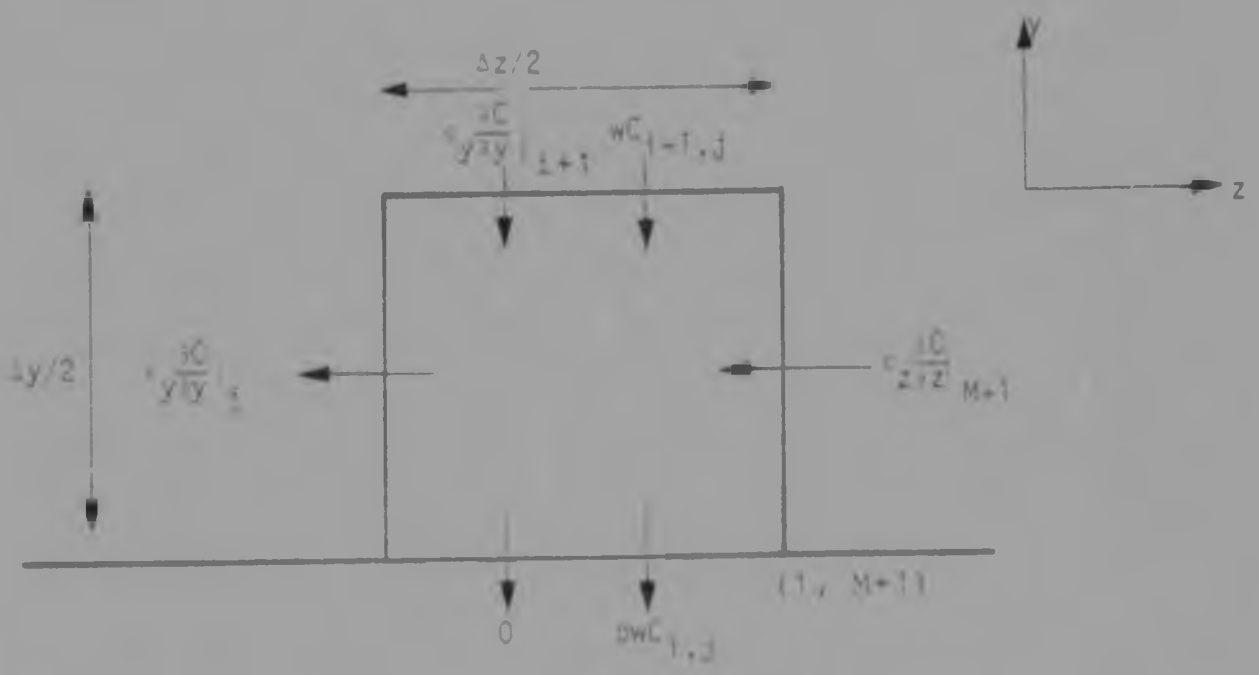


Fig. 3.8 Fluid element at the intersection of the plain bed and the solid vertical boundary

The resulting finite difference equation for point (1,M+1), obtained by mass balance is

$$[\frac{E_y(i+1)}{\Delta y^2} + \frac{w}{\Delta y}]C_{i+1,j} + [-\frac{E_z(j)+E_z(j-1)}{\Delta z^2}]C_{i,j-1} + [-\frac{E_y(i+1)}{\Delta y^2} - \frac{E_z(j)}{\Delta z^2}$$

$$+ \frac{bw}{\Delta y}]C_{i,j} + \frac{E_z(j-1)}{\Delta z^2} C_{i,j-2} = 0 \qquad (3.25)$$

3.4 Numerical Solution

Application of the appropriate finite difference equation to all points in the finite difference grid leads to a system of algebraic simultaneous equations whose solution gives concentration values at all grid points. Many methods have been proposed for solving such a system of equations and these can be divided into two classes, viz. direct and iterative methods.

In direct methods the solution is obtained in a known number of arithmetic operations. These methods are basically solutions by elimination, the best known being the systematic Gaussian elimination method. Direct methods have generally not been favoured because of excessive computer storage requirements. The algorithms for direct solution procedures are often complicated although very efficient techniques have been proposed for cases where the matrix of coefficients has some special property or structure. Direct methods are particularly useful if several sets of equations with the same matrix of coefficients but different right hand sides are to be solved.

Iterative methods involve the repeated application of some algorithm to an initial approximation of the solution. The solution is modified according to some rule at each iterative step until the difference between successive values is within an acceptable tolerance. The algorithms are generally simple and easily programmed and can often be modified to take advantage of particular characteristics of the coefficient matrix and to improve convergence.

The diffusion settling model is likely to be applied to situations which will require a large number of grid points to define the concentration distribution adequately. The number of equations to be solved could

therefore be large and computer storage requirements could be excessive if a direct method of solution is used. Although the matrix of coefficient will be sparse, it will not be symmetric and the more efficient direct techniques cannot be used.

Iterative techniques do not perform calculations on zero coefficients so the storage required for a sparse coefficient matrix is considerably less than for direct methods. An iterative solution method is therefore ideal for solving the diffusion-settling problem and the Successive Over-Relaxation (SOR) or Accelerated Gauss-Seidel Method is used.

For simplification the general finite difference equation for interior points (Equation 3.18) can be written as

$$A_1C_{i+1,j} + A_2C_{i,j+1} + A_3C_{i-1,j} + A_4C_{i,j-1} + A_5C_{i,j} = 0 \qquad (3.26)$$

in which the coefficients A_1 to A_5 are defined by equation (3.18).

Equation (3.26) can be expressed as an equation for the new value of $C_{i,j}$ at a particular iteration in terms of the most recently calculated values of the other concentrations, i.e.

$$C_{i,j}^{n+1} = \frac{1}{A_5}[-A_1C_{i+1,j} - A_2C_{i,j+1} - A_3C_{i-1,j} - A_4C_{i,j-1}] \qquad (3.27)$$

in which all concentrations on the right hand side are the most recently calculated values.

Equation (3.27) can be applied to each grid point recursively until the difference between concentration values at successive iterations is within the acceptable tolerance. This procedure is known as Gauss-Seidel iteration.

Equation (3.27) can also be written so that the

concentration value for each point at a particular iteration is expressed as the value at the previous iteration plus a correction or 'displacement', i.e.

$$C_{i,j}^{n+1} = C_{i,j}^{n} + \{\frac{1}{A_5}[-A_1C_{i+1,j}-A_2C_{i,j+1}-A_3C_{i-1,j}-A_4C_{i,j-1} - A_5C_{i,j}^{n}]\} \qquad (3.28)$$

in which the terms within the large brackets constitute the displacement. Concentrations on the right hand side are again the most recently calculated values.

If successive displacements all have the same sign, which is generally the case for elliptic problems, convergence can be accelerated by using a displacement value which is larger than indicated by equation (3.28). To effect this the displacement value from equation (3.28) is multiplied by an accelerator, ω, which normally lies in the range $1 \leq \omega < 2$.

The new concentration value is then

$$C_{i,j}^{n+1} = C_{i,j}^{n} + \omega\frac{1}{A_5}[-A_1C_{i+1,j}-A_2C_{i,j-1}-A_3C_{i-1,j}-A_4C_{i,j-1} - A_5C_{i,j}^{n}]) \qquad (3.29)$$

or

$$C_{i,j}^{n+1} = \frac{\omega}{A_5}[-A_1C_{i+1,j}-A_2C_{i,j+1}-A_3C_{i-1,j}-A_4C_{i,j-1}] - (\omega-1)C_{i,j}^{n} \qquad (3.30)$$

The use of the accelerator as described above is known as Successive Over-Relaxation (SOR), which reduces to Gauss-Seidel iteration for $\omega = 1$.

Equation (3.30) is the SOR equation for interior points. For points on the boundaries some coefficients on the right hand side will be zero or have values as defined by the relevant finite difference equation.

The [illegible] of the SOR method deperds on [illegible] the accelerator . Computation [illegible] significantly if it is chosen [illegible] convergence is inversely [illegible] magnitude of the spectral radius [illegible] of the iteration matrix, and [illegible] value will therefore be that [illegible] spectral radius. For certain [illegible] type a formula has been developed [illegible] accelerator in terms of the spectral [illegible] limited usefulness, however, because [illegible] spectral radius is not simple.

[illegible] computing the optimum accelerator in [illegible] displacement at each iteration has [illegible] Habetler and Asaacs 1977 [illegible] the maximum [illegible] iteration k is

$$[illegible]^{k-1}_{i,j} - C^{*}_{i,j} \quad \text{for all } i \text{ and } j \qquad (3.31$$

[illegible] procedure begins with an accelerator [illegible] continues with this value until it is [illegible] decreasing monotonically from [illegible] max. Thereafter the optimum acceler- [illegible] updated at each cycle by

(3.32)

(3.33)

[illegible] variable in acceler- [illegible] maximize the rate of [illegible] convergent system. There is, [illegible] system will converge at [illegible] satisfied.

A necessary and sufficient condition for the convergence of iterative solutions for elliptic partial differential equations is that the spectral radius of the iteration matrix (G) be less than unity, i.e.

$$\rho(G) < 1,0 \qquad (3.34)$$

According to Gershgorin's first theorem, the largest of the moduli of the eigenvalues of a square matrix cannot exceed the largest sum of the moduli of the elements along any row or column of the matrix. Therefore a sufficient condition for convergence can be established, namely that the infinity norm (or largest sum of moduli) of the iteration matrix must be less than unity, i.e.

$$||G|| < 1,0 \qquad (3.35)$$

Examination of the iteration equations for the SOR solution of the diffusion-settling model shows that this sufficient condition will never be met. If the probability of deposition is 1,0 the norm will be exactly unity and for any smaller probability of deposition the norm will exceed unity. Therefore the more stringent condition that the spectral radius be less than unity must be applied.

The spectral radius cannot be determined explicitly from the input for a particular case. It can be calculated by an iterative procedure once the iteration matrix has been set up. Because of the computational effort required to calculate the spectral radius it is not worthwhile checking each problem for convergence. If divergence occurs it will be apparent from the results. In such a case the finite difference grid parameters can be changed in order to satisfy the convergence condition. This would have to be done by trial as it is not possible to express the convergence criterion explicitly in terms of grid spacings. Slow convergence tends to be associated with large hydraulic

gradients and flow depths and smal particle fall velocities and deposition probabilities

4. TRANSFER COMPONENTS

4.1 Introduction

The distribution of suspended sediment in two directions across a section normal to the direction of flow depends on the magnitude and variation of the turbulent diffusivities in the vertical and transverse directions. This chapter describes the theory used to estimate values for the diffusivities and convection components for sediment particles. Diffusivities depend on the turbulence characteristics of the flow as expressed by the shear velocity; estimation of shear velocity is therefore also explained. Calculation of turbulent diffusivities also requires estimates of the average flow velocities in the channel and over the plain. Different approaches for making this estimate are reviewed and the adopted procedure is explained.

4.2 Turbulent Diffusivities for Sediments

It is usually assumed that the transfer of sediment particles by diffusion is similar to that of fluid particles and momentum. Most generally accepted models for computing discharge rates of suspended sediments are based on a vertical distribution of sediment concentration which depends on this assumption.

The equivalence of diffusivity for sediment particles and fluid mass is generally accepted for particles with fall velocities in the Stokes range. Sand and gold particles do not fall in this range and for such particles it is normally assumed that

$$\varepsilon_s = \beta \varepsilon_m \qquad (4.1)$$

in which ε_s is the diffusivity for sediment, ε_m is the diffusivity for momentum and β is a constant. According

to the Reynolds analogy for the equivalence of mass and momentum transfer the diffusivity for mass is, for practical purposes, identical to the diffusivity for linear momentum.

Estimation of ε_s for a particular flow situation therefore requires evaluation firstly of the process of momentum transfer and secondly of the relationship between momentum transfer and solid particle transfer.

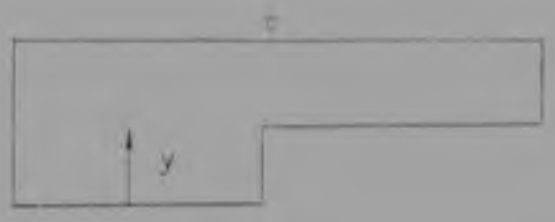
Linear momentum can be transferred from one region in the flow to another by several physical mechanisms. In increasing order of effectiveness these mechanisms are: molecular motion and intermolecular forces, eddies generated by flow along solid boundaries,eddies generated in mixing zones between regions of different velocity, and secondary currents. The aggregate effect of these mechanisms is reflected in the value of effective diffusivity. In turbulent flow situations the molecular scale mechanisms are negligible compared with the others and can be ignored.

In channels of simple cross section the dominant mechanism for vertical momentum transfer is by eddies generated by flow over the bed. Transverse momentum transfer is the result of a combination of eddies generated by boundaries and secondary currents, usually with secondary current effects dominating. In compound section channels a strong interaction exists between deep and shallow flows which have different velocities and hence different values of momentum. This interaction takes the form of a bank of eddies with vertical axes which develop along the interface between the regions of different flow depth. These eddies transfer longitudinal momentum from the deep region to the shallow region, decreasing velocity and boundary shear in the deep region and increasing them in the shallow. The presence of the eddies has been demonstrated

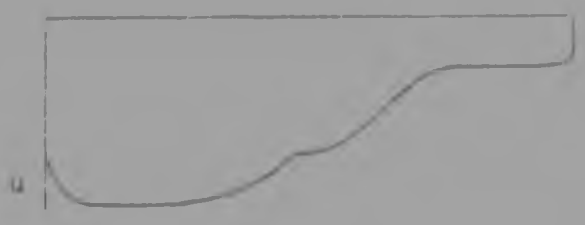
photographically by Sellin (1964) and the effects of the momentum transfer have been evaluated for various conditions. Wright and Carstens (1970) measured velocity and shear stress distributions in a compound air duct. Townsend (1968) used photographic techniques to determine the turbulent characteristics in the interaction zone of a compound channel. Myers and Elsawy (1975) measured shear stress distributions in a compound channel and Myers (1978) extended this study to evaluate apparent shear stress on vertical sections within the flow. Rajaratnam and Ahmadi (1979 and 1981) measured shear stress and velocity distributions for a compound channel and proposed generalized relationships to describe these distributions. The general forms of velocity and bed shear distributions are shown in Figure 4.1.

The effective transverse diffusivity must obviously be increased by the lateral transfer of momentum across the interface. The vertical diffusivity will also be affected because it is related to the boundary shear stress which is affected by the momentum transfer. The interaction will affect flow conditions only within a certain distance of the interface and therefore the diffusivities must be determined for both the interaction zone and the regions of undisturbed flow.

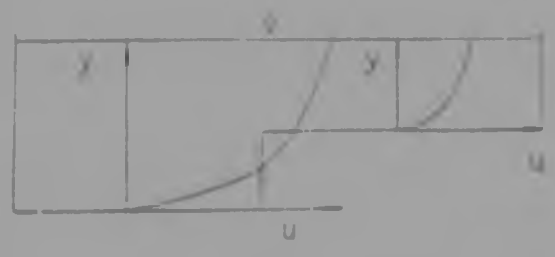
Once the magnitudes and variations of the vertical and transverse diffusivities for momentum have been determined they can be used to estimate the diffusivities for sediment if the Reynolds analogy applies and the relationship between mass and sediment transfer is known. Many researchers have attempted to evaluate β in equation (4.1). Most experiments have been conducted in conditions where turbulence is composed of rectilinear velocity fluctuations. Under these conditions it is generally concluded that $\beta < 1,0$ because the inertia of sediment particles prevents them from responding fully



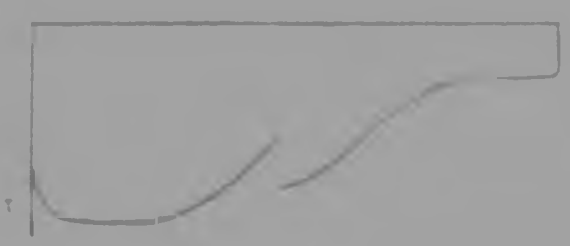
a. Channel section



b. Transverse velocity profile



c. Vertical velocity profile



d. Bed shear profile

Fig. 4.1 Velocity and bed shear profiles for compound section.

to the velocity fluctuations. Very different results have been obtained in conditions where turbulence consists of eddies with a strong element of vorticity. In such cases sediment particles would be thrown outwards by the centrifugal force resulting from eddy motion, which would be greater than on fluid particles. Singamsetti (1966) examined the diffusion of sediment in a submerged jet where the turbulence has strong vorticity and concluded that $\beta > 1{,}0$. Jobson and Sayre (1970) reconciled these apparent contradictions by dividing the diffusivity for sediment into two components,

$$\varepsilon_s = \varepsilon_c + \varepsilon_t \qquad (4.2)$$

in which ε_c is the component which describes the transfer due to curvature of fluid path lines and ε_t describes the transfer due to tangential components of the turbulent velocity fluctuations.

The tangential component ε_t, is similar to ε_m and therefore equation (4.1) should be valid when ε_t is much greater than ε_c. In such cases $\beta < 1{,}0$. When flow conditions are such that eddies are large compared with particle size the radial component ε_c will be significant. This component cannot be related to ε_m because ε_c would be zero for fluid particles.

The diffusivity of linear momentum in the vertical direction depends on the intensity of turbulence and therefore varies with distance above the stream bed. A distribution of vertical diffusivity based on considerations of shear stress and velocity is in general use for computing sediment concentration profiles. This distribution assumes a linear variation of shear stress with depth, i.e.

$$-\frac{\tau_y}{\rho} = \frac{D-y}{D} \qquad (4.3)$$

in which τ_y is the shear stress at depth y, τ_0 is the shear stress at the bed and D is the total flow depth.

From Prandtl's mixing length theory

$$\frac{du}{dy} = \frac{\sqrt{\tau_0/\rho}}{\kappa y} = \frac{u_*}{\kappa y} \qquad (4.4)$$

in which u is the velocity in the flow direction, ρ is the fluid density, κ is Karman's constant and u_* is the shear velocity.

According to the Reynolds analogy the diffusivities of mass and momentum are identical and the shear stress in turbulent flow can be expressed as

$$\tau_y = \rho \epsilon_m \frac{du}{dy} \qquad (4.5)$$

From equations (4.3), (4.4) and (4.5) the distribution of diffusivity for mass can be written as

$$\epsilon_m = \kappa u_* \frac{y}{D}(D-y) \qquad (4.6)$$

If $\beta = 1$ in equation (4.1) this equation also describes the distribution of diffusivity for sediment, ϵ_s.

Equation (4.6) can be used to determine the diffusivity at any depth in the flow. The Karman constant κ has a value of 0,4 for clear water but tends to be reduced by heavy suspended loads. The shear velocity u_* can be calculated from the bed shear stress with the equation.

$$u_* = \sqrt{\frac{\tau_0}{\rho}} \qquad (4.7)$$

For wide channels and no bed forms the bed shear stress is given by

$$\tau_0 = \gamma RS = \gamma DS \qquad (4.8)$$

in which R is the hydraulic radius.

Equation (4.8) does not apply within the interaction zone between regions of different flow depths because the transfer of momentum increases the bed shear stress

in the shallow region. It can therefore be expected that the vertical diffusivity will vary in the transverse direction as well as the vertical.

Rajaratnam and Ahmadi (1981) have found that the distribution of velocity in a vertical section is logarithmic at all points in the interaction zone if the local value of u_* is used. Equation (4.4) is therefore applicable in the interaction zone and the vertical distribution of diffusivity can still be described by equation (4.6), using the local value of u_*. Local values of bed shear stress are therefore required. Rajaratnam and Ahmadi (1981) measured bed shear stresses in a channel-flood plain model and developed some general relationships to describe the variation of bed shear stress in the interaction zone. The local bed shear stress is given by

$$\tau_b' = \tau_{b\infty} \left(\tau_b'_m - \tau_{b\infty} \right) e^{-0,693(z'/b_\tau)^2} \qquad (4.9)$$

where $\tau_{b\infty}$ is the undisturbed bed shear stress on the plain and z' is the distance over the plain measured from the interface. τ_b' is the bed shear stress at the interface and is given by

$$\tau_b'_m = \tau_{b\infty}(1+0,24(D_c/D_p - 1)) \qquad (4.10)$$

in which D_c is the flow depth in the channel and D_p is the flow depth on the plain. b_τ is a length scale given by

$$b_\tau = 0,64\, D_p (D_c/D_p - 1) \qquad (4.11)$$

The incremental term in equation (4.9) becomes negligible for large values of z'/b_τ. To avoid computational problems it is assumed that $\tau_b' = \tau_{b\infty}$ if z'/b_τ exceeds 3,0.

Equations (4.6) to (4.11) can be used to describe completely the vertical and transverse distribution of vertical diffusivity over the shallow flow region.

The transverse diffusivity for momentum depends on flow conditions and various attempts have been made to relate the diffusivity to variables describing the flow conditions. Miller and Richardson (1974) found that for straight rectangular channels

$$\epsilon_z = 0,23Ru_* \qquad (4.12)$$

in which ϵ_z is the average transverse diffusivity, R is the hydraulic radius and u_* is the shear velocity. Other tests for rectangular channels have yielded similar relationships but in natural streams with bends and meanders the factor 0,23 is increased significantly.

Several researchers have demonstrated the important effects of friction factor and secondary circulation. Lau and Krishnappan (1977) consider the dominant mechanism in transverse spreading to be secondary circulation, which is governed by width to depth ratio. They performed experiments in a rectangular flume with different widths and roughnesses and produced relationships between friction factor (f), width to depth ratio (W/D) and $\epsilon_z/u_* W$ or $\epsilon_z/u_* W$. The variation with W/D is very much more significant than with f and the following relationship has been derived from their data

$$\frac{\epsilon_z}{u_* W} = 0,001(32,77-8,03 \ln(W/D)) \qquad (4.13)$$

This relationship was developed for rectangular channels and therefore does not apply directly to the situation where the vertical boundaries are replaced by zones of interaction with deeper flows. Secondary circulation can be expected to develop between the interaction zones, however, and equation (4.13) should give a reasonable estimate of ϵ_z if the distance between the interaction zones is used as the width. The extent of the interaction can be inferred from the distributions of velocity and shear stress over the shallow flow region. Rajaratnam and Ahmadi (1981) described the distribution of bed shear

stress by equation (4.9) which also describes the distribution of velocity in the flow direction, i.e.

$$u = u_\infty + (u'-u_\infty)e^{-0,693(z'/b_f)^2} \qquad (4.14)$$

where u is the velocity at distance z' from the interface, u' is the velocity at the interface and u_∞ is the undisturbed velocity. The length scale b_f is identical to b_t, given by equation (4.11). Equations (4.9) and (4.14) show that at a distance of $2b_f$ from the interface the excess of both shear stress and velocity over the undisturbed value is about 5% of the excess at the interface. This distance is assumed to define the extent of the interaction zone.

The transverse diffusivity in the undisturbed region is therefore calculated by equation (4.13), using for W the distance between adjacent regions of deep flow less the extent of the interaction zone on each side, which is calculated as twice the length scale given by equation (4.11). It is, in fact, unnecessary to determine W with great accuracy as the transverse diffusivity tends to become constant as W/D increases, and large values are likely to be used in application of the model.Equation (4.13) is not very accurate for values of W/D less than about 10 where ε_z appears to be very sensitive to W/D. It is further assumed for the undisturbed region that $\beta = 1,0$ in equation (4.1).

Transverse diffusivity within the interaction zone is considerably enhanced by the increased eddy turbulence. Rajaratnam and Ahmadi (1981) have proposed the following distribution of eddy kinematic viscosity or diffusivity for momentum within the interaction zone

$$\frac{\varepsilon_z}{(u_m-u_*)D_p} = \frac{0,145(D_z/D_p-1)^2}{(u_m-u_*)/u_*} \qquad (4.15)$$

... shear velocity, U_* is ... and the function $A(n_\tau)$ ... shown in Fig ...

Equation 4.15 was developed from data obtained for a single flood plain width and consequently does not allow for the effect of width to depth ratio at the limit of the interaction zone. For this reason it is specified that the value of transverse diffusivity derived from the distribution of eddy kinematic viscosity given by equation (4.15) must not decrease below the value determined for the undisturbed region (equation (4.13)).

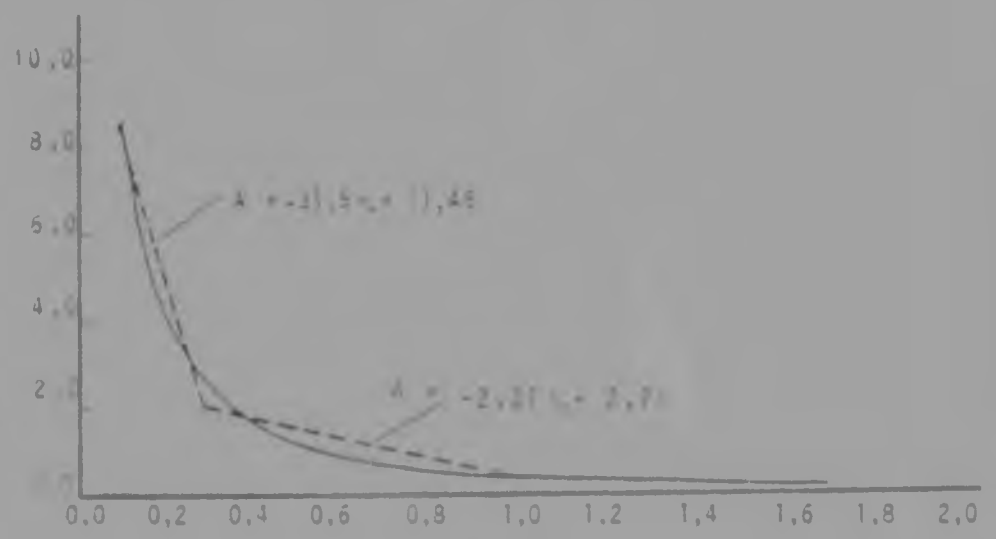


Fig 4.2 Function for evaluating transverse diffusivity in the interaction zone (Rajaratnam and Ahmadi (1981))

In Fig 4.2 A is not defined for very small values of n_τ. An upper limit was determined by studying the results of Townsend (1968). Using photographic techniques, Townsend measured the distribution of the root mean square of turbulent fluctuations of transverse velocity, $\sqrt{v^2}$. His distribution shows that the value of $\sqrt{v^2}$ at the interface is about 1,7 times the value in the undisturbed region. The transverse diffusivity for momentum is related to

$$\varepsilon_z = \ell^2 \left| \frac{\partial u}{\partial z} \right| \qquad (4.16)$$

where ℓ is Prandtl's mixing length. In the interaction zone ℓ will be of the same order of magnitude as the flow depth. In the undisturbed region ℓ is given by

$$\ell = \kappa y \qquad (4.17)$$

where κ is Karman's constant (0,4 for clear water) and y is the height above the bed. A representative value of y in the undisturbed region is half the flow depth. Applying equation (4.17) and the aforementioned assumption for ℓ to Townsend's results indicates that the eddy kinematic viscosity at the interface will be about 20 times that in the undisturbed region. Applying this relationship to equation (4.15) and assuming that the undisturbed region begins at approximately $\eta_r = 1,0$ suggests a maximum value for A of about 9,0, which is very close to the value given in fig. 4.1 for $\eta_r = 0,1$.

Equation (4.15) is therefore used to estimate the eddy kinematic viscosity in the interaction zone subject to an upper limit for A of 9,0. For computational purposes the distribution of A is approximated by the straight lines shown on fig. 4.1, i.e.

$$\begin{aligned} A &= -31,5\eta_r + 11,45 \quad \text{for } \eta_r \leq 0,3 \\ A &= -2,37\eta_r + 2,71 \quad \text{for } \eta_r > 0,3 \end{aligned} \qquad (4.18)$$

and $A \leq 9,0$

Also, when determining transverse diffusivity the minimum value is as calculated by equation (4.13).

In the interaction zone the turbulence will have strong vorticity and the ε_z component in equation (4.2) will be large. Singamsetti (1966) conducted experiments to study the diffusion of sediment in a submerged jet. Although the interaction zone between free surface flows with different depths is different from a submerged jet because of the significant effect of bed shear, the

transfer mechanism will be similar because of the generation of large-scale vortices in both cases. Singamsetti's conclusions should therefore be valid, at least as a first approximation. He maintains that in turbulence with circulatory motion the ratio of the diffusivities of fluid mass to momentum is not 1,0 but about 1,2. The ratio of diffusivities of sediment to fluid mass will be 1,0 in the Stokes range and will increase for larger particles. The constant β in equation (4.1) is the product of these two ratios and will therefore have a minimum value of 1,2 in the Stokes range and will also increase for larger particles. The variation of β with particle Reynolds number (in terms of fall velocity) is shown in fig. 4.3. For computation purposes the variation is approximated by the straight lines shown on fig. 4.3, i.e.

$$\begin{aligned} \beta &= 1,22 \text{ for } R_e < 5,0 \\ \beta &= 1,01 + 0,125 \ln R_e \text{ for } R_e \geq 5,0 \end{aligned} \qquad (4.19)$$

and $\beta > 1,5$

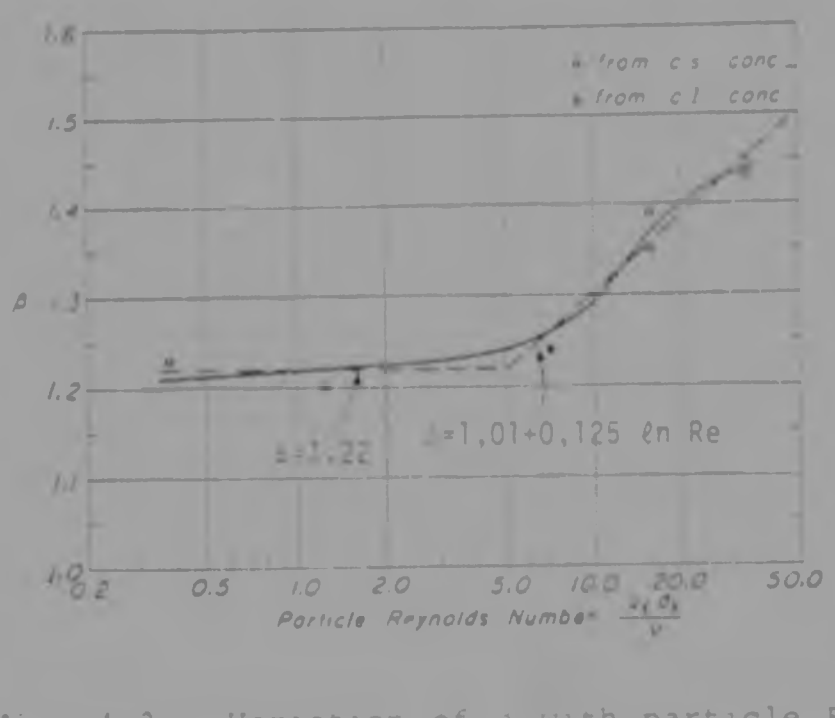


Fig. 4.3 Variation of β with particle Reynolds number for interaction zone (Singamsetti (1966))

The effect of β on the diffusivity for sediment is obviously much less than the variation across the interaction zone. It is worth considering β, however, because it describes the difference in behaviour of particles with different characteristics.

The transverse diffusivity for sediment within the interaction zone is therefore based on the distribution of eddy kinematic viscosity proposed by Rajaratnam and Ahmadi (1981), equation (4.15). The value at the interface is assumed to be approximately the same as at 0,1 δ, over the plain. The constant β in equation (4.1) is determined from the results of Singamsetti (1966).

No results are available regarding variations of ε_z in the vertical direction. Such variations are unlikely to be as significant as for vertical diffusivity and a uniform distribution has been assumed.

4.3 Shear Velocity

Both vertical and transverse diffusivities are related to the turbulence characteristics of the flow which depend on the hydraulic resistance of the bounding surfaces. The relationships are expressed in terms of the shear velocity which is a representation of boundary shear in velocity dimensions.

Hydraulic resistance in a natural channel results from the effect of two different roughness elements of different magnitudes. Firstly there is a component of resistance resulting from skin friction caused by the roughness of sediment grains on the surface of the bed. Secondly there is a form resistance component associated with bedforms; separation occurs immediately downstream of bedforms and a significant amount of energy is dissipated through turbulence in the separation zones.

The total shear stress associated with the bed can therefore be divided into two components,

$$\tau_o = \tau' + \tau'' \qquad (4.20)$$

in which τ' represents the skin friction component and τ'' the form resistance component. In the absence of bed forms the total boundary shear stress results from skin friction only. Form resistance is significant when bedforms are present and depends on the nature of the bedforms. Fig. (4.4) illustrates qualitatively the contributions of the two components in the lower and upper flow regions.

The movement and entrainment of sediment on the bed is obviously related to τ' only. The velocity profile and other flow characteristics outside the separation zones are also determined only by skin friction effects. If bedforms are present, therefore, bed concentrations and turbulent diffusivities should be calculated in terms of τ' rather than τ_o.

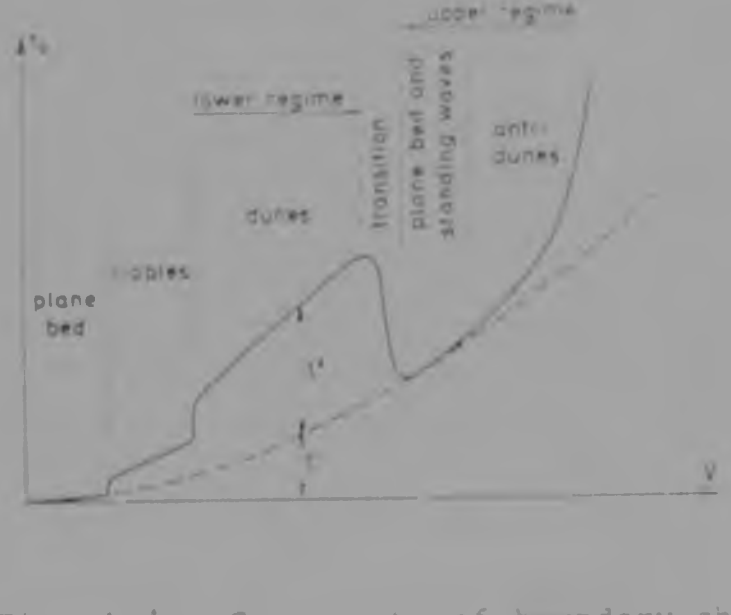


Fig. 4.4 Components of boundary shear stress (Engelund and Hansen (1967))

The total shear stress associated with the bed can therefore be divided into two components,

$$\tau_b = \tau' + \tau'' \qquad (4.20)$$

in which τ' represents the skin friction component and τ'' the form resistance component. In the absence of bed forms the total boundary shear stress results from skin friction only. Form resistance is significant when bedforms are present and depends on the nature of the bedforms. Fig. (4.4) illustrates qualitatively the contributions of the two components in the lower and upper flow regions.

The movement and entrainment of sediment on the bed is obviously related to τ' only. The velocity profile and other flow characteristics outside the separation zones are also determined only by skin friction effects. If bedforms are present, therefore, bed concentrations and turbulent diffusivities should be calculated in terms of τ' rather than τ_b.

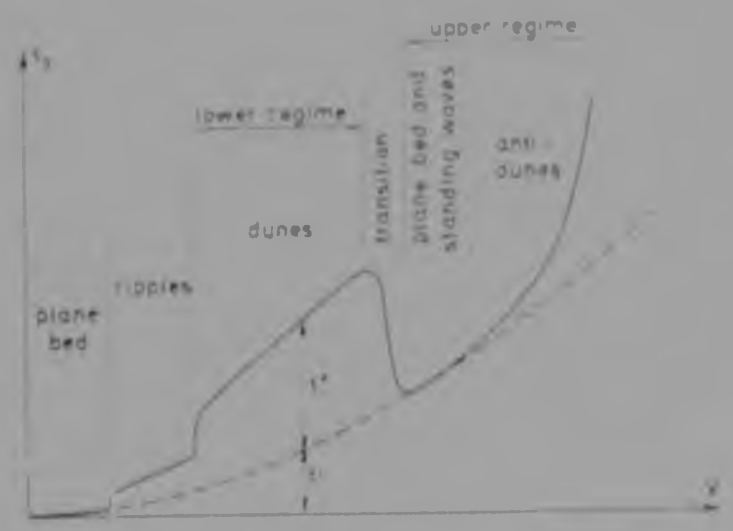


Fig. 4.4 Components of boundary shear stress (Engelund and Hansen (1967))

The two components of the total boundary shear stress can be evaluated by dividing either the hydraulic radius or the energy gradient into components associated with skin friction and form resistance. For no bedforms the boundary shear stress is given by

$$\tau_0 = \gamma RS \qquad (4.8)$$

and when bedforms exist by

$$\tau_0 = \gamma(R'+R'')S \qquad (4.21)$$

$$\text{or } \tau_0 = \gamma R(S'+S'') \qquad (4.22)$$

in which the superscript ' denotes the skin friction component and the superscript '' the form resistance component. Both methods of subdivision have been assumed by different researchers. Einstein (1950) assumed the hydraulic radius to be divided, in which case the appropriate shear stress is

$$\tau' = \gamma R'S \qquad (4.23)$$

and the appropriate shear velocity is

$$u_*' = \sqrt{\tau'/\rho} = \sqrt{gR'S} \qquad (4.24)$$

Einstein proposed an equation for the average velocity (V) in terms of the modified shear velocity

$$\frac{V}{u_*'} = 5{,}75 \log_{10}(12{,}27\frac{R'}{k}) \qquad (4.25)$$

in which k is the grain roughness assumed to be 2,5 times the representative size of bed particles. Equation (4.24) can also be expressed as

$$\frac{V}{\sqrt{gR'S}} = 6{,}25 + 2{,}5\ell n \frac{R'}{k} \qquad (4.26)$$

If the average velocity is known, equation (4.26) can be solved iteratively for R' which can then be used in equation (4.24) to calculate u_*'.

In the transverse distribution model this estimate of u_*' replaces u_* in all the relationships for diffusivity in order to account for the possible presence of bedforms.

4.4 Transverse Convection

The transverse convection component in the transfer equation arises from the flow over the plain being not parallel to the flow in the channel. Convection caused by secondary circulation is assumed to be accounted for in the transverse diffusivity. The flow velocity components parallel to the channel V_c, normal to the channel V_n, and in the direction parallel to the steepest plain gradient V_p, are related by the deviation of the channel direction from the direction of the steepest plain gradient, δ.

These velocity components and their associated gradients (S_c, S_p and S_n) are defined in Fig. 4.5.

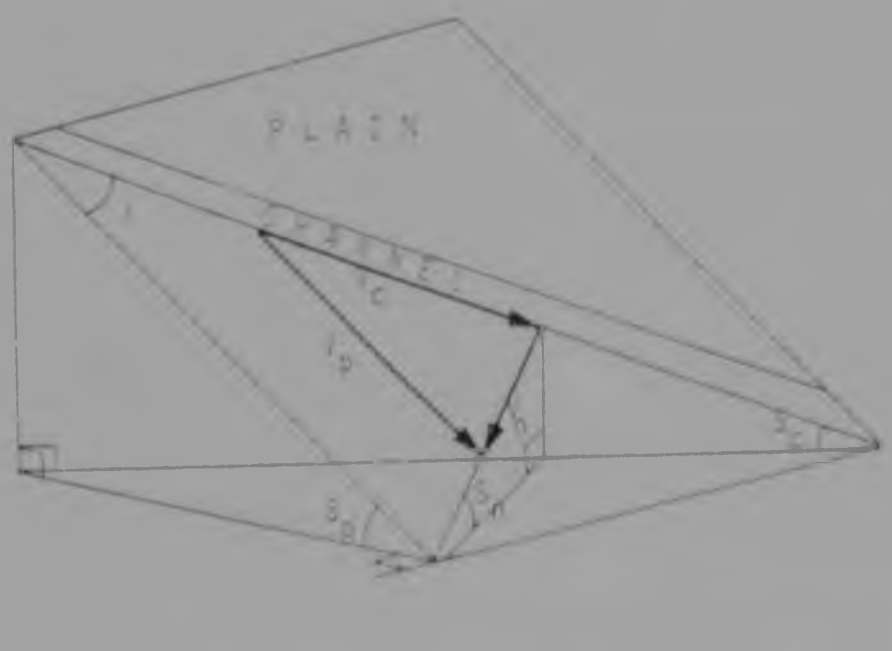


Fig. 4.5 Relative flow directions over plain

From the geometry of Fig. 4.5 the following relationships between the different gradients can be derived.

$$\sin S_c = \sin S_p \cos \delta \tag{4.27}$$

$$\sin S_n = \sin S_c \tan \delta \tag{4.28}$$

It is assumed that the flow velocity in any direction is proportional to the square root of the gradient in that direction. The flow velocity parallel to the plain direction can therefore be calculated from the velocity component parallel to the channel from equation (4.29)

$$V_p = V_c \sqrt{S_p/S_c} \tag{4.29}$$

and the velocity component normal to the channel from equation (4.30)

$$V_n = V_c \sqrt{S_n/S_c} \tag{4.30}$$

These velocities represent the flow velocities of water in the relevant directions. The velocity of suspended sediment particles is always less than the water velocity by an amount which depends on the flow turbulence characteristics and the sediment particle characteristics. Sumer (1974) developed an analytical relationship between water and particle (average) velocities for free surface flow over a smooth boundary. This relationship (Fig. 4.6) is used to approximate the average velocity of sediment particles parallel to V_c.

In Fig. 4.6 μ and μ_s are dimensionless forms of average velocities of water and sediment, defined by

$$\mu = U\, h/D \tag{4.31}$$

$$\mu_s = U_s\, h/D \tag{4.32}$$

in which U is the average water velocity, U_s the average particle velocity, h is the flow depth and D is the average diffusivity in the flow direction, given by

$$D = 1/6\, \kappa h u_* \tag{4.33}$$

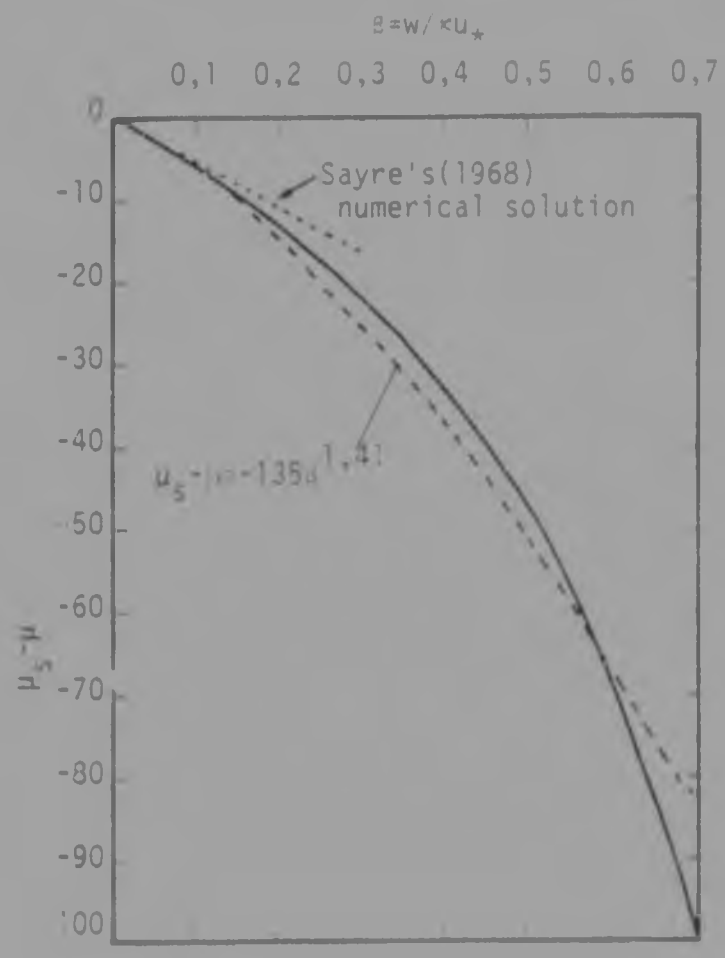


Fig. 4.6 Mean velocity of heavy particles relative to the mean flow velocity vs. the fall velocity parameter $\beta = w/\kappa u_*$ (Sumer, 1974)

For computation purposes the relationship described by Fig. 4.8 has been approximated by the power curve

$$u_s - u = -135\,\beta^{1,41} \tag{4.34}$$

Using this relationship the velocity of sediment particles in the direction of V_s can be calculated. The required convective component, u, is the component of this particle velocity normal to the channel. This can be calculated by assuming that sediment velocities are also proportional to the square root of the gradient, i.e.

$$u = U_s \sqrt{S_n/S_p} \tag{4.35}$$

This average particle velocity is assumed to apply at all depths.

The transverse velocity component will also affect the vertical distribution of sediment within the channel, tending to increase concentrations on one side and decrease concentrations on the other side. This effect is not accounted for but should be borne in mind when interpreting results.

The above description of the transverse convection component is very simplified and assumes that flow within the channel is unaffected by the transverse gradient of the plain. This is obviously not true but should be a reasonable approximation for small deviations of the channel direction from the steepest plain gradient.

If channels are not straight the transverse distribution of sediment cannot be described by a two-dimensional model. Application of the model should be restricted to cases where channels can be considered to be straight for a distance which is long relative to the distance particles can travel before depositing.

4.5 Calculation of Flow Velocities

The transfer of linear momentum between flow in a channel and flow over an adjacent plain as discussed in section 4.2 is the direct result of the difference in flow velocities between the two sections. In the transverse sediment distribution model the distributions of shear stress and hence vertical diffusivity over the plain are described by empirical relationships involving the ratio of flow depths and therefore, implicitly, the difference in flow velocities. The distribution of transverse diffusivity is calculated directly from the difference in flow velocities as well as the ratio of flow depths. Flow velocities are also required in the calculation of shear velocity for both channel and plain. It is therefore necessary to calculate average flow velocities for the

channel and plain sections.

The average flow velocity (V) in a channel of regular cross-sectional shape can be calculated using a uniform flow resistance equation such as the Manning equation,

$$V = \frac{1}{n} R^{2/3} S^{\frac{1}{2}} \qquad (4.36)$$

in which n is a roughness coefficient, R is the hydraulic radius given by the ratio of area to wetted perimeter and S is the energy gradient which is equal to the physical gradient for uniform flow.

Application of the Manning and other resistance equations to the different sections of a compound channel is not straightforward because the hydraulic radius is difficult to define correctly. The interaction between the deep and shallow flow sections gives rise to longitudinal shear stresses (known as apparent shear stresses) on the interface separating them. These shear stresses constitute an increase in the boundary shear resistance for the channel flow and an effective decrease in boundary shear resistance for flow on the plain.

Sellin (1964) demonstrated the effect of the flow interaction by comparing the discharge in a compound channel with the sum of the discharges in channel and plain when separated by thin dividing walls. He found that the sum of the separate discharges was up to 30% greater than the compound channel discharge for a plain depth of 0,16 times the bankfull channel depth.

If a resistance equation is used to calculate the flow velocities the hydraulic radius must account for the apparent shear stresses. This can be done either by evaluating the shear on the interface or by locating an interface on which the apparent shear stress is zero.

Various methods have been proposed for accounting for the apparent shear losses by making different assumptions regarding the position and nature of the channel-plain interface. Different assumptions have been made and tested experimentally by various researchers. Posey (1967) considered a rectangular channel with inward sloping plains. He obtained good agreement between measured and calculated discharges by assuming a vertical interface extending from the channel sidewalls. For plain depths greater than 0,4 times the bankfull channel depth the resistance of the interfaces was ignored, i.e. the interfaces were assumed to be planes of zero shear. For plain depths less than 0,4 times the bankfull channel depth the interface was assumed to have the same roughness as the channel boundaries for channel flow calculations, thereby reducing the discharge, and ignored for plain flow calculations. Using horizontal flood plains Zheleznyakov (1971) found that Posey's method for shallow plain flow depths slightly underestimates plain discharges but significantly over-estimates channel discharges. Deutler Poebes and Udeozo (1977) proposed separating flow regions by a horizontal interface across the channel at bankfull level.

Wright and Carstens (1970) considered horizontal flood plains and analysed flow with flood plain depths equal to and times the bankfull channel depth and larger. They used vertical interfaces and recommended applying an effective shear stress on the interfaces equal to the mean shear stress in the channel. This effective shear stress resists flow in the channel and propels flow on the plains.

Yen and Overton (1973) proposed that planes of zero shear stress exist, extending from the plain-channel junction towards the centre of the main channel at an angle to the vertical which varies with stage, roughness and other geometrical factors. If such planes are located and used

to define the flow areas, when apparent shear stresses can be ignored.

None of the approaches described gives satisfactory results over a range of discharges. Wormleaton, Allen and Hadjipanos (1982) performed a series of experiments to evaluate the different approaches and establish criteria for selecting the best approach for particular conditions. They investigated the interfaces shown in Fig. 4.7 and considered four different plain roughnesses.

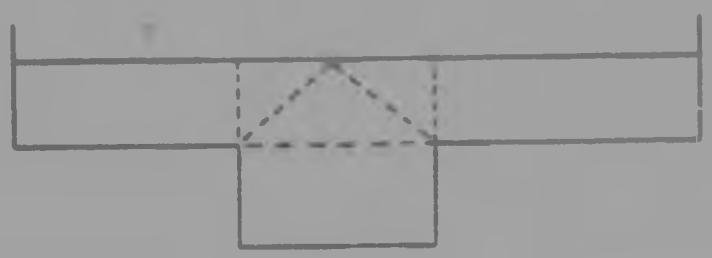


Fig. 4.7 Compound channel section showing alternative interface planes.

The accuracies of various methods of discharge calculation were related to the ratio of apparent shear stress on the assumed interface to the average main channel shear stress. This ratio was proposed as a criterion for selecting the best method for a given flow condition. It was found that the diagonal and horizontal interfaces gave better overall results than the vertical and the value of the apparent shear stress ratio could be used to indicate whether the interface should be included in the main channel wetted perimeter or not. No intermediate values of apparent shear stress were considered for discharge calculations; the interface was assumed either to offer the same resistance as the average for the rest of the channel perimeter or no resistance at all.

There is no clear superiority of either the diagonal or

the horizontal subdivisions and the former has been adopted for use in the transverse distribution model. In accordance with the results of Wormleaton, Allen and Hadjipanos the interface is included in the main channel wetted perimeter for values of the apparent shear stress ratio below 0,5 and excluded for all values above 0,5. The interface is always excluded from the plain's wetted perimeter because generally wide plains will be considered and the propelling effect of the interface would be small.

The apparent shear stress ratio is calculated from the apparent shear stress on the diagonal interface and the average shear stress on the channel boundary. These shear stresses can be determined by considering the equilibrium of all forces acting on an element of water in the channel.

In the transverse distribution model the main channel is assumed to have a trapezoidal section with a bottom width equal to half the width at bankfull level. This shape is more realistic than the rectangular section used by Wormleaton, Allen and Hadjipanos. It is assumed that their apparent shear stress ratio criterion applies to the trapezoidal section without significant error. The assumed crosssection and interface planes are shown in Fig. 4.8.

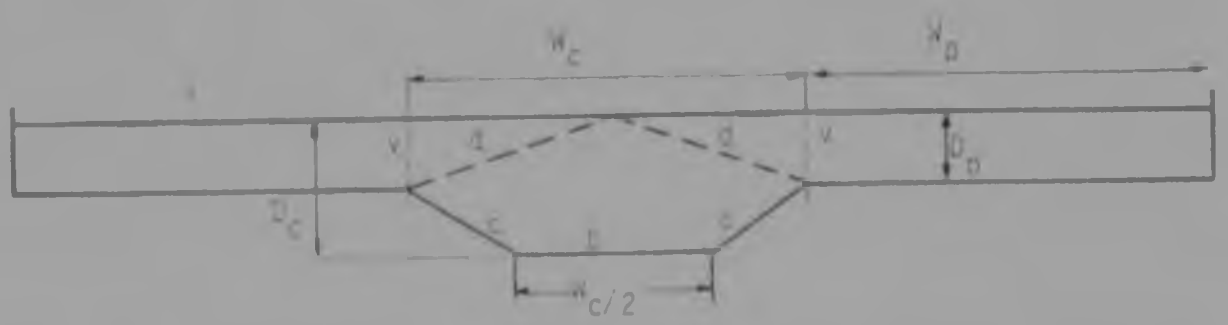


Fig. 4.8 Assumed channel section and interface planes

The average boundary shear stress for the channel section (τ_c) will be equal to the component in the flow direction of the weight of water contained within the channel section divided by the total wetted perimeter, i.e.

$$\tau_c = \frac{\gamma A_r S}{p+2(c+d)} \qquad (4.37)$$

in which γ is the unit weight of water, A_r is the area bounded by the assumed boundary and interface planes, and S is the bed slope of the channel.

The apparent shear stress on the diagonal interface planes (τ_{ad}) can be expressed in terms of the apparent shear stress on the vertical interface planes (τ_{av}) by considering forces associated with the shear stresses. For equilibrium

$$2\tau_{ad}{}^{d} = 2\tau_{av}{}^{v} - \gamma(A_v - A_T)S \qquad (4.38)$$

in which A_v is the channel area assuming vertical interface planes. Equation (4.38) leads to the following expression for the apparent shear stress on the diagonal planes

$$\tau_{ad} = \frac{D_p}{2d}[2\tau_{av} - \tfrac{1}{2}\gamma W_c S] \qquad (4.39)$$

The apparent shear stress on the vertical planes can be calculated using the following empirical equation proposed by Wormleaton, Allen and Hadjipanos

$$\tau_{av} = 13,34(\Delta V)^{1,862}\left(\frac{D_c}{D_c+D_p}\right)^{-3,123}\left(\frac{W_p}{W_c}\right)^{-0,727} \qquad (4.40)$$

in which Δv is the difference in flow velocity between channel and plain in m/s.

Using equations (4.3[illegible], (4.39) and (4.40) the apparent

shear stress ratio can be calculated as

$$\lambda = \tau_{ad} / \tau_c \qquad (4.41)$$

Because equation (4.40) involves Δv which is unknown until the velocities have been calculated some iteration is necessary and the velocity calculations are performed as follows. The channel and plain velocities are calculated using Manning's equation and excluding the diagonal interfaces from the wetted perimeters. The apparent shear stress ratio is then calculated. A value less than 0,5 is consistent with the assumption of excluding the diagonal interfaces and the velocities are accepted. A value greater than 0,5 implies that the interfaces should be included in the wetted perimeter for the channel. The channel velocity is therefore recalculated with the wetted perimeter included and if the apparent shear stress ratio is confirmed to be greater than 0,5 the new channel velocity is accepted. Because the channel velocity will be less if the interfaces are included than if they are not, it is possible that the apparent shear stress ratio will now be less than 0,5, suggesting that the first assumption was correct after all. This implies that the apparent shear stress on the interface is actually some value between zero and the average boundary shear for the channel. In such cases the velocity is assumed to be the average of the values obtained by including and excluding the interface in the wetted perimeter. Refinement of these calculations is not justified because the apparent shear stress ratio criterion is rather vague and requires further experimental investigation.

Using the diagonal interface as described above can result in the channel velocity being calculated to be less than the plain velocity if the flow depth on the plain is large. This occurs because the channel flow area is made unreasonably small by a diagonal subdivision even when the interface is excluded from the wetted perimeter

for shear stress calculations. The resulting small hydraulic radius leads to an underestimation of velocity. The results presented by Wormleaton, Allen and Hadjipanos show in fact that for high depth ratios ($D_c/(D_c-D_p)$) the best estimates for channel velocity are obtained if a vertical interface is used to define the area but excluded from the wetted perimeter. In the model the diagonal interface is therefore used only if the depth ratio is less than 2,0, otherwise a vertical interface excluded from the wetted perimeter is assumed.

5. BOUNDARY CONDITIONS

5.1 Vertical Boundary Conditions

The domain of integration for the diffusion-settling equation is bounded by a channel on one or both sides (see Fig. 3.1). The bounding surface associated with a channel is assumed to be a vertical plane on which the boundary conditions are specified in terms of concentration values. The concentrations on this surface are assumed to be determined purely by the hydraulic conditions in the channel.

Suspension of solid particles in the channel is governed by the same processes as over the plain and the concentration distribution can therefore also be described by a diffusion-settling equation. Equation (3.2) was derived to determine the transverse and vertical distribution of suspended material over the plain, i.e.

$$0 = \frac{\partial}{\partial y}\left(\epsilon_y \frac{\partial C}{\partial y}\right) + \frac{\partial}{\partial z}\left(\epsilon_z \frac{\partial C}{\partial z}\right) + w\frac{\partial C}{\partial y} - u\frac{\partial C}{\partial x} \qquad (3.2)$$

If it is assumed that there is no transverse variation of concentration within the channel then $\frac{\partial C}{\partial z} = 0$ and equation (3.2) can be simplified further

$$0 = \frac{\partial}{\partial y}\left(\epsilon_y \frac{\partial C}{\partial y}\right) + w\frac{\partial C}{\partial y} \qquad (5.1)$$

Equation (5.1) can be integrated once to yield

$$0 = \epsilon_y \frac{\partial C}{\partial y} + wC + A \qquad (5.2)$$

where A is a constant of integration. A will be equal to zero if it is assumed that the concentration is zero near to the water surface. Partial derivatives are no longer necessary and so the vertical concentration distribution is given by

$$0 = \epsilon_y \frac{dC}{dy} + wC \qquad (5.3)$$

The vertical diffusivity varies with depth in the flow according to equation (4.6), i.e.

$$\epsilon_y = \kappa u_* \frac{y}{D}(D-y) \qquad (4.6)$$

Introducing equation (4.6) into equation (5.3) and separating variables yields

$$\frac{dC}{C} = -\frac{w}{\kappa u_*}\frac{D}{y}\left(\frac{dy}{D-y}\right) \qquad (5.4)$$

Equation (5.4) can be integrated from a reference level a to the depth in the flow to give

$$\frac{C}{C_a} = \left(\frac{D-y}{y}\,\frac{a}{D-a}\right)^{z} \qquad (5.5)$$

in which C_a is the concentration at depth a and z is given by

$$z = \frac{w}{\kappa u_*} \qquad (5.6$$

Equation (5.5) was introduced by Rouse in 1937. It can be used to describe the vertical distribution of suspended sediment relative to the concentration at a known level.

The transverse distribution model is intended to describe the distribution of deposits in relative terms only. It is therefore not necessary to determine an actual value for C_a. Any suitable value can be used and all concentrations on the vertical boundary and within the domain of integration will be relative to that value. If actual values were required C_a could be determined by means of a bed load equation, assuming a certain thickness for the active layer of the bed. In the model the chosen value for C_a is assumed to occur at a distance above the bed equal to twice the mean diameter of bed particles.

The actual sediment concentration at the bed depends on the hydraulic conditions in the channel. Therefore if the plain is bounded by channels on both sides and the channels are not identical then arbitrary values for C_a cannot be assigned to both boundaries. If an arbitrary value is selected for one boundary then the value for the other boundary will be uniquely determined by the relative capacities of the two channels to transport bed

material. When considering two channel boundaries it is therefore necessary to determine the bed load capacities of the channels, at least in a relative sense.

Many bed load equations have been proposed and these can be classified into three basic types. The duBoys type equations express sediment discharge in terms of the excess of bed shear over the critical value at which bed particles begin to move. The Schoklitsch type equations consider an excess of discharge or velocity over a critical value. The Einstein type equations are based on a consideration of the statistical characteristics of hydrodynamic lift forces acting on particles.

The Einstein bed load equation is probably the most advanced but it is rather complicated to apply and difficult to code for solution by computer. The equation of Meyer-Peter and Muller has been used in this study; it is easy to use and gives close agreement with the Einstein equation over a wide range of conditions.

Meyer-Peter and Muller acknowledged that movement of bed material is associated with the skin friction component of total shear stress only. They evaluated this component by dividing the total energy gradient into components for skin friction and form resistance. From theoretical and experimental studies they developed the following equation

$$\frac{\gamma R (k/k')^{3/2} S}{d} - 0,047(\gamma_s - \gamma) = \frac{0,25 \rho^{1/3} (g_s')^{2/3}}{d} \qquad (2.10)$$

in which γ and γ_s are the unit weight of water and sediment respectively, R is the total hydraulic radius, S is the energy gradient, d is the representative particle size, ρ is the density of water and g_s' is the sediment discharge as submerged weight per unit width. The factor $(k/k')^{3/2}$ represents the proportion of the total energy gradient associated with skin friction,

S'. The total resistance is represented by k, which is the reciprocal of Manning's n, and the skin friction by k', which can be calculated from bed particle size using an empirical relationship.

In equation (2.10) the term $\gamma R(k/k')^{3/2}S$ represents the boundary shear stress due to skin friction, τ'. This can also be calculated by using the total energy gradient and the component of hydraulic radius associated with skin friction. In other words, τ' can be calculated from equation (4.23), i.e.

$$\tau' = \gamma R'S \qquad (4.23)$$

using the value of R' determined from equation (4.26), i.e.

$$\frac{V}{\sqrt{gR'S}} = 6,25 + 2,5\ \ell n\frac{R'}{k} \qquad (4.26)$$

Because equations (4.23) and (4.26) are used elsewhere in the transverse distribution model their result for τ' is substituted in equation (2.10) in place of $\gamma R(k/k')^{3/2}S$.

By dividing through by $(\gamma_s-\gamma)$, equation (2.10) can be expressed in dimensionless terms,

$$\theta' - 0,047 = \frac{0,25\,\theta^{1/3}}{(\gamma_s/\gamma-1)^{2/3}}\,(g_s')^{2/3} \qquad (5.7)$$

in which θ' is the dimensionless shear stress due to skin friction,

$$\theta' = \frac{\tau'}{(\gamma_s-\gamma)d} \qquad (5.8)$$

The sediment concentration at the bed is proportional to g_s' and therefore equation (5.7) can be used to calculate the relationship between values of C_a in the two channels. If a value of C_a is arbitrarily selected for one channel the value for the second channel will therefore be given by

$$C_{a2} = C_{a1}\left(\frac{\delta'_2{}^{-0,0047}}{\delta'_1{}^{-0,0047}}\right)^{3/2} \qquad (5.9)$$

in which the subscripts 1 and 2 denote the first and second channels respectively.

By applying equation (5.9) the concentration values throughout the domain of integration will be calculated relative to the single, arbitrarily selected value for C_{a1}.

5.2 Probability of Deposition

The domain of integration of the diffusion-settling equation is bounded at the bottom by the plain surface. The boundary condition at this surface is specified in derivative form, defining the rate of transport of sediment particles across the surface. Because vertical diffusivity decreases to zero at the boundary the only mechanism for transport across the boundary is settling, i.e. the convective component of the diffusion-settling equation.

The deposition of a particle on the bed depends on the hydraulic conditions close to the bed and on the roughness of the bed surface. A particle reaching the bed surface will not deposit if the hydraulic lift and drag forces exceed the stabilizing forces of weight and friction. The hydraulic forces will be applied only to particles on exposed areas of the bed; if a small particle settles to the region between larger bed particles it will be shielded from disturbing forces.

If the deposition of particles is inhibited the sediment concentration close to the bed will be increased by particles settling from above. The rate of diffusion is proportional to concentration gradient and therefore a

higher concentration near the bed will enhance net diffusion in an upward direction. All concentrations in a vertical section will therefore be increased. This effect is most pronounced close to the main channel where vertical diffusivity, disturbing hydraulic forces at the bed, and sediment availability are greatest. The transverse concentration gradient will therefore also tend to be increased thus enhancing transverse diffusion. The net result is a more extensive spreading of sediment across the plain. The final distribution of deposited material therefore depends on the probability that a particle reaching the plain surface will deposit.

The probability of deposition is the probability that the hydraulic disturbing forces acting on a particle at the bed surface are less than the stabilizing forces. This is equal to unity minus the probability of erosion which is used in some bed load models to determine the proportion of bed particle that will move.

Einstein was the first researcher to calculate the transport of sediment by considering the probability of motion of individual particles resting on the bed. He found the probability to be distributed according to the normal-error law and proposed an expression for the probability in terms of hydraulic and particle characteristics. This expression would, however, be difficult to include in a computer program and involves certain empirical constants which have been evaluated for uniform bed material only.

Engelund and Fredsoe (1976) proposed a much simpler equation for calculating the probability of motion in terms of sediment characteristics and the imposed shear stress. The probability, p, is given by

$$p = \left\{1 + \left[\frac{\theta}{\theta_c}\right]^4\right\}^{-1/4} \qquad (5.10)$$

in which θ is the non-dimensional shear stress (Shields parameter). This is given by

$$\theta = \frac{u_*^2}{(s-1)gd} \tag{5.11}$$

in which u_* is the shear velocity, s is the relative density, g is the acceleration due to gravity and d is the representative particle size. θ_c is the non-dimensional shear stress at which the particle will begin to move. This could be obtained from the Shields diagram for different particle sizes, but because use of this diagram is not straightforward a single representative value of 0,056 is used for all cases. This value applies to fully turbulent flow conditions which should generally be the case in practical applications of the model. There is some doubt concerning the accuracy of Shields's values where density differences are large, as will be the case with gold particles, but the deposition probability is not very sensitive to θ_c.

In equation (5.10) $\tan\phi$ is the dynamic friction coefficient of the sediment particles. A value of tan 27° which is typical for sand is used.

Equation (5.10) gives the probability of entrainment from a reasonably smooth bed. The probability of entrainment of a single particle can also be interpreted as the proportion of bed area over which entrainment will occur. Because of the extreme size difference between gold and gravel particles many gold particles will pass directly through the interstices between the gravel particles on the bed. They will be subjected to re-entraining forces only if they settle on top of gravel particles. The area to which the entrainment probability is applied must therefore be less than the total area of the bed.

The proportion of the bed over which the re-entrainment

forces apply can be determined if it is assumed that the bed is composed of spherical particles as shown in Fig. 5.1. If a particle settles on the top of the bed particle, i.e. within length ℓ, it will be momentarily retained and therefore exposed to re-entrainment. The probability of deposition for such a particle will be similar to that on a smooth bed. If the particle falls within length m it will continue through the top bed layer unimpeded.

It is further assumed that a particle can settle on a sloping surface only if the slope is less than the angle of repose of the particle. The length ℓ will therefore be the diameter of the circular locus of points on the sphere where the surface angle is equal to the angle of repose. Assuming a representative angle of repose to be 30° the length ℓ will be as defined in Fig. 5.2

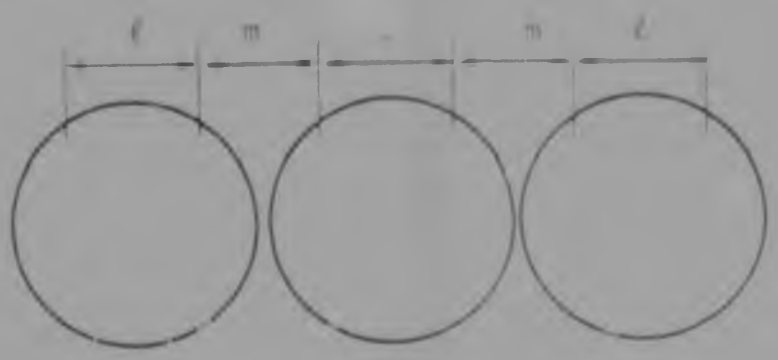


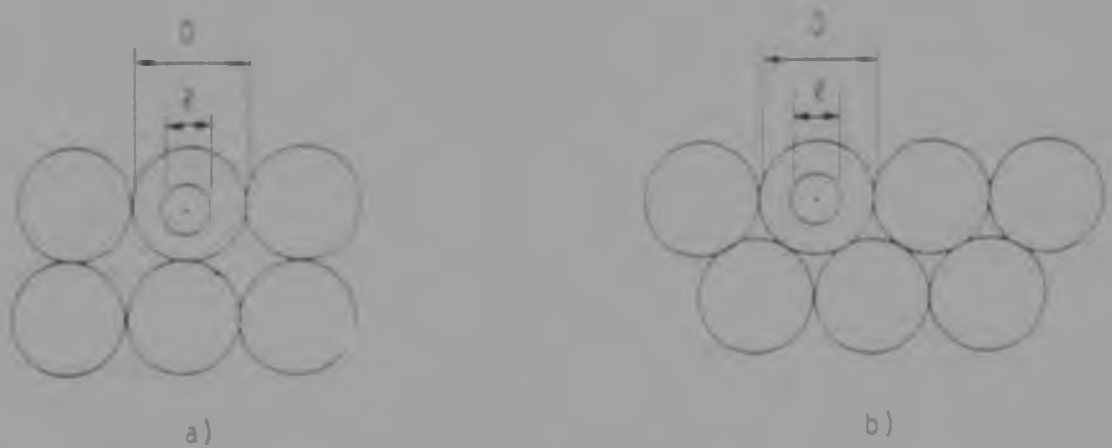
Fig. 5.1 Bed area subject to entrainment forces

From the geometry of Fig. 5.2 it can be shown that length ℓ is equal to half the diameter of the spherical bed particle. To calculate the proportion of bed area within length ℓ the packing arrangement of bed particles must be assumed.



Fig. 5.2 Definition of length ℓ

Two packing arrangements are considered, as shown in Fig. 5.3.



a) b)

Fig. 5.3 Alternative packing arrangements

From the geometries of Fig. (5.3) it can be shown that the proportion of total area within diameter ℓ is 0,196 for packing arrangement a) and 0,227 for packing arrangement (b). Packing on the plain surface will be random and the average of the above two values is assumed for general cases, i.e. 0,21.

For calculating the probability of deposition it is therefore assumed that equation (5.10) applies over 21 percent of the bed while over the remaining portion the probability of deposition is 1,0. The probability that a settling particle will reach an exposed portion of bed is therefore 0,21. It's probability of being immediately re-entrained from this portion is p as defined by equation (5.10). The probability of any settling particle being immediately re-entrained is therefore 0,21 p and the probability of any particle being permanently deposited must be

$$\text{probability of deposition} = 1-0,21\ p \qquad (5.12)$$

Equation (5.12) will apply only if the settling particles are small enough to pass easily through the interstices between the bed particles. It can be shown that for packing arrangement (b) in Fig. 5.3 a particle will just pass between spheres of diameter D if its diameter, d, is such that

$$\frac{D}{d} > 6,46 \qquad (5.13)$$

It is likely that particles even smaller than D/6,46 will bridge and block the opening so the maximum particle size will be smaller than defined by equation 5.13. Einstein (1968) performed experiments to study the deposition of suspended particles in a gravel bed and found that the maximum size, such that clogging of interstices would not occur, is given by

$$\frac{D}{d} > 15 \qquad (5.14)$$

All suspended particles must satisfy this condition, or clogging will occur and equation (5.12) will not apply. However, if all particles in suspension other than gold are larger than 15 times the gold particle diameter, gold would still be able to pass through the interstices in the bed.

Equation (5.12) does not account for the shielding effect of the large bed particles on particles settling within the exposed area. On the other hand it also does not account for the decreased stability of a particle on a sloping surface, which would have a compensating effect.

6. EXPERIMENTAL VERIFICATION OF THE TRANSVERSE DISTRIBUTION MODEL

6.1 Introduction

A number of experiments were performed to determine the transverse distribution of fine sand deposited on the shallow flow (or plain) region of a channel with a compound section. The experimental channel was parallel to the flow direction so the distribution was a result of transverse diffusion only, there being no transverse convective component. The mathematical model described previously indicated that for this condition the parameters which have the most significant effect on the distribution are the particle size, the ratio of the flow depths on the plain and in the main channel, and the probability that a particle settling to the plain surface will be deposited. The experiments were therefore designed to enable these parameters to be varied so that comparisons could be made. Results for different particle sizes were obtained by using a graded sand in the experiments. The deposits were separated into several fractions, enabling distributions for different sizes to be measured for each experiment. Different flow depth ratios were obtained by varying the flow rate and the flow depth in the channel section. Two extreme deposition probabilities were obtained by using different materials to cover the plain surface.

Distributions of deposits for the same conditions as in the experiments were computed using the mathematical model and the results from the two approaches are compared.

6.2 Description of Apparatus

The experiments were performed in a 380 mm wide glass

6. EXPERIMENTAL VERIFICATION OF THE TRANSVERSE DISTRIBUTION MODEL

6.1 Introduction

A number of experiments were performed to determine the transverse distribution of fine sand deposited on the shallow flow (or plain) region of a channel with a compound section. The experimental channel was parallel to the flow direction so the distribution was a result of transverse diffusion only, there being no transverse convective component. The mathematical model described previously indicated that for this condition the parameters which have the most significant effect on the distribution are the particle size, the ratio of the flow depths on the plain and in the main channel, and the probability that a particle settling to the plain surface will be deposited. The experiments were therefore designed to enable these parameters to be varied so that comparisons could be made. Results for different particle sizes were obtained by using a graded sand in the experiments. The deposits were separated into several fractions, enabling distributions for different sizes to be measured for each experiment. Different flow depth ratios were obtained by varying the flow rate and the flow depth in the channel section. Two extreme deposition probabilities were obtained by using different materials to cover the plain surface.

Distributions of deposits for the same conditions as in the experiments were computed using the mathematical model and the results from the two approaches are compared.

6.2 Description of Apparatus

The experiments were performed in a 380 mm wide glass

sided flume which had the bed built up with bricks over a length of approximately 10,0m to form the compound section shown in Fig. 6.1. At the upstream end of the compound section the plain surface was tapered gradually down to the channel bed level over a length of approximately one metre.

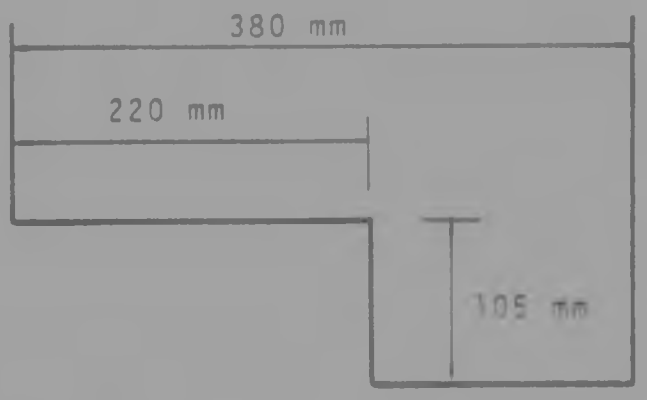


Fig. 6.1 Compound section

The flume was tilted over the length of the built-up section. Preliminary tests were run to determine the gradient necessary to entrain and transport in suspension significant quantities of sediment at reasonable flow depths. On the basis of these tests the flume slope was set at 0,004 for all experiments.

It was necessary to install a control device at the downstream end of the flume so that drawdown of the water surface profile could be eliminated and uniform flow conditions ensured over the test sections. An adjustable weir with a horizontal crest existed at the end of the flume but this was unsuitable for the compound section. Flow in both sections would have to be controlled without causing sediment accumulation in the main channel. The flow was therefore constricted by means of movable vertical bars, each 12 mm in diameter, set across the flow section as shown in Fig. 6.2. The number and spacing of these bars could be adjusted until the desired effect was obtained.

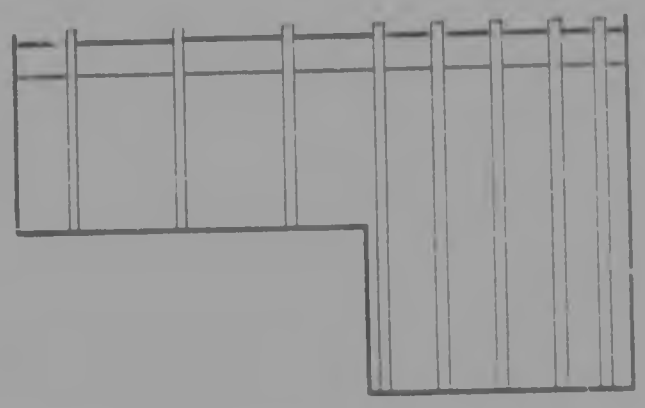


Fig. 6.2 Upstream view of downstream control device

Because of the dependence of the sediment distribution on the probability of deposition on the plain surface it was necessary to conduct experiments with different types of surfaces. Two different surfaces were used: a completely absorbing surface and a completely non-absorbing surface. (Real conditions are somewhere between these extremes, a coarse gravel bed being close to the completely absorbing condition.) An absorbing surface was obtained by covering the whole plain area with 'Nomad' matting. This is a synthetic spun filament type of material with an open 'pile' about 10 mm thick, attached to a solid backing. The surface is uniform and fairly even and it provides a very effective trap for sediment. Trapped particles would settle rapidly through the pile so that surface conditions would not be changed until very large quantities of sediment had been deposited. The matting was glued to galvanized steel sheeting to prevent floating or other movement during testing. The non-absorbing surface was obtained by reversing the matting strips so that the smooth steel was uppermost.

Two test sections were provided for collecting deposited sediment. These were located 1,8m apart with the

downstream section 2,8m from the end of the flume. Each test section was 0,5m long and consisted of 8 longitudinal strips of matting each 27,5mm wide. (See Fig. 6.3).

This arrangement was unsatisfactory for the non-absorbing surface test because the distribution adjusted to that for an absorbing surface over the lengths of the test sections. It was therefore necessary to use test sections which would trap the sediment at the boundary but which were short enough not to distort the distribution. The 0,5m strips were therefore replaced by 15mm blocks for tests with the non-absorbing surface.

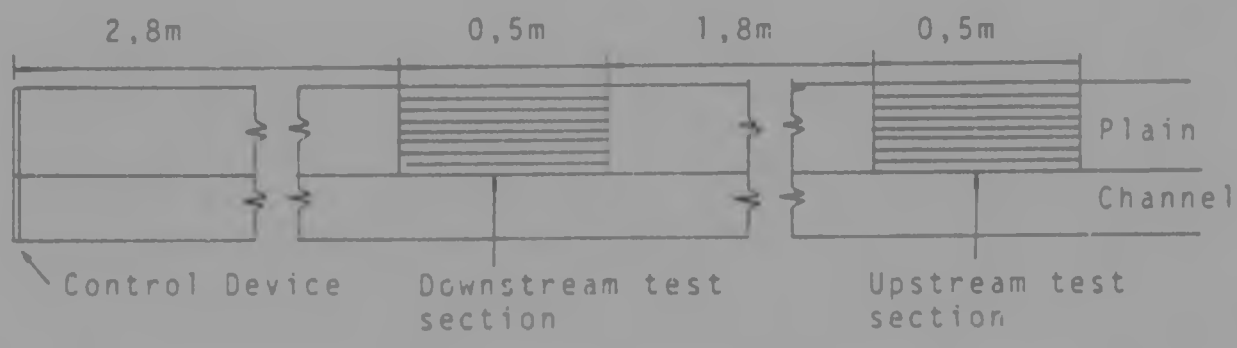


Fig. 6.3 Location of test sections

The same type of sand was used for all tests. This was a fine sand with a median particle size of 0,25mm and a size distribution as shown in Fig. 6.4. A layer of fresh sand was placed on the channel bed before each test. The thickness of the sand layer was determined by the channel flow depth required for the particular test.

No facilities were available in the laboratory for recirculating sediment so all sand transported to the end of the flume was collected in a trap at the end of the flume.

Flow velocities were measured using a propeller-type 'Streamflo' meter. Discharges were measured with a Venturi meter installed in the supply line. Water surface levels were measured with a pointer gauge mounted on a traversing mechanism.

6.3 Experimental Procedure

Results were obtained for four different conditions, three for the absorbing boundary (tests 2, 3 and 4) and one for the non-absorbing boundary (test 6). Table 6.1 summarizes the conditions for each of the four tests.

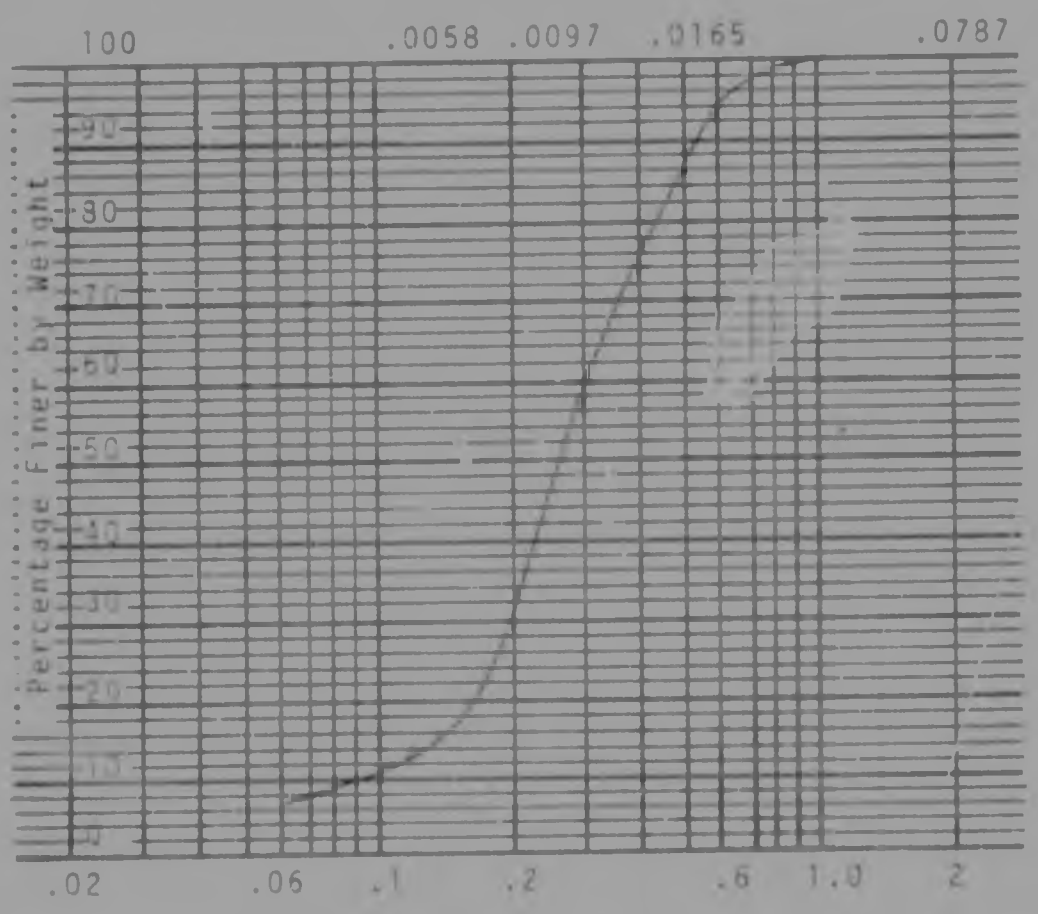


Fig. 6.4 Particle size distribution

The channel flow depths given in Table 6.1 represent average values for the duration of the test. The actual flow depth varied during the tests as sand was removed

from the bed and the thickness of the sand layer reduced The original thickness of the sand layer was 30mm for tests 2 and 3, and 50mm for tests 4 and 6. The greater thickness for the latter two tests enabled the tests to be continued for considerably longer than for the first two before the solid flume bed became exposed at the upstream end of the compound reach.

Table 6.1 Conditions for Experiments

Test	S	Q (l/s)	D_p (mm)	V_p (m/s)	D_c (mm)	V_c (m/s)	D_c/D_p	T (mins)
2	0,004	11,9	45	0,42	145	1,00	3,22	40
3	0,004	9,9	20	0,20	120	0,90	6,00	40
4	0,004	9,5	30	0,30	100	0,75	3,33	72
6	0,004	8,3	20	0,43	95	0,82	4,75	270

where S : gradient
Q : discharge
D_p : flow depth on plain
V_p : average flow velocity over plain
D_c : flow depth in channel
V_c : average flow velocity in channel
T : duration of test

Before each test water was passed through the flume without sand on the channel bed so that the discharge and control device could be adjusted to give approximately the correct water level. This was done so that only minor adjustments would be necessary during the test and the desired conditions obtained quickly. The flume was then emptied and sand spread evenly to the required depth over the channel bed and for a short distance (about one metre) upstream of the compound reach. Samples of bed material adjacent to each test section were analysed by sieving. The particle size distribution was never significantly different from

that shown in Fig 6.4. The test was then started by passing water through the flume at the predetermined valve and control device settings and any necessary fine adjustments were made.

During the course of the test, the water level, flow velocity profiles and discharge were measured periodically. The sand surface was also observed continually so that bed forms, local sorting and any changes in particle entrainment could be noted. After some time most fine particles were removed from the surface layers of the sand and the suspended load was reduced significantly. This segregation occurred progressively further downstream and once the supply of suspended material to the upstream test section was affected the test was ended.

After the test the flume was drained and the test strips removed from the plain surface. The sand remaining on the channel bed was discarded and not used in subsequent tests as segregation changed its grading characteristics.

The test strips were allowed to dry and then the deposited sand was removed. The sand removed from each strip was weighed and then separated into fractions by sieving. For most tests four size fractions could be obtained, viz. greater than 300 microns, 150 to 300 microns, 75 to 150 microns and less than 75 microns. Each fraction from each test strip was then weighed to determine the transverse distribution of the deposited material across the strips.

6.4 Results

The mass distributions for all size fractions at both upstream and downstream test sections for all four tests are presented in tables 6.2 to 6.5.

The test strips are numbered as shown in Fig. 6.5. In the tables the numbers are prefixed by U to denote the upstream section and D to denote the downstream section.

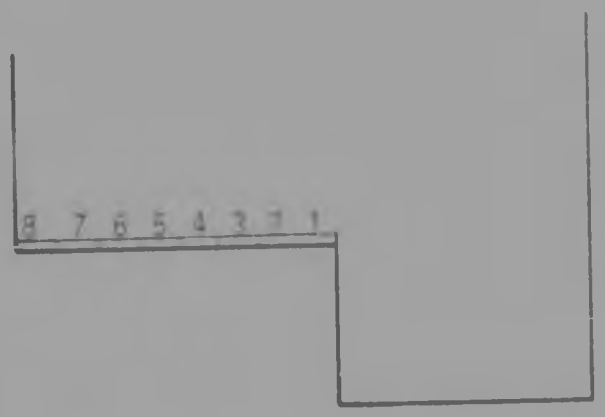


Fig. 6.5 Location of test strips

For test 6 (non-absorbing boundary) the quantities of sand in the test strip were very small and the distribution changed rapidly near to the channel. To improve accuracy the samples were split for some of the test strips at the upstream test section. Sand was removed and weighed separately from each half of strips 1 to 3.

The mathematical model is intended to predict the relative distribution of deposits and not masses. For comparison with the model the experimentally determined distributions were expressed relative to the deposit on the test strip adjacent to the channel. An exception was made with the results for the upstream test section of test 6 where data were obtained for half strip widths; here the distributions were calculated relative to the average of the first two values in order to maintain consistency with the other results. The relative distributions are also presented in tables 6.2 to 6.5.

Table 6.2 Results for Test 2

Size Fraction	>300μ		150-300μ		75-150μ		<75μ	
Test Strip	Mass (g)	Rel.	Mass (g)	Rel.	Mass (g)	Rel.	Mass (g)	Rel.
U1	0,045	1,000	1,235	1,000	1,544	1,000	0,445	1,000
U2	0,015	0,333	0,574	0,465	1,119	0,725	0,381	0,856
U3	0,007	0,156	0,235	0,190	0,663	0,429	0,275	0,618
U4	0,006	0,133	0,099	0,080	0,398	0,258	0,247	0,555
U5	0,006	0,133	0,039	0,032	0,310	0,201	0,214	0,481
U6	0,007	0,156	0,024	0,019	0,299	0,194	0,209	0,470
U7	0,009	0,200	0,021	0,017	0,363	0,235	0,259	0,582
U8	0,007	0,156	0,023	0,019	0,339	0,220	0,228	0,572
D1	0,019	1,000	0,489	1,000	1,680	1,000	0,695	1,000
D2	0,009	0,474	0,231	0,472	1,000	0,595	0,465	0,669
D3	0,006	0,316	0,097	0,198	0,587	0,349	0,300	0,432
D4	0,007	0,368	0,040	0,082	0,334	0,199	0,176	0,253
D5	0,009	0,474	0,022	0,045	0,189	0,113	0,118	0,170
D6	0,007	0,368	0,015	0,031	0,148	0,088	0,122	0,176
D7	0,010	0,526	0,017	0,035	0,127	0,076	0,116	0,167
D8	0,007	0,368	0,023	0,047	0,116	0,069	0,091	0,131

Table 6.3 Results for Test 1

Size Fraction	>300μ		150-300μ		75-150μ		<75μ	
Test Strip	Mass (g)	Rel.	Mass (g)	Rel.	Mass (g)	Rel.	Mass (g)	Rel.
U1	0,016	1,000	0,106	1,000	0,533	1,000	0,209	1,000
U2	0,007	0,438	0,033	0,311	0,193	0,362	0,108	0,517
U3	0,002	0,125	0,007	0,066	0,053	0,099	0,032	0,153
U4	0,001	0,063	0,003	0,028	0,013	0,024	0,011	0,053
U5	0,000	0,000	0,000	0,000	0,006	0,011	0,004	0,019
U6	0,001	0,063	0,000	0,000	0,003	0,006	0,015	0,072
U7	0,001	0,063	0,001	0,009	0,007	0,013	0,011	0,053
U8	0,002	0,125	0,004	0,038	0,022	0,041	0,021	0,100
D1	0,056	1,000	0,387	1,000	2,024	1,000	0,778	1,000
D2	0,018	0,321	0,129	0,333	0,983	0,486	0,504	0,648
D3	0,011	0,196	0,042	0,109	0,385	0,190	0,265	0,341
D4	0,006	0,107	0,018	0,047	0,128	0,063	0,148	0,190
D5	0,000	0,000	0,001	0,003	0,004	0,002	0,006	0,008
D6	0,003	0,054	0,003	0,008	0,016	0,008	0,023	0,030
D7	0,003	0,054	0,003	0,008	0,009	0,004	0,011	0,014
D8	0,005	0,089	0,003	0,008	0,006	0,003	0,006	0,008

Table 6.4 Results for Test 4

Size Fraction	>300µ		150-300µ		75-150µ		<75µ	
Test Strip	Mass (g)	Rel.	Mass (g)	Rel.	Mass (g)	Rel.	Mass (g)	Rel.
U1	0,037	1,000	0,320	1,000	1,742	1,000	0,676	1,000
U2	0,013	0,351	0,105	0,328	0,657	0,377	0,346	0,512
U3	0,007	0,189	0,025	0,078	0,206	0,118	0,159	0,235
U4	0,006	0,162	0,008	0,025	0,054	0,031	0,062	0,092
U5	0,002	0,054	0,003	0,009	0,013	0,007	0,021	0,031
U6	0,002	0,054	0,002	0,006	0,007	0,004	0,014	0,021
U7	0,003	0,081	0,002	0,006	0,005	0,003	0,014	0,021
U8	0,004	0,108	0,004	0,013	0,009	0,005	0,019	0,028
D1	0,041	1,000	0,641	1,000	5,163	1,000	1,695	1,000
D2	0,031	0,756	0,255	0,398	2,543	0,493	1,166	0,688
D3	0,011	0,268	0,089	0,139	1,066	0,206	0,683	0,403
D4	0,008	0,195	0,026	0,041	0,392	0,076	0,323	0,191
D5	0,004	0,098	0,010	0,016	0,103	0,020	0,113	0,067
D6	0,004	0,098	0,006	0,009	0,031	0,006	0,051	0,030
D7	0,003	0,073	0,006	0,009	0,013	0,003	0,021	0,012
D8	0,006	0,146	0,011	0,017	0,012	0,002	0,016	0,009

Table 6.5 Results for Test 6

Size Fraction	>300μ		150-300μ		75-150μ		<75μ	
Test Strip	Mass (g)	Rel.	Mass (g)	Rel.	Mass (g)	Rel.	Mass (g)	Rel.
U1a	0,005	0,714	0,017	0,708	0,062	0,574	0,025	0,490
U1b	0,009	1,286	0,030	1,250	0,154	1,426	0,077	1,510
U2a	0,012	1,714	0,034	1,417	0,180	1,667	0,092	1,804
U2b	0,004	0,571	0,018	0,750	0,121	1,120	0,064	1,255
U3a	0,008	1,143	0,009	0,375	0,050	0,463	0,031	0,608
U3b	0,003	0,429	0,002	0,083	0,012	0,111	0,007	0,137
U4	0,004	0,286	0,004	0,083	0,021	0,097	0,014	0,137
U5	0,015	1,071	0,013	0,271	0,011	0,051	0,015	0,147
U6	0,009	0,643	0,011	0,229	0,005	0,023	0,005	0,049
U7	-	-	-	-	-	-	-	-
U8	-	-	-	-	-	-	-	-
D1	0,012	1,000	0,030	1,000	0,214	1,000	0,131	1,000
D2	0,008	0,667	0,052	1,733	0,583	2,724	0,352	2,687
D3	0,005	0,417	0,017	0,567	0,250	1,168	0,214	1,634
D4	0,001	0,083	0,003	0,100	0,052	0,243	0,067	0,511
D5	0,000	0,000	0,000	0,000	0,007	0,033	0,016	0,112
D6	-	-	-	-	-	-	-	-
D7	-	-	-	-	-	-	-	-
D8	-	-	-	-	-	-	-	-

The two test sections were used to obtain extra data for the same hydraulic conditions. It is interesting to note that in terms of mass of deposited sediment the results from the two sections do not compare well but the relative distributions are generally in close agreement. For example, in test 2 the total mass deposited in the 150 to 300 micron fraction was 2,4 times as great at the upstream section compared with the downstream section. The relative distributions were, however, almost identical.

The reason for the mass discrepancy was the varying availability of particles of different sizes in the bed material along the length of the channel. The sediment at the surface of the bed, which was available for entrainment and transport, changed continuously in composition during testing. Because of the continual interchange of bed material and transported sediment the bed material upstream became depleted of fine material sooner than further downstream - fine particles were removed more rapidly than they were replaced. Fine sediment was therefore being supplied to the downstream test section for longer than to the upstream section. The data confirm that the mass deposited is generally greater at the downstream section for the finer fractions and vice versa for coarser fractions.

The availability of sediment for entrainment is also affected by the movement of bedforms. During test 4 a bedform about 1,5m long and composed of coarse material advanced downstream over the original bed surface, thereby inhibiting the entrainment of fine material for some time.

The difference in deposit masses and the close agreement of relative distributions between the two test sections indicates that the mechanism of transverse diffusion of sediment is not affected by

The two test sections were used to obtain extra data for the same hydraulic conditions. It is interesting to note that in terms of mass of deposited sediment the results from the two sections do not compare well but the relative distributions are generally in close agreement. For example, in test 2 the total mass deposited in the 150 to 300 micron fraction was 2,4 times as great at the upstream section compared with the downstream section. The relative distributions were, however, almost identical.

The reason for the mass discrepancy was the varying availability of particles of different sizes in the bed material along the length of the channel. The sediment at the surface of the bed, which was available for entrainment and transport, changed continuously in composition during testing. Because of the continual interchange of bed material and transported sediment the bed material upstream became depleted of fine material sooner than further downstream - fine particles were removed more rapidly than they were replaced. Fine sediment was therefore being supplied to the downstream test section for longer than to the upstream section. The data confirm that the mass deposited is generally greater at the downstream section for the finer fractions and vice versa for coarser fractions.

The availability of sediment for entrainment is also affected by the movement of bedforms. During test 4 a bedform about 1,5m long and composed of coarse material advanced downstream over the original bed surface, thereby inhibiting the entrainment of fine material for some time.

The difference in deposit masses and the close agreement of relative distributions between the two test sections indicates that the mechanism of transverse diffusion of sediment is not affected by

variations in absolute concentration, at least over small ranges.

6.5 Comparison of Measured and Simulated Distributions

Each of the four flume tests was simulated with the mathematical model and sediment deposit distributions were predicted for particle sizes of 75, 150 and 300 microns.

It was assumed in all cases that the relative density of the sediment was 2,65 and fall velocities were estimated from results presented by Graf (1971), as shown in Fig. 2.3

Manning's n values for the plain and channel were calculated from the flow velocities measured during testing.

Appropriate dimensions for the finite difference grid were determined by trial. A fairly coarse mesh was used initially and made progressively finer until there was no significant difference between successive results. The iteration tolerance, i.e. the maximum allowable difference in sediment concentration at any point between successive iterations, was determined in the same way.

A statement was inserted in the computer program to override the probability of deposition as normally calculated. A value of 1,0 was inserted when simulating the fully absorbing boundary.

The deposition distributions generated by the model were expressed in relative form in the same way as the measured distributions. The deposition at the point corresponding to the centre of test strip 1 was calculated by interpolating linearly between values at

the nearest grid points on either side. Depositions at other points were then divided by this value.

The simulated distributions were calculated for a single particle size in each case whereas the experimentally determined distributions represent a range of sizes. For comparison the average values of the simulated distributions for the extreme particle sizes in each fraction were calculated and plotted together with the measured values. This enabled direct comparisons to be made for the 150 to 300 micron and 75 to 150 micron fractions. Comparisons for the fractions greater than 300 microns and less than 75 microns could not be made in the same way because the size distributions beyond these limits were not known. Representative sizes for these fractions are therefore difficult to determine.

The experimental and simulated distributions for tests 2, 3 and 4, (i.e. the absorbing bed condition) are compared graphically in Figs. 6.6 to 6.11.

It will be noticed that in several cases the experimental distributions show a slight increase in sediment near to the side wall of the flume. This tendency is not predicted by the model and is probably due to enhanced transverse diffusivity resulting from the transfer of linear momentum by eddies generated along the solid side wall. The effect is most pronounced in the results for experiment 2, for which the flow depth over the plain, and therefore the effect of the vertical boundary, were greatest. In practical application of the model very large width to depth ratios for plain flow will be used and the effect should be insignificant.

Simulation of the distributions for the non-absorbing bed was attempted by inserting a constant probability

of deposition equal to zero in the model. This however caused convergence problems in the solution algorithm. It was found that for very small probabilities of deposition a decrease in the iteration tolerance led to solutions which deviated more and more from the measured distributions. No convergence problems were encountered for high deposition probabilities.

For verification of the model with experimental results an indirect approach was followed to simulate the distribution for a non-absorbing bed. Distributions were obtained for different low probabilities of deposition and the results were extrapolated to obtain a distribution for zero probability. The comparison of measured and simulated results for the 150 to 300 micron fraction for test 6 is shown in Fig. 6.12.

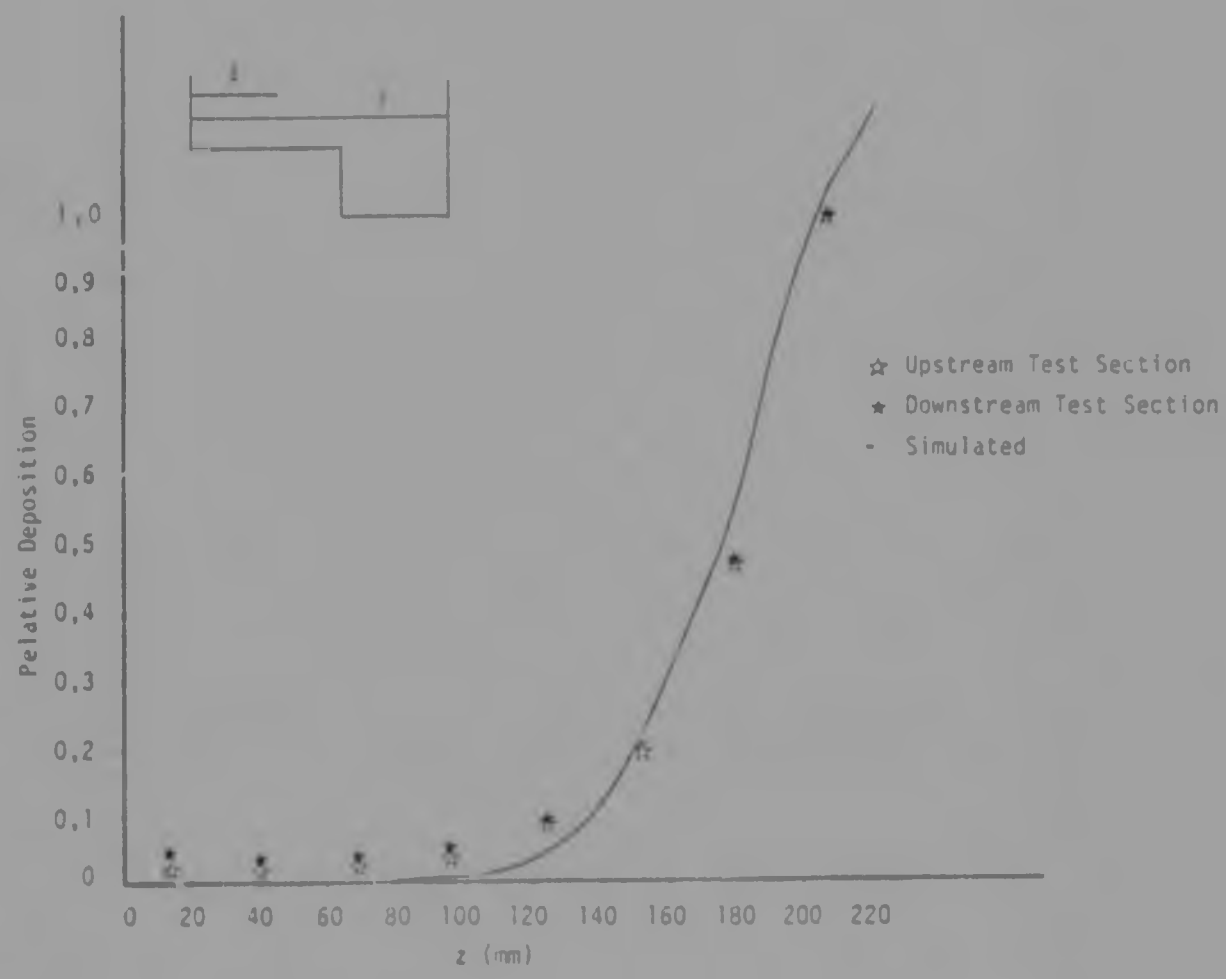


Fig. 6.6 Comparison of measured and simulated distributions for Test 2, 150 - 300 μ fraction

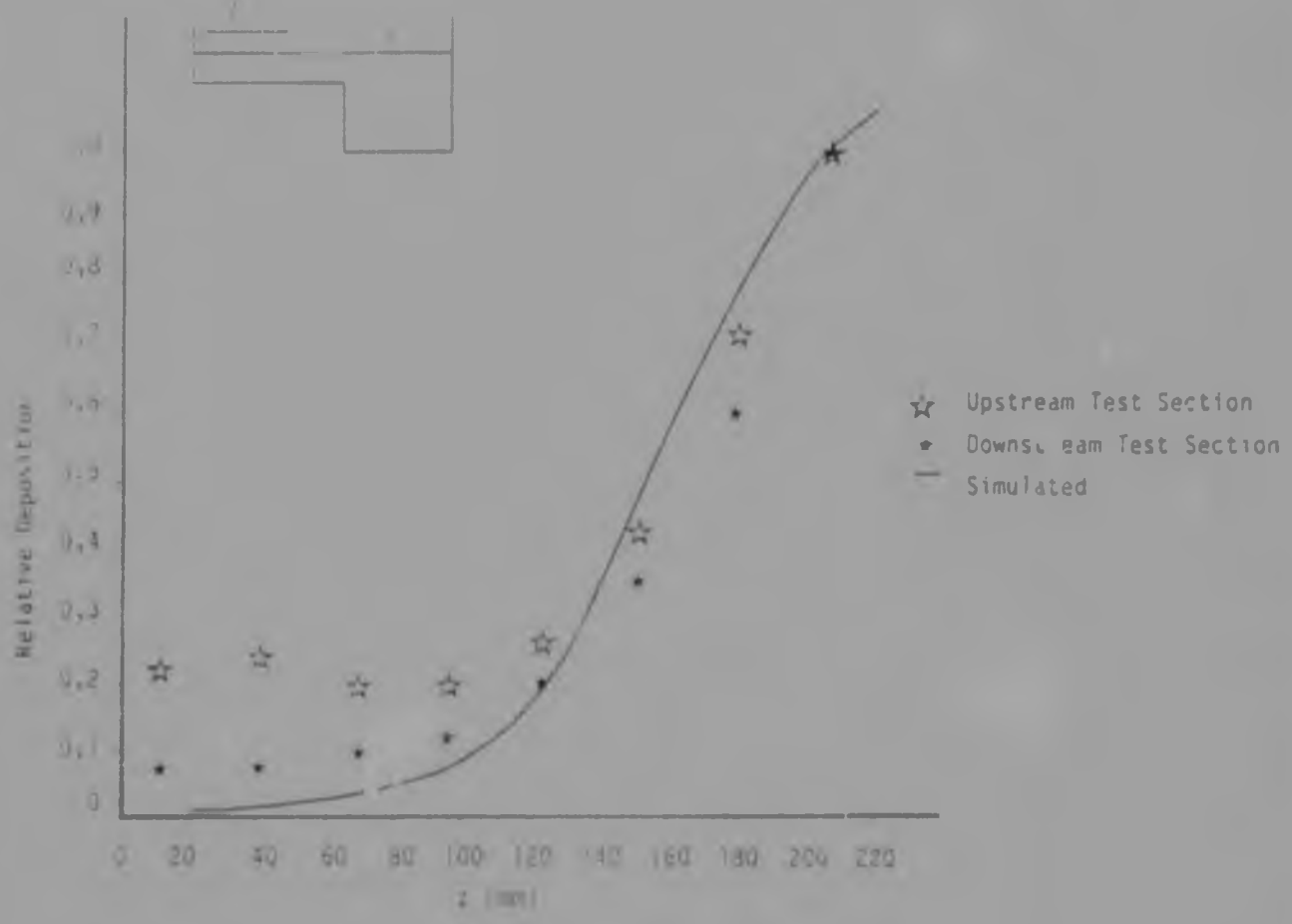


Fig. [illegible] Comparison of measured and simulated [illegible] for Test 2, 75 - 150 μ fraction

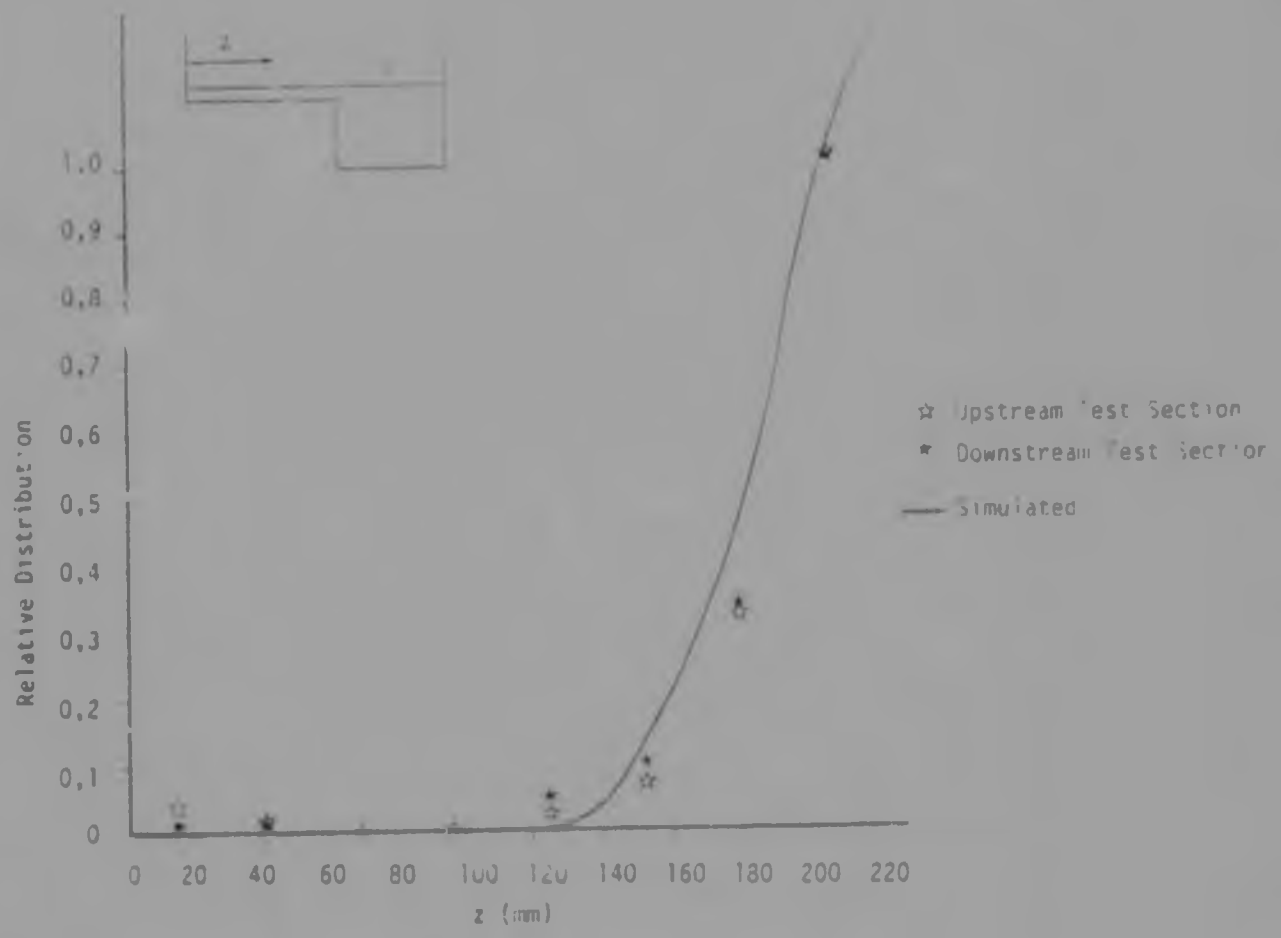


Fig. 6.8 Comparison of measured and simulated distributions for Test 3, 150 - 300 μ fraction

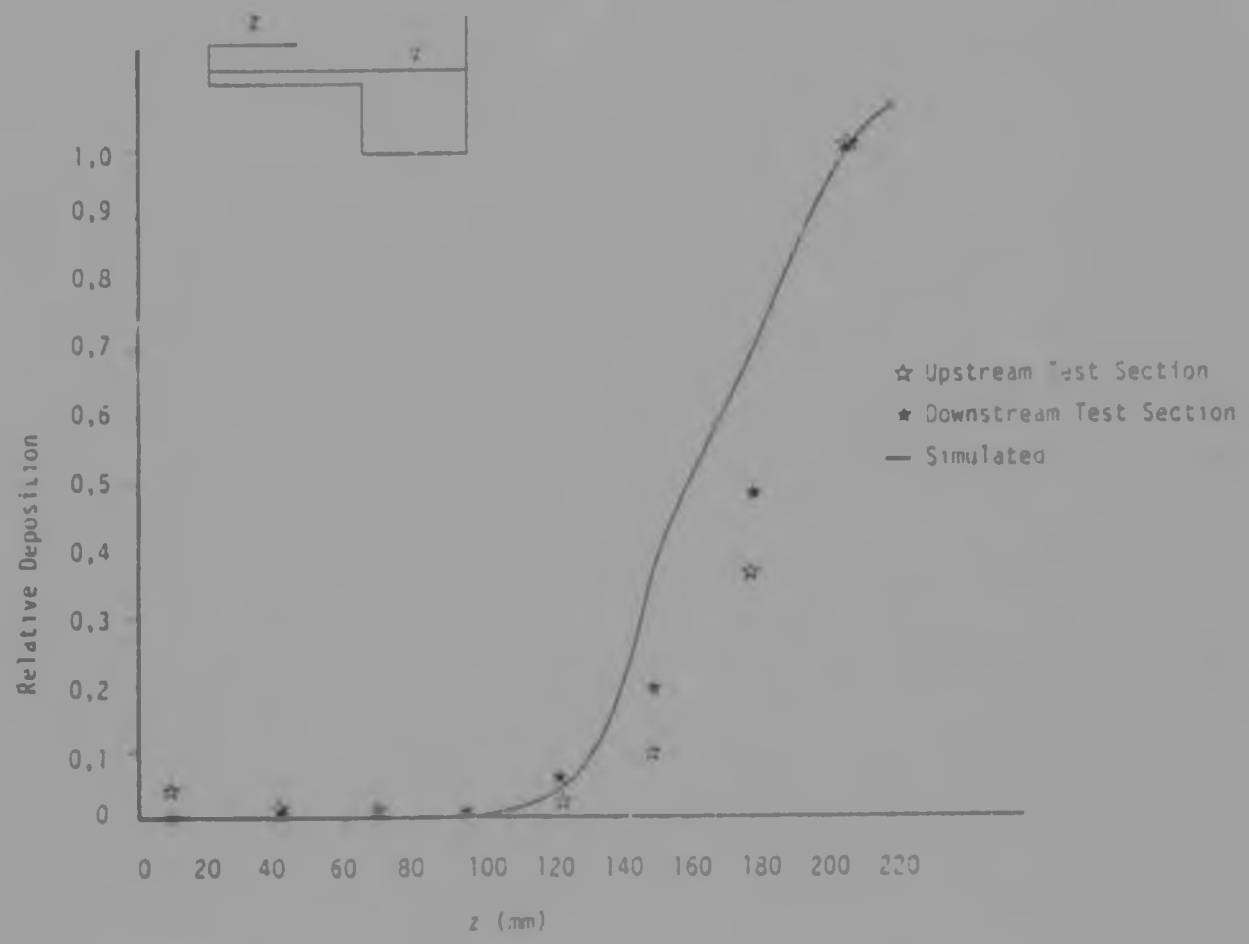


Fig. 6.9 Comparison of measured and simulated distributions for Test 3, 5 - 150 μ fraction

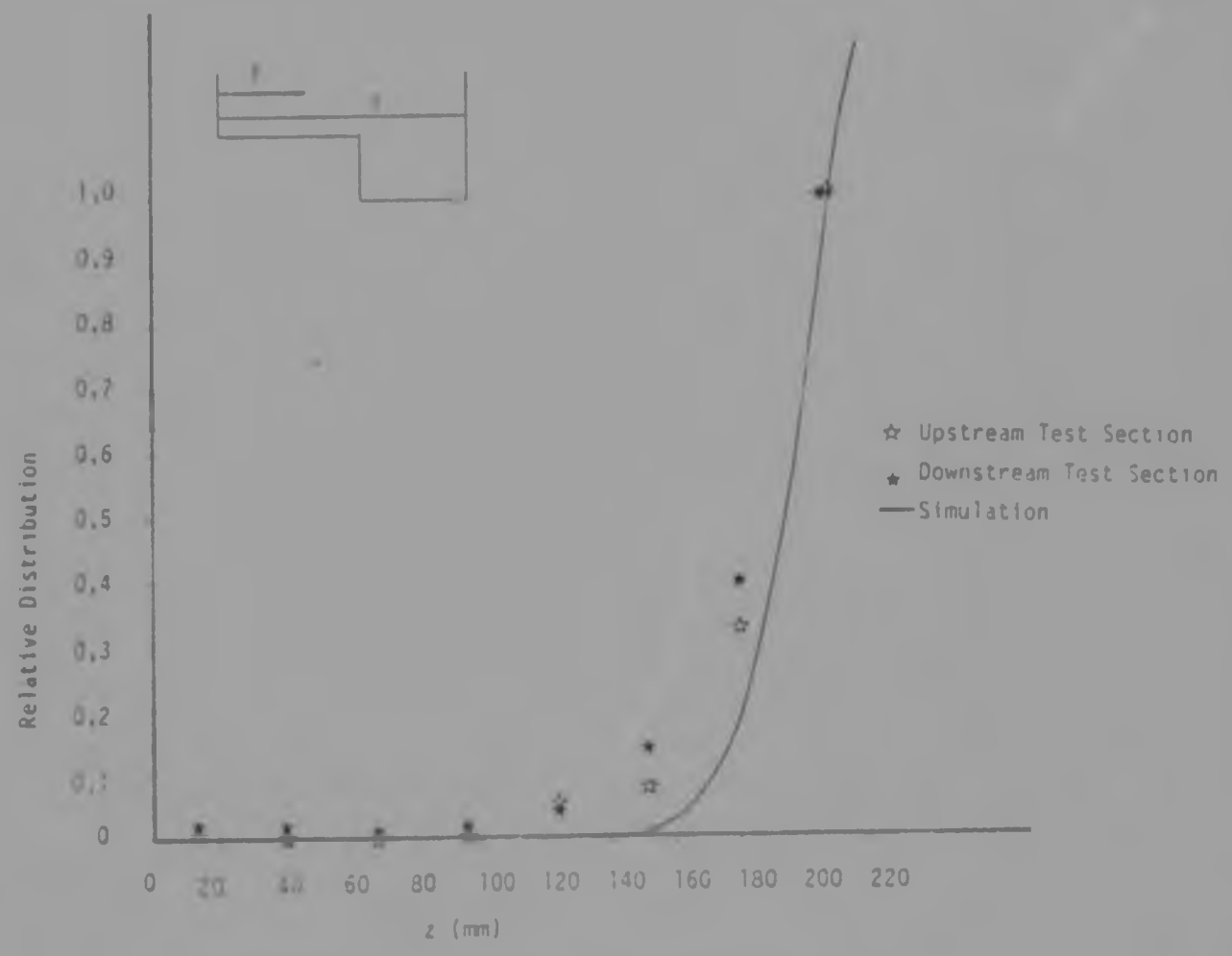


Fig. 6.10 Comparison of measured and simulated distributions for Test 4, 150 - 300 μ fraction

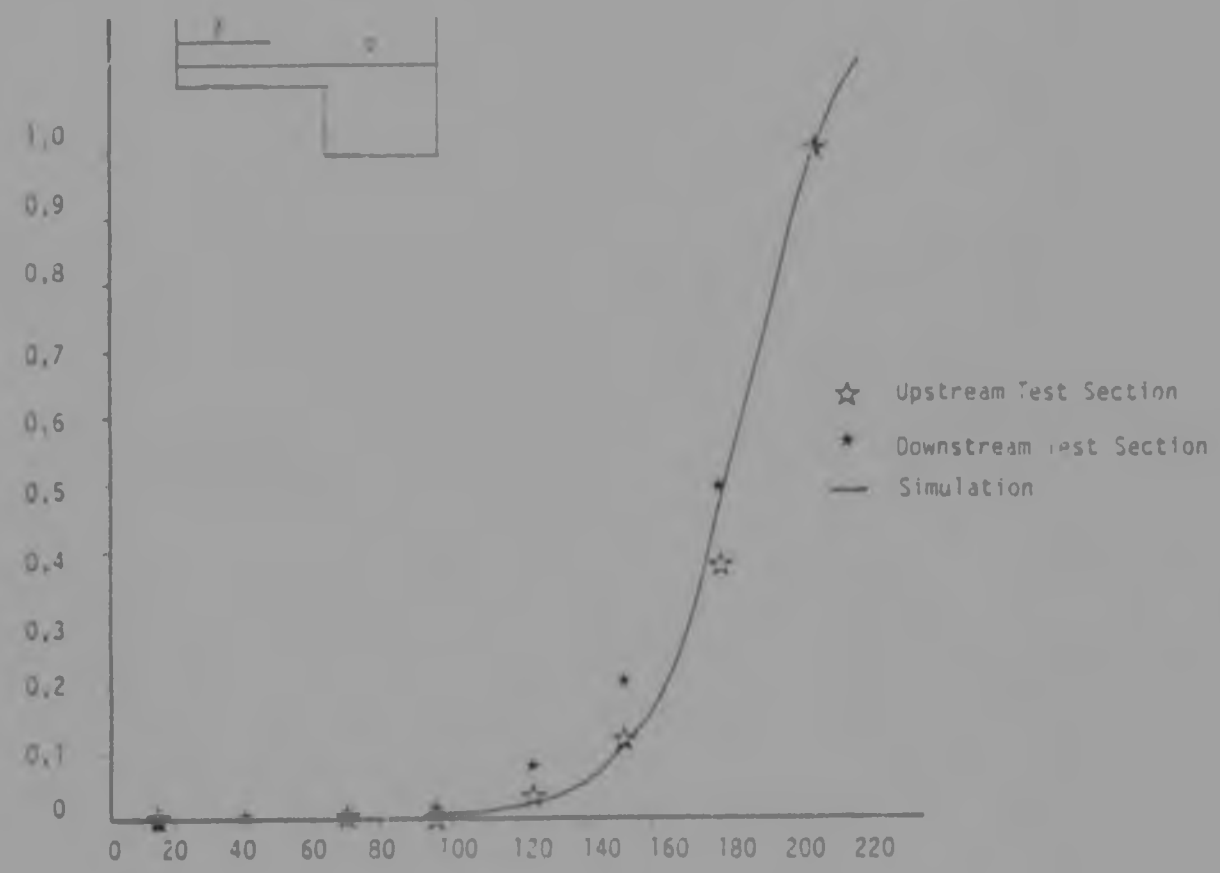


Fig. 6.11 Comparison of measured and simulated distributions for Test 4, 75 - 150 μ fraction

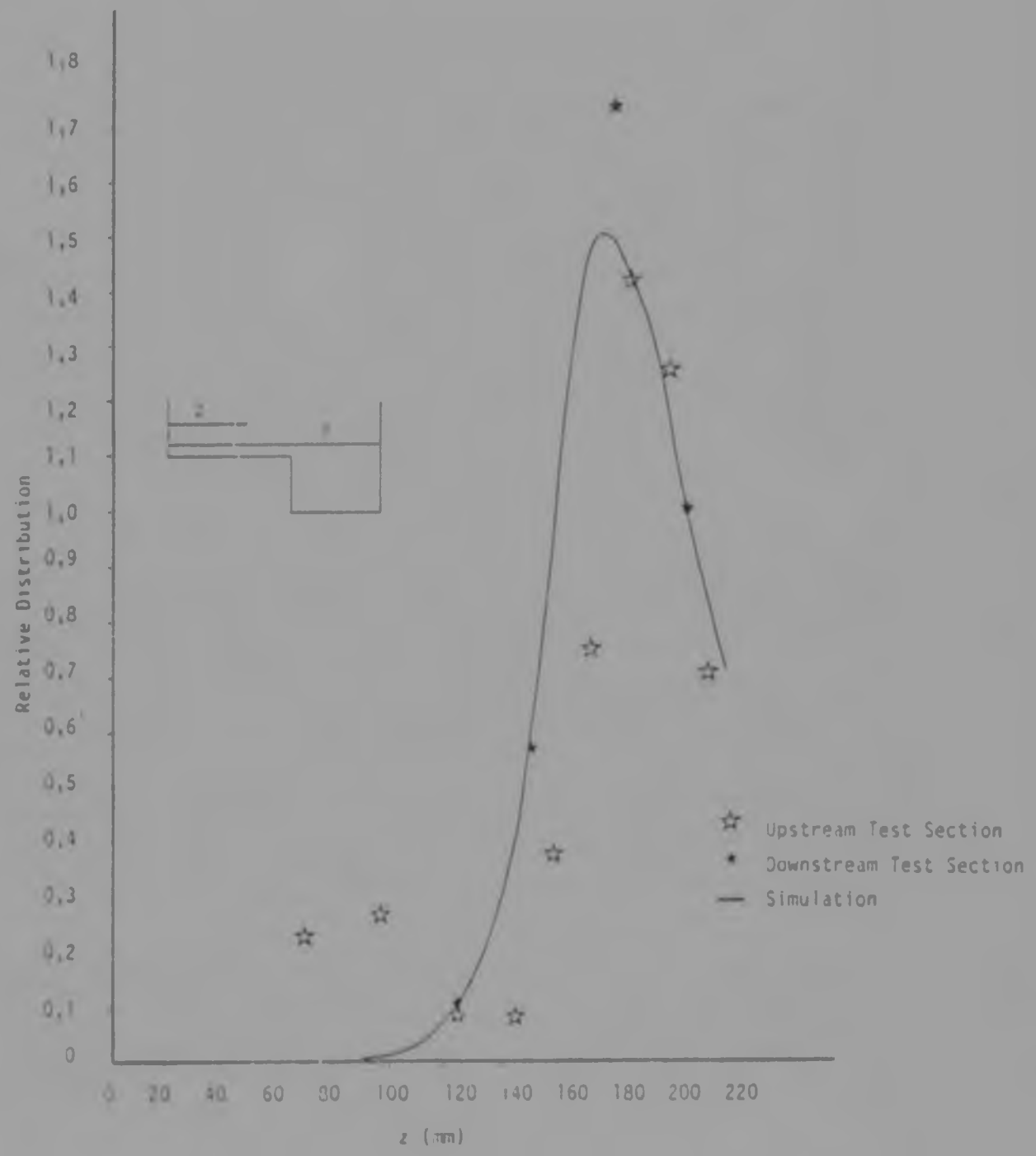


Fig. 6.12 Comparison of measured and simulated distributions for Test 6, 150 - 300 μ fraction

7. APPLICATION OF THE TRANSVERSE DISTRIBUTION MODEL

7.1 Introduction

The model has been used to predict the distribution of gold deposits on plain areas adjacent to well-defined channels. Two different types of application were performed. Firstly a hypothetical channel geometry was used to analyse the sensitivity of the deposit distribution with respect to various parameters. Secondly, distributions were generated for channel geometries measured in the reef and these were compared with observed distributions.

7.2 Sensitivity Analysis

A hypothetical channel was used to examine the effect of various input and model parameters on the distribution of gold deposits on the plain in the vicinity of the channel. This was done so that sensitive parameters could be identified. This would help to isolate dominant effects and provide a guide for identifying important features in the reef when applying the model to practical cases.

The cross-sectional geometry of the hypothetical channel is shown in Fig. 7.1. As a basis for comparison a flow depth of 0, m and a longitudinal gradient of 0,001 were

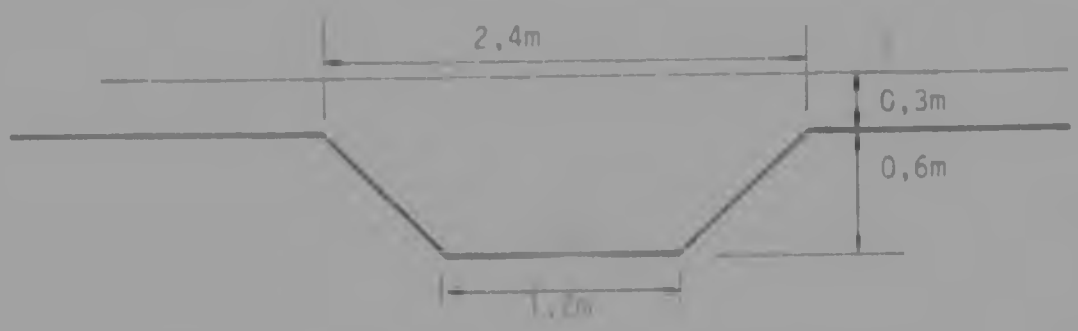
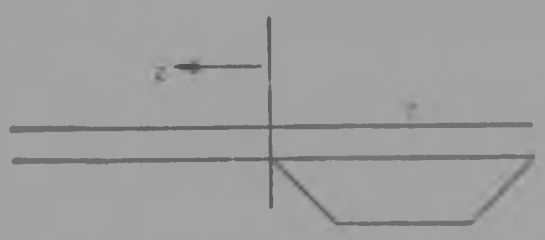


Fig. 7.1 Hypothetical channel geometry



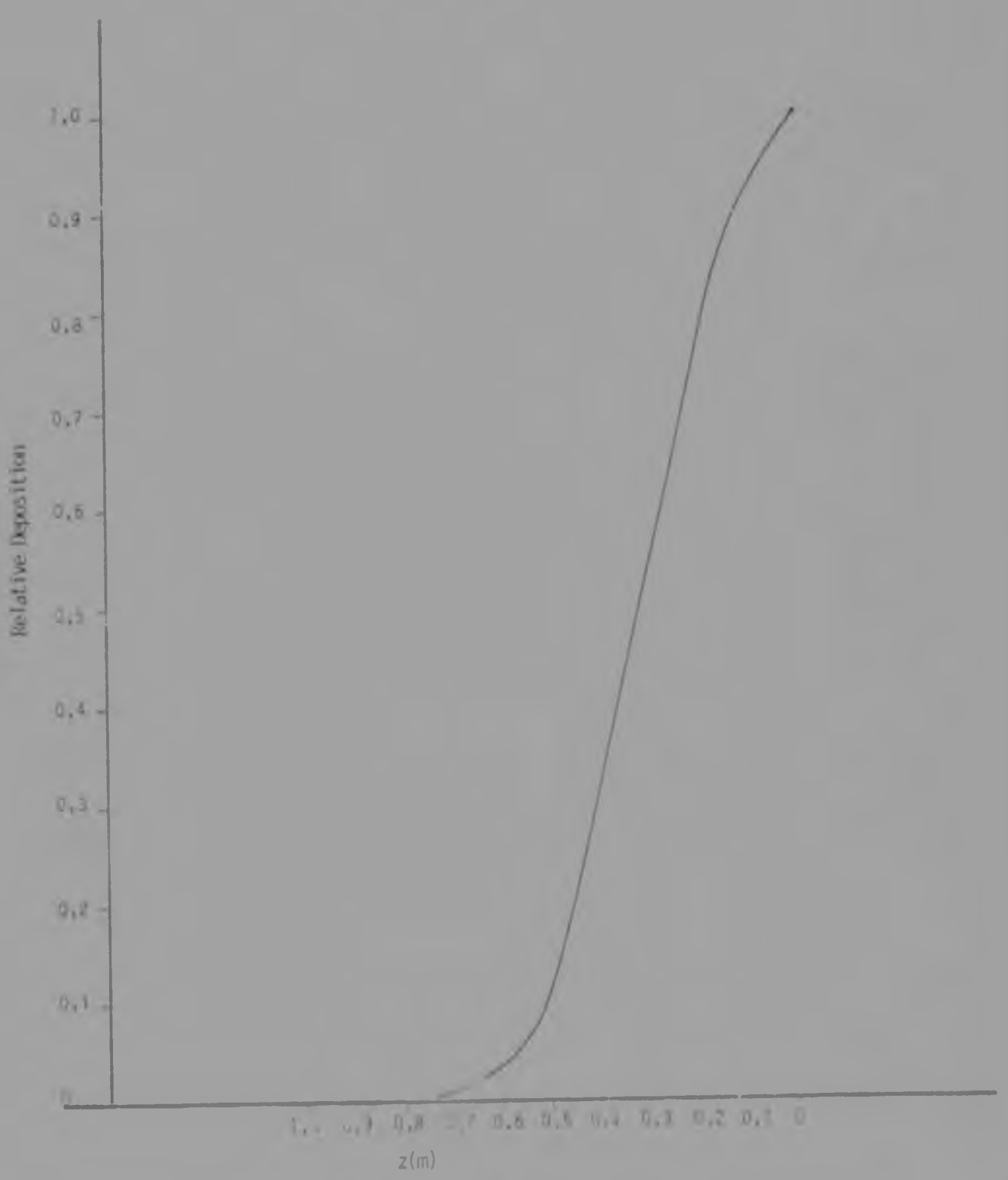


Fig. 7.2 Relative transverse distribution of deposited gold for standard conditions



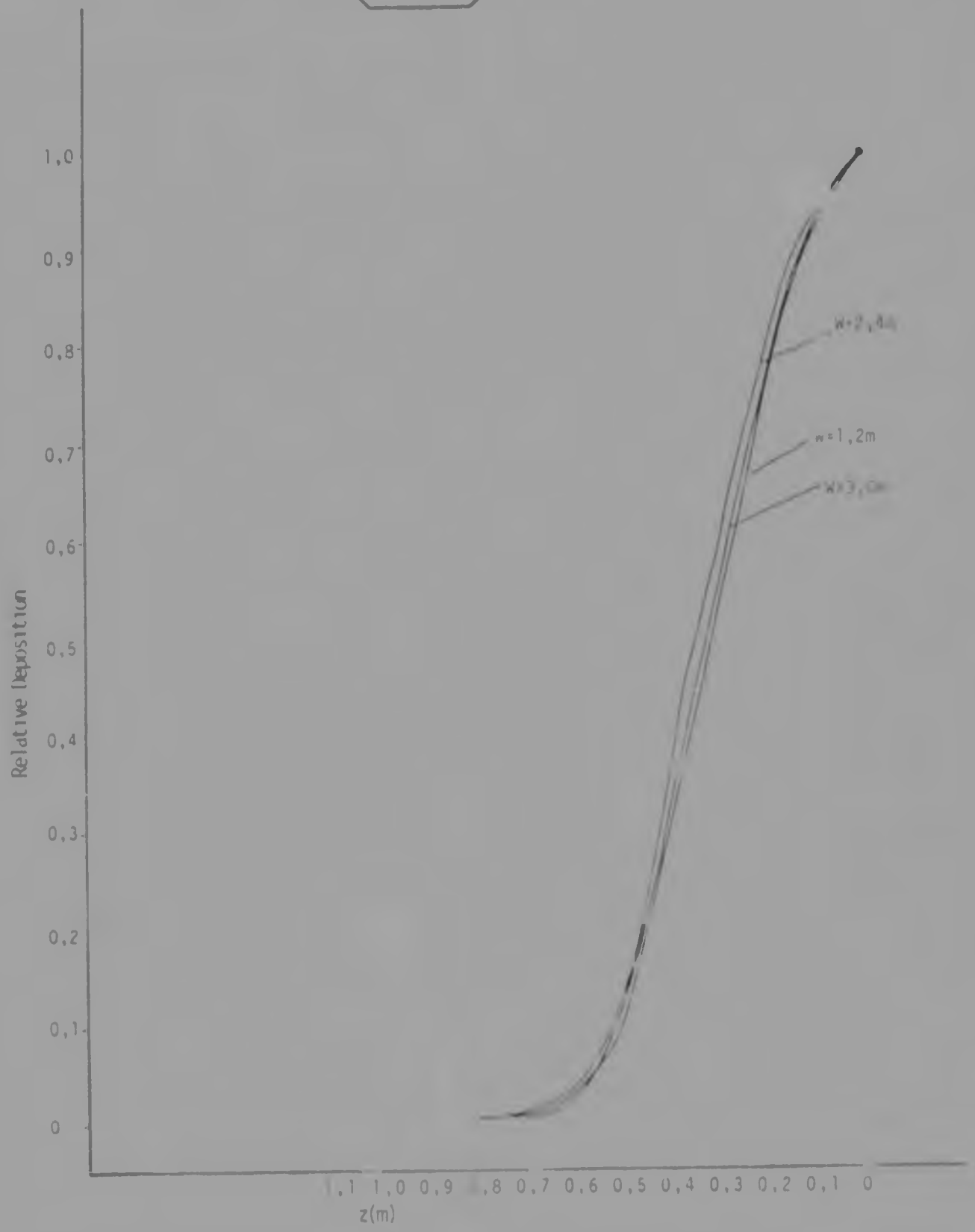
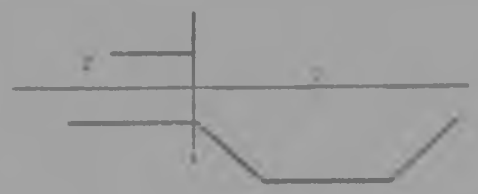


Fig. 7.3 Effect of plain width on gold distribution



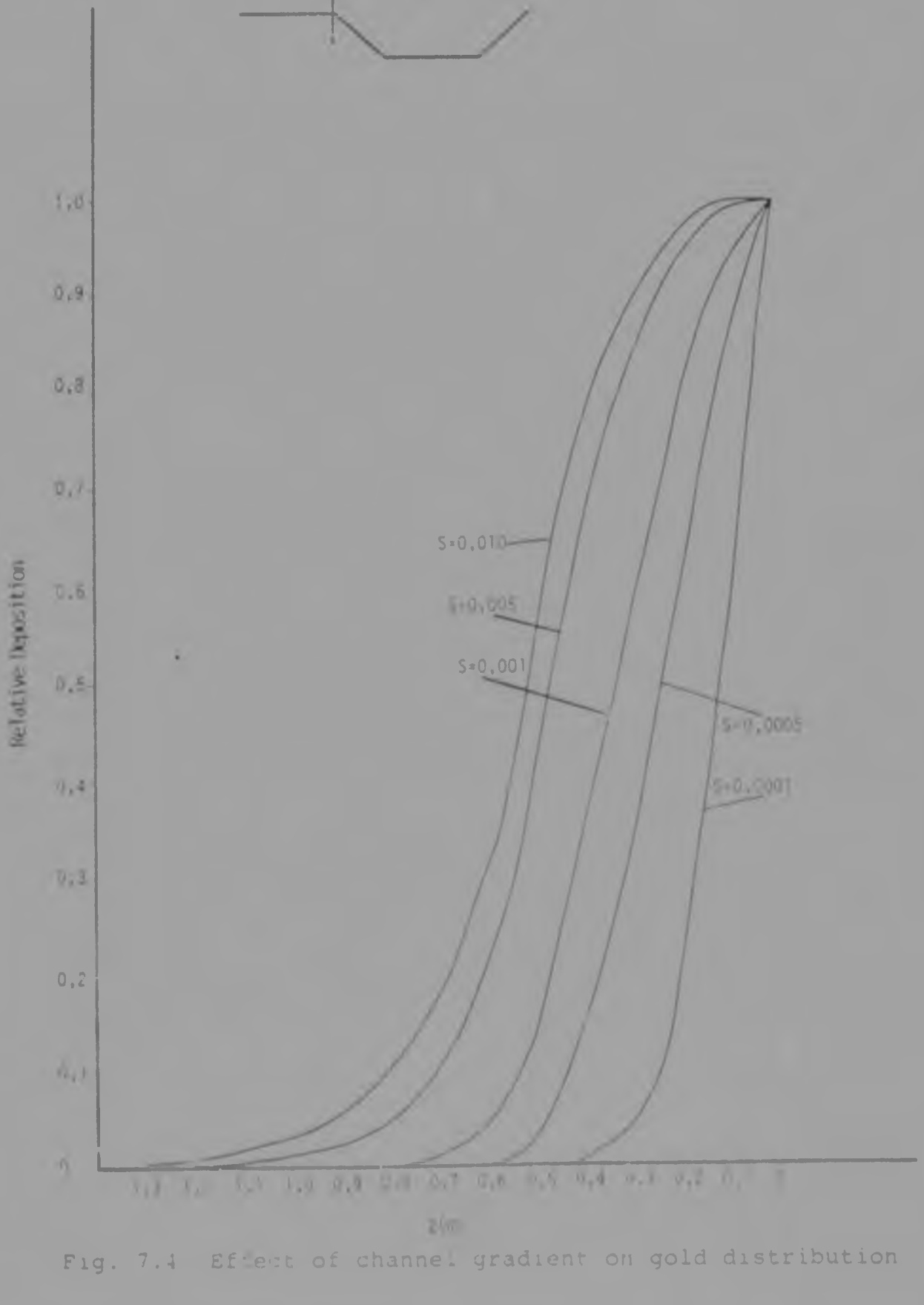


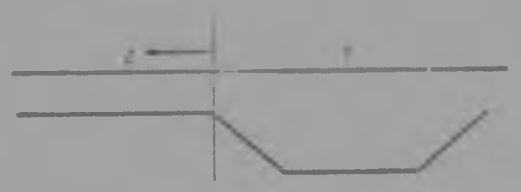
Fig. 7.4 Effect of channel gradient on gold distribution

assumed and the channel was assumed to be parallel to the steepest gradient of the plain. It was further assumed for most analyses that the plain was 2,40m wide and bounded by a solid vertical boundary on the side opposite to the channel. Gold particles in suspension were assumed to have an average diameter of 0,140 mm, a fall velocity of 0,035 m/s and a specific gravity of 19,3. A suitable grid size for the finite difference solution of the diffusion-settling equation was determined by using a progressively finer mesh until halving the spacing in both directions had a negligible effect on the results.

The relative distribution of deposited gold for the above conditions is shown in Fig. 7.2.

The first parameter to be varied was the width of the plain to confirm that the width assumed for the other analyses would be too large to affect the distribution. The width was kept small to keep computational time short. The lower limit is equal to the width of the interaction zone which is twice the length scale defined by equation 4.11) and is 0,07m for this case. A range of widths between 1,2m and 3,0m were used and the effect on the distribution was negligible, as shown in Fig. 7.3. This indicated that the distribution would be unaffected as long as the plain width exceeded the extent of the deposit. A width of 2,40 m was nevertheless used for the other analyses to allow for more extensive distributions as other factors were varied.

The hydraulic gradient proved to be a relatively sensitive parameter although a wide range of values were used. As can be seen in Fig. 7.4 the extent of the deposit increased by a factor of about three as the gradient was increased from 0,0001 to 0,01. This trend is to be expected as increasing the gradient would



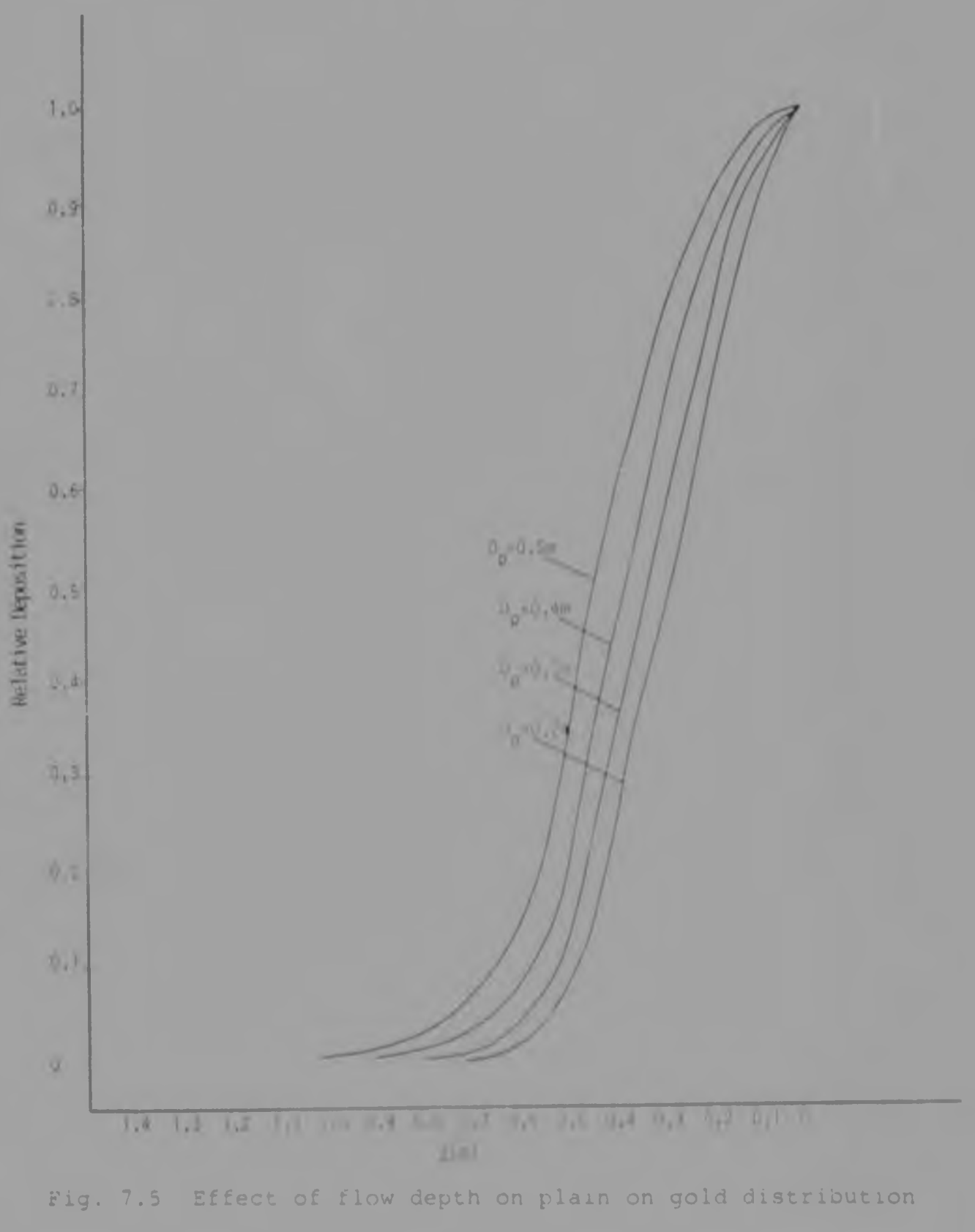
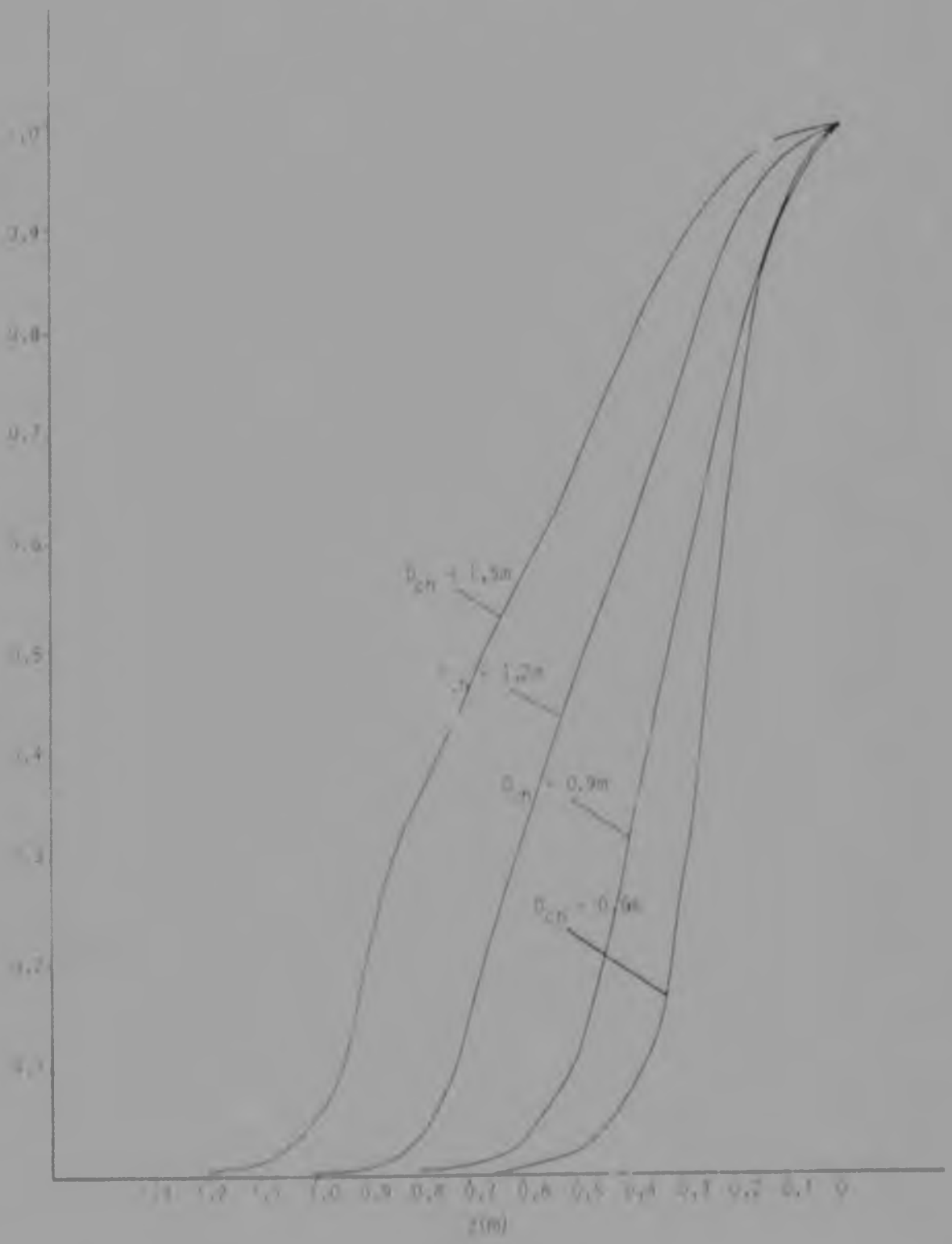


Fig. 7.5 Effect of flow depth on plain on gold distribution





Effect of flow depth on channel on gold distribution



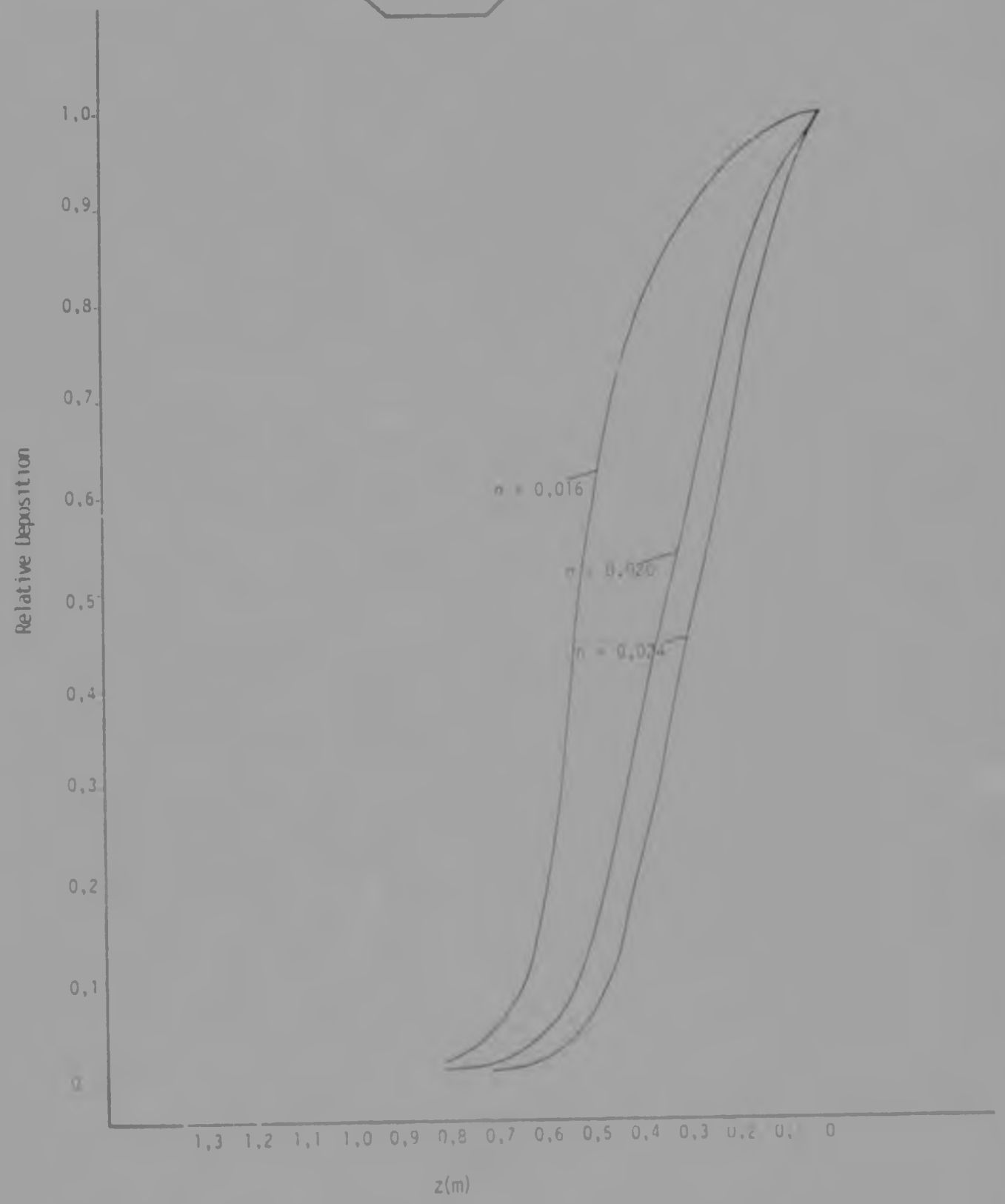


Fig. 7.7 Effect of Manning's n on plain on gold distribution

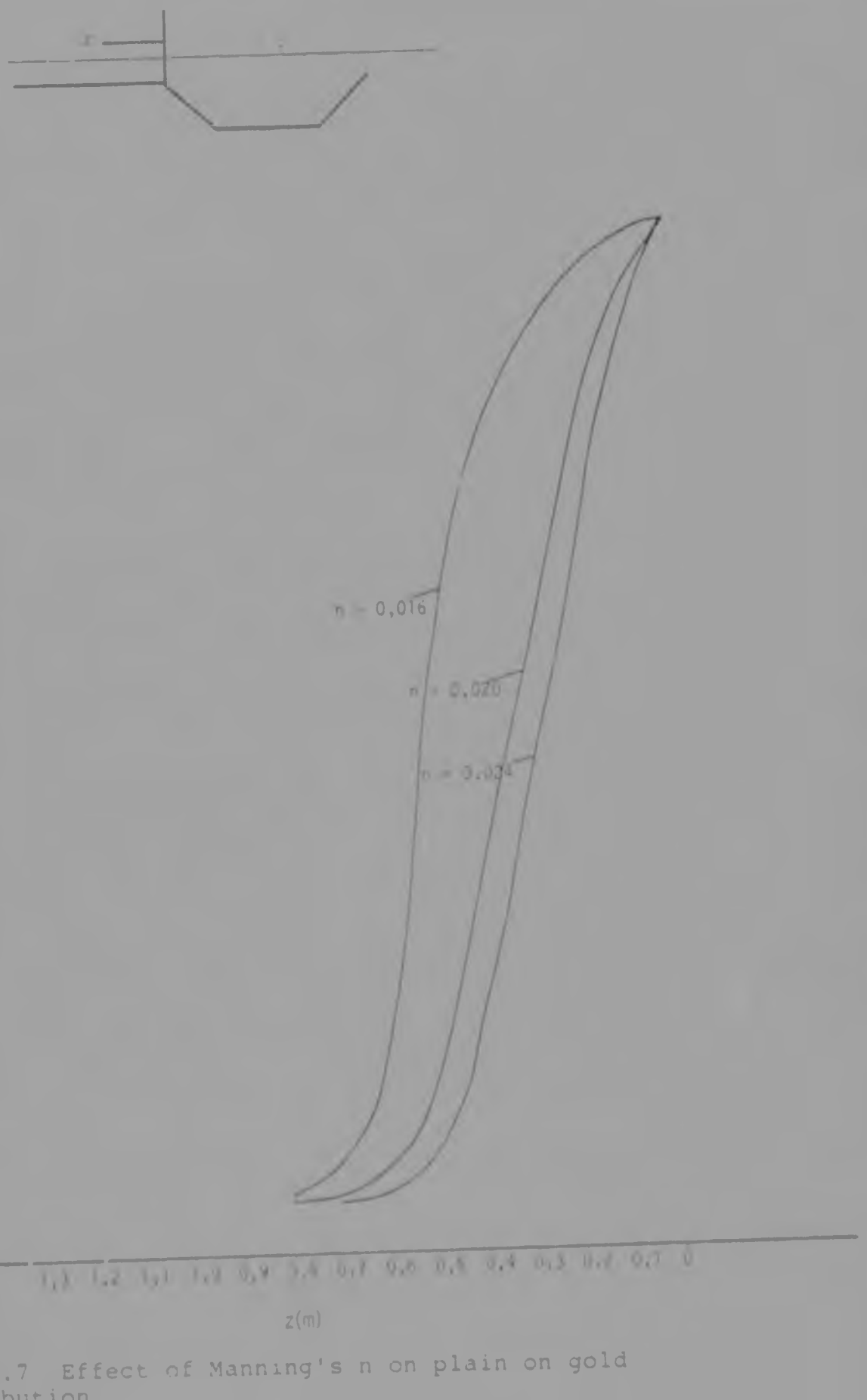
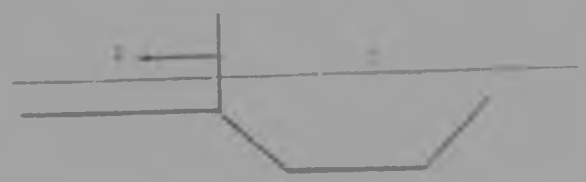


Fig. 7.7 Effect of Manning's n on plain on gold distribution



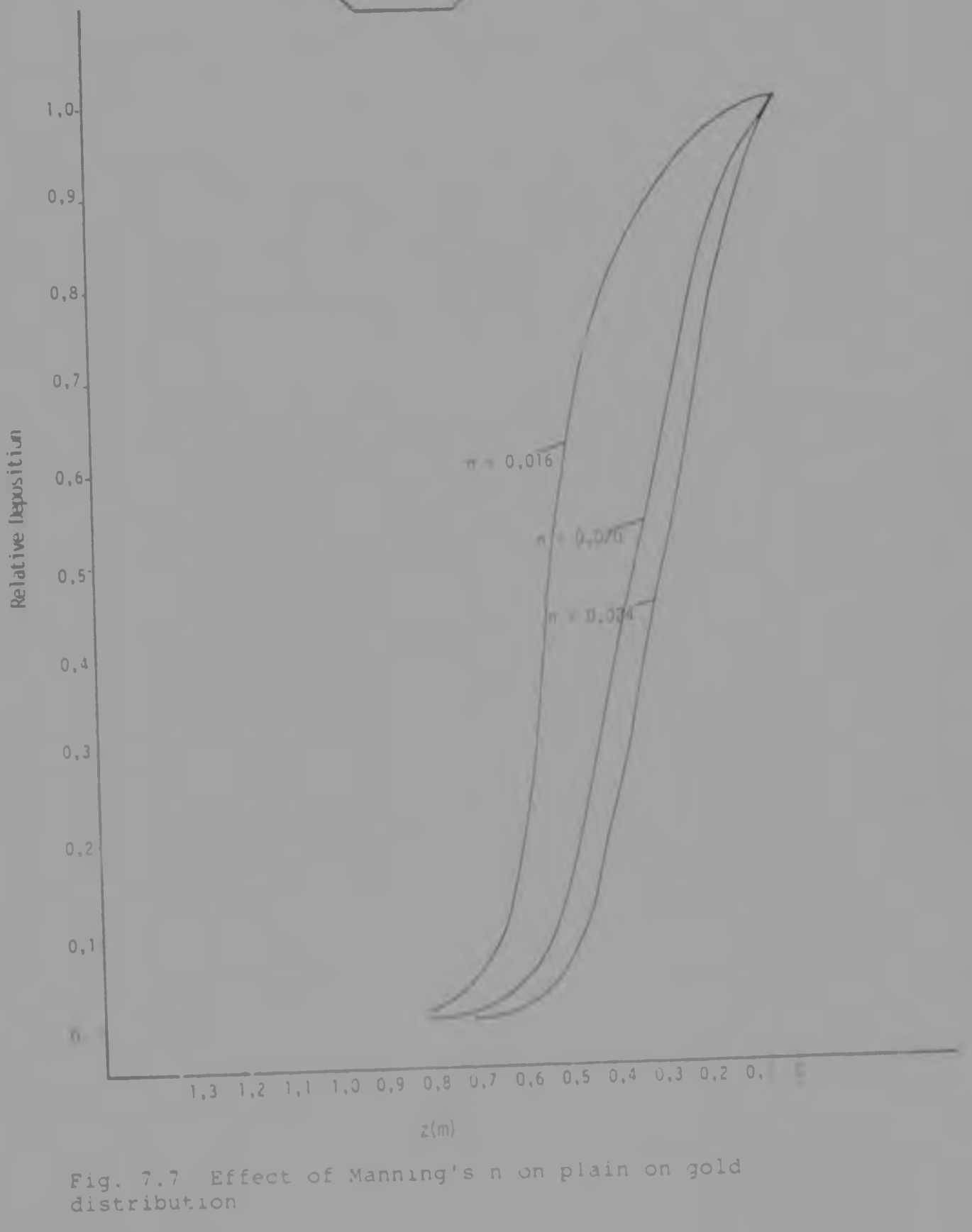


Fig. 7.7 Effect of Manning's n on plain on gold distribution



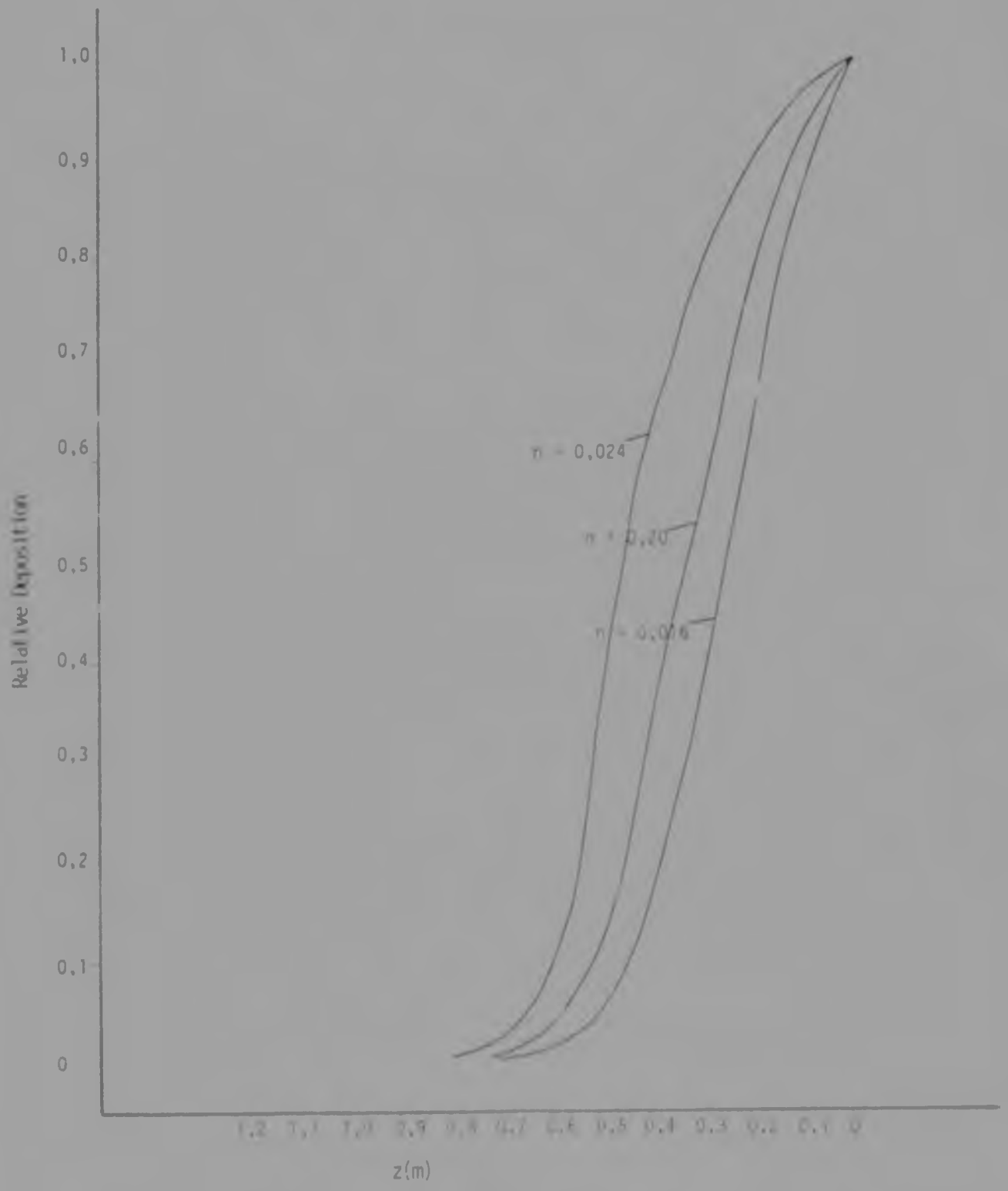


Fig. 7.8 Effect of Manning's n in channel on gold distribution

increase the flow velocity and hence the intensity of turbulence in the interaction zone.

The depth of flow on the plain had a relatively minor effect on the distribution, as shown in Fig. 7.5. An increase in depth of about 2,5 times caused the extent of the deposits to increase by about 40%. This suggests that variations in discharge and hence depth during a particular flood event would not affect the distribution significantly. The relative distribution (but not the mass of deposits) is therefore probably not affected by duration and frequency of flood events as much as by other factors.

The size of the channel was varied while keeping the same cross-sectional shape. Both transverse diffusivity (equation (4.15)) and vertical diffusivity (equations (4.6) to (4.11)) are directly proportional to the channel flow depth. An increase in channel depth would therefore considerably enhance transport of sediment by diffusion. The significant effect of the channel depth as the distribution of plain deposits is shown in Fig. 7.6. An increase in channel depth from 0,6m to 1,5m caused the extent of deposits to increase by a factor of about 2,25.

The effect of resistance to flow in the channel and on the plain was examined by varying Manning's n independently for both surfaces. Fig. 7.7 and Fig. 7.8 show that as the plain is made smoother relative to the channel the extent of the deposits is increased slightly. Equation (4.15) shows that transverse diffusivity through the interaction zone is indirectly proportional to the velocity difference between channel and plain but the dependence is not as strong as on the channel depth.

The surface roughness on both channel and plain surface



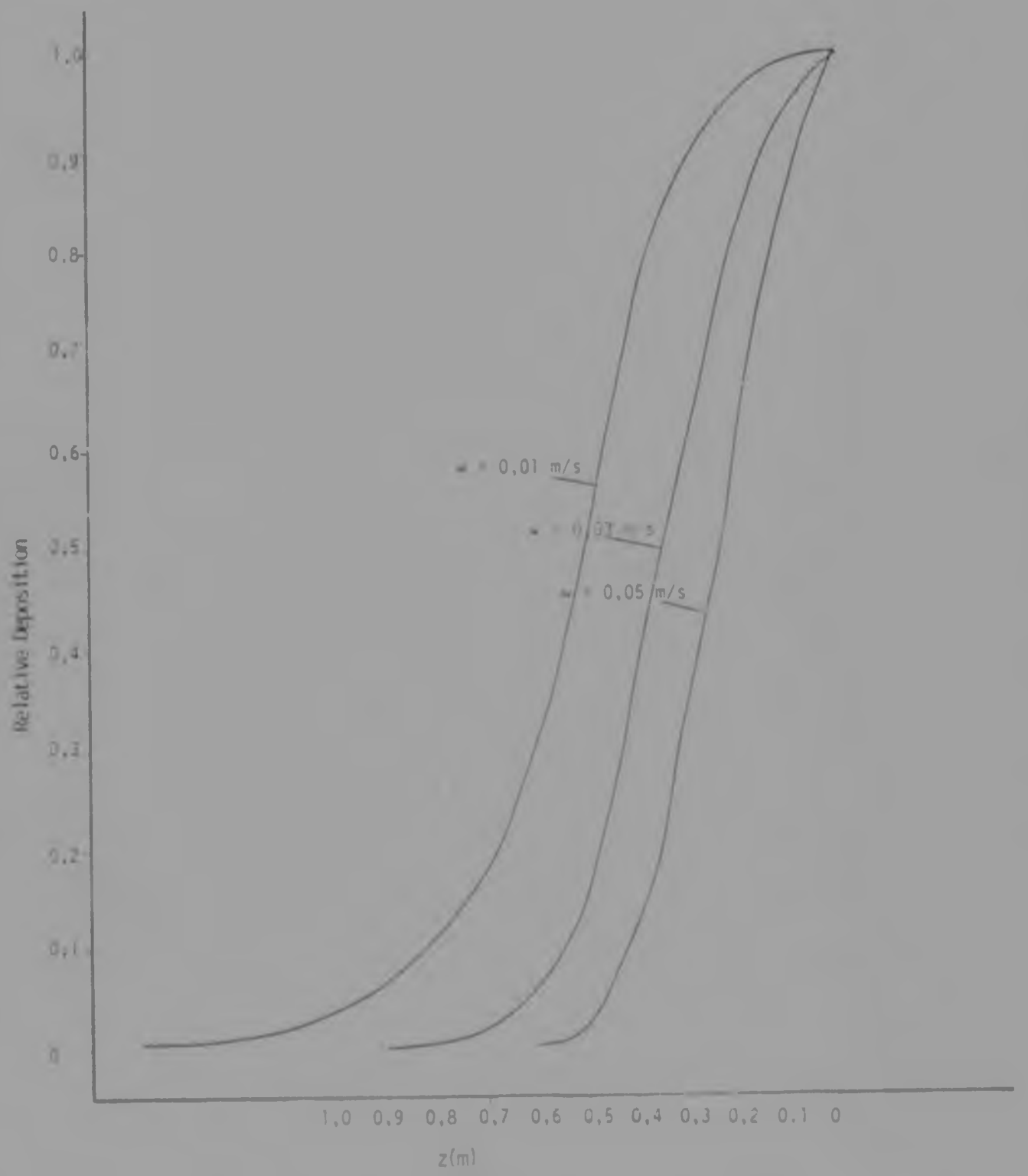


Fig. 7.9 Effect of particle fall velocity on gold distribution



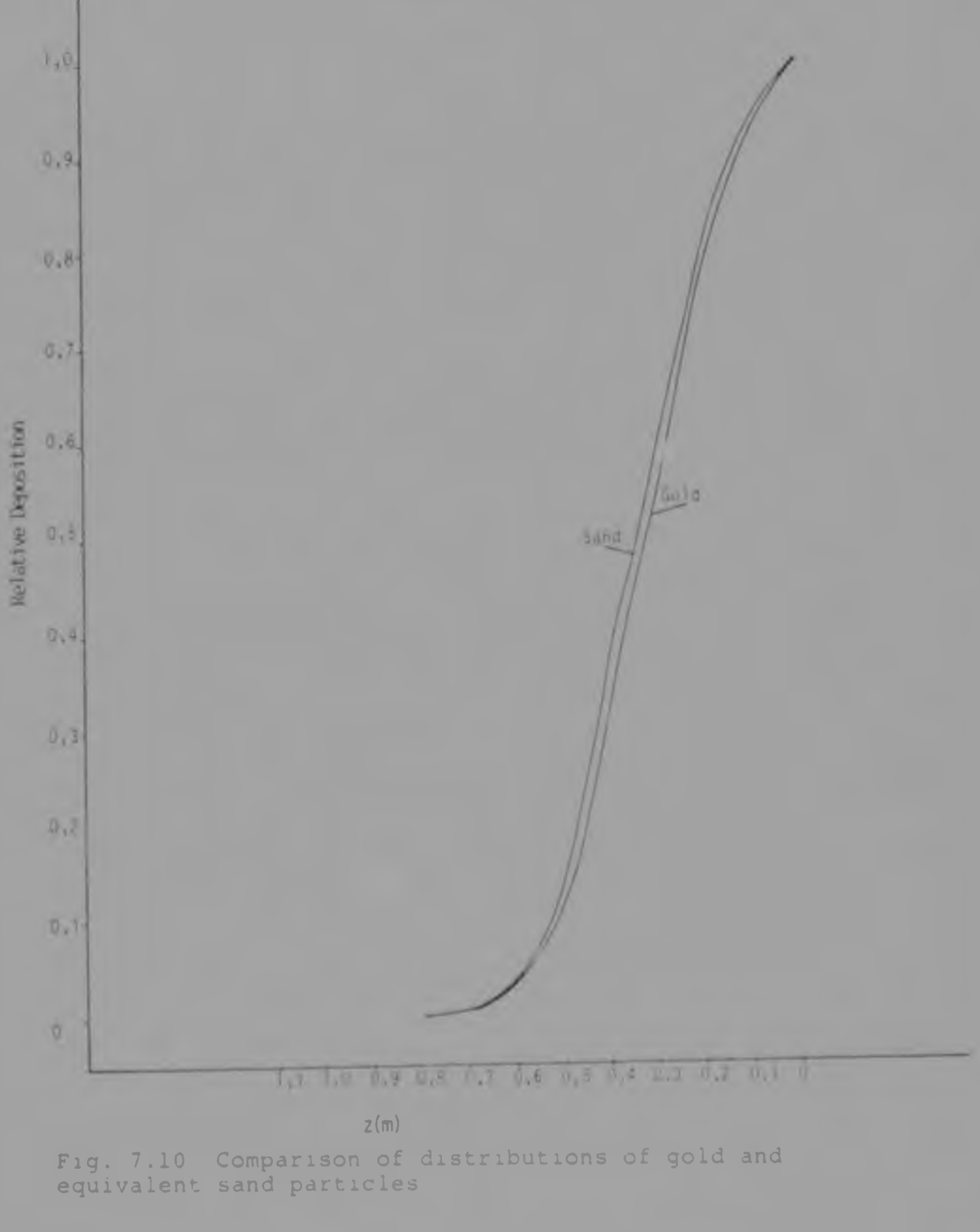


Fig. 7.10 Comparison of distributions of gold and equivalent sand particles

was varied over a wide range and the effect in both cases was negligible. Surface roughness affects the velocity distribution in the vertical direction (equation (4.26) and hence the value of shear velocity which is used to evaluate vertical and transverse diffusivities. Sediment distribution is shown to be insensitive to this effect. The surface roughness is also used in the model to define the height above the channel bed at which the reference concentration is specified; the reference concentration is assumed to occur at a height above the bed equal to twice the diameter of bed particles, or surface roughness. This height will therefore have a very significant effect on the vertical boundary concentrations. The insensitivity of the distribution to the surface roughness implies that the distribution of deposits is also not unduly affected by the vertical distribution of suspended material in the channel.

The fall velocity of the gold particles was varied between 0,01 m/s and 0,05 m/s and the effect of this variation on the deposit is shown in Fig. 7.9. Although the distribution is fairly sensitive to fall velocity the characteristics of gold particles are known and the fall velocity can be predicted quite accurately.

The model was also run using quartz density particles with a mean diameter of 0,3mm which have the same fall velocity as 0,140 mm gold particles. The deposit distribution was almost identical (Fig. 7.10) indicating that the allowance for the dependence of the ratio of diffusivities of sediment and momentum on particle size (equations (4.19) is relatively unimportant. It must be stated, however, that the deposition and entrainment characteristics of the gold and sand particles could be very different although their behaviour while in suspension is similar. Simulation of deposition in the model assumes that settling particles

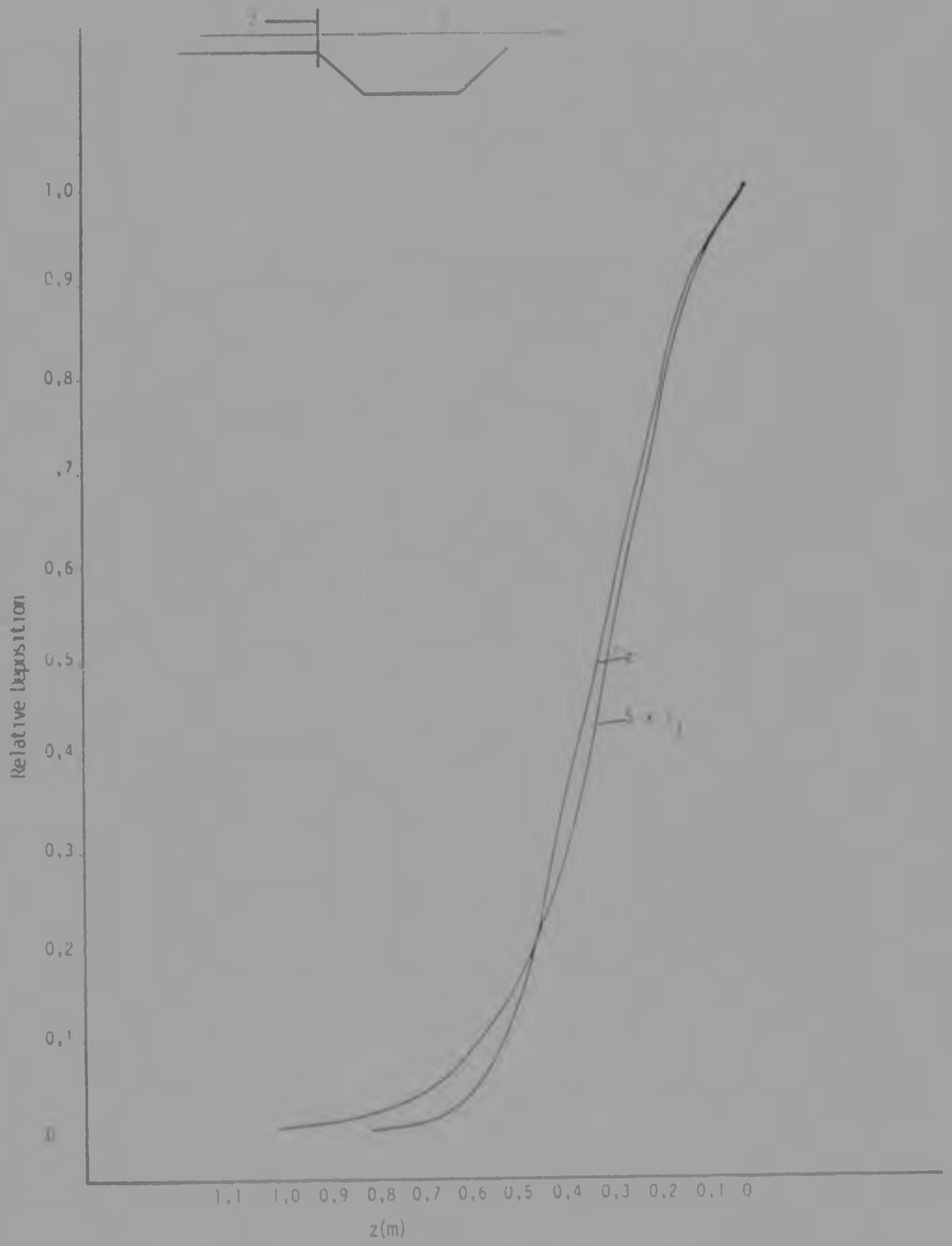


Fig. 7.11 Effect of transverse diffusivity on gold distribution

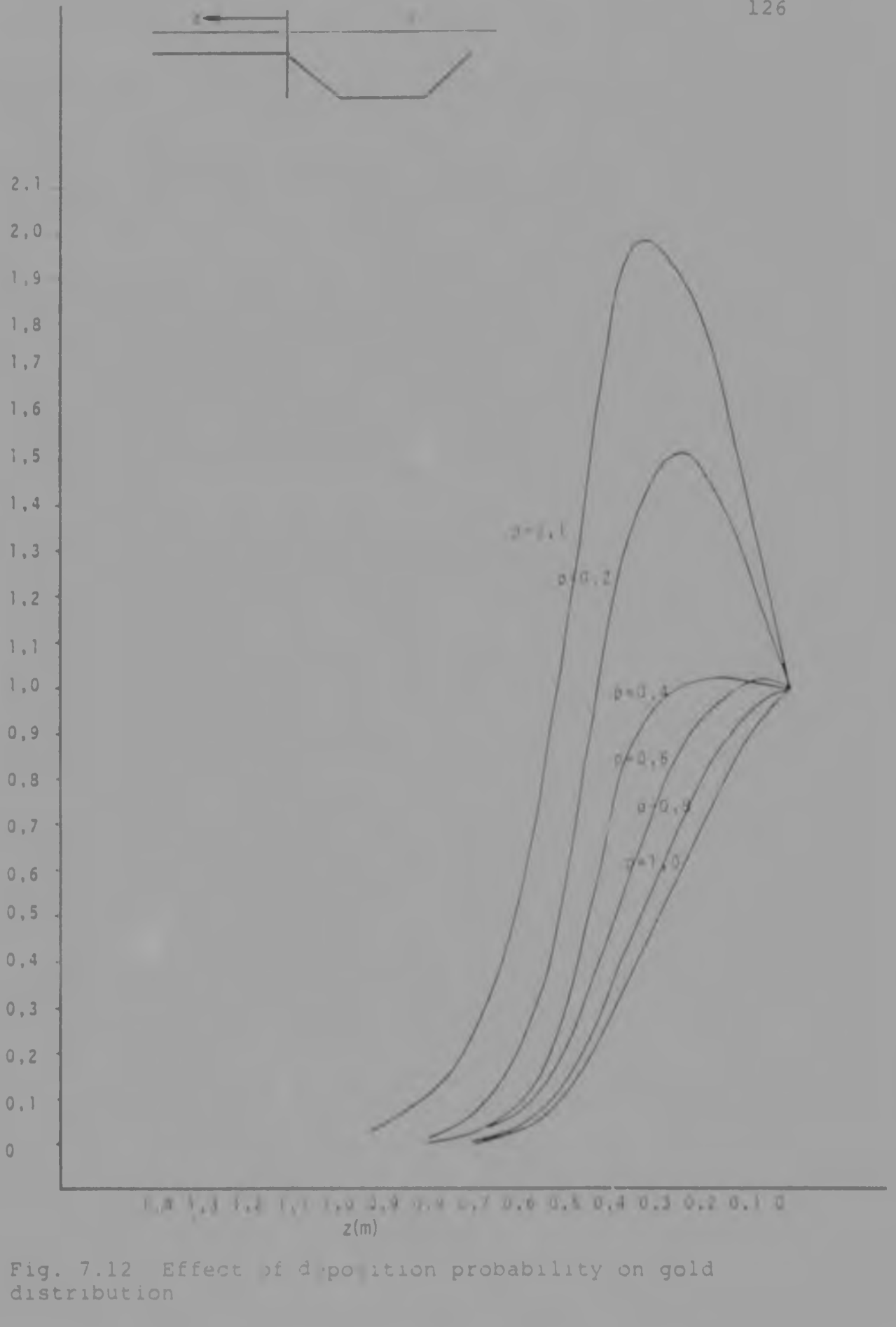


Fig. 7.12 Effect of deposition probability on gold distribution

are small compared with bed particles. On a granular bed it is possible that gold particles would be deposited while 'equivalent' sand particles would be immediately re-entrained on reaching the surface because their larger size causes them to be more exposed to drag and lift forces than the gold particles. It is also possible that if both sand and gold are deposited a subsequent flood event could cause removal of sand particles but not gold particles. Deposition characteristics have a pronounced effect on the distribution and the model should not be used for particles which are not small compared with the bed particles without modifying the deposition calculation procedures.

Because of the uncertainty associated with the calculation of the undisturbed transverse diffusivity on the plain, especially for small width to depth ratios the model was run with a value of diffusivity equal to five times the usual value. As can be seen in Fig. 7.11 the effect was small and refinement of this calculation is therefore unnecessary.

The probability that a particle settling to the plain bed will deposit and not be available for re-entrainment has a very significant effect on the shape of the relative distribution of deposits. The model incorporates a routine for calculating this probability, which varies across the plain. The effect of deposition probability was analysed by overriding the computed probabilities by various values which were constant across the plain. The relative depositions for values between 0,1 and 1,0 are shown in Fig. 7.12. The shapes of the distributions for the extreme values differ significantly, confirming the results of the laboratory tests. It should be noted that although the peak relative deposit is much higher for low deposition probabilities than for high values, the mass of

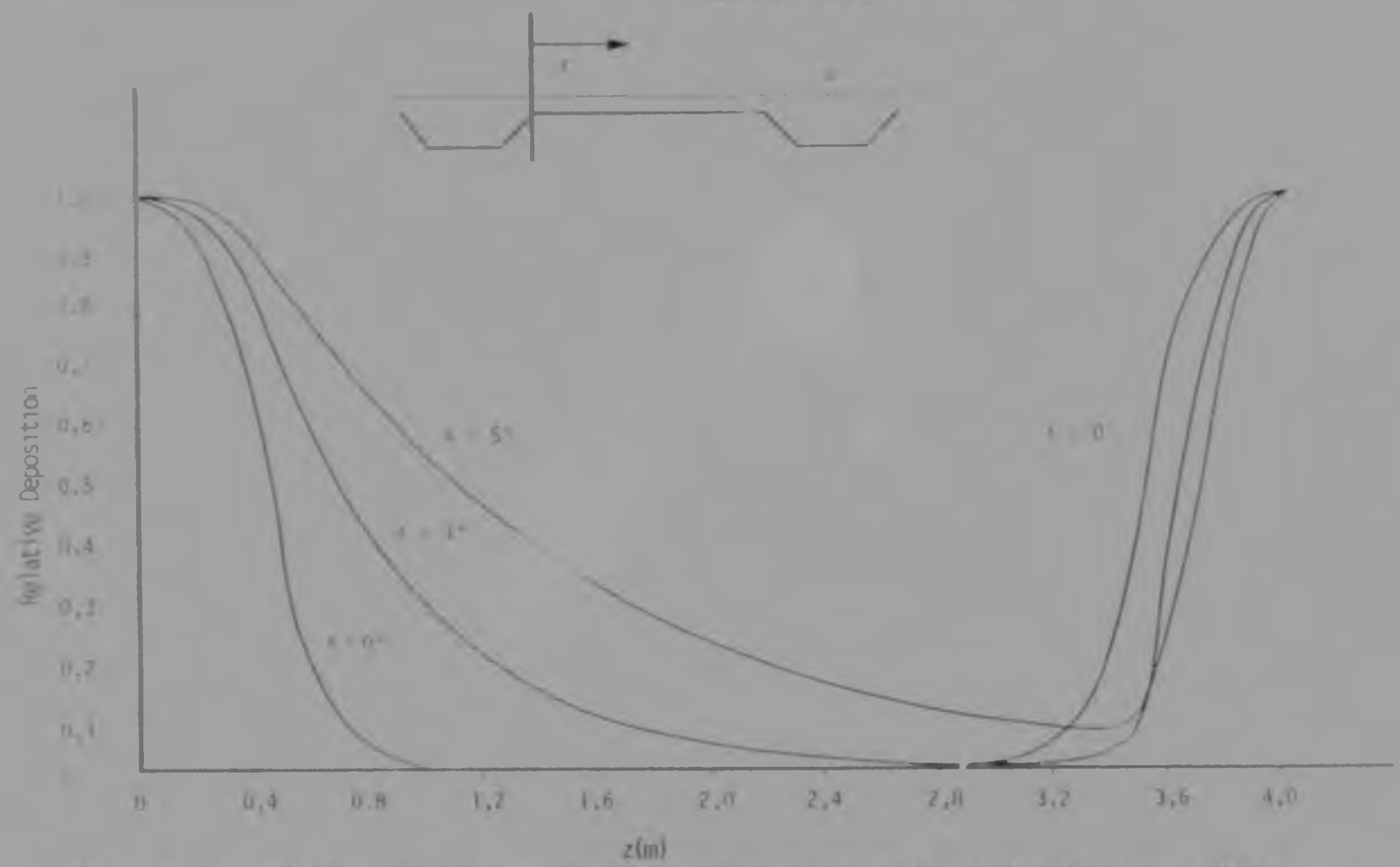


Fig. 7.13 Effect of tran rse convection on gold distribution. (Flow depth and hydraulic gradie.t constant)

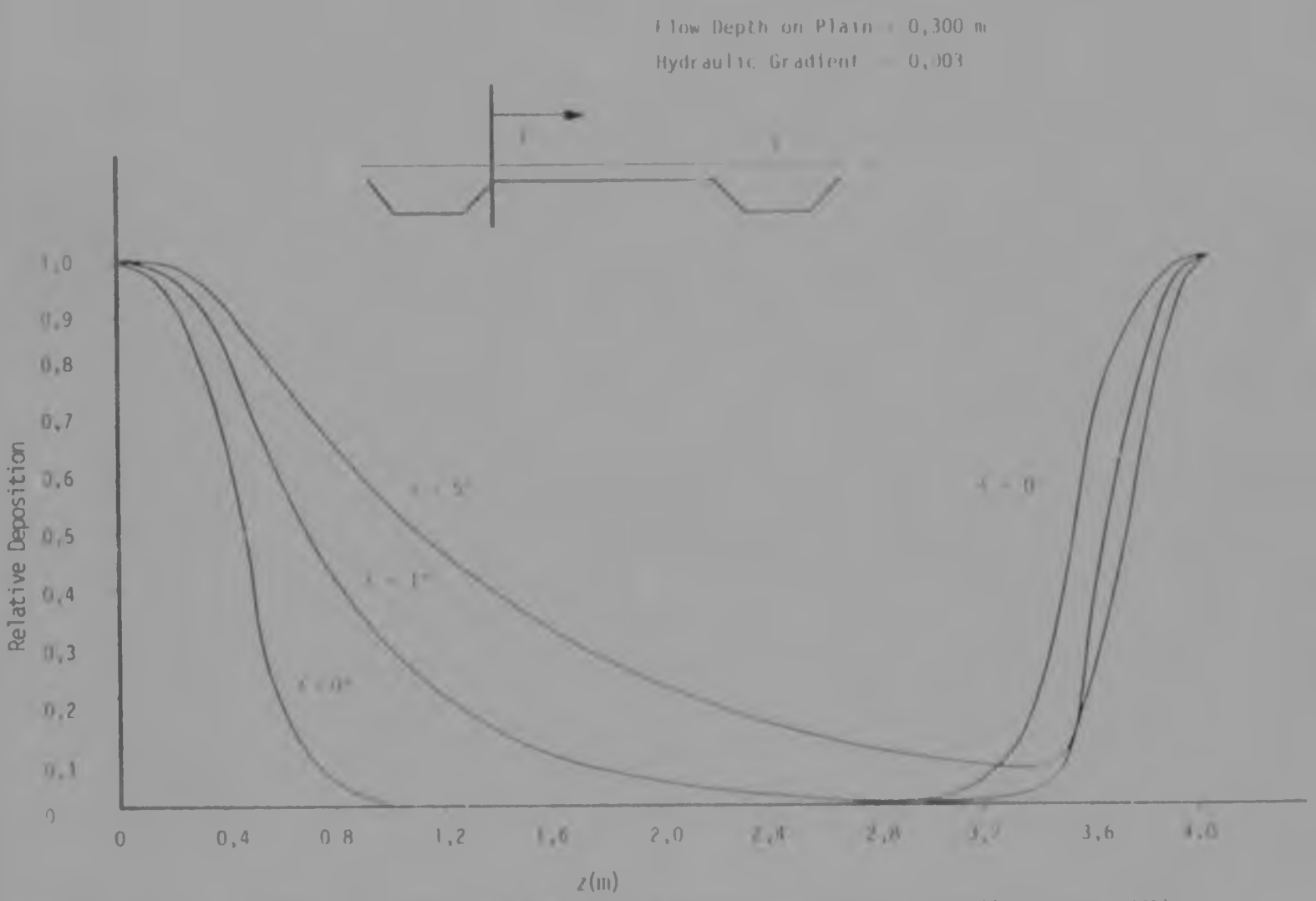


Fig. 7.13 Effect of transverse convection on gold distribution (Flow depth and hydraulic gradient constant.)

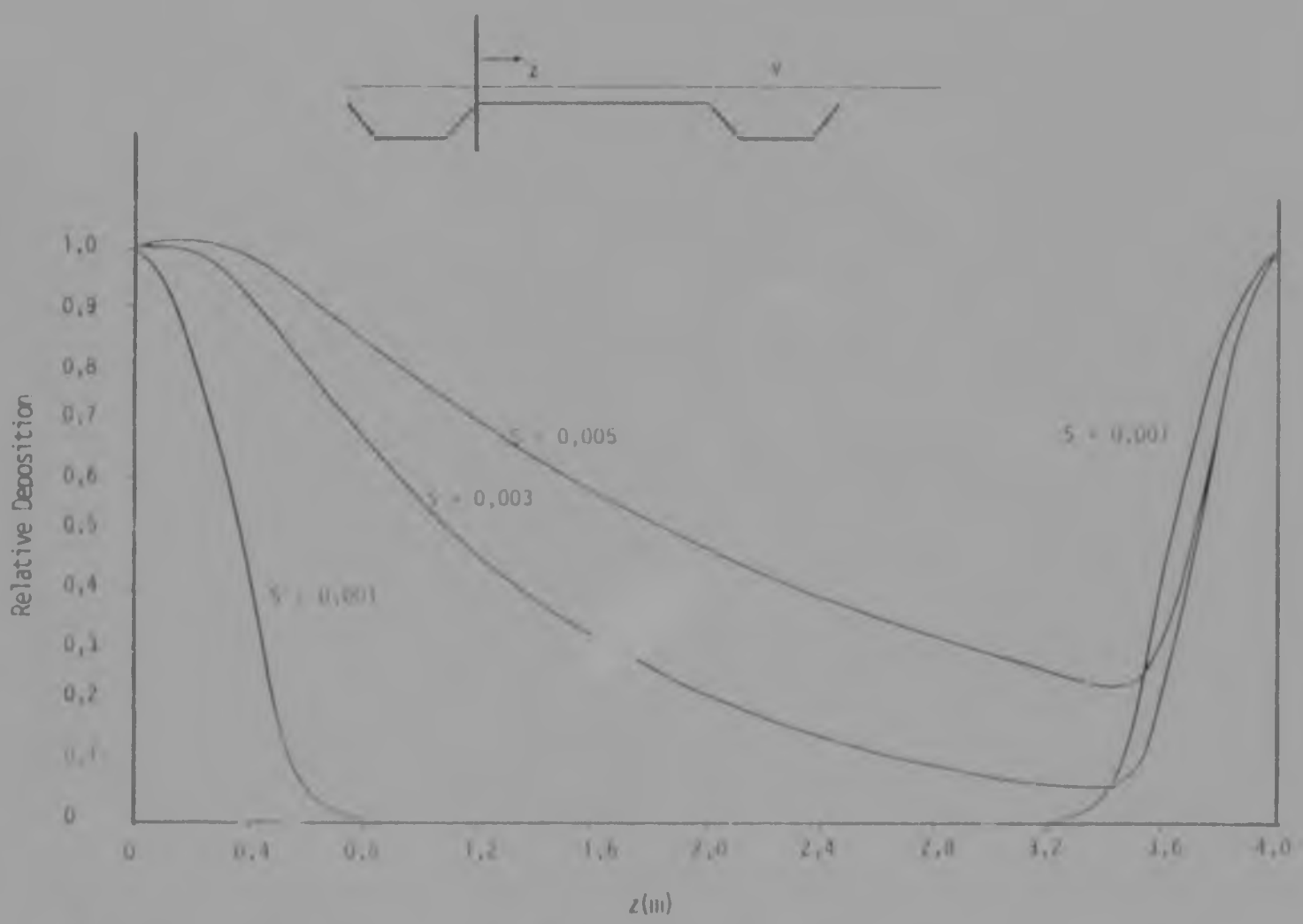


Fig. 7.14 Effect of transverse convection on gold distribution (Flow depth and channel deviation constant)

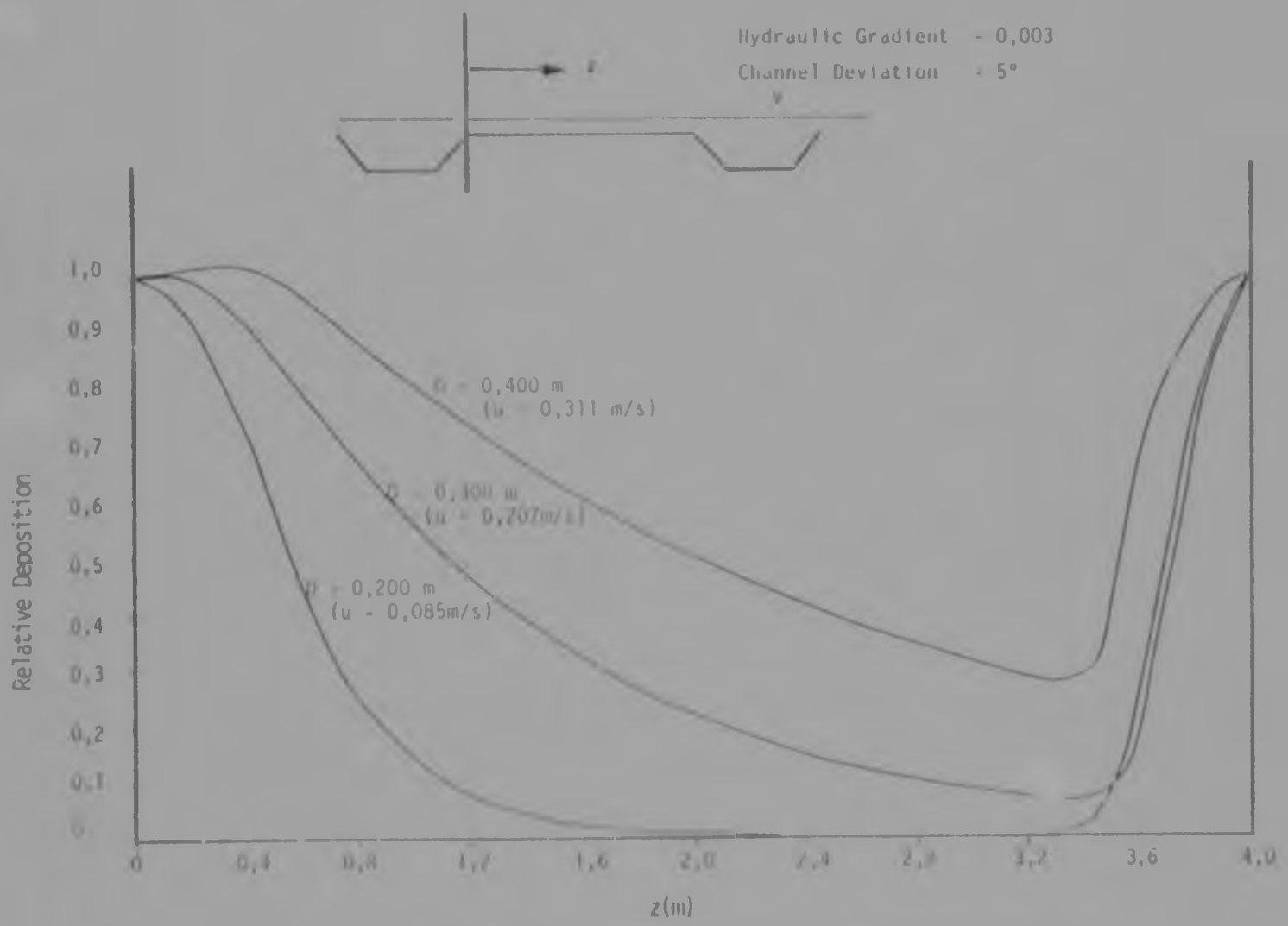


Fig. 7.15 Effect of transverse convection on gold distribution. (Hydraulic gradient and channel deviation constant)

deposited material would actually be much lower for the same event duration.

Although the shape of the distribution is sensitive to deposition probability the extent of deposits is not. The sensitivity is therefore not practically significant. The extent of deposits is likely to be the important result and local variations of deposits caused by other factors in real situations would be just as significant as the effect of deposition probability on the shape of the distribution. Also, although the deposition probability at the time of deposition is not known exactly it should be possible to make an estimate sufficiently accurate for the sensitivity not to be serious.

To analyse the effect of the transverse convective transport component the channel configuration was modified slightly. The distribution between adjacent parallel channels was simulated because a solid vertical boundary is inconsistent with a normal velocity component. These channels were assumed to be 4,0m apart to allow for more extensive deposits. The two channels were assumed to be identical in cross-sectional shape and size and the distribution could therefore be interpreted to obtain the distributions on either side of the same channel.

The transverse convection effect is accounted for by specifying the angle of deviation between the channel direction and the direction of the steepest gradient of the plain. Convective transport is determined by flow velocity and therefore also depends on the longitudinal gradient and the flow depth. Results have therefore been presented in three different diagrams. Fig. 7.13 shows the effect of the angle of deviation for a given flow depth (300mm) and hydraulic gradient (0,003). Fig. 7.14 shows the effect of hydraulic gradient for the

same flow depth and a deviation of 5°. Fig. 7.15 shows the effect of flow depth for a hydraulic gradient of 0,003 and a deviation of 5°. These results show that at small hydraulic gradients and low flow depths the distribution is far less affected by channel deviation than at large hydraulic gradients and deep flows. The effect is small on the side of the channel where diffusive and convective transport components are in opposite directions but where the two components are additive the effect is significant and very extensive deposits result.

This sensitivity analysis has enabled the identification of the parameters which have the most significant effects on the relative distributions of gold on plain areas in the vicinity of channels. The most important parameter is the angle of deviation between the channel direction and the direction of the steepest gradient of the plain. This is the parameter which introduces a convective transport component which can be significantly larger than the diffusive component beyond the interaction zone. The hydraulic gradient and size of the channel affect the extent of deposits, particularly if the channel is not parallel to the direction of the steepest gradient of the plain, in which case their effect is very significant. The most important factor in determining the shape of the relative distribution is the probability of deposition of the particles on the plain surface.

7.3 Comparison with Observed Distributions

Four measured distributions of reef gold concentrations were supplied by the Chamber of Mines. For each distribution a cross-section of the reef structure was provided, which shows clearly the size and cross-sectional shape of the channel and the thickness of the overlying pebble band. The gold is dispersed through

the material within the channel and concentrated at the base of the pebble band over the plain. Measured gold concentrations are given at 15cm intervals over a distance of about 4m along the cross-section. These samples represent single point values of gold concentration. It was not possible to obtain more than one section for each channel because sampling in the mines generally does not proceed in the direction of the channels. If several cross-sections were available for each channel a more representative average distribution could have been obtained. The angle of the cross-sections to the channel direction is also not known. If a cross- section is not perpendicular to the channel the lateral extent of the deposits will be exaggerated.

The sensitivity analysis showed that the most important parameters determining the extent of the deposits are the hydraulic gradient, the flow depth, the deviation of the channel flow direction and the size of the channel. For the measured distributions the only significant parameter that can be obtained from the information available is the size of the channel. The size and shape of each channel were measured directly from the cross-sections and approximated by a symmetrical trapezoidal section. The other three parameters could not be inferred from the cross-sections and realistic values were assigned to them and these were varied until a reasonable fit with the measured distribution was obtained. A hydraulic gradient of 0,01 and flow depths of 0,30 m or 0,5 m were assumed as first estimates. The deviation of the channel direction was then varied to change the distribution. The final measured and simulated distributions are shown in Figs. 7.16 to 7.19.

Simulated distributions are expressed in relative terms only. A relative distribution of 1,0 is assumed to occur at the edge of the channel and this is plotted to

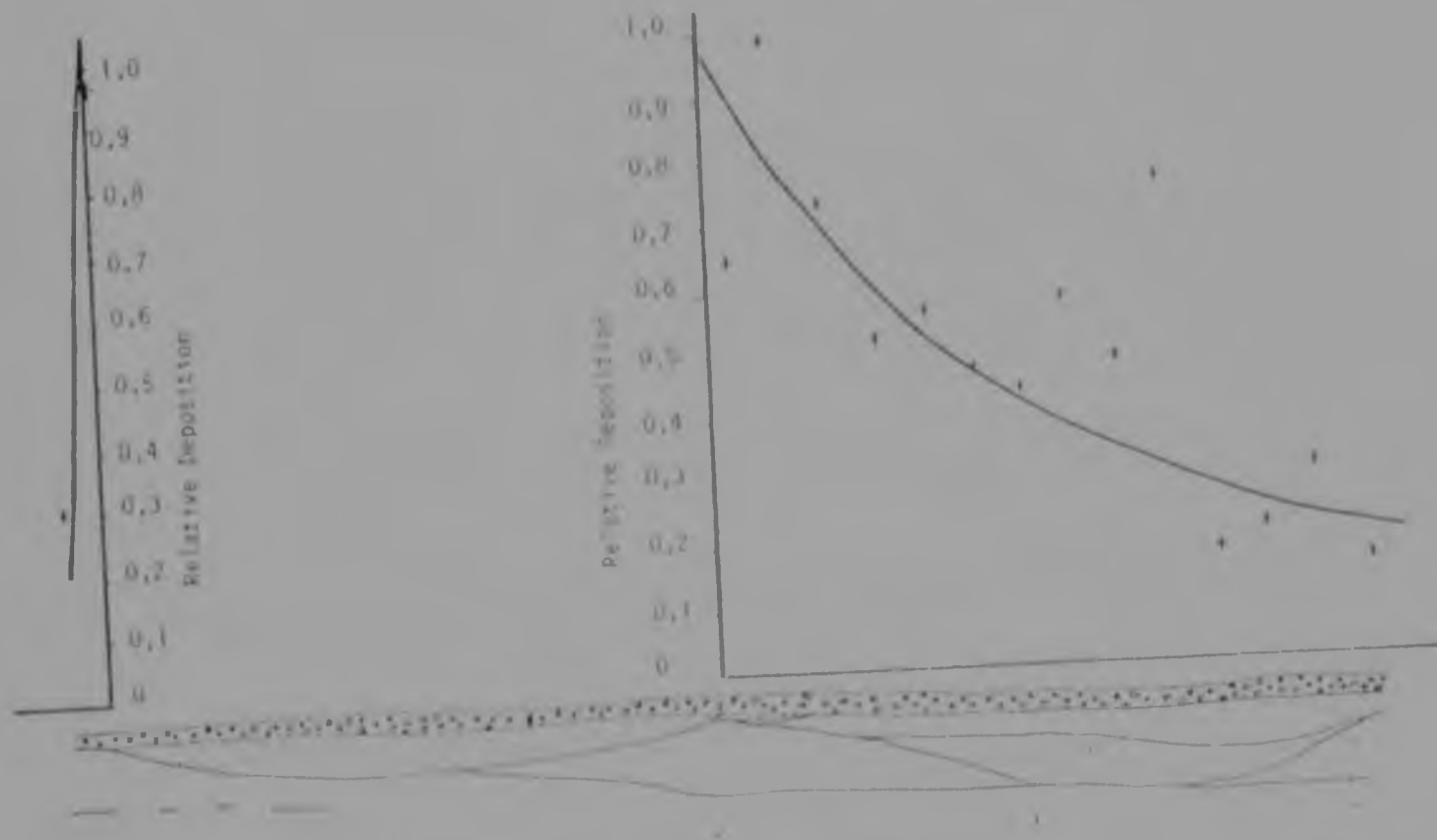


Fig. 7.16 Comparison of observed and simulated gold distributions ((East shaft pillar (a))

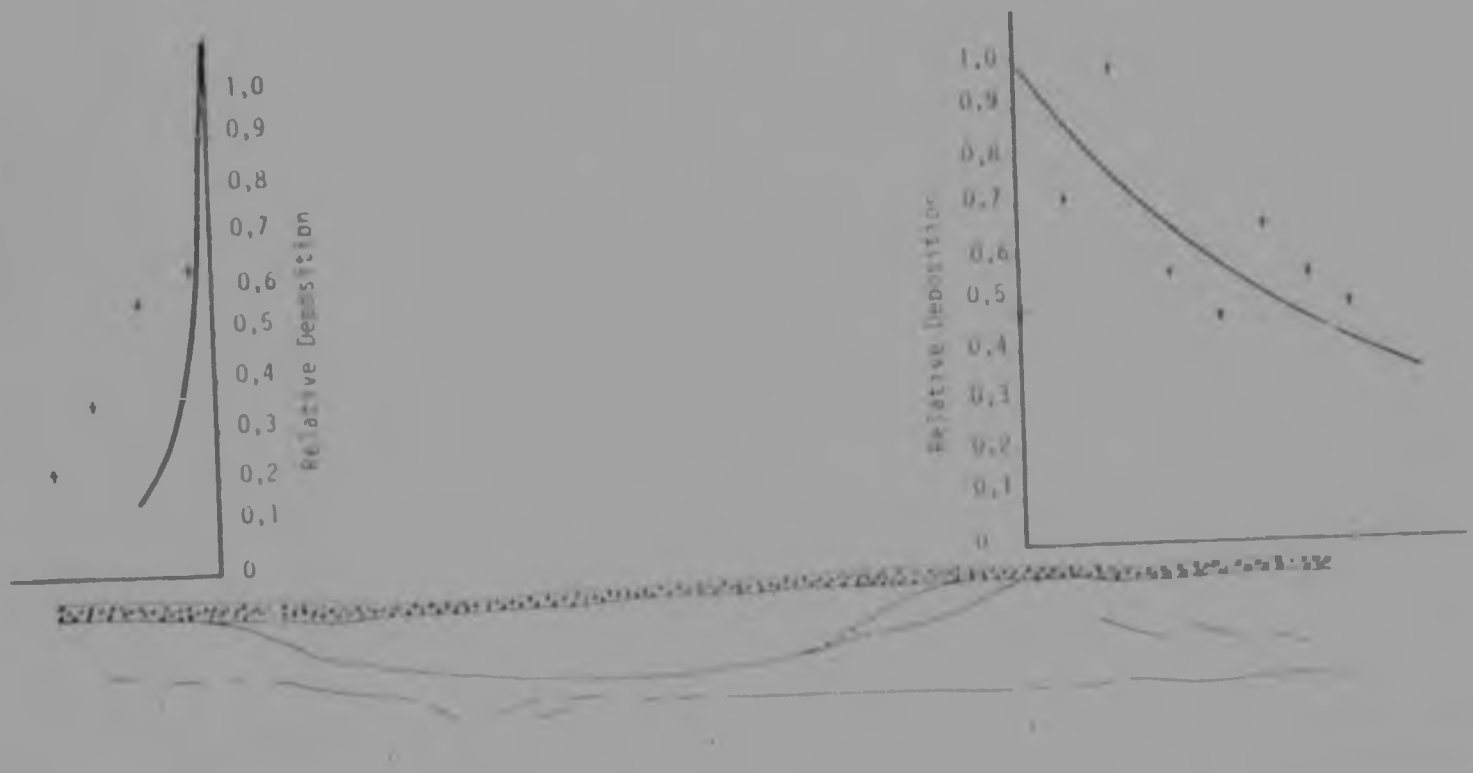
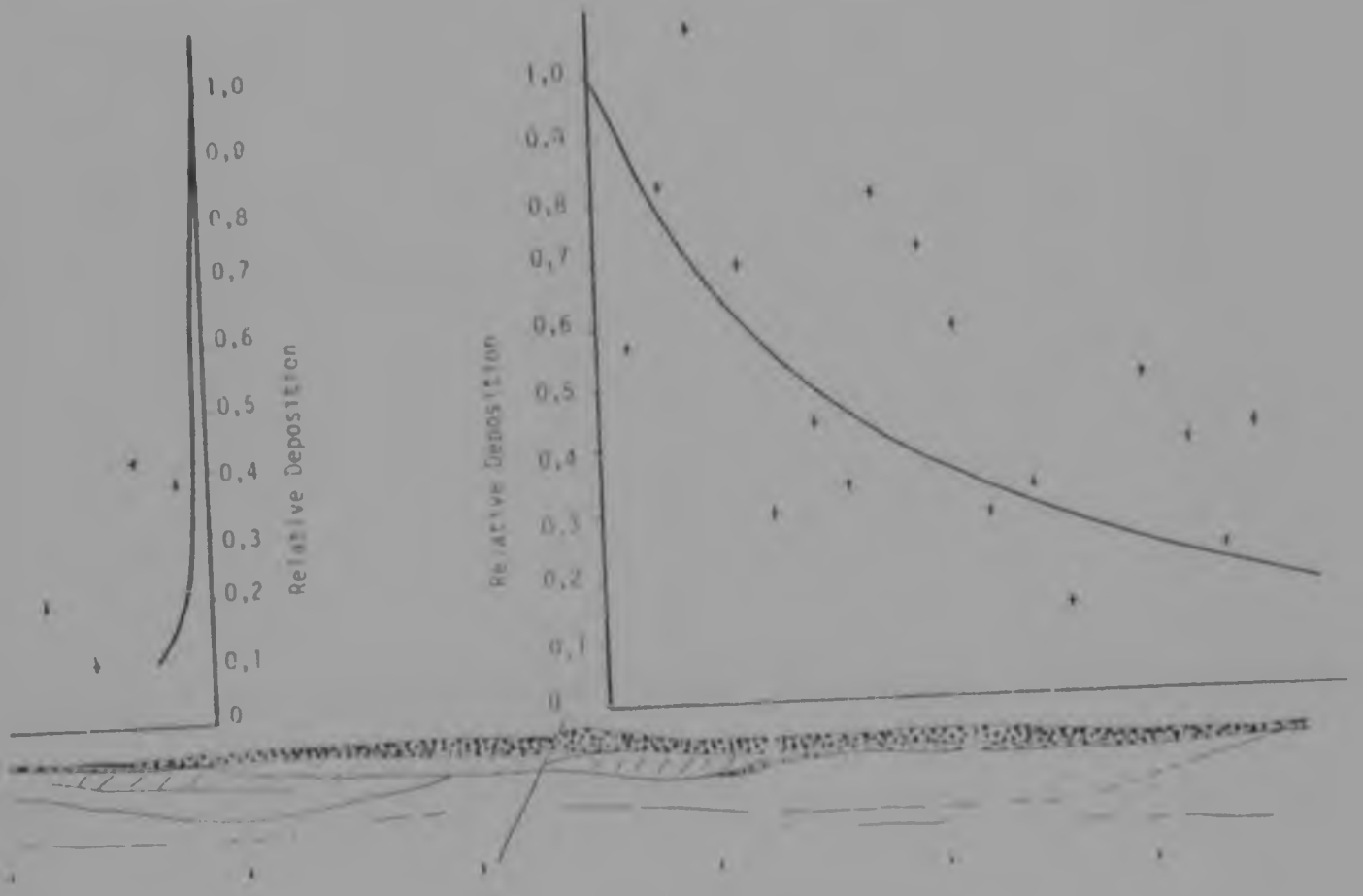


Fig. 7.17 Comparison of observed and simulated gold distributions. (East shaft pillar (b))



Cross-section scales:
Vertical - 1:10
Horizontal - 1:20

• Measured Distribution
- Simulated Distribution for
Flow Depth on Plain = 0,30 m
Hydraulic Gradient = 0,01
Channel Deviation = 10°

Fig. 7.18 Comparison of observed and simulated gold distributions (NIB 13)

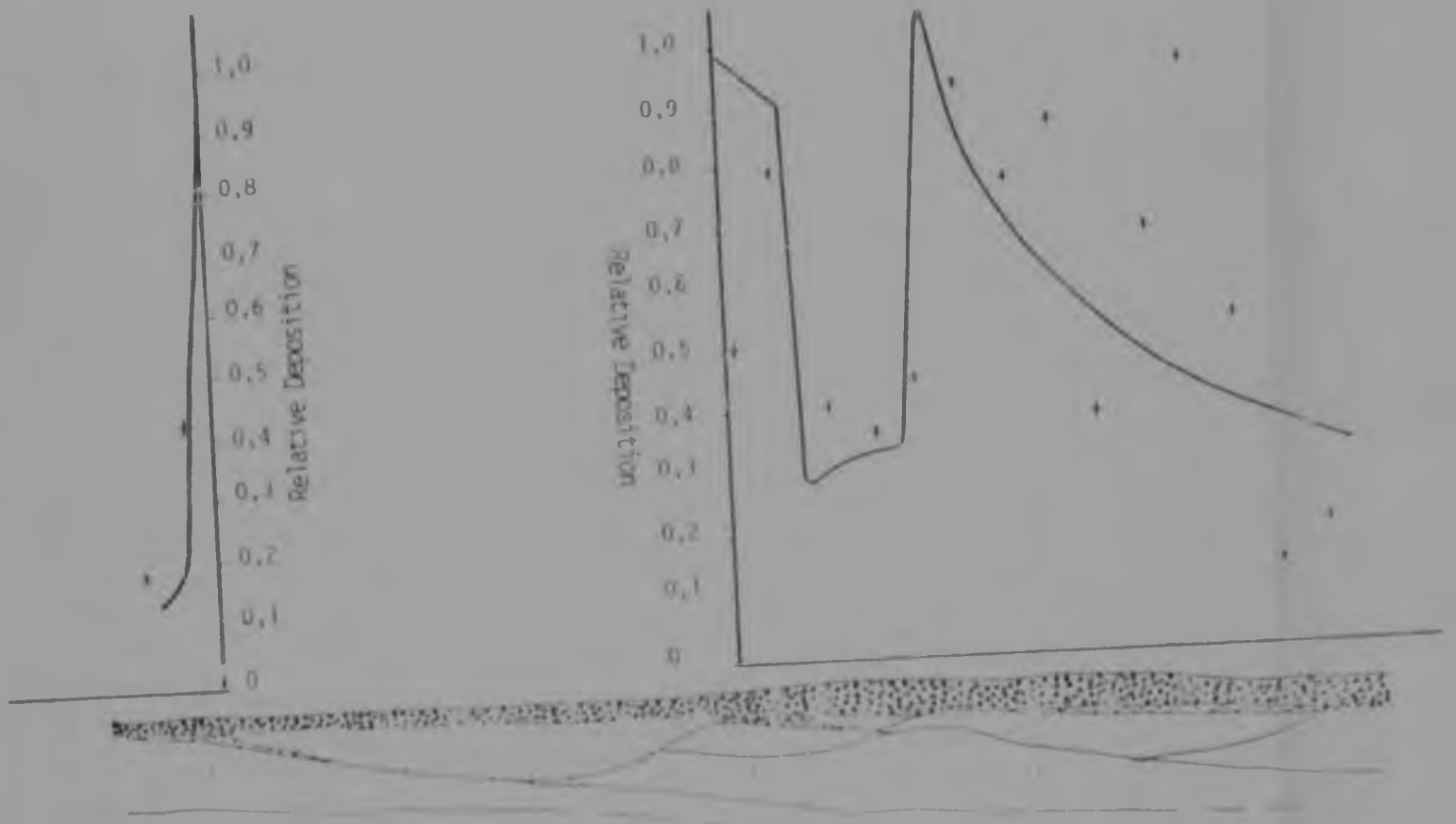


Fig. 7.19 Comparison of observed and simulated gold distributions (W11 f3)

approximately the same ordinate as the highest measured concentration for comparison purposes.

Section W11 f3, shown in Fig. 7.19 has some interesting features. The channel cross-section is distorted so that the deepest point is off centre. This suggests that the section is at a bend in the channel with the concave bank to the right. For such a case there would be a significant convective transport component to the right which is confirmed by the measured gold distribution, which is very extensive on the right bank and drops off very rapidly on the left bank. In addition there is a minor channel on the right bank about 0,3m from the main channel, probably a distributary from the main channel some distance upstream. This minor channel is small compared with the main channel and would probably have contributed very little suspended material to the plain. Over the width of this minor channel, however, deposition of gold would have been severely inhibited by the increased boundary shear. To account for the presence of the minor channel in the simulation the probability of deposition over its width was set to a small value (0,2 compared with the rest of the plain. This had the desired effect of reducing the deposit over the minor channel width and increasing the deposit immediately to the right to a value slightly greater than between the main and minor channels.

Agreement between measured and simulated distributions was obtained by adjusting values of three parameters which could not be estimated from the information available. Obviously agreement could also have been obtained with a set of values for these parameters different from those finally adopted. Agreement with any set of realistic values does confirm that the fundamental processes involved in the distribution of gold have been accounted for. As further information becomes available it will be possible to determine the

important parameters with more confidence and use the model to infer general conclusions regarding gold distribution for predictive use.

The sediment distribution model is based on certain flow characteristics which have been established for clear water and which are known to be affected by heavy suspended loads. Although the concentration of gold during transport was probably very small there may have been enough accompanying sediments to alter the flow characteristics. This could affect the distribution of gold deposits and therefore cause some discrepancy between predicted and observed distributions.

Experiments have shown that the distribution of velocity is affected by sediment in suspension. This has been attributed to changes in the value of the Karman constant which defines the mixing length or scale of macroturbulence and therefore the relationship between shear stress and velocity gradient. As sediment concentration increases the value of the Karman constant decreases, mixing becomes less effective and the velocity distribution becomes less uniform. This effect is discussed by Yalin (1977). Data are available which relate the Karman constant to concentration and preliminary proposals have been made for determining velocity gradients but it is not worthwhile making modifications to the model until more is known about hydraulic conditions associated with reef formation.

Suspended sediment also affects the viscosity of the fluid, as discussed by Graf (1971). The most important effect of this would be on the particle fall velocity. Equations have been developed for predicting changes of viscosity with concentration. The variation in size of gold particles would, however, have a greater effect on fall velocity than changes in viscosity due to suspension concentrations

Secondary circulation is also believed to be enhanced by suspended load and can cause uneven distributions (Graf (1971)). Local changes in flow direction caused by channel irregularities can also occur and are not described by the model.

Considering the degree of uncertainty associated with the description of system geometry and hydraulic conditions the effects of the above-mentioned factors should be relatively minor and should not detract from the validity of general interpretations of model results.

8. THE LONGITUDINAL DISTRIBUTION MODEL

8.1 Theory

The general three-dimensional equation for diffusive and convective transfer of a neutrally buoyant solute was given in Chapter 3 as

$$\frac{\partial C}{\partial t} + \sum_{i=1}^{3} u_i \frac{\partial C}{\partial x_i} = \sum_{i=1}^{3} \frac{\partial}{\partial x_i}\left(\varepsilon_i \frac{\partial C}{\partial x_i}\right) \qquad (3.1)$$

For heavy particles the vertical convective velocity is the particle fall velocity (w), which is assumed to be positive downwards, and the transverse convective velocity (u) is the particle velocity normal to the channel direction, as described in chapter 4.4. The longitudinal convective velocity (v) is the velocity of particles in the flow direction. According to Sarikaya (1977) the transport of particles by longitudinal diffusion is insignificant compared with longitudinal convection and can be ignored. For steady state conditions the concentration will not vary with time and $\frac{\partial C}{\partial t} = 0$.

For steady flow equation (3.1) can therefore be written as

$$0 = -v\frac{\partial C}{\partial x} + w\frac{\partial C}{\partial y} + \frac{\partial}{\partial y}\left(\varepsilon_y \frac{\partial C}{\partial y}\right) - u\frac{\partial C}{\partial z} + \frac{\partial}{\partial z}\left(\varepsilon_z \frac{\partial C}{\partial z}\right) \qquad (8.1)$$

Equation (8.1) can be used to describe the distribution of sediment in the vertical and longitudinal directions along a flow reach. The first three terms on the right hand side are the same as used by Sarikaya (1977) to describe the longitudinal distribution of sediment in a channel with a simple cross section. The last two terms account for the transverse movement of sediment across the interface between deep and shallow flow sections of a compound section. These two terms can be evaluated using the transverse distribution model and are considered as constants in the formulation of the longitudinal model.

Equation (8.1) can be classified by comparing it with the general form given by equation (3.3)

$$a\frac{\partial^2 \phi}{\partial x^2} + b\frac{\partial^2 \phi}{\partial x \partial y} + c\frac{\partial^2 \phi}{\partial y^2} + d\frac{\partial \phi}{\partial x} + e\frac{\partial \phi}{\partial y} + f\phi + g = 0 \qquad (3.3)$$

For equation (8.1) the value of the discriminant (b^2-4ac) will be equal to zero and the equation is therefore parabolic and can be solved in finite difference form using an explicit method.

Initial conditions are specified as concentration values along a vertical section at the beginning of the reach. Boundary conditions need to be specified at the water surface and the channel bed. These boundary conditions are of the derivative type and require that there can be no transport of suspended material across the water surface and that the rate of transfer to the bed is defined by the probability that a particle reaching the bed will be deposited. The boundary conditions are satisfied by applying appropriate finite difference formulations of equation (8.1) at all boundary points.

8.2 Finite Difference Solution

The longitudinal distribution equation is solved numerically by using a finite difference approach. The domain of integration is defined by the water surface, channel bed and vertical planes at the beginning and end of the reach. This domain is divided into N equal vertical increments and M equal horizontal increments as shown in Figure 8.1. Finite difference grid lines are numbered vertically from i=1 on the channel bed to i=N+1 at the water surface and longitudinally from j=1 at the beginning of the reach to j=M+1 at the end of the reach.

A grid must also be defined in the y-z plane so that the transverse transport component can be specified.

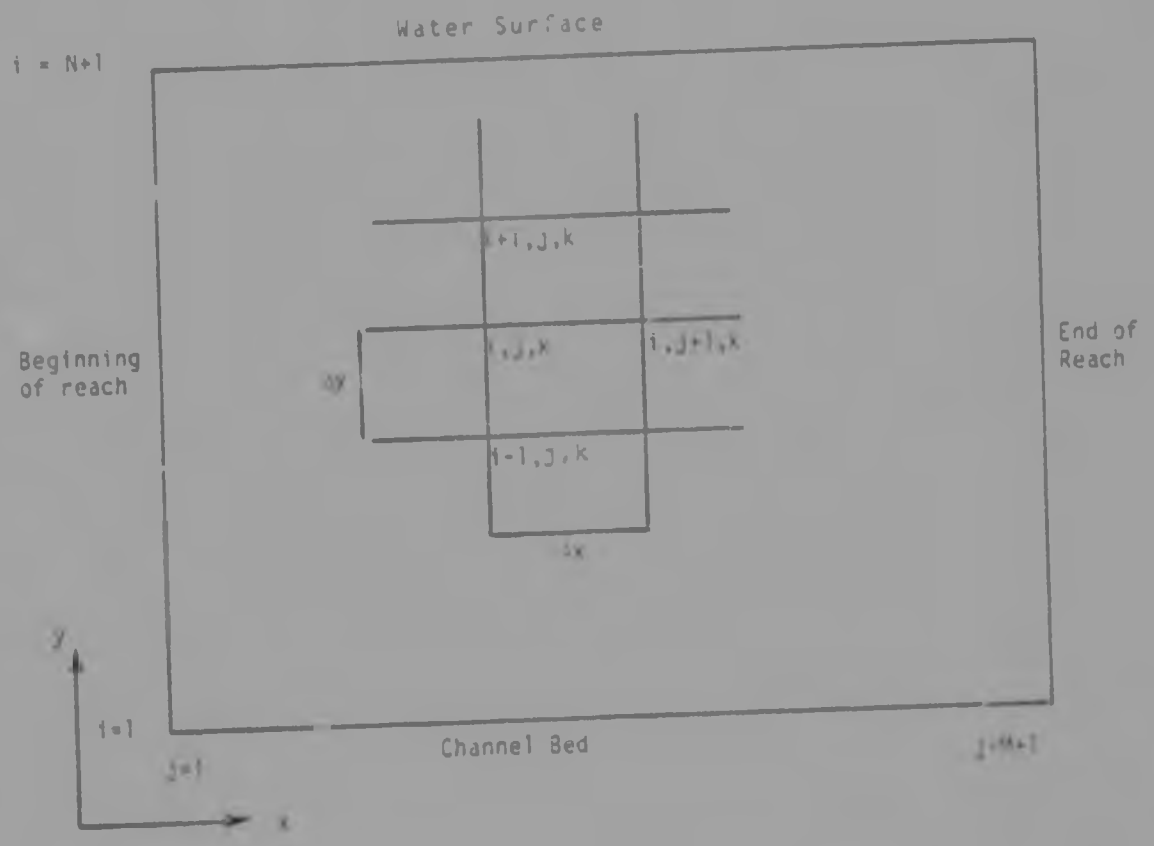


Fig. 8.1 Integration domain and finite difference grid

It is assumed that sediment concentrations will not vary across the width of the channel. Points on both sides of the channel can therefore be represented by the same grid point, as shown in Figure 8.2

The finite difference equations can be formulated by considering the mass balance of suspended material entering and leaving a fluid element. Material transported by diffusion across a boundary is equal to the product of diffusivity and concentration gradient and material transported by convection across a boundary is equal to the product of convective velocity and concentration.

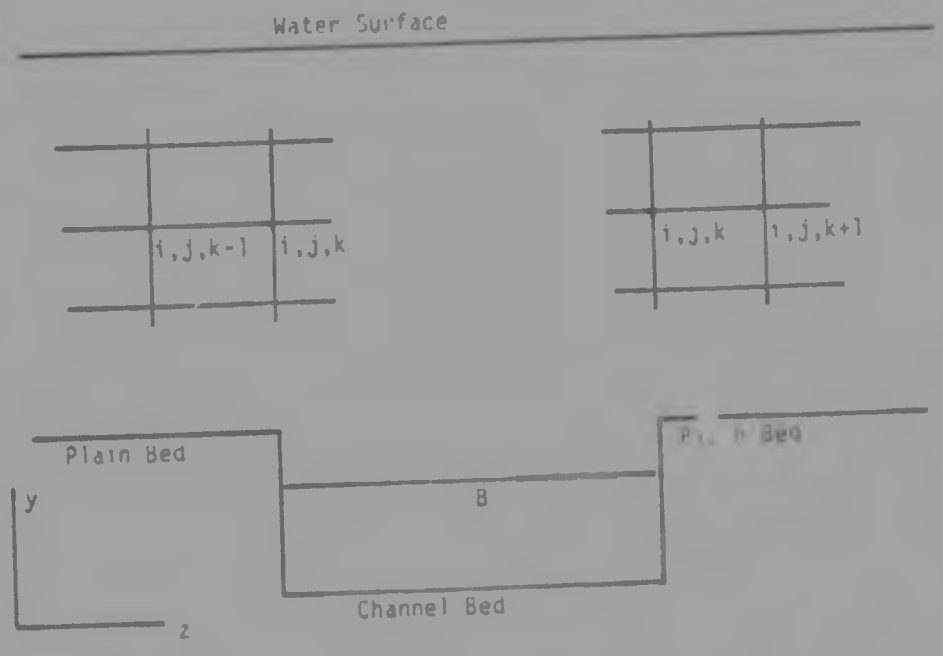


Fig. 3.2 Finite difference grid in Y-Z plane

For interior grid points a fluid element will have dimensions of Δy, Δx and $(\Delta z+B)$, where B is the channel width. A typical element is shown in Figures 8.3 and 8.4 with the transport components in the x and directions and the z direction respectively.

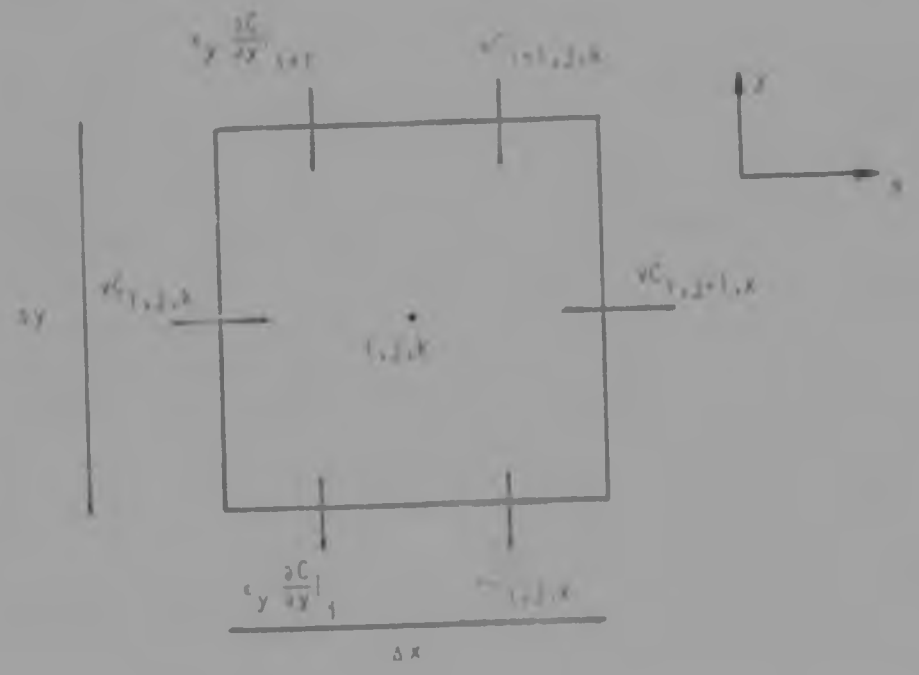


Fig. 8 3 Fluid element for interior points showing transport components in x and y directions

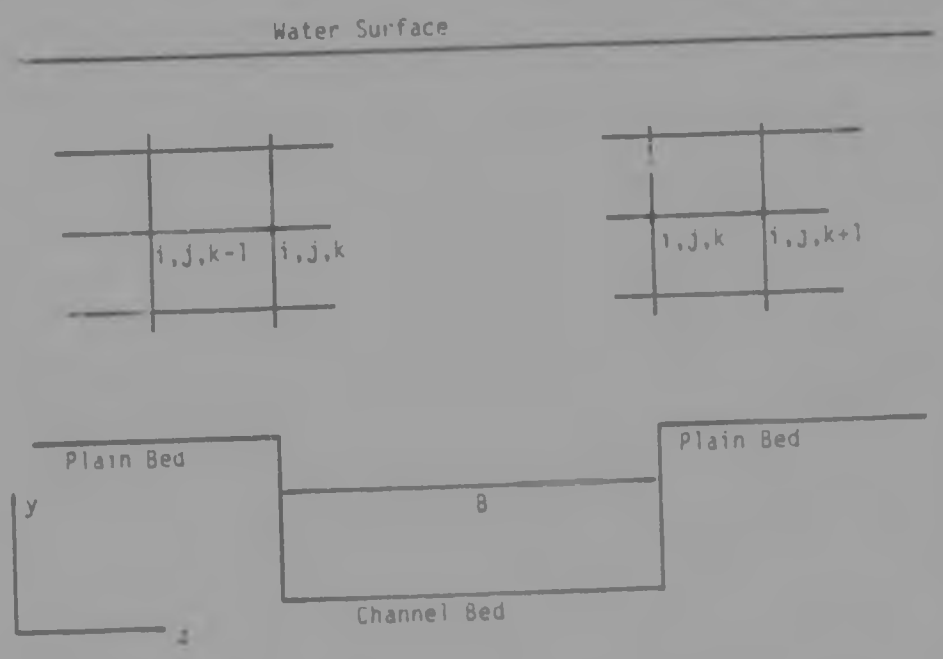


Fig. 8.2 Finite difference grid in Y-Z plane

For interior grid points a fluid element will have dimensions of Δy, Δx and $(\Delta z+B)$, where B is the channel width. A typical element is shown in Figures 8.3 and 8.4 with the transport components in the x and y directions and the z direction respectively.

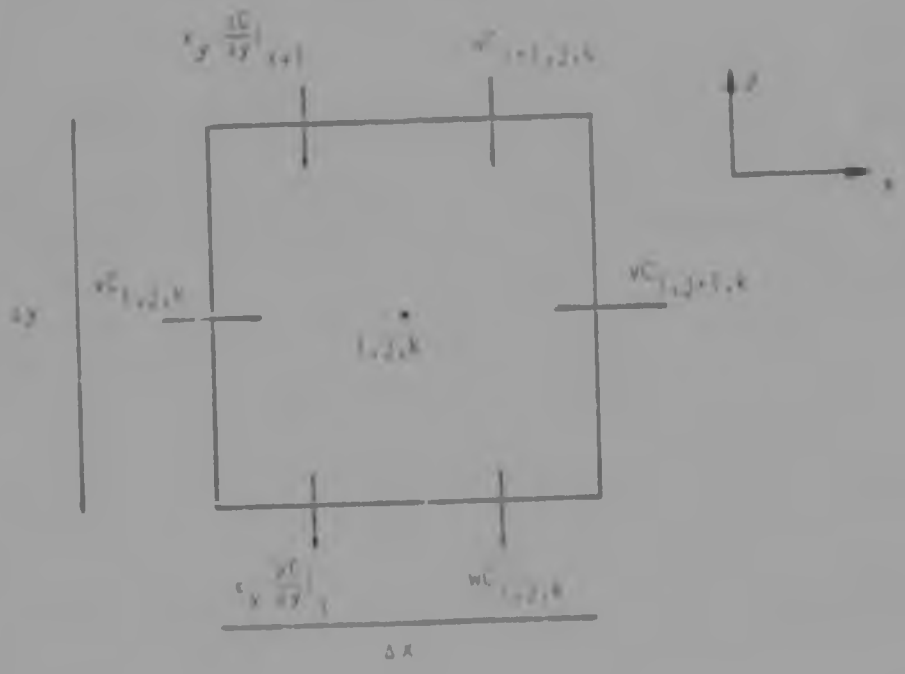


Fig. 8.3 Fluid element for interior points showing transport components in x and y directions

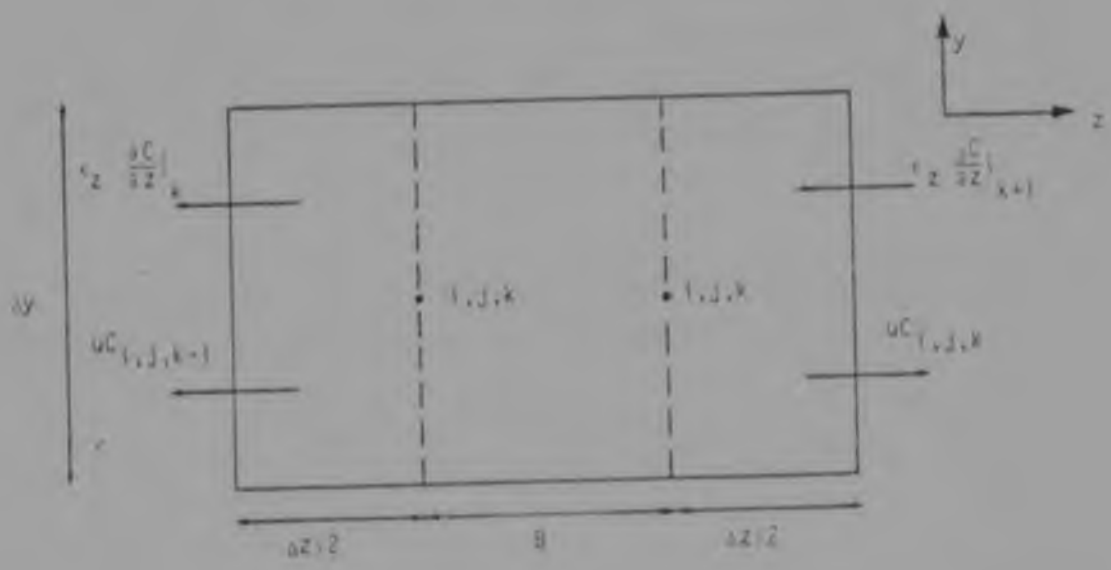


Fig. 8.4 Fluid element for interior points showing transport components in the z direction

The net mass of material entering the element in the y, x and z directions are given by expressions (8.2), (8.3) and (8.4) respectively.

$$(\epsilon_y \frac{\partial C}{\partial y}\Big|_{i+1} + wC_{i+1,j,k} - \epsilon_y \frac{\partial C}{\partial y}\Big|_{i} - wC_{i,j,k})(\Delta z + B)\Delta x \qquad (8.2)$$

$$(vC_{i,j,k} - vC_{i,j+1,k})(\Delta z + B)\Delta y \qquad (8.3)$$

$$(\epsilon_z \frac{\partial C}{\partial z}\Big|_{k+1} + uC_{i,j,k-1} - \epsilon_z \frac{\partial C}{\partial z}\Big|_{k} - uC_{i,j,k})\Delta y \Delta x \qquad (8.4)$$

For a steady process the net mass entering the element from all directions is zero and therefore

$$(\epsilon_y \frac{\partial C}{\partial y}\Big|_{i+1} + wC_{i+1,j,k} - \epsilon_y \frac{\partial C}{\partial y}\Big|_{i} - wC_{i,j,k})(\Delta z + B)\Delta x$$

$$+(vC_{i,j,k} - vC_{i,j+1,k})(\Delta z + B)\Delta y$$

$$+(\epsilon_z \frac{\partial C}{\partial z}\Big|_{k+1} + uC_{i,j,k-1} - \epsilon_z \frac{\partial C}{\partial z}\Big|_{k} - uC_{i,j,k})\Delta y \Delta x = 0 \qquad (8.5)$$

The following finite difference approximations are made

$$\frac{\partial C}{\partial y}\Big|_{i} \longrightarrow \frac{C_{i,j,k} - C_{i-1,j,k}}{\Delta y} \qquad (8.6)$$

$$\frac{\partial C}{\partial y}\Big|_{i+1} \longrightarrow \frac{C_{i+1,j,k} - C_{i,j,k}}{\Delta y} \qquad (8.7)$$

The terms for concentration gradient in the z direction will be evaluated using the transverse distribution model and supplied as input for the longitudinal model. It is therefore not necessary to express these terms in finite difference form.

The diffusivity value between adjacent grid points are calculated as the average of the point values, i.e.

$$E_y(i) = \frac{{}^{-}y_{i,j,k} + {}^{-}y_{i-1,j,k}}{2} \qquad (8.8)$$

$$\text{and } E_y(i+1) = \frac{\epsilon_{y_{i+1,j,k}} + \epsilon_{y_{i,j,k}}}{2} \qquad (8.9)$$

The concentration value $C_{i,j,k-1}$ is expressed in terms of $C_{i,j,k}$ and the concentration gradient, i.e.

$$C_{i,j,k-1} = C_{i,j,k} - \frac{\partial C}{\partial z}\Big|_k \Delta z \qquad (8.10)$$

Substituting expressions (8.6) to (8.10) in equation (8.5) and dividing by $\Delta x \Delta y (\Delta z + B)$ gives

$$\frac{E_y(i+1)}{\Delta y^2} C_{i+1,j,k} - \frac{E_y(i+1)}{\Delta y^2} C_{i,j,k} - \frac{w}{\Delta y} C_{i+1,j,k}$$

$$- \frac{E_y(i)}{\Delta y^2} C_{i,j,k} + \frac{E_y(i)}{\Delta y^2} C_{i-1,j,k} - \frac{w}{\Delta y} C_{i,j,k} + \frac{v}{\Delta x} C_{i,j+1,k}$$

$$- \frac{v}{\Delta x} C_{i,j+1,k} + \frac{u}{(\Delta z + B)} (C_{i,j,k} - \frac{\partial C}{\partial z}\Big|_k \Delta z) - \frac{u}{(\Delta z + B)} C_{i,j,k}$$

$$+ (\epsilon_z \frac{\partial C}{\partial z}\Big|_{k+1} - \epsilon_z \frac{\partial C}{\partial z}\Big|_k) \frac{1}{(\Delta z + B)} = 0 \qquad (8.11)$$

Equation (8.11) can be rearranged to give an expression for the unknown $C_{i,j+1,k}$ in terms of known values, i.e.

$$C_{i,j+1,k} = \frac{\Delta x}{v}\left\{\left(\frac{E_y(i-1)}{\Delta y^2} + \frac{w}{\Delta y}\right)C_{i+1,j,k} + \frac{E_y(i)}{\Delta y^2}C_{i-1,j,k}\right.$$

$$- \left(\frac{E_y(i+1)}{\Delta y^2} + \frac{E_y(i)}{\Delta y^2} + \frac{w}{\Delta y} - \frac{v}{\Delta x}\right)C_{i,j,k}$$

$$\left. + \frac{\varepsilon_z}{(\Delta z+B)}\left(\frac{\partial C}{\partial z}\right)_{k+1} - \left(\frac{\varepsilon_z}{(\Delta z+B)} + \frac{u\Delta z}{(\Delta z+B)}\right)\left(\frac{\partial C}{\partial z}\right)_k\right\} \quad (8.12)$$

The last two terms in equation (8.12) are omitted for all points below the level of the plain surface, where transverse transport obviously does not occur.

The mass balance approach is used to derive finite difference equations which satisfy the relevant boundary conditions for water surface and channel bed points.

At the water surface the fluid element associated with each grid point will have dimensions of $\Delta y/2$, Δx and $(\Delta z+B)$, as shown in Figures 8.5 and 8.6.

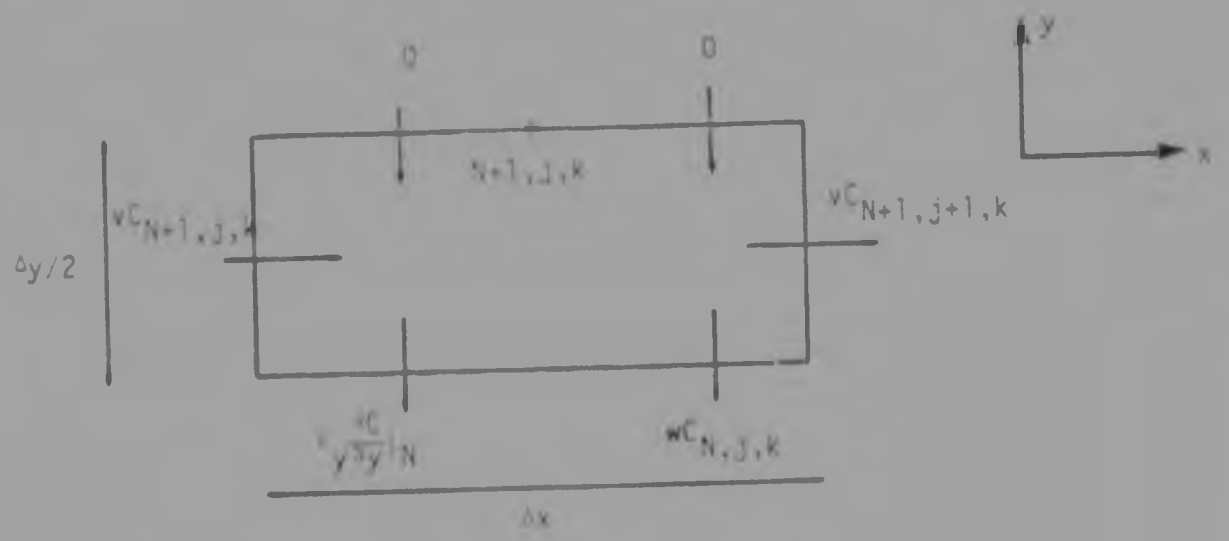


Fig. 8.5 Fluid element for water surface points showing transport components in x and y directions

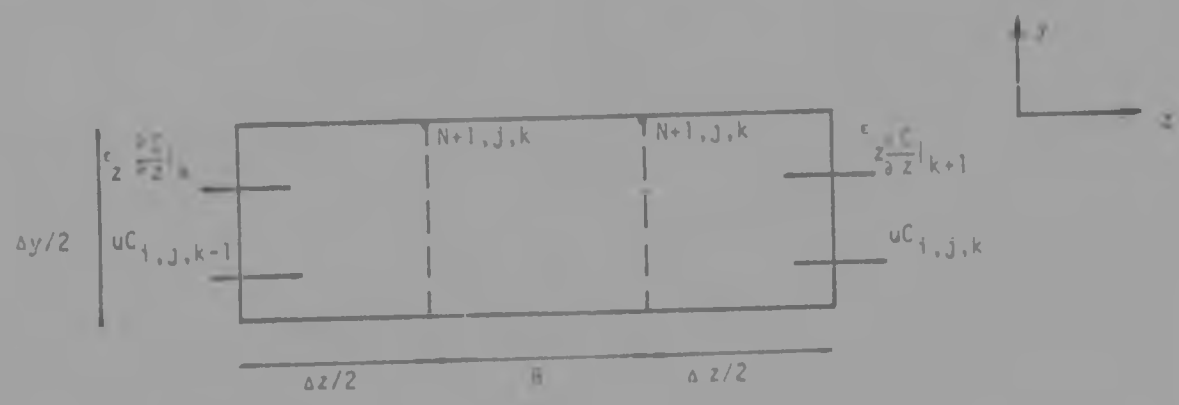


Fig. 8.6 Fluid element for water surface points showing transport components in the z direction

The diffusion component at the water surface is zero because vertical diffusivity decreases to zero at the surface and the convective term is zero because there can be no settling of material from above the surface. By following the same mass balance approach as for the interior points the following equation can be derived for concentrations at points on the water surface

$$C_{i,j+1,k} = \frac{\Delta x}{V}\left\{\frac{E_y^{(i,j)}}{\Delta y^2}C_{i-1,j,k} - \left(\frac{E_y^{(i,j)}}{\Delta y^2} + \frac{w}{\Delta y} - \frac{Q}{\Delta x}\right)C_{i,j,k}\right.$$

$$\left. + \frac{\varepsilon_z}{\Delta x(\Delta z+B)}\frac{\partial C}{\partial z}\Big|_{k+1} - \left(\frac{\varepsilon_z}{\Delta x(\Delta z+B)} + \frac{u\Delta z}{2\Delta x(\Delta z+B)}\right)\frac{\partial C}{\partial z}\Big|_{k}\right\} \quad (8.12)$$

At the channel bed the fluid element associated with each grid point will again have dimensions of $\Delta y/2$, Δx and $(\Delta z+B)$. The vertical diffusion component will be zero because diffusivity decreases to zero at the bed. The rate of convective transfer across the bed boundary will be determined by the probability of deposition, as discussed for the transverse distribution model in chapter 3. There is no transport in the z direction at the bed because the bed will always be below the level of the plain. The element and transport components in the x and y directions are shown in Figure 8.7.

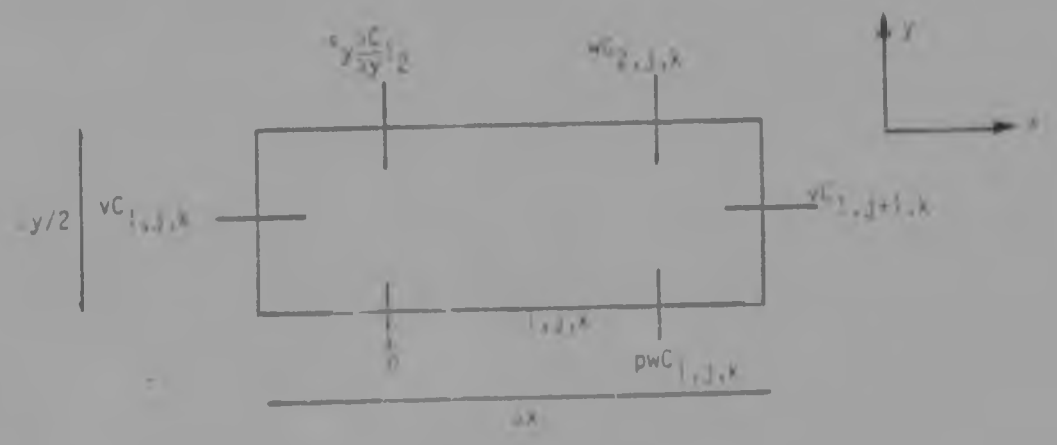


Fig. 8.7 Fluid element for channel bed points showing all transport components

The mass balance approach leads to the following equation for concentrations at channel bed points.

$$C_{i,j+1,k} = \frac{2\Delta x}{v}\left\{\left(\frac{E_y(i+1)}{\Delta y^2}+\frac{w}{\Delta y}\right)C_{i+1,j,k}-\left(\frac{E_y(i+1)}{\Delta y^2}+\frac{pw}{\Delta y}\right.\right.$$

$$\left.\left.-\frac{v}{2\Delta x}\right)C_{i,j,k}\right\} \qquad (8.1$$

Equations (8.12) to (8.14) enable calculation of the concentration values at all grid points in a vertical section explicitly from known values at the previously calculated section.

Sarikaya (1977) established a criterion for stability and convergence of his explicit solution in terms of Δx and Δy. Sarikaya's diffusion-settling equation differs from equation (8.1) only in that it does not include the transverse components which are treated as constants in the formulation of the longitudinal model. The stability and convergence conditions should therefore be similar for the two equations. Sarikaya's criterion is

$$\frac{\Delta x}{\Delta y^2} \leq \frac{2Z + T\Delta y}{4Z^2+4TZ\Delta y+T^2\Delta y^2} \qquad (8.15)$$

$$\text{in which} \quad Z = \frac{y_{max}}{D_c v_{max}} \qquad (8.16)$$

and $\frac{}{v_{max}}$ (8.17)

This criterion has been applied to the longitudinal distribution model and found to give a good indication of stability conditions.

8.3 Turbulent Diffusivities for Sediment

The longitudinal distribution of suspended sediment in a channel depends largely on the magnitude and variation of the turbulent diffusivity in the vertical direction. In the longitudinal direction the diffusive transport component is small compared with the convective component and is ignored. The loss of sediment from the channel associated with the interaction between channel and overbank flows is calculated in terms of an effective transverse diffusivity at the channel-plain interface. It is assumed that within the channel sediment concentration is uniform in the transverse direction, implying complete mixing between adjacent sections.

The relationship between turbulent diffusivities for sediment, fluid mass and momentum has been discussed in chapter 4 and equations are presented for calculating diffusivities. Vertical diffusivities are calculated according to the equation

$$\varepsilon_z = \kappa u_* \frac{Y}{D_c}(D_c - y) \qquad (8.18)$$

using a value of 0,4 for the Karman constant, κ. The shear velocity, u_*, is calculated using a reduced depth to account for possible form resistance as described in chapter 4.3.

The transverse diffusivity at the channel plain interface is calculated according to the empirical relationship developed by Rajaratnam and Ahmadi 1981 for diffusivity within the interaction zone, i.e.

$$\frac{\varepsilon_z}{(u_m-u_\infty)D_p} = \frac{0,3(D_c/D_p-1)^2}{((u_m-u_\infty)/u_{*_m})A(\eta_z)} \qquad (4.15)$$

and

$$\begin{aligned} A &= -31,5\eta_z + 11,45 \text{ for } \eta_z \leq 0,3 \\ A &= -2,37\eta_z + 2,71 \text{ for } \eta_z > 0,3 \\ A &\geq 9,0 \end{aligned} \qquad (4.16)$$

The flow velocities in the channel (u_m) and on the plain (u_∞) are calculated according to the procedure described in chapter 4.5

The transfer of sediment from the channel to the plain areas is determined by the concentration gradients at the interface as well as the transverse diffusivity. The concentration gradients can be determined by running the transverse distribution model to obtain concentration values on the first and second vertical rows of grid points. The gradients can then be calculated by dividing the differences between horizontally adjacent concentration values by the transverse grid spacing, Δz.

8.4 Convective Transport Components

The longitudinal distribution equation (equation 8.1) includes terms for convective transport in all three directions. The vertical component is represented by the particle fall velocity which is assumed to be the terminal settling velocity in quiescent water and can be estimated from equation (2.5) and Figure 2.2.

The longitudinal distribution of sediment in a channel has been shown to be sensitive to the magnitude and

The transverse diffusivity at the channel plain interface is calculated according to the empirical relationship developed by Rajaratnam and Ahmadi (1981) for diffusivity within the interaction zone, i.e.

$$\frac{\varepsilon_z}{(u_m - u_\infty) D_p} = \frac{0,3(D_c/D_p - 1)^{}}{((u_m - u_\infty)/u_{*\infty})^{A}} \qquad (4.15)$$

and

$$\begin{aligned} A &= -31,5\eta_\tau + 11,45 \text{ for } \eta_\tau \leq 0,3 \\ A &= -2,37\eta_\tau + 2,71 \text{ for } \eta_\tau > 0,3 \\ A &\geq 9,0 \end{aligned} \qquad (4.18)$$

The flow velocities in the channel (u_m) and on the plain (u_∞) are calculated according to the procedure described in chapter 4.5

The transfer of sediment from the channel to the plain areas is determined by the concentration gradients at the interface as well as the transverse diffusivity. The concentration gradients can be determined by running the transverse distribution model to obtain concentration values on the first and second vertical rows of grid points. The gradients can then be calculated by dividing the differences between horizontally adjacent concentration values by the transverse grid spacing, Δz.

8.4 Convective Transport Components

The longitudinal distribution equation (equation (8.1) includes terms for convective transport in all three directions. The vertical component is represented by the particle fall velocity which is assumed to be the terminal settling velocity in quiescent water and can be estimated from equation (2.5) and Figure 2.2.

The longitudinal distribution of sediment in a channel has been shown to be sensitive to the magnitude and

The transverse diffusivity at the channel plain interface is calculated according to the empirical relationship developed by Rajaratnam and Ahmadi (1981) for diffusivity within the interaction zone, i.e.

$$\frac{\varepsilon_z}{(u_m - u^\infty)D_p} = \frac{0,3(D_c/D_p - 1)^2}{((u_m - u^\infty)/u_*^\infty)} A(\eta_z) \qquad (4.15)$$

and

$$\begin{aligned} A &= -31,5\eta_z + 11,45 \text{ for } \eta_z \leq 0,3 \\ A &= -2,37\eta_z + 2,71 \text{ for } \eta_z > 0,3 \\ A &> 9,0 \end{aligned} \qquad (4.18)$$

The flow velocities in the channel (u_m) and on the plain (u^∞) are calculated according to the procedure described in chapter 4.5

The transfer of sediment from the channel to the plain areas is determined by the concentration gradients at the interface as well as the transverse diffusivity. The concentration gradients can be determined by running the transverse distribution model to obtain concentration values on the first and second vertical rows of grid points. The gradients can then be calculated by dividing the differences between horizontally adjacent concentration values by the transverse grid spacing, Δz.

8.4 Convective Transport Components

The longitudinal distribution equation (equation (8.1) includes terms for convective transport in all three directions. The vertical component is represented by the particle fall velocity which is assumed to be the terminal settling velocity in quiescent water and can be estimated from equation (2.5) and Figure 2.2.

The longitudinal distribution of sediment in a channel has been shown to be sensitive to the magnitude and

variation of longitudinal velocity (see chapter 9.2). The mean flow velocity in the channel is calculated according to the procedure described in chapter 4.5. Suspended particles are transported at a velocity which is lower than the flow velocity by an amount which depends on the turbulence of the flow and the particle characteristics. The average particle velocity is estimated from the relationship presented by Sumer (1974) and discussed in Chapter 4.4. The average particle velocity (U_s) is given by

$$U_s = -135\beta^{1.41}\frac{D}{D_c} + U \qquad (8.19)$$

in which U is the average flow velocity, D_c is the channel flow depth, D is the average diffusivity in the flow direction given by

$$D = 1/6\ D_c\ U_* \qquad (8.20)$$

and β is the fall velocity parameter given by

$$\beta = w/kU_* \qquad (8.21)$$

The flow velocity varies in the vertical direction and it is assumed that the particle velocity will follow the same form of variation. The variation is best described by the von Karman-Prandtl logarithmic velocity distribution. The particle velocity in the flow direction (v) at any depth (y) is given by

$$v = \frac{u_*}{\kappa}\left(\ln\frac{y}{D_c} + 1\right) + U_s \qquad (8.22)$$

If the channel is not parallel to the direction of the steepest gradient of the plain a transverse convective transport component will exist. This component is estimated as described in Chapter 4.4

8.5 Probability of Deposition

The boundary condition at the channel bed specifies the rate at which particles close to the bed are trans-

ferred to the bed material. This transfer rate is the product of the particle fall velocity and the probability that surface and flow conditions permit deposition.

The probability of deposition on the plain surface is discussed in Chapter 5.2. An expression for estimating this probability was derived under the assumption that the plain surface consisted of particles which were large compared with the suspended particles. The extent of deposits on the plain was found to be relatively insensitive to probability of deposition and this approximation is reasonable. The longitudinal distribution of suspended sediment within the channel is also fairly insensitive to the probability of deposition on the plain.

The channel bed cannot be considered to consist of large particles. For significant quantities of gold and equivalent sand particles in suspension there would be a very high concentration of fine material close to the bed and most likely a large bed load component of relatively fine material. Reef observations also indicate relatively fine bed material. The longitudinal distribution of suspended sediment proves to be very sensitive to the deposition probability and the approach used for the plain surface is clearly unsuitable for the channel bed. The equation proposed by Engelund and Fredsoe (1976) for the probability of erosion is therefore applied without reducing the bed area to account for large particles. The probability of erosion is given by

$$p = \left\{1 + \left(\frac{\sqrt{\theta}}{\theta - \theta_c}\right)^4\right\}^{-1/4} \qquad (5.10)$$

in which

$$\theta = \frac{u_*^2}{(s-1)gd} \qquad (5.11)$$

and θ_c is the critical value of θ at which particles begin to move.

The probability of deposition is then equal to unity less the probability of erosion given by equation (5.10).

9. APPLICATION OF THE LONGITUDINAL DISTRIBUTION MODEL

9.1 Introduction

The longitudinal distribution of suspended sediment in a channel with a compound cross section is determined to a large degree by the rate of transfer of sediment to the overbank sections. This transfer depends on the values of transverse diffusivity, concentrations and concentration gradients at the channel-plain interface. The concentration gradients vary significantly with changing flow conditions and accurate estimates of these values can be obtained only by solving the transverse distribution problem for the conditions being considered. Many other parameters required for the longitudinal model, such as shear velocity, flow velocities and diffusivities, are also calculated by the transverse distribution model. Because the transverse model must always be run to determine the concentration gradients the values of these other parameters are also obtained as output and are not recalculated in the longitudinal model. Each longitudinal distribution analysis therefore involves an initial application of the transverse distribution model to obtain input data for the longitudinal distribution model.

No data were available from the reefs which could be used to relate the longitudinal distribution of gold to channel geometry and configuration. Application of the model has therefore been restricted to hypothetical situations and two cases were considered. A sensitivity analysis was performed on a single channel reach to determine the effect of various parameters on the longitudinal distribution of sediment. A hypothetical distributary system was also analysed to illustrate application of the model and to enable general conclusions regarding gold distribution to be drawn.

9.2 Sensitivity Analysis

A single hypothetical channel was used to examine the effects of various channel, flow and sediment characteristics on the longitudinal distributions of suspended and deposited particles. An analysis was performed using a particular set of characteristics as a standard and different parameters were then varied individually for subsequent analyses.

The standard channel was assumed to have an average width of 2,0 m, a depth below plain level of 0,50 m and a gradient of 0,005. For calculation of average flow velocities in the transverse distribution model the channel was assumed to have a trapezoidal section with a top width of 2,4 m and a bottom width of 1,2 m. Manning's n was assumed to be 0,020 for the channel bed and 0,025 for the plain surface. The size of surface roughness elements used for velocity profile and concentration profile calculations was assumed to be 5,0 mm for both channel and plain. A channel reach 100 m long was considered.

Gold particles in suspension were assumed to have an average diameter of 0,140 mm, a fall velocity of 0,035 m/s and a specific gravity of 19,3. At the head of the channel reach the concentration of suspended gold was assumed to be 100 units, distributed uniformly along the vertical section. As for the transverse distribution studies, relative concentrations are considered and concentration units are arbitrary.

The standard discharge was such that the flow depth on the plain would be 0,5 m. It was assumed that flow velocity was uniformly distributed within the channel and that the velocity of sediment particles was the same as the flow velocity.

Results of the longitudinal distribution analysis for the standard channel are summarized in Figures 9.1, 9.2 and 9.3. Figure 9.1 shows the variation of the vertical concentration profile along the reach. The uniform distribution specified at the beginning of the reach adjusts fairly rapidly and has attained an equilibrium form after about 50 m. Thereafter the change is gradual with the profile shape remaining essentially constant and concentration values decreasing as suspended material is transferred to the bed and plain areas.

The variations of the rates of transfer to bed and banks are shown in Figure 9.2. This diagram shows deposition rates per unit longitudinal distance relative to the value for the channel bed at the beginning of the reach. As for the concentration profile, there is a fairly rapid change until the uniform concentration profile adjusts to some sort of equilibrium. Deposition on the channel bed increases rapidly as the concentration close to the bed increases, while transfer to the plains decreases as the concentrations above the plain level decrease. Once the profile has adjusted both transfers decrease gradually as the amount of material in suspension decreases. It should be noted that at the end of the reach the rate of transfer to the plains is about 380 times that to the bed. This factor varies significantly with channel characteristics, as can be seen in the analysis of the effect of longitudinal gradient.

Figure 9.3 shows the variation of the average concentration along the reach. The distribution of average concentration is a concise representation of the net effect of longitudinal transport and transfer to bed and plains and is used as a basis for comparison between different conditions.

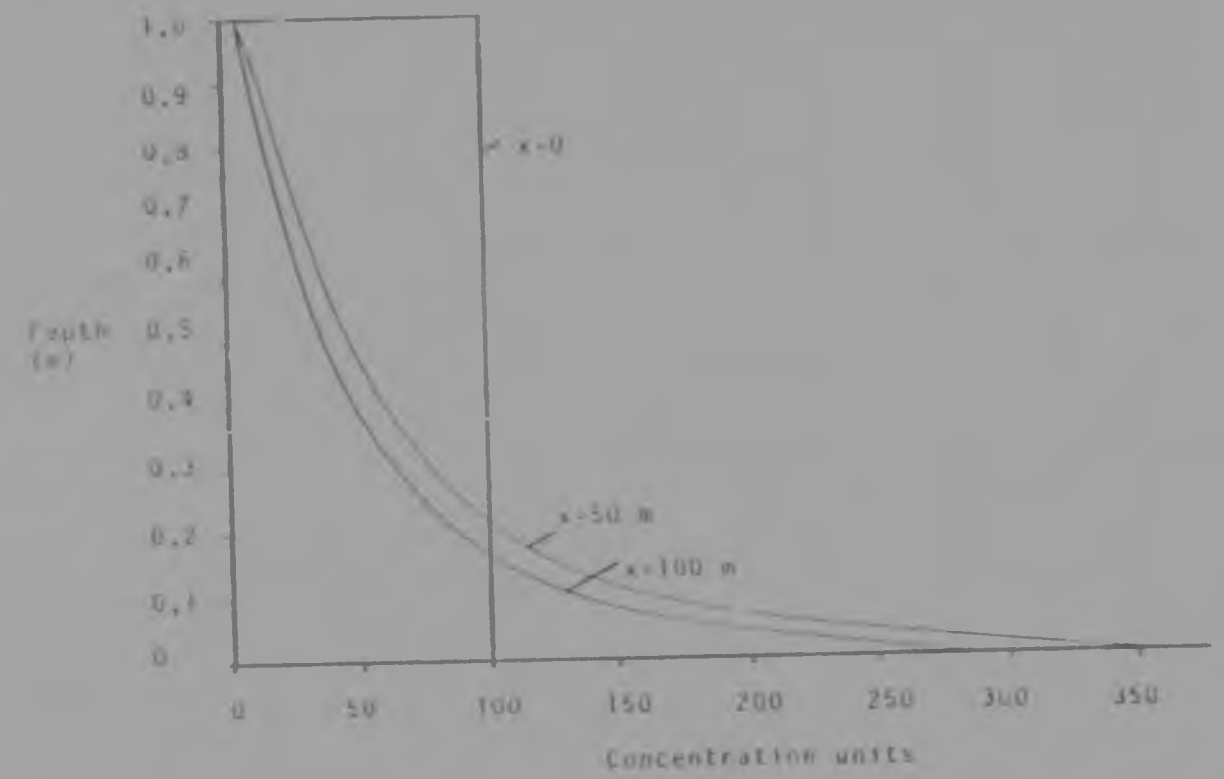


Fig. 9.1 Concentration profiles in standard channel

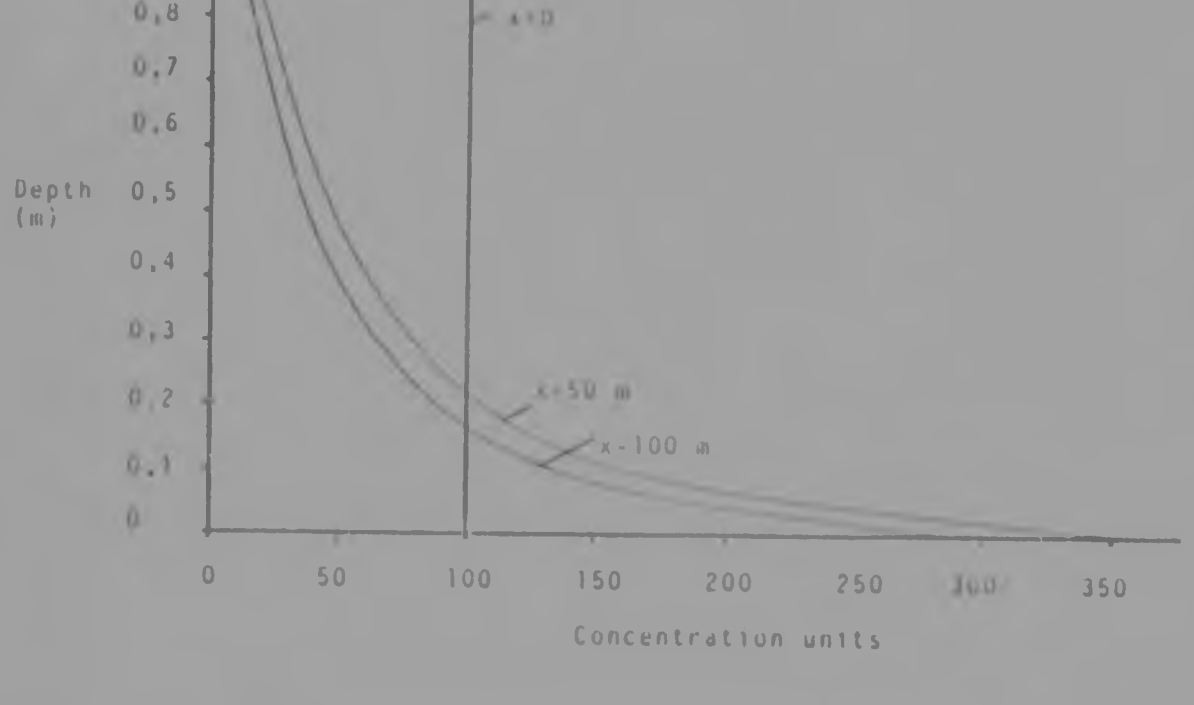


Fig. 9.1 Concentration profiles in standard channel

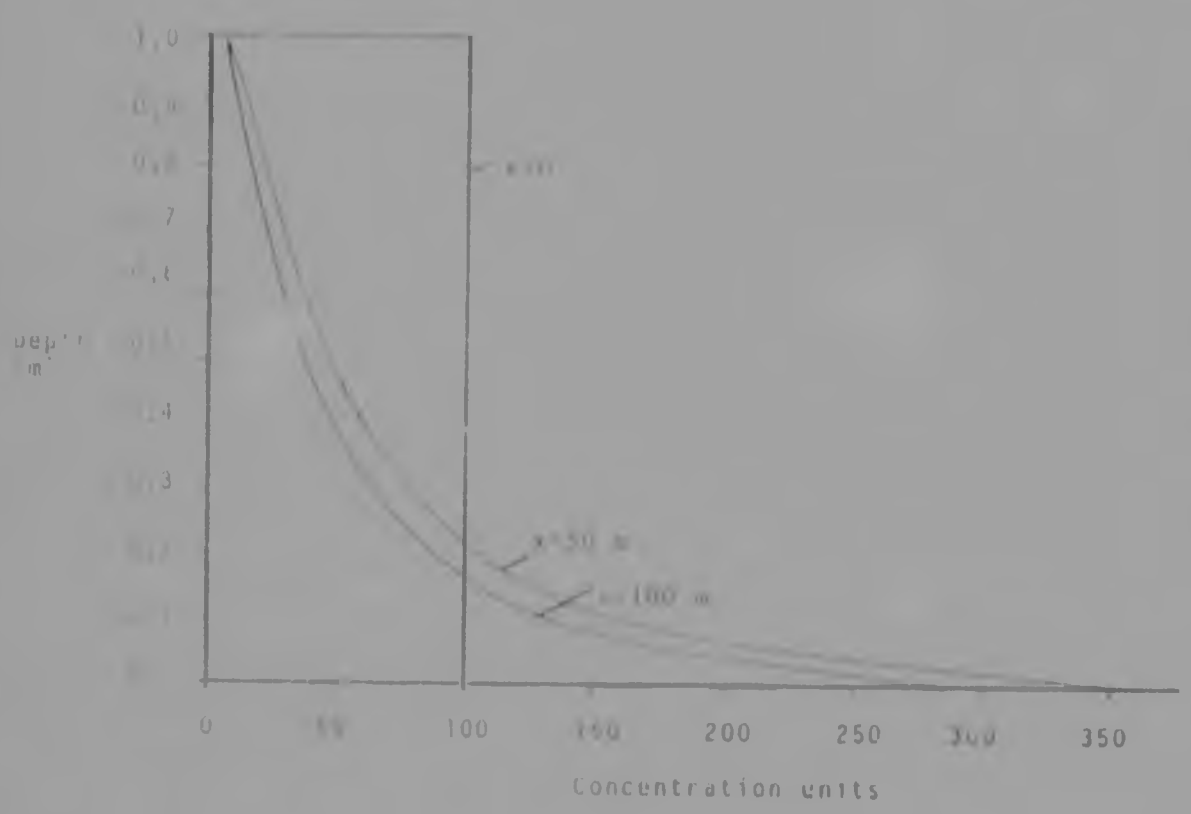


Fig [illegible] Concentration profiles in standard channel

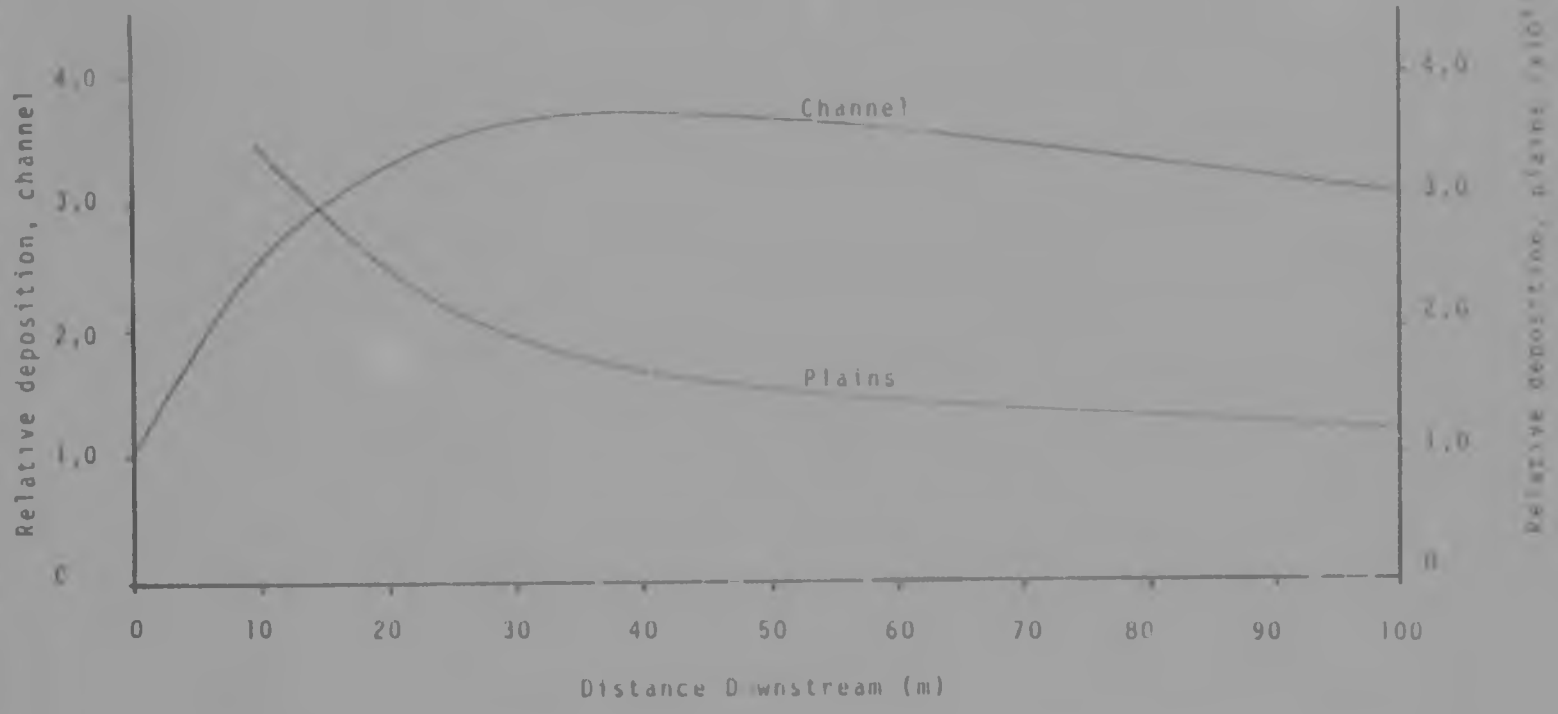


Fig. 9.2 Relative deposition on standard channel bed and plains

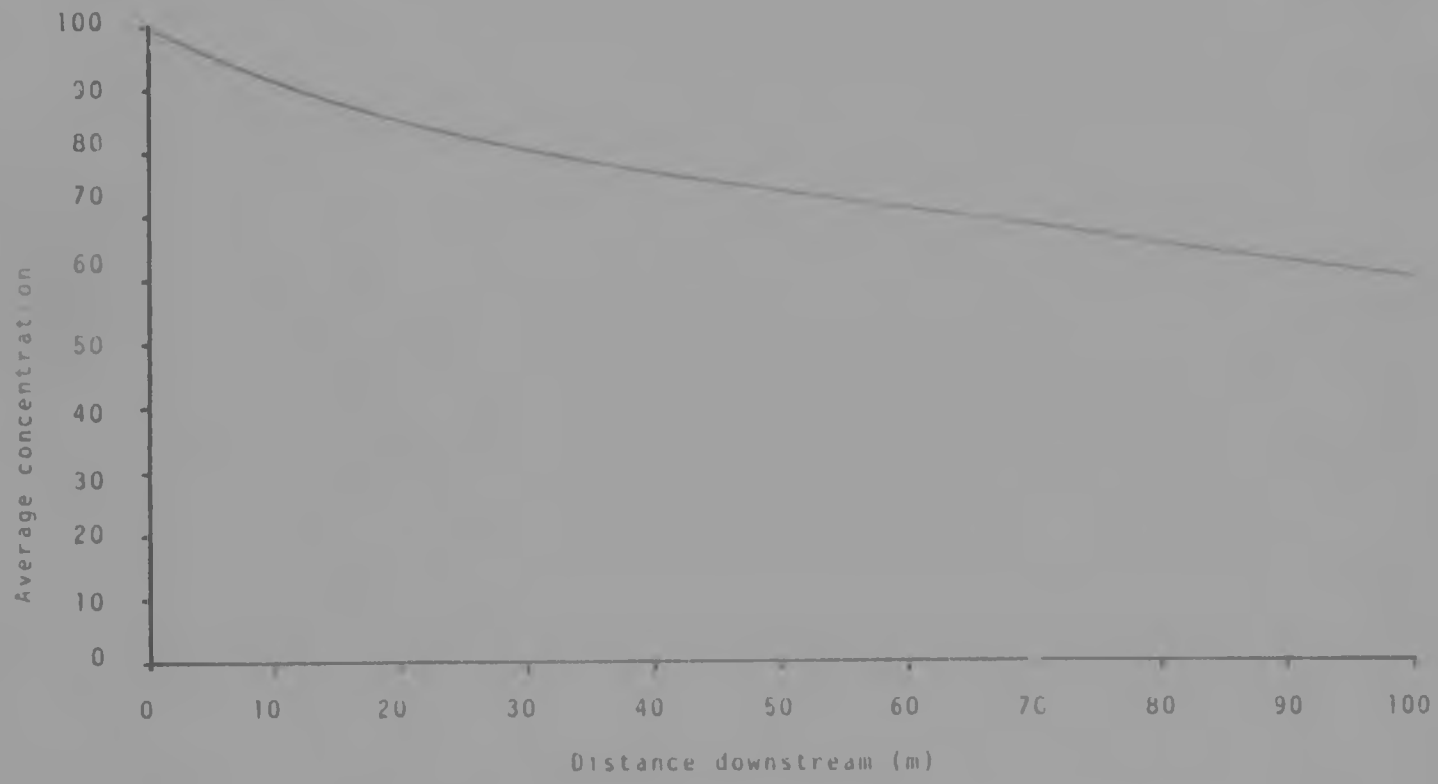


Fig. 9.3 Average concentration along standard channel reach

The width of the channel can be expected to have a significant influence on the longitudinal variation of sediment in suspension. Sediment is transferred to the plain areas across vertical planes at the sides of the channel. The closer these planes are together the higher will be the transverse transfer rate relative to the rate of transport in the flow direction. This tendency was quantified by varying the width of the standard section without making any other changes. The average concentration distributions in Figure 9.4 show that the amount of sediment remaining within the channel at its downstream end is reduced by about 28% if the width is reduced from 2,0 m to 1,0 m and increased by about 15% if the width is increased to 3,0 m. The concentration distribution for an infinitely wide channel was simulated by suppressing all transverse transfer. For this case the reduction in suspended sediment is negligible, which is realistic considering the insignificant bed deposition as compared with transverse transfer (Figure 9.2).

The longitudinal gradient of the channel determines the flow velocities in the channel and on the plains. The transverse diffusivity over the plain is a function of the difference in velocity between the channel and the plain. The probability of deposition of sediment on the channel bed depends on the shear velocity which is also determined by the gradient. The distribution of sediment should therefore be affected by longitudinal gradient and several values were assumed, giving results as shown in Figure 9.5. Changing the gradient from 0,005 to 0,002 has a relatively minor effect on the longitudinal distribution of average concentration. Once the gradient drops below 0,002, however, the effect is dramatic and for a gradient of 0,001 the average concentration at the end of the reach is only about 6% of the value for 0,005. This threshold effect can be ascribed to the increase in deposition probabil-

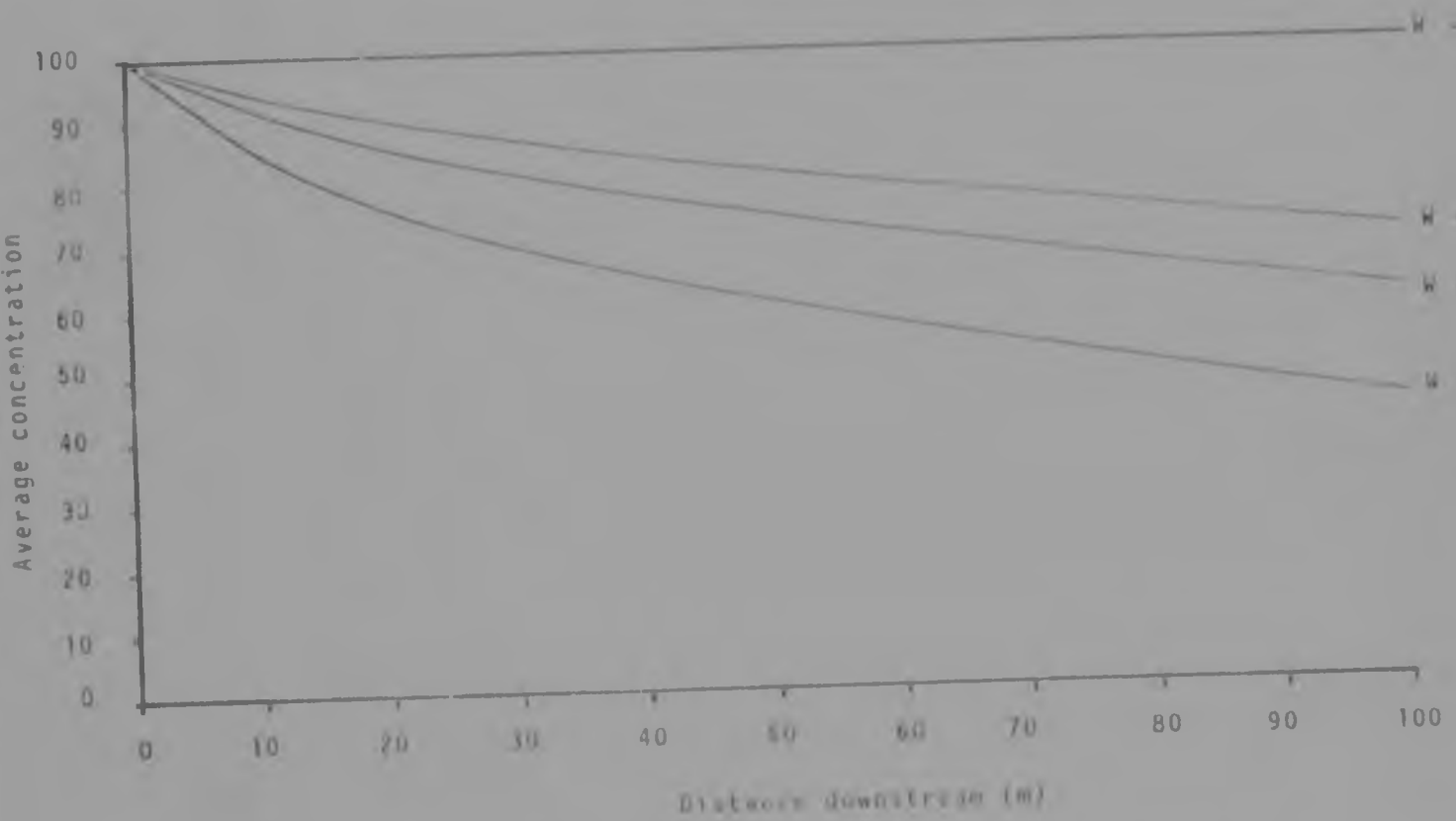


Fig. 9.4 Effect of channel width on sediment distribution

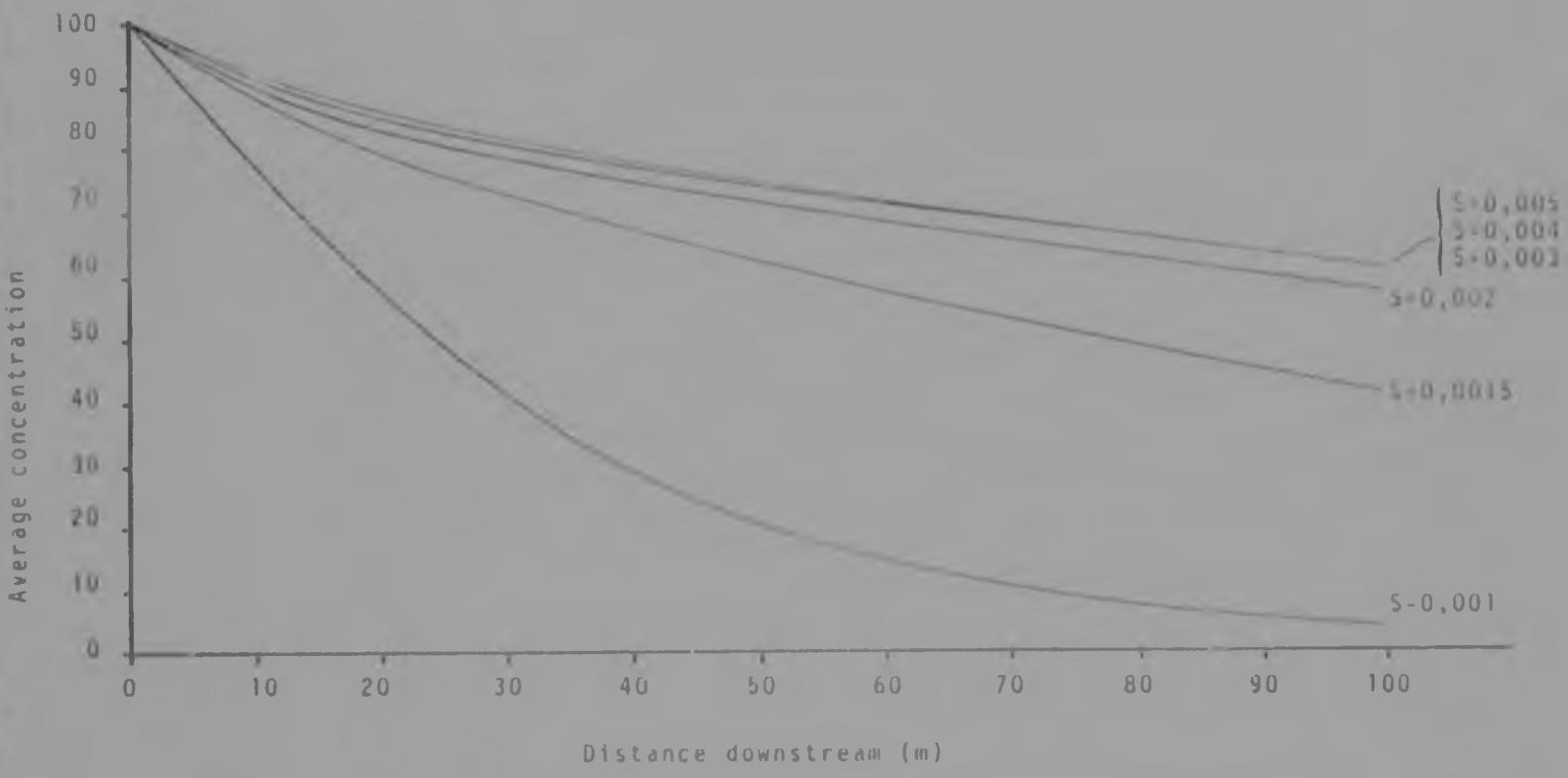


Fig. 9.5 Effect of channel gradient on sediment distribution

ity more than to a reduction in transverse diffusivity. Between gradients of 0,003 and 0,001 the probability of deposition increases from 0,0012 to 0,1200 while the transverse diffusivity decreases from 0,036 m^2/s to 0,021 m^2/s. For a gradient of 0,001 more sediment is deposited within the channel than is transferred to the plain. The ratio of plain transfer to bed deposition at the end of the reach is 0,124 compared with 385 for a gradient of 0 005. The variation of this ratio with gradient is shown in Figure 9.6.

Figure 9.7 shows the effect of changing the probability of deposition on the channel bed with the transverse diffusivity remaining unchanged. The high sensitivity apparent in these results confirms the interpretation of the effect of varying channel gradient.

The probability of deposition on the plain areas was shown in Chapter 7 to have a sigificant effect on the distribution of sediment in the transverse direction. This distribution determines the concentration gradients at the channel-plain interface and can therefore be expected to affect the longitudinal distribution. The deposition probability on the plain for the standard flow conditions is 0,79 as calculated by the model described in Chapter 5.2. Different values were imposed by overriding the calculation routine in the transverse distribution model. The effect on the longitudinal distribution proved to be relatively small, as shown in Figure 9.8.

The resistance to flow on the plain affects the difference in flow velocity between channel and plain and therefore influences the transverse diffusivity according to equation (4.1 . The resistance, as expressed by Manning's n, was varied to determine its effect on the longitudinal distribution of sediment. As shown in Figure 8.9 the effect is not very significant

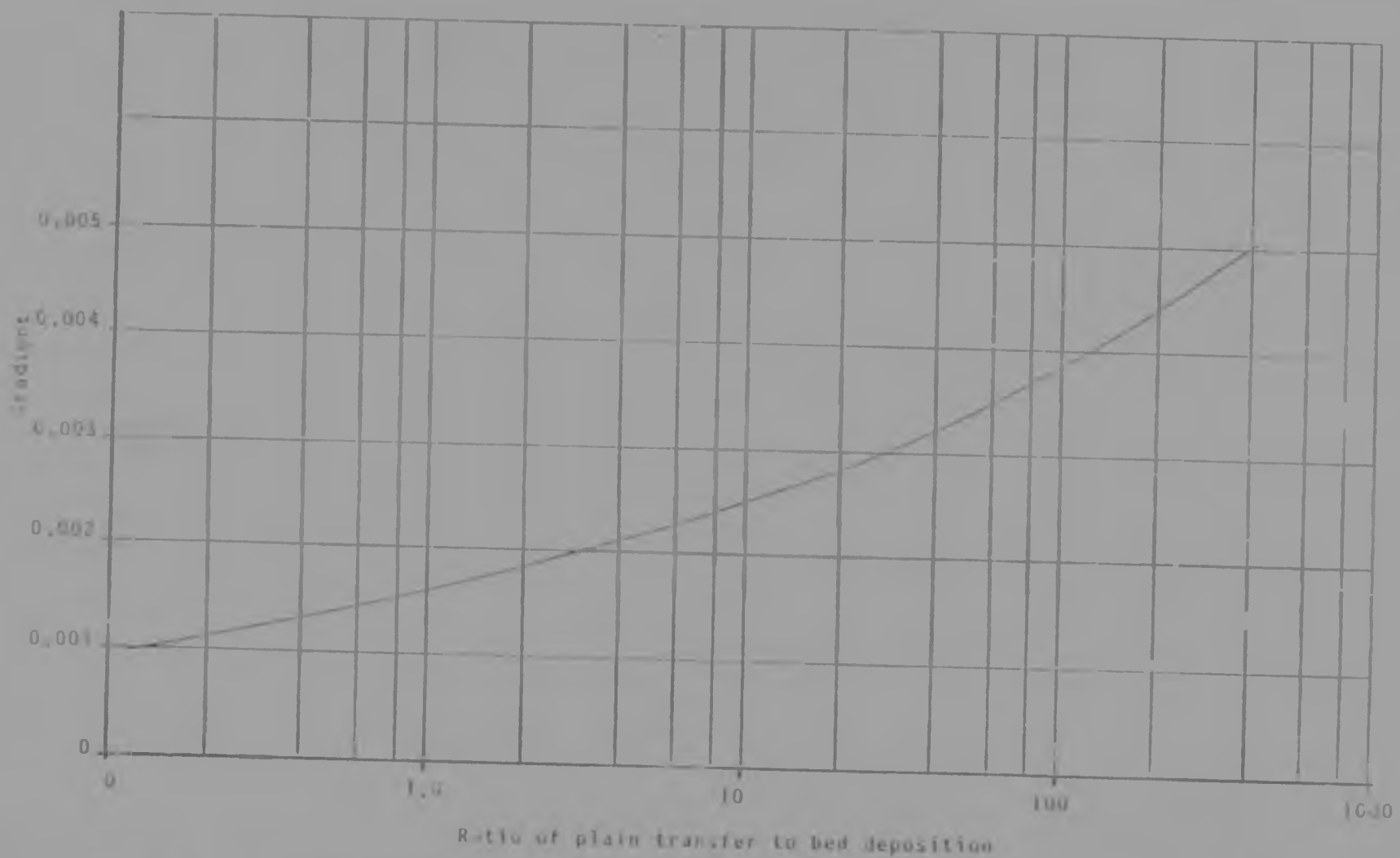


Fig. 9.6 Variation of plain deposits relative to channel deposits with gradient

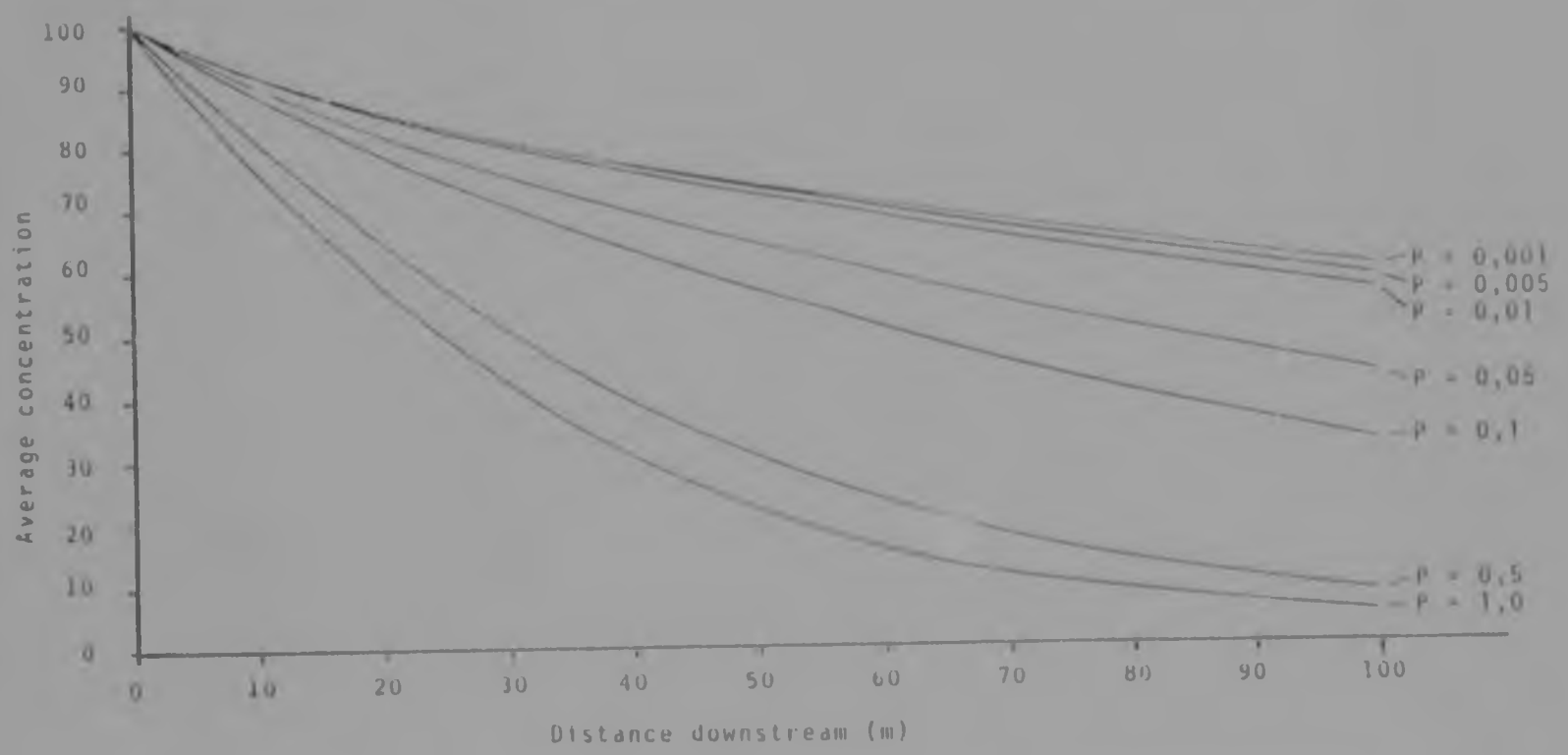


Fig. 9.7 Effect of deposition probability in channel on sediment distribution

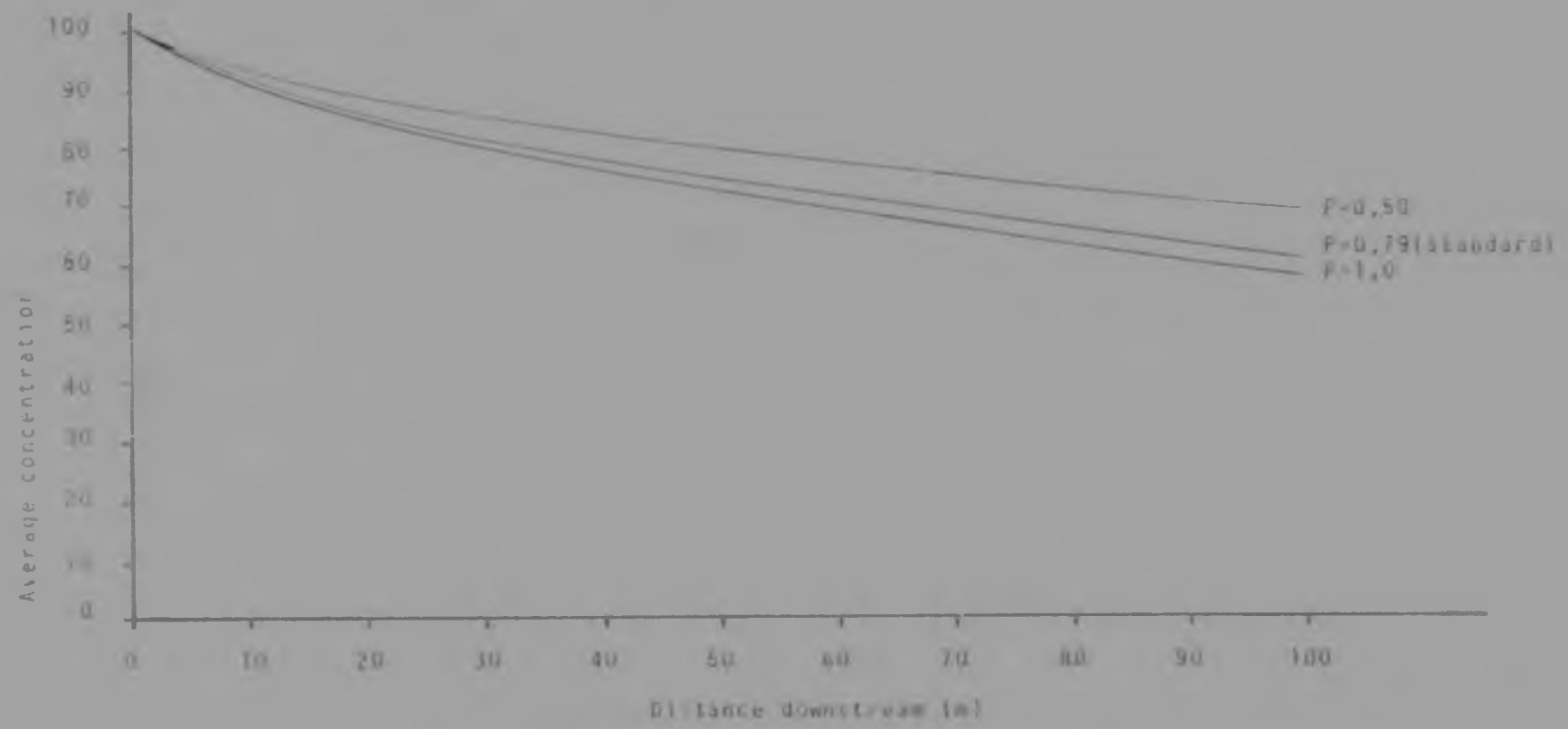


Fig. 9.8 Effect of deposition probability on plain on sediment distribution

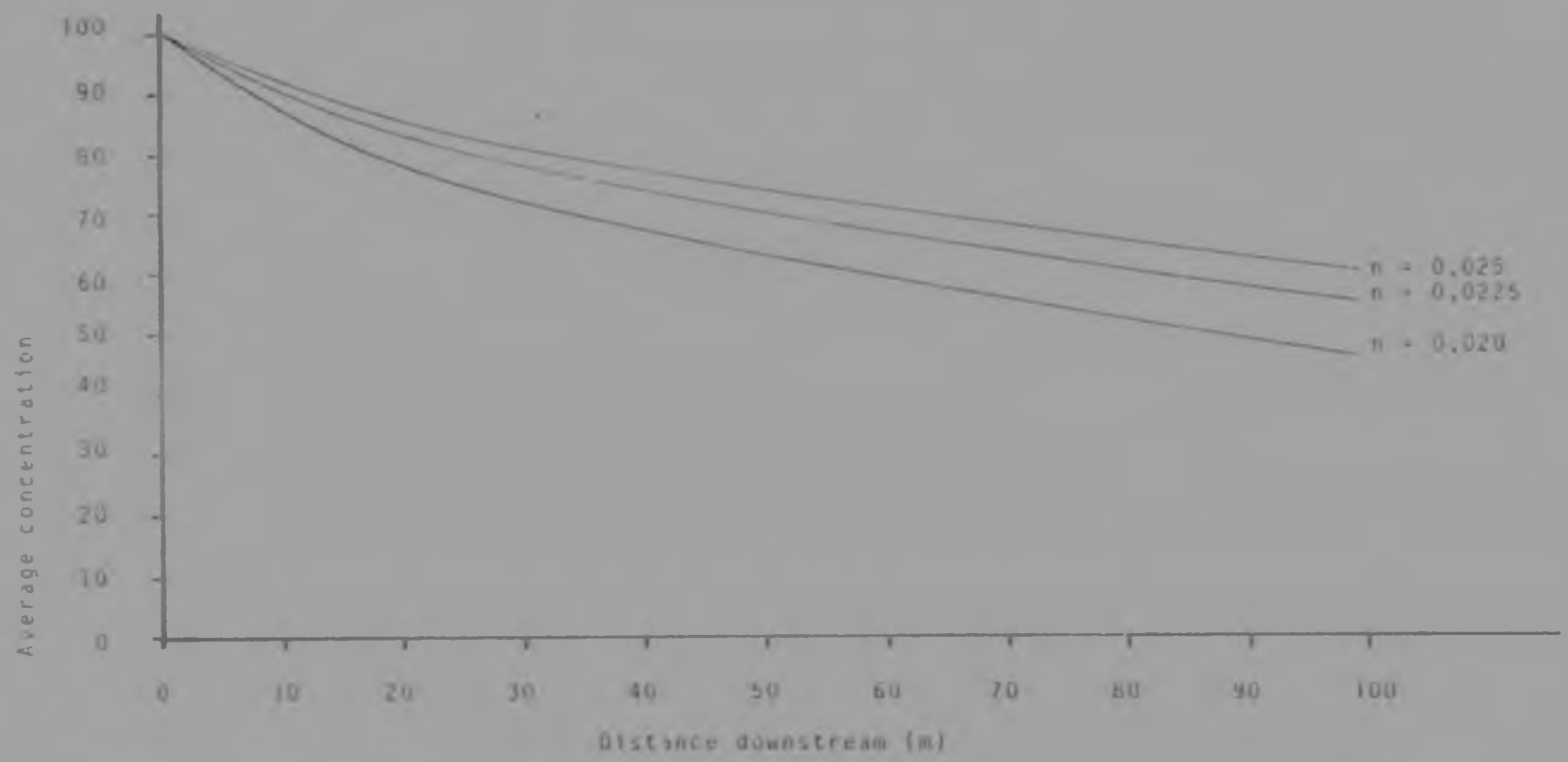


Fig. 9.9 Effect of plain resistance on sediment distribution

considering the reliability of estimates of n. Sensitivity to Manning's n for the channel would be much the same.

According to equation (4.15) the transverse diffusivity is also affected by the flow depths in the channel and on the plain. Their effect on longitudinal distribution of sediment was examined by varying firstly the depth of the channel bed below the plain surface and secondly the flow depth on the plain. In both cases the sediment concentration reached a minimum when the flow depth in the channel was about twice that on the plain (figures 9.10 and 9.11). This complex behaviour reflects a balance between the potential rate of transfer to the plains and the availability of sediment for transfer. As the flow depth in the channel increases relative to that on the plain so the transverse diffusivity increases. At the same time, however, the amount of sediment in suspension in the channel above the plain surface level decreases according to the form of the concentration profile. The amount of sediment transferred therefore increases initially as the transverse diffusivity increases but subsequently decreases as the amount of sediment available becomes less.

Transfer of sediment to the plain is considerably enhanced on one side of the channel and inhibited on the other if a transverse convective transport component exists, such as would result from a deviation (δ) of the channel direction from the direction of the steepest gradient of the plain. The effect of such a deviation on the longitudinal distribution of sediment is shown on Figure 9.12 for the standard flow conditions. As shown in Chapter 7.2 the sensitivity of transverse transfer to channel deviation varies considerably as flow conditions change and the results of Figure 9.12 should not be construed as generally representative.

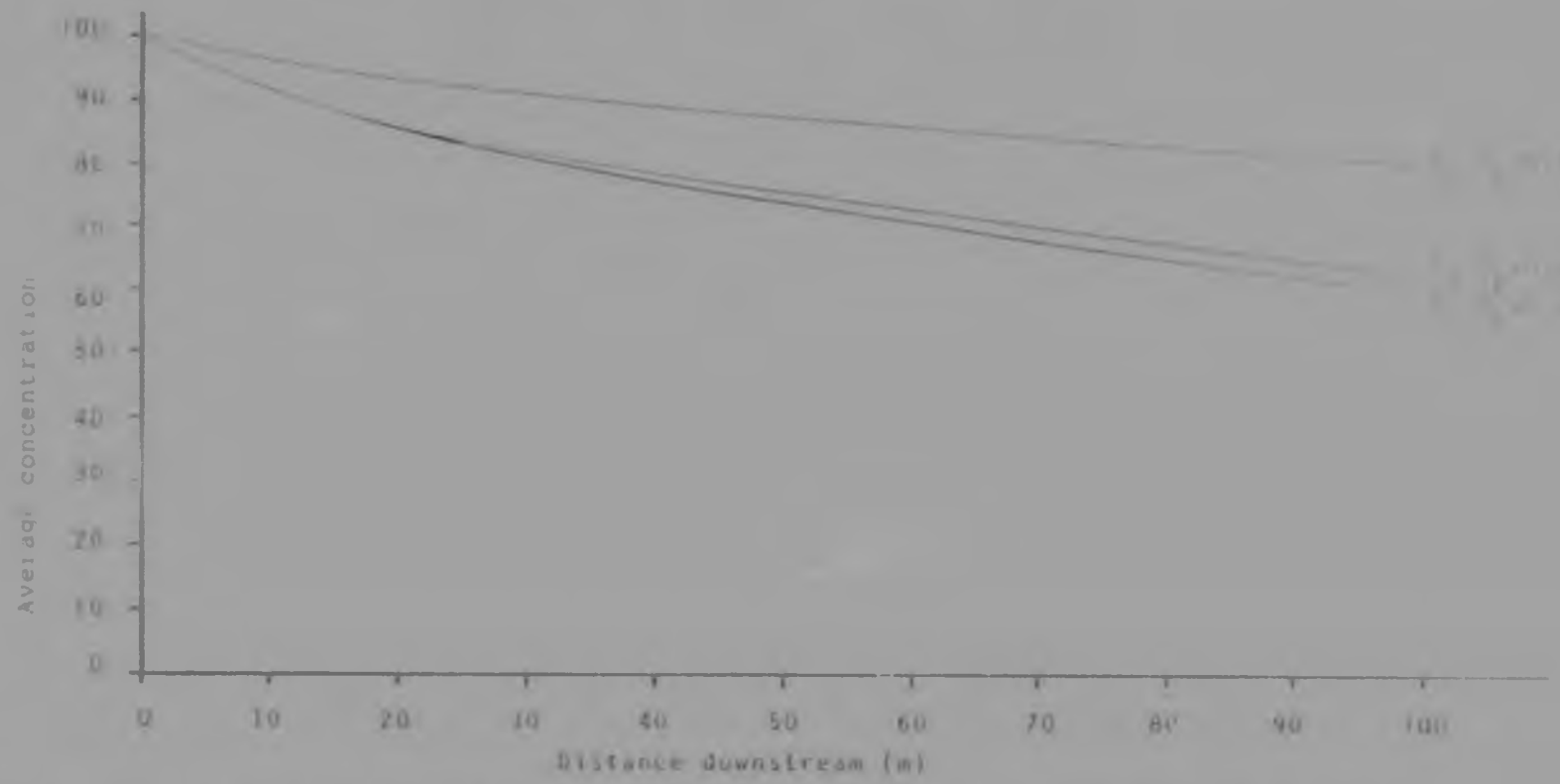


Fig. 9.20 Effect of bankfull channel depth (D_c-D_p) on sediment distribution

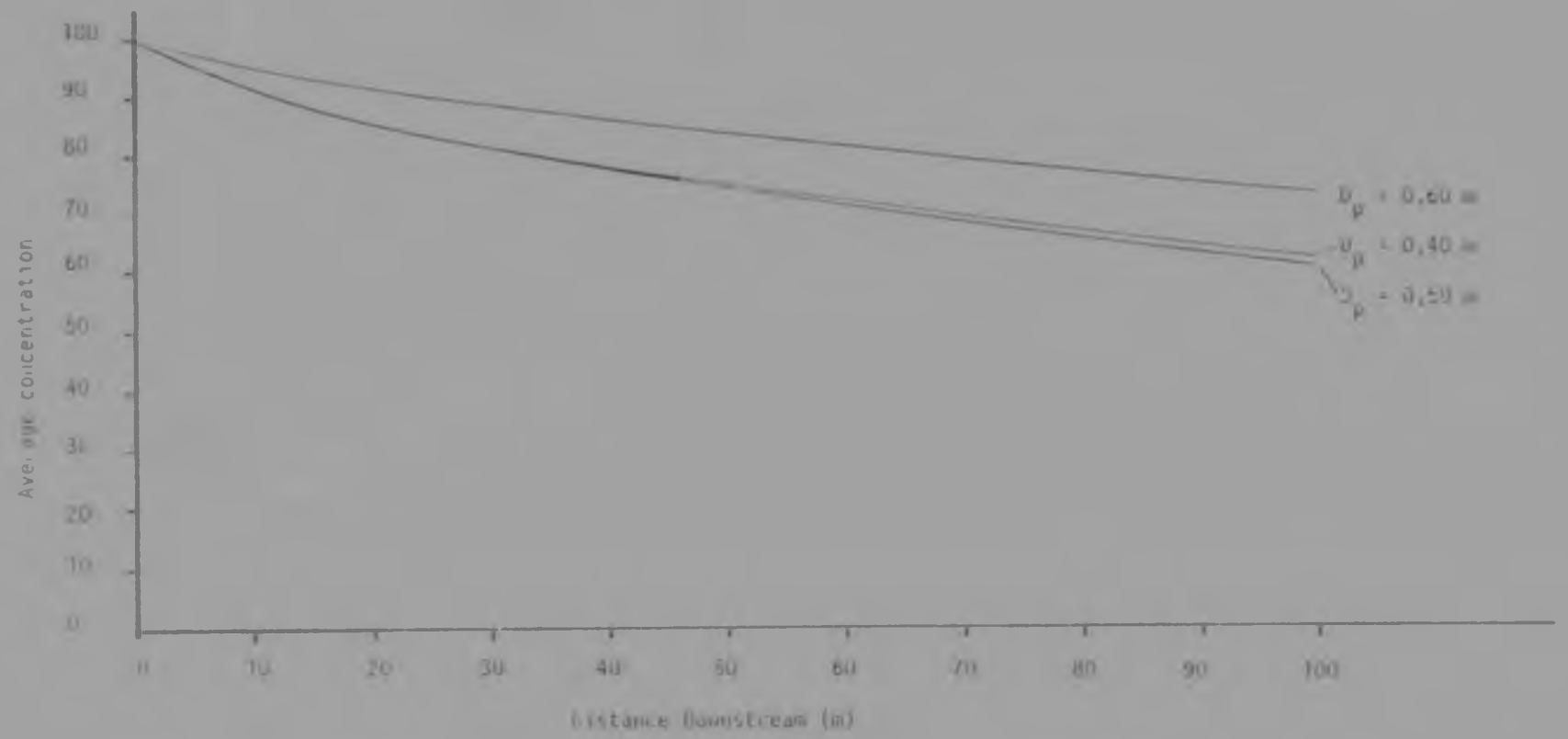


Fig. 9.11 Effect of water level on sediment distribution

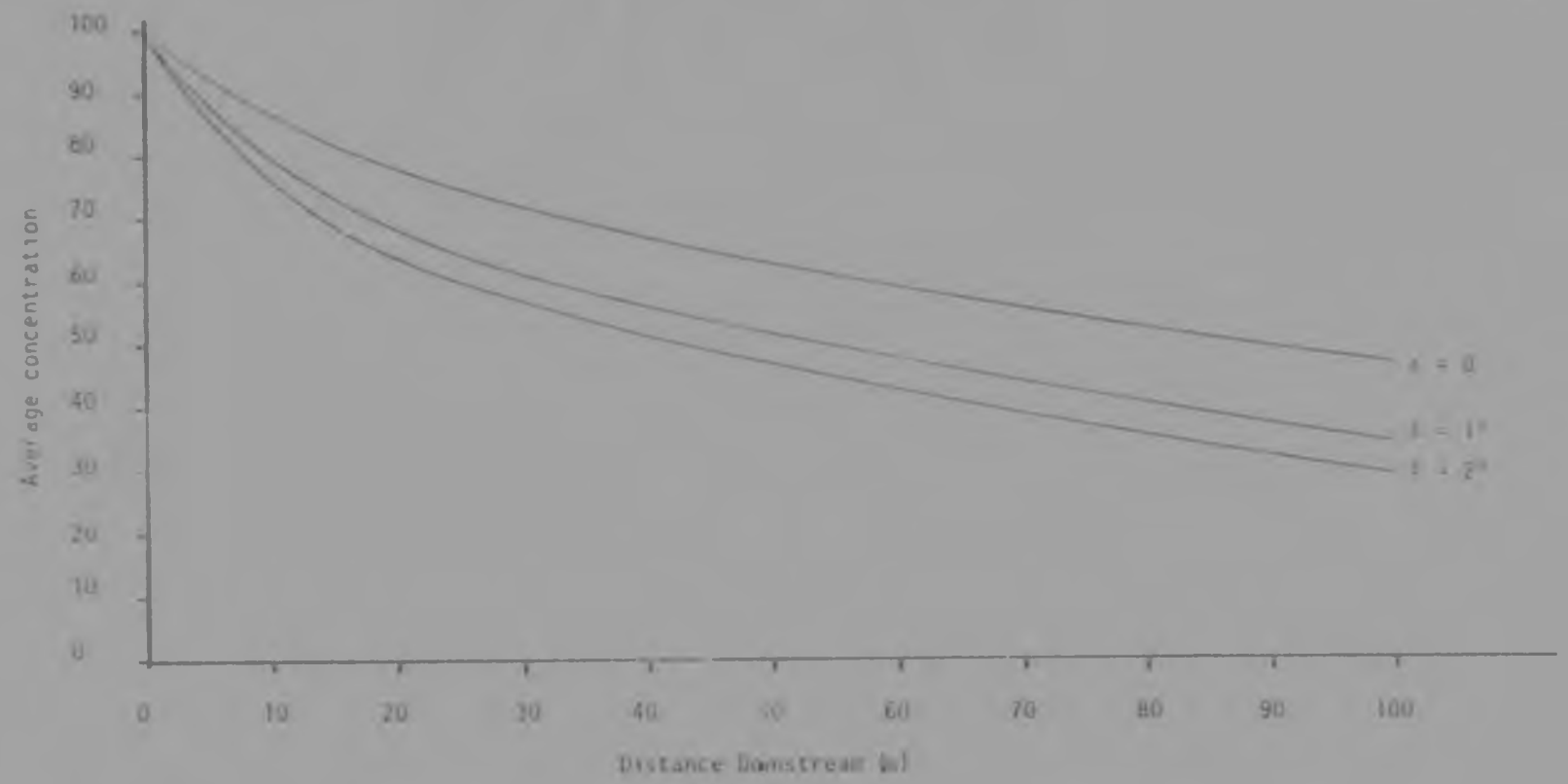


Fig. 9.12 Effect of transverse convection on sediment distribution

The fall velocity of a sediment particle has a strong influence on its behaviour in suspension. Fall velocities ranging from 0,10 m/s to 0,02 m/s were used and the resulting longitudinal sediment distributions are shown in Figure 9.13. It will be noticed that the average concentration at the end of the reach is a minimum for a fall velocity of 0,03 m/s while 30 m from the beginning of the reach the average concentration is the same for fall velocities of 0,10 m/s, 0,07 m/s and 0,05 m/s. This dependence on position within the reach is caused by the non-equilibrium concentration profile specified at the beginning of the reach. Adjustment to an equilibrium concentration profile is most rapid for heavier particles, and this profile is such that most sediment is concentrated close to the bed and relatively little is above the plain surface and available for transverse transfer. The loss of sediment from the channel is therefore relatively small and the rate of decrease of average concentration with distance is relatively low. For smaller particles the concentration profile is more uniform and more sediment is in suspension above the plain surface and available for transfer, resulting in a relatively high transfer rate along the reach. If an equilibrium concentration profile were input at the beginning of the reach the average concentration at the end of the reach would decrease monotonically with decreasing fall velocity.

It is known that the velocity of a suspended particle in the flow direction is less than the flow velocity. For all the sensitivity analyses described previously it was assumed that the average particle velocity was identical to the average flow velocity. The effect of this assumption was determined by generating sediment distributions with reduced particle velocities. The effect proved to be significant, as illustrated in Figure 9.14.

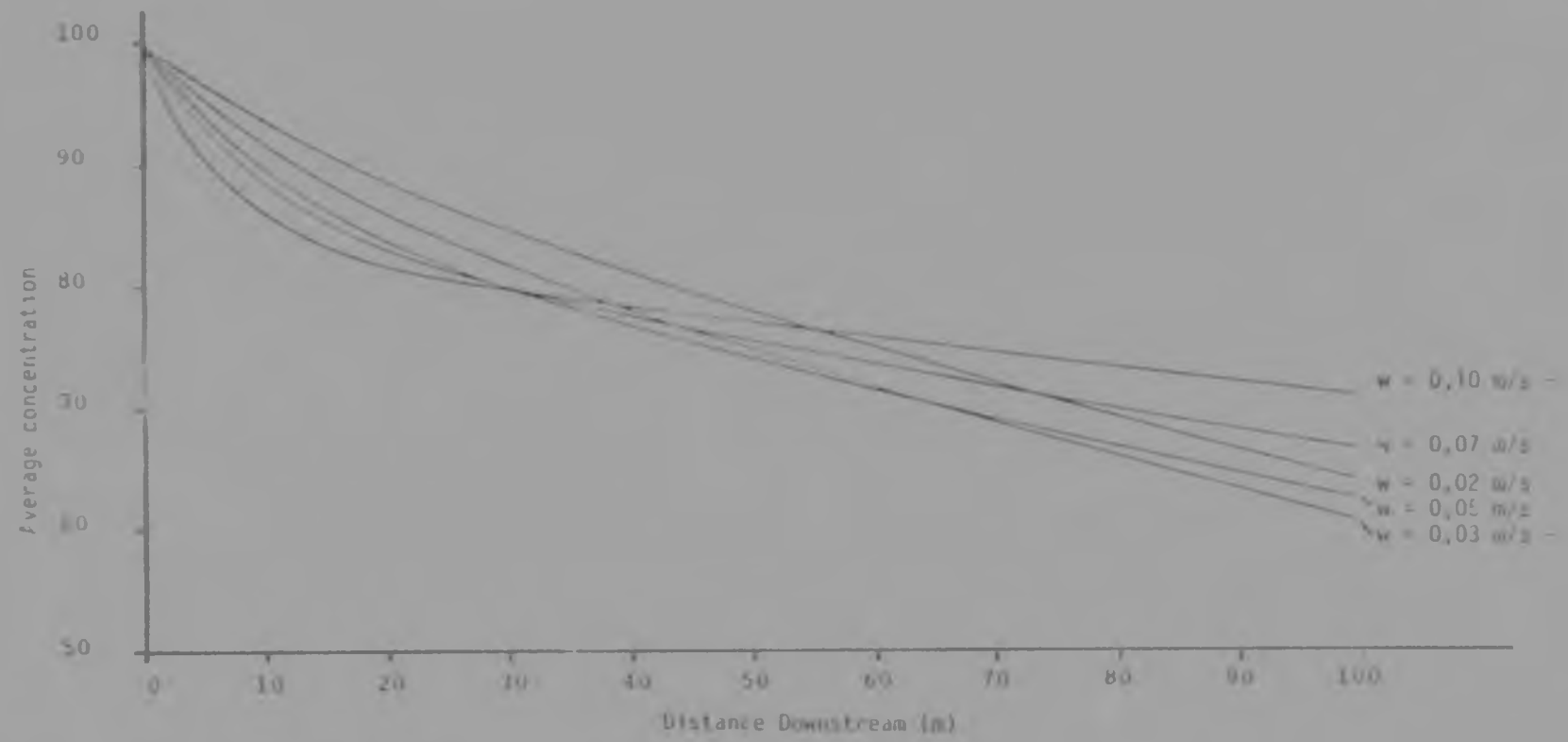


Fig. 9.13 Effect of fall velocity on sediment distribution

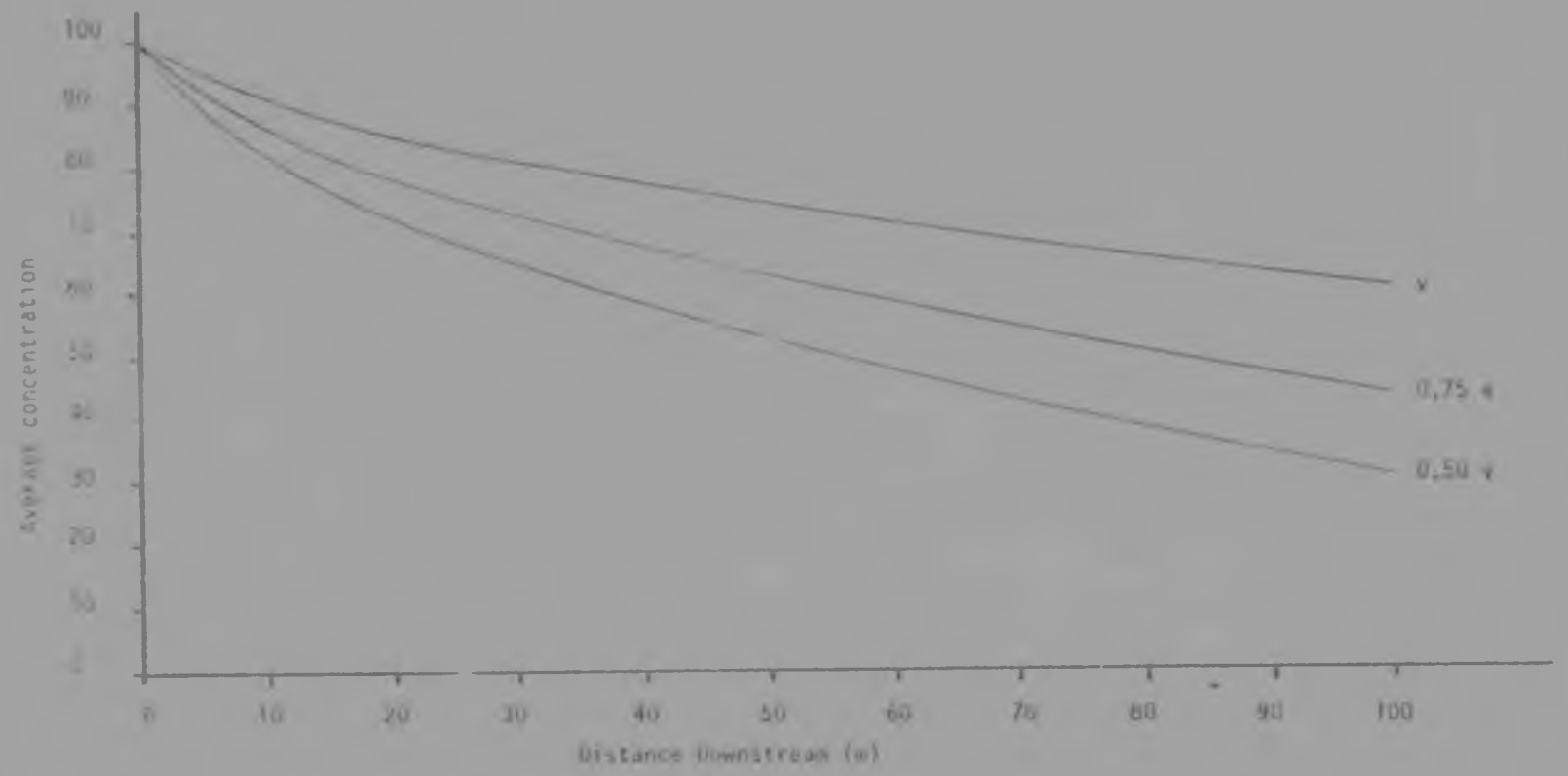


Fig. 9.14 Effect of reduced particle velocity on sediment distribution

In all of the previous analyses it was also assumed that the flow velocity was distributed uniformly along a vertical section. The velocity is known to be distributed logarithmically and the von Karman-Prandtl distribution was substituted. The result was a more gradual adjustment to the equilibrium concentration profile but thereafter a higher rate of decrease of average concentration, as shown in Figure 9.15. It must be noted that the very steep concentration gradient near the channel bed can lead to exaggerated estimates of average concentration unless very small vertical grid spacing is used. The low velocities near the bed also tend to exacerbate stability problems, particularly for small channels on mild stopes.

On the strength of the results shown in Figures 9.14 and 9.15 the model was modified to include a reduction in particle velocity and an option for a logarithmic flow velocity distribution, as described in Chapter 8.4.

9.3 Hypothetical Distributary System

A simple idealized distributary system was synthesized and used to illustrate application of the sediment distribution models.

The first channel in the distributary system was assumed to have the same characteristics as the standard channel used for the sensitivity analyses. This channel was assumed to be 100 m long and then to divide into two equal distributaries. Each of these distributaries was also assumed to be 100 m long and then to divide into two further distributaries. This pattern was assumed to be repeated twice more, resulting in the configuration shown in Figure 9.16.

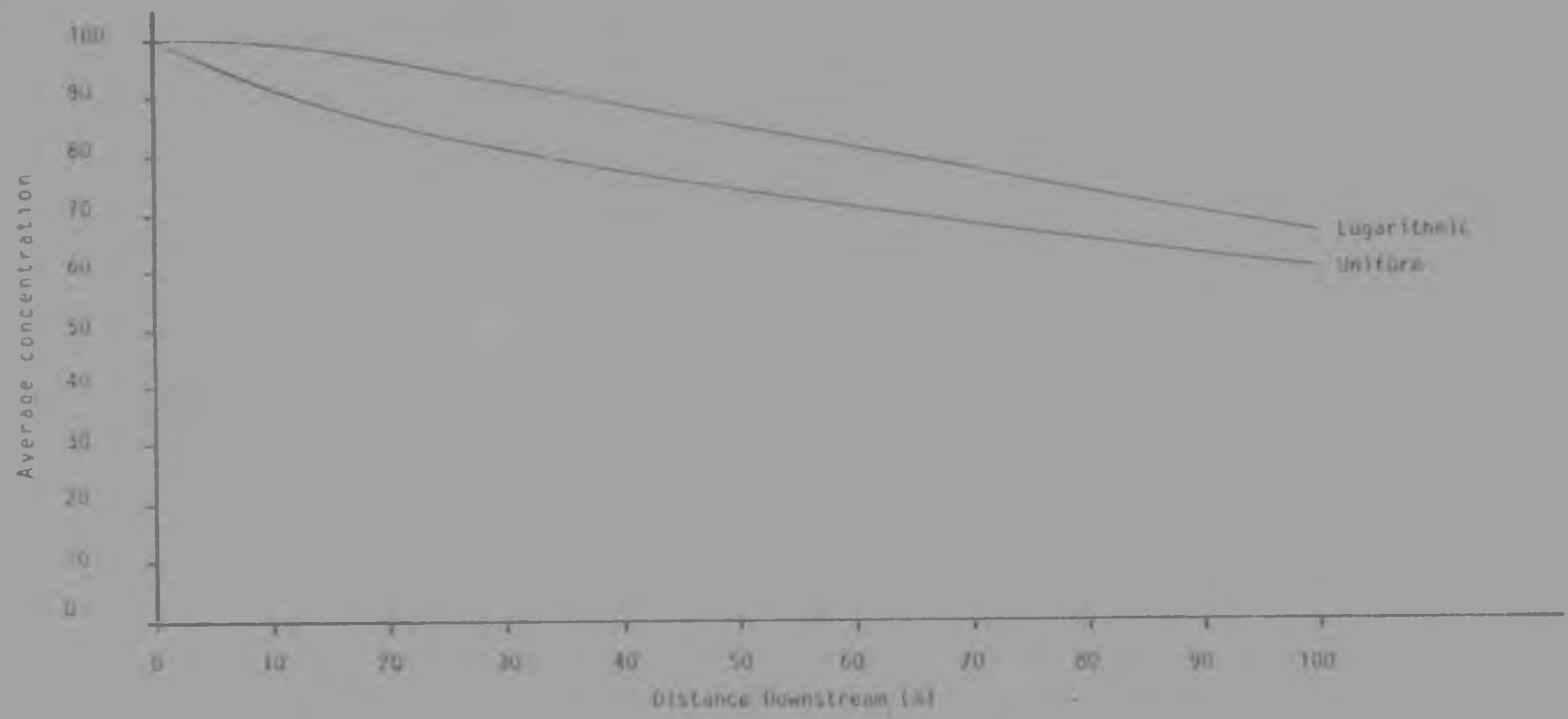


Fig. 9.15 Effect of velocity distribution on sediment distribution



Reach 1	Channel width	= 2,0 m
	Channel depth	= 0,50 m
	Gradient	= 0,005
	Average total width	= 22,0 m
	Flow depth on plain	= 0,50 m
	Reach length	= 100 m
Reach 2	Channel width	= 1,61 m
	Channel depth	= 0,40 m
	Gradient	= 0,004
	Average total width	= 35,4 m
	Flow depth on plain	= 0,40 m
	Reach length	= 100 m
Reach 3	Channel width	= 1,31 m
	Channel depth	= 0,325 m
	Gradient	= 0,003
	Average total width	= 57,6 m
	Flow depth on plain	= 0,325 m
	Reach length	= 100 m
Reach 4	Channel width	= 1.09 m
	Channel depth	= 0,27 m
	Gradient	= 0,002
	Average total width	= 95,8 m
	Flow depth on plain	= 0,27 m
	Reach length	= 100 m

Fig. 9.16 The hypothetical distributary system

Channel gradient was assumed to be constant along each reach but to decrease from reach to reach in a downstream direction. The gradients selected for the four reaches were 0,005, 0,004, 0,003 and 0,002. Channel sizes were calculated to be such that the bankfull discharge capacity of the system would be constant along its entire length. Using the same width-to-depth ratio for all channels and a discharge for each channel equal to half that of the channel immediately upstream, channel dimensions were calculated by Manning's equation with an n value of 0,02. The total width of the system was determined by assuming the plain areas associated with each channel to extend an average distance of five times the channel width on either side of the channel. The flow depths over the plains were then calculated using Manning's equation with n equal to 0,025 and assuming the depth to be constant over the whole width.

It must be emphasized that this system geometry is completely arbitrary. The geometry of a real distributary system is determined by the bed material characteristics and hydraulic conditions prevailing during its formation.

The distribution of gold particles in the hypothetical distributary system was determined for steady flow conditions using the transverse and longitudinal distribution models. The effect of transverse convection was ignored, i.e. it was assumed that channel flow and plain flow were parallel throughout the system.

The concentration profile input at the beginning of the first reach was the equilibrium profile calculated from the characteristics of the first channel using a bed concentration of 1000 units. The concentration profile input to each subsequent reach was determined from the profile obtained at the end of the preceding reach.

These profiles had to be adjusted slightly because the uniform flow depths are different in each reach and the longitudinal model does not account for the nonuniform drawdown towards the end of each reach. The same number of grid points was used in successive reaches and it was assumed that the concentration values were the same at corresponding grid points at reach junctions, although the grid spacing was not identical. This is a reasonable assumption for small differences in uniform flow depth because the accelerating flow in the nonuniform region towards the end of a reach would tend to maintain the same total amount of material in suspension despite the reduction in depth.

The distributions of average concentration of suspended gold within the channels is shown in Figure 9.17. The concentration decreases progressively through reaches 1, 2 and 3 and then very rapidly at the beginning of reach 4 so that after about 15 m no gold remains in suspension. The analysis was repeated with a gradient of 0,004 in reach 3. As can be seen on Figure 9.17 the concentration decreases less rapidly in reach 3 but the gold extends no further into reach 4.

The distribution of gold deposits in the channels and on the plains are shown in Figures 9.18 and 9.19 for third reach gradients of 0,003 and 0,004 respectively. All deposition values are relative to the deposition in the channel at the beginning of the first reach. Channel deposits are shown along one flow path through the system. The plain deposit distribution represents the total amount of gold deposited on the plain areas in the whole system, i.e. the deposits associated with all channels in each reach were added together.

Both channel deposit distributions show clearly the sudden increase in deposition at the beginning of each reach as the deposition probability increases and the

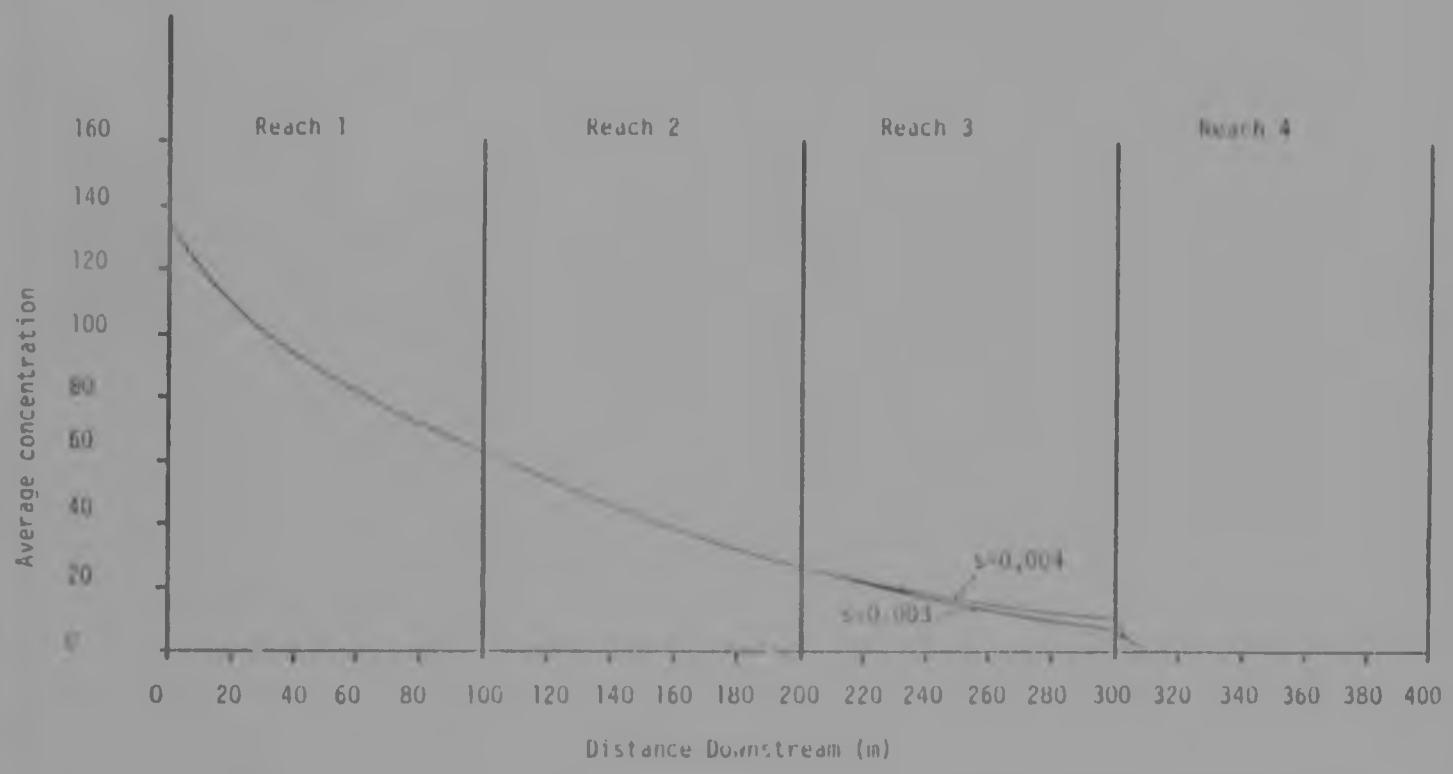


Fig. 9.17 Distribution of suspended gold in distributary channels

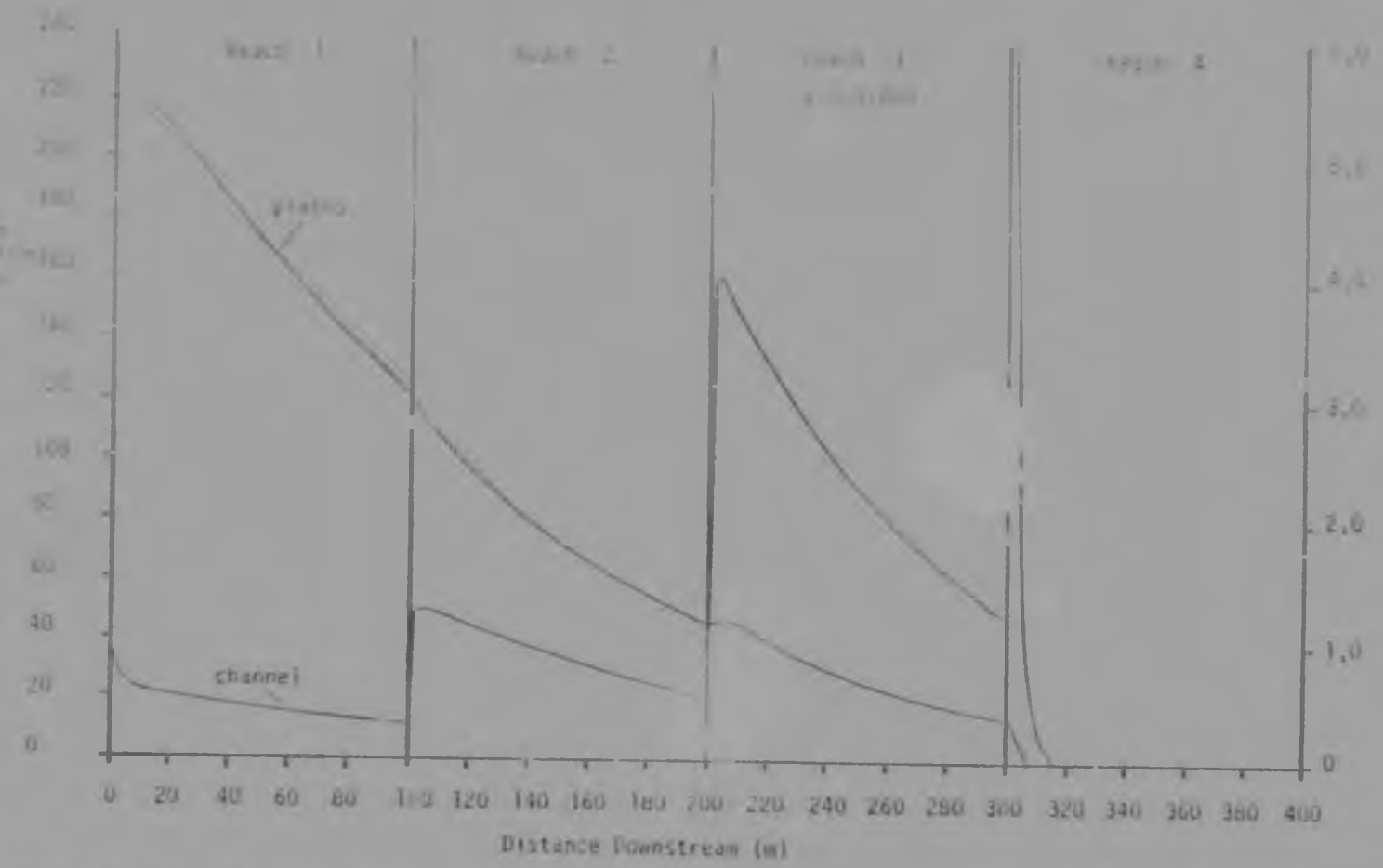


Fig 9.18 Distribution of gold deposits in hypothetical distributary systems

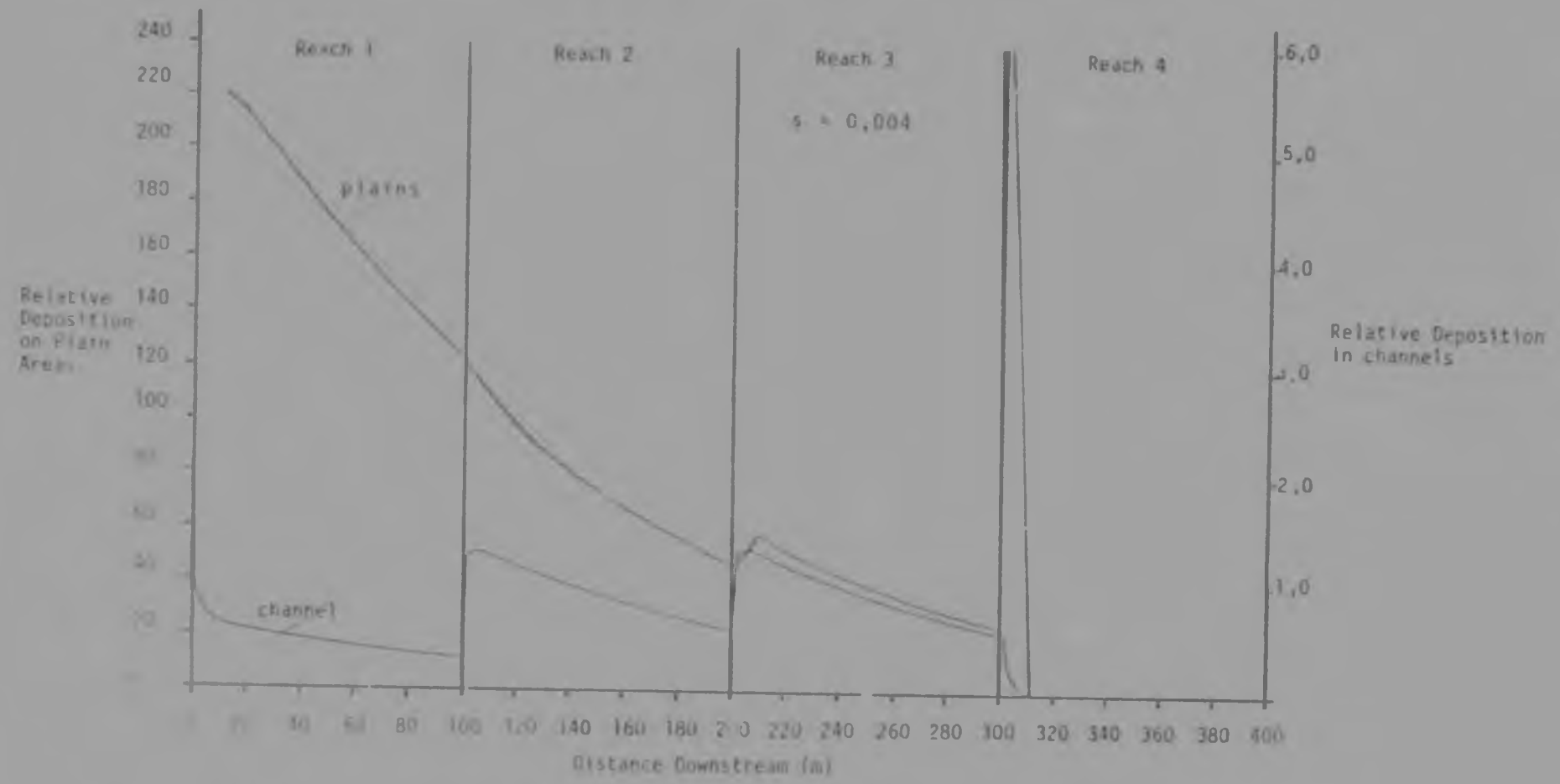


Fig. 5.14 Distribution of gold deposits in hypothetical distributary system

input concentration profile adjusts to a new equilibrium with a higher bed concentration. This is particularly remarkable in the fourth reach where all the gold in suspension is deposited over a short distance. Increasing the gradient of reach 3 has the effect of reducing channel deposits in that reach and increasing the supply of gold to reach 4.

Plain deposits decrease progressively through the system except for a slight increase at the beginning of reach 3, particularly noticeable for the higher gradient. It is possible that local increases in plain deposits could be significant in certain real system configurations.

It should be noted that channel deposits increase downstream through the system while plain deposits decrease. At the beginning of reach 1 the plain deposits exceed channel deposits by a factor of about 230. At the beginning of reach 4 this factor has reduced to 0,14, i.e. there is more gold in the channel bed than on the plains. In the first reach the gold is deposited in narrow bands along the edges of the channel with negligible amount within the channel. In lower reaches the plain deposits become progressively less concentrated and more extensive with less difference between channel and plain concentrations.

10. CONCLUSION

Two numerical models have been developed which can be used together to describe the transport and deposition of small suspended sediment particles in a compound channel system. Each model describes the distribution of particle concentration in two dimensions, the first in the vertical and transverse directions and the second in the vertical and longitudinal directions. The use of these two models obviates the need for a three-dimensional model which would require excessive computation time.

That the gold now present in the Witwatersrand reefs was transported mainly in suspension has been confirmed by comparing the hydraulic conditions necessary for suspension with those prevailing when the reefs were formed. Established criteria for suspension in terms of particle fall velocity and the shear velocity of the flow were used to define combinations of hydraulic gradient and flow depth capable of suspending typical gold particles. These conditions were confirmed by applying Einstein's sediment transport model to hydraulically equivalent sand grains. A relationship between drag coefficient and Reynolds number was determined experimentally for estimating fall velocities of gold particles. The hydraulic conditions prevailing when the reefs were formed were inferred from the size of the largest particles present. The Shields criterion for sediment motion and the Meyer-Peter and Muller equation for bed load were used to determine the hydraulic gradients and flow depths required to move such particles. These conditions were well within the range capable of suspending gold. Deposition patterns of gold are therefore closely related to the distribution of gold particles in suspension.

The distribution models are based on the diffusion analogy for suspended sediment. The transverse distribution of suspended material is described by a two-dimensional elliptic partial differential equation which expresses continuity for sediment in terms of diffusive and convective transport components. The equation is expressed in finite difference form and solved numerically by the method of Successive Over-Relaxation using an accelerator which is optimized at each iteration step. The solution describes the distribution of sediment concentration in the flow region between adjacent channels from which the relative distribution of plain deposits can be determined.

Solution of the transverse distribution equation requires estimates of turbulent diffusivities and particle velocities in both the transverse and vertical directions. Turbulent diffusivities for sediment are related to momentum diffusivities which are calculated from the flow geometry using theoretical and empirical relationships. The vertical particle velocity is assumed to be the terminal fall velocity in quiescent water. The transverse velocity is calculated as the component of sediment velocity over the plain normal to the channel direction. Convection associated with secondary circulation is assumed to be accounted for in the transverse diffusivity term. Flow velocities in the channel and over the plain are calculated using Manning's equation. The appropriate wetted perimeters depend on the flow condition and are selected by a procedure based on experimental results for rectangular compound channels.

The integration domain for the transverse distribution equation is bounded by the water surface, the plain bed and either two channel boundaries or one channel boundary and a solid vertical surface. Boundary conditions must be specified for all of these surfaces

The distribution models are based on the diffusion analogy for suspended sediment. The transverse distribution of suspended material is described by a two-dimensional elliptic partial differential equation which expresses continuity for sediment in terms of diffusive and convective transport components. The equation is expressed in finite difference form and solved numerically by the method of Successive Over-Relaxation using an accelerator which is optimized at each iteration step. The solution describes the distribution of sediment concentration in the flow region between adjacent channels from which the relative distribution of plain deposits can be determined.

Solution of the transverse distribution equation requires estimates of turbulent diffusivities and particle velocities in both the transverse and vertical directions. Turbulent diffusivities for sediment are related to momentum diffusivities which are calculated from the flow geometry using theoretical and empirical relationships. The vertical particle velocity is assumed to be the terminal fall velocity in quiescent water. The transverse velocity is calculated as the component of sediment velocity over the plain normal to the channel direction. Convection associated with secondary circulation is assumed to be accounted for in the transverse diffusivity term. Flow velocities in the channel and over the plain are calculated using Manning's equation. The appropriate wetted perimeters depend on the flow condition and are selected by a procedure based on experimental results for rectangular compound channels.

The integration domain for the transverse distribution equation is bounded by the water surface, the plain bed and either two channel boundaries or one channel boundary and a solid vertical surface. Boundary conditions must be specified for all of these surfaces

in terms of either derivatives or concentration values. Channel boundaries are defined in terms of concentration values calculated by a theoretical solution of a one-dimensional diffusion-settling equation applied to sediment in the channels. No sediment can be transferred across the water surface and at the bed the rate of transfer is defined by the probability that a particle reaching the bed will deposit; this probability is determined by flow characteristics and surface properties. The solid vertical surface is defined in terms of derivatives calculated from conditions close to the boundary.

The transverse distribution model was verified by comparing predicted and measured distributions of deposits in a laboratory flume with a compound section. Fine sand was placed on the bed of the deep section of the laboratory channel and distributions of deposits on the plain section were measured for a range of particle sizes and flow depths for two different types of plain surface. The measured distributions agreed well with those predicted by the model.

The longitudinal distribution of suspended particles in a channel is described by a parabolic partial differential equation which includes terms for diffusion and convection in the vertical, longitudinal and transverse directions. Rates for the transverse terms are calculated by the transverse distribution model which enables the longitudinal distribution to be solved as a two-dimensional problem. The equation is expressed in finite difference form subject to appropriate boundary conditions and solved explicitly. The solution describes the distribution of suspended sediment concentration over flow depth and distance along the channel, from which the relative amounts of sediment deposited on the channel bed and transferred to the plains along the reach are determined. Various flow parameters

required for the solution are obtained from output from the transverse model which must therefore always be run before applying the longitudinal model.

The grid spacings required for the finite difference solutions depend on the accuracy required. The vertical spacing should be selected to give a reasonable description of the sediment concentration profile above the level of the plain surface. The horizontal spacing must then be selected to ensure stability and convergence of the solution.

In the forms presented the models can be applied to straight channels under longitudinally uniform, steady flow conditions. Nonuniform conditions could be analysed by performing preliminary flow calculations and applying the longitudinal model, with relatively minor modification, to reasonably short reaches. The transverse model would be adequate for nonuniform conditions provided changes in conditions take place gradually with respect to the distance required for a particle to settle through the depth of flow. A certain degree of unsteadiness could also be considered by assuming consecutive periods of steady flow. Unsteady, nonuniform analysis would not be warranted, however, until the conditions prevailing at the time of deposition are better understood.

The models have been applied to hypothetical systems to identify the factors which would have the greatest effects on gold distributions. These studies indicate that the transverse extent of plain deposits is determined primarily by the magnitude of the transverse convective transport component. This component is related to the direction of the channels relative to the steepest gradient of the plain and would obviously enhance the diffusive transport on one side of the channel and detract from it on the other. The most

extensive deposits of gold can therefore be expected to be unsymmetrical about the associated channel, which would be changing direction or inclined to the general flow direction. The convective component is strongly related to channel direction, flow depth and hydraulic energy gradient. There would be no transverse convective component for channels which are straight and parallel to the steepest gradient of the plain. In such cases the distribution would result from diffusive transport only and would be the same on both sides of the channel. This distribution has been found to depend primarily on hydraulic gradient, size of channel, particle fall velocity and the probability that a particle settling to the bed will deposit. The effects of these parameters are very local, however, and deposits can be expected to be confined to within a distance from the channel of about three times the flow depth on the plain. Symmetrical distributions can therefore be expected to be limited in extent. The shape of the distribution close to the channel is not very important for prediction of gold concentrations but would be very useful for inferring hydraulic conditions.

Transverse distributions of gold observed in the reefs were reproduced by the transverse model. Although the hydraulic conditions associated with the observed distributions are completely unknown, acceptable agreement was obtained by choosing reasonable values for flow parameters.

The longitudinal distribution of deposits is closely related to the transverse distribution because the variation in the amount of suspended sediment in the channel depends on the rate of transfer to the plain. Any parameters which increase the rate of transfer to the plain will obviously decrease the amount of sediment in the channel further downstream. The para-

meters which affect the longitudinal distribution most significantly were found to be the channel width, particle fall velocity, downstream transport velocity, the probability of deposition on the channel bed and the longitudinal gradient. The last two parameters are closely related and the ratio of plain deposition to channel deposition was found to be extremely sensitive to gradient. This ratio could be a valuable indicator of gradient when attempting to reconstruct channel configurations from reef samples.

Results of the hypothetical applications of the models lead to some general conclusions regarding the distribution of gold in distributary channel systems in which channel size and gradient may normally be expected to decrease in a downstream direction. The highest concentrations of gold can be expected on plain areas adjacent to relatively large channels in the upper reaches of the system. The gradients of these channels would be relatively steep and the ratio of plain deposits to channel deposits would be high. The larger channels would tend to be more closely aligned to the plain slope than smaller channels. Transverse convection would therefore be relatively less significant and gold deposits would tend to be confined to narrow bands along the sides of the channels. Concentrations within these channels would be very low.

As channels become smaller and less steep the ratio of plain deposits to channel deposits decreases. Plain deposits would generally be less than for larger channels but are likely to be more extensive as the likelihood of transverse convective transport increases. Total deposits decrease progressively as transport capacity and hence supply rates decrease until eventually all the gold will have deposited.

Local regions of high concentration can be expected

both within channels and on plains immediately downstream of channel divisions, particularly where the size difference between successive channel reaches is large. This results from rapid deposition as transport capacity is reduced. The effect is more noticeable within channels as the suspended load becomes more concentrated near the channel bed, below the plain surface.

These conclusions should be regarded as general indications only as distributions will be determined by specific characteristics of local channel configuration. Reworking of deposits by subsequent events would also have significant effects on distributions.

The transverse and longitudinal models could be used to predict patterns of gold distribution for most situations for which the channel geometry and prevailing hydraulic conditions are known. The limited knowledge of geometry and hydraulic conditions for the reefs, however, restricts their usefulness as predictive tools although there would certainly be some useful predictive applications on a fairly small scale during mining operations. Until more information about reef channels is available the models would probably be more useful for hydraulic interpretation of observed deposition patterns. The experimental verification and comparisons with observed deposits conducted in this study indicate that the models describe the fundamental processes reliably and therefore provide a link between observed deposits and their causative events. A deterministic interpretation of observed deposits should lead to a more thorough understanding of reef formation and ultimately to improved predictions of gold distribution.

Much research must still be done before the distribution of gold in the reefs can be satisfactorily

explained and predicted. The approach followed in this study should yield more valuable insight if pursued further in parallel with other methods. The models presented can be used to develop general relationships between gold distribution and reef structure. For accurate predictions some of the empirical relationships incorporated in the models should be verified generally and refined if necessary.

The interaction between channel and plain flows requires further investigation. Relationships for evaluating transverse diffusivity through the interaction zone, boundary shear stress distributions and the average flow velocities in the channel and over the adjacent plain are based on experimental results obtained for rectangular compound sections. Natural channels are not rectangular and these relationships should be verified for different shapes. Ideally, a theoretical model is required which could predict the distribution of velocity and momentum transfer in a channel of arbitrary section. Some advances have already been made in this direction. Querner and Doyle (1980), for example, presented a finite element model for predicting the distribution of velocity across a channel. This model however, requires a priori description of the distribution of momentum diffusivity which is unreasonable, especially for compound sections.

The models presented in this report indicate that concentrated gold deposits would tend to occur immediately downstream of channel junctions. The models cannot describe the local distributions accurately in such regions and a more detailed three-dimensional model would be required. Such a model would also require better understanding of turbulent structure.

The model proposed for evaluating the probability of

particles on a coarse bed is tentative. Results are not particularly sensitive to this parameter but the model should be calibrated experimentally if greater accuracy is required. The deposition probability models for coarse and fine beds incorporate a critical shear stress for particle motion. This critical condition requires further experimental work for particles with high density and different shapes and for mixtures of different particle sizes. Improved understanding of differential entrainment and deposition would also help to explain heavy mineral concentration on a bedform scale.

Improved knowledge of the processes of gold transport and deposition will not enable gold distribution to be described adequately until the hydraulic conditions prevailing during reef formation are better understood. The highest priority for research should therefore be given to hydraulic interpretation of reef structures. Extensive data are required describing the stratigraphy and lateral variation of channels within the reefs and the distributions of particle sizes as well as the associated patterns of gold concentrations. The models presented in this report could be useful for hydraulic interpretation and could be refined and developed as more information becomes available.

APPENDIX A: TRANSVERSE DISTRIBUTION MODEL PLAINDEP

A.1 Description of Computer Program

The transverse distribution model described in the main body of this report has been coded in FORTRAN for solution by computer. The program comprises a main program and three subroutines, which are discussed briefly below.

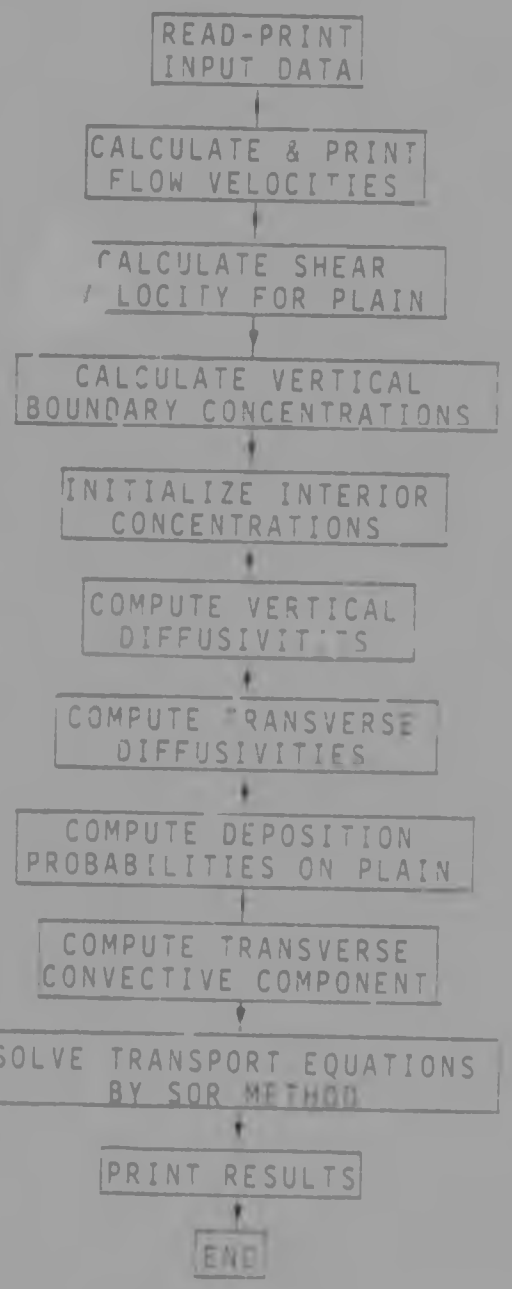


Fig. A.1 General flow diagram for program PLAINDEP

A.1.1 Main Program PLAINDEI

Computations proceed as shown in Fig. A.1

Input data are read off a file appended to the program. Data describing the flow geometry and sediment characteristics are immediately printed on the output file.

Flow velocities for the plain and channel or channels are calculated using Manning's equation. The wetted perimeter for the plain is assumed to be the plain width if two channels are specified and the plain width plus the flow depth if one channel only is specified. The flow areas and wetted perimeters for the channels are calculated according to the procedure described in chapter 4.5. If the ratio of total flow depth in a channel to the depth below the plain surface is greater than 2,0, a vertical interface between channel and plain is assumed and excluded from the wetted perimeter. If the ratio is less than 2,0 then a diagonal interface is assumed and included or excluded from the wetted perimeter depending on the value of the apparent shear stress ratio. The interface is excluded initially and the velocity and apparent shear stress ratio calculated in subroutine FLOVEL. If this ratio is greater than 0,5 the velocity is recalculated with the interface included and the apparent shear stress ratio calculated again. If the new value is less than 0,5 the velocity is assumed to be the average of the values obtained by including and excluding the interface.

The shear velocity for the plain is calculated by subroutine SHVEL.

The sediment concentrations on the vertical boundaries are calculated according to the theory explained in chapter 5.1. The shear velocity for the channel is

calculated by subroutine SHVEL and the concentration profile generated by subroutine BCPROF. If two channels are specified the reference concentration for the second channel is calculated from the value input for the first channel in proportion to the excess dimensionless boundary shear stress raised to the power of 1,5.
Before iteration of the sediment concentrations begins, the concentrations at all interior grid points are initialized to zero.

Vertical diffusivities are calculated for all grid points using the equations presented in chapter 4.2. For values within the interaction zones the appropriate channel is identified by comparing the loop counter with the number of the grid point halfway across the plain; all points before the half-way point are related to the first channel, and all points after the half-way point to the second channel. For all points further from a channel than three units of the dimensionless transverse distance scale, the boundary shear stresses and hence the vertical diffusivities are assumed to be unaffected by the channel-plain interaction. These values are calculated from the shear velocity for the plain.

Transverse diffusivity is assumed to be constant on any vertical section. Values are calculated for all vertical sections as described in chapter 4.2. A value for sections unaffected by the interaction zones is calculated first. This value depends on the plain width and a reduced width is determined by subtracting the width of the interaction zone on both sides of the plain from the total width. Within the interaction zones the values are calculated using the equations given in chapter 4.2. All transverse diffusivities are restricted to values greater than or equal to the undisturbed value. Transverse diffusivities are adjusted for particle size in terms of the particle Reynolds number by multiplying by the factor described in chapter 4.2.

The probability of deposition is calculated for each point on the plain bed according to the procedure explained in chapter 5.2. The probability of erosion from a solid surface is calculated, multiplied by the exposed fraction of the bed and subtracted from unity.

The transverse convective transport component is calculated as described in chapter 4.4. The flow velocity in the direction of the steepest gradient of the plain is calculated from the channel gradient and direction. The velocity of sediment in this direction is then calculated and the component normal to the channel direction is taken and checked to be positive. This component is then printed.

Once all preliminary calculations have been completed the transverse transport equation is solved. At each iteration the SOR accelerator is re-estimated by means of the algorithm described in chapter 3.3. The coefficients for the concentrations in the transport equation are calculated, depending on the location with respect to the boundaries of the grid point being considered. The new concentration for each grid point is then calculated using the appropriate form of the transport equation. This value is compared with the value at the previous iteration and if the largest difference for all grid points is within the specified tolerance the computation is terminated.

Two options are available for printing output. If required the sediment concentrations at all grid points are printed. If this detail is not required only the bed shear stress, transverse diffusivity, probability of deposition and the deposition concentration relative to that at the edge of the first channel are printed for each grid point on the plain bed. The relative deposition at each point is calculated by multiplying

the bed concentration by the probability of deposition and dividing this product by the value obtained for the point adjacent to the first channel. The number of iterations required for the solution and the final value of the SOR accelerator are also printed.

A.1.2 Subroutine BCPROF

This subroutine computes sediment concentrations at all points on the vertical boundary or boundaries defined by channels. The procedure is based on a one-dimensional diffusion model described in chapter 5.1

A.1.3 Subroutine SHVEL

This subroutine calculates the shear velocity associated with grain roughness for channel or plain flow. A reduced hydraulic radius is calculated from the equation for average velocity given in chapter 4.3. This hydraulic radius and the longitudinal gradient are then used to calculate the shear velocity.

A.1.4 Subroutine FLOVEL

This subroutine calculates the flow velocities in the channels using Manning's equation and the wetted perimeter as defined in the main program. For certain extreme conditions it is possible that the procedure used for computing velocities in compound channels can result in channel velocities being less than plain velocities. Such conditions are unlikely to occur, but as the transport model depends on the velocity difference between channel and plain all computation is stopped if this difference is negative and a message to this effect is printed. Subroutine FLOVEL also calculates the apparent shear stress ratio on the diagonal

interface between channel and plain. This ratio is used in the main program as a criterion for including or excluding the interface in the wetted perimeter.

A.2 Users' Guide

The input data required by program PLAINDEP describe the flow geometry and conditions, the sediment characteristics and the finite difference grid parameters. The data are inserted immediately following the program coding. Numerical data are all entered in 8-column fields and should be right justified as some variables are integer type. Each input line and each data item is discussed in the following paragraphs in order of input.

Lines 1 and 2 Title

Any alphanumeric information may be entered in columns 1 to 70 in the first two cards to serve as a run identification title. This information will be printed at the beginning of the output. Two title lines must always be included; if no title is required two blank lines should be inserted.

Line 3 Channel Configuration

Item 1. The number of channels to be simulated, either 1 or 2. If one channel is specified the plain is assumed to be bounded by a channel on one side and a solid vertical boundary on the other. If two channels are specified the deposition on the plain area between the channels is computed. Deposition on either side of a single channel can be predicted by specifying two channels of equal size and shape.

Item 2: The channel direction, in degrees. This is the

angle between the direction of the channels and the direction of the steepest gradient of the plain and is used for computing the transverse convective sediment transport component. The value should be zero if one channel is specified. If two channels are specified they are assumed to be parallel and the direction applies to both.

Line 4 Plain Data

Item 1: Flow depth on plain (m).

Item 2: Plain width (m). This is the distance between adjacent channels if two were specified on Line 3, or between the channel and the solid vertical boundary if one channel was specified. The width must be greater than the combined widths of the interaction zones adjacent to the channels. The width of each interaction zone is given by 1,28 times the depth of the relevant channel below the plain surface.

Item 3: Hydraulic gradient (m/m). This applies to the plain in the direction of the channel/s and to the channel/s.

Item 4: Manning's n. This should be estimated from the total roughness of the plain surface.

Item 5: Grain Roughness (mm). This can be represented by the median size of bed particles.

Line 5.A Data for First or Only Channel

Item 1: Flow depth in channel (m). This is the total depth of flow, i.e. from the water surface to the lowest point on the channel bed.

Item 2: Top width of channel (m). This is the width of the channel at the level of the plain surface.

Item 3: Bottom width of channel (m). Channels are assumed to be trapezoidal and symmetrical in section. This item represents the width at the lowest point of the channel.

Item 4: Manning's n for channel. This should be estimated from the total roughness of the channel boundary.

Item 5: Grain roughness (mm). This can be represented by the median size of the bed particles.

Item 6: Reference sediment concentration. All concentrations computed by the model are related to the concentration close to the bed of the first channel. All concentrations are relative and therefore the units and value of this item are arbitrary. A suitable value depends on the output requirements, channel geometry and the tolerance specified for the SOR solution. If detailed output is specified the concentrations are printed to four decimal places; the reference concentration should be chosen to give results consistent with this format. The concentrations on the vertical channel boundary decrease rapidly with distance from the channel bed. If the channel bed is much lower than the plain surface the reference concentration should be specified large enough for reasonable values to occur over the depth of flow on the plain. The iteration tolerance specified for the SOR solution is a concentration value and the number of iterations will obviously depend on the relative values of the tolerance and the computed concentrations. The tolerance and reference concentration should be specified such that the number of iterations is reasonable.

Line 5.B Data for Second Channel

This line is required only if two channels are specified

on line 3. The items are exactly the same as for Line 5.A except that no reference concentration is specified; this is calculated by the program.

Line 6 Sediment Data

Item 1: Particle size mm). This is the equivalent diameter of the particles being considered, i.e. the diameter of a sphere with the same density and fall velocity.

Item 2: Particle fall velocity (m/s). This is the terminal settling velocity of the particles and can be estimated from the equivalent diameter (Item 1) and the information provided in chapter 2.

Item 3: Relative density of particles. This is the density of the particle material relative to that of water.

Line 7 Finite Difference Parameters

The accuracy of the results depends on the spacing of the finite difference grid as well as on the tolerance specified for the solution. The grid spacing should be selected by using a progressively finer grid until the results converge to a reasonable degree.

Item 1: Number of grid intersections in the vertical direction. This includes the water surface and plain bed points.

Item 2: Vertical grid spacing. This is the distance between adjacent horizontal grid lines and is constant over the whole depth. The spacing can be calculated from the number of intersections and the total depth.

Item 3: Number of grid intersections in the horizontal direction. This includes both vertical boundaries.

Item 4: Horizontal grid spacing. This is the distance between adjacent vertical grid lines and is constant over the whole plain width. The spacing can be calculated from the number of intersections and the plain width.

Item 5: Iteration tolerance. Computation iterations are terminated when the maximum difference between point concentration values at successive iterations is within this specified tolerance. The value selected depends on the accuracy required and the value specified for the reference concentration in Line 5.A (q.v.).

Item 6: Initial accelerator for SOR solution. The accelerator value is adjusted at each iteration during computation. This value is required for the first iteration and must be between 1,0 and 2,0.

Line 8 Output Requirements

Item 1: Output indicator. Standard output includes input data, flow velocities, transverse convective velocity, and the distributions over the plain of bed shear stress, transverse diffusivity, probability of deposition and relative deposition concentration. If required a more detailed output including concentration values at all grid points can be printed. This item should have a value of 1 for the standard output and 2 for the detailed output.

A.3 List of Variables

A.3.1 Input

Variable	Description
AF	Initial value for SOR accelerator
CA1	Reference sediment concentration at bed of first channel
DCH1	Flow depth in channel 1 (m)
DCH2	Flow depth in channel 2 (m)
DELY	Vertical grid spacing (m)
DELZ	Horizontal grid spacing (m)
DEPTH	Flow depth on plain (m)
DIAM	Particle size (mm)
DIRN	Channel direction (degrees)
DM	Grain roughness on plain (mm)
DM1	Grain roughness in channel 1 (mm)
DM2	Grain roughness in channel 2 (mm)
IBC	Number of channels
IPRINT	Indicator for output requirements
M	Number of horizontal grid points
N	Number of vertical grid points
RMAN	Manning's n for plain
RM1	Manning's n for channel 1
RM2	Manning's n for channel 2
S	Relative density of sediment
SLOP	Hydraulic gradient
TITLE1(35)	First line for alphanumeric title
TITLE2(35)	Second line for alphanumeric title
TOL	Tolerance for SOR iteration
W	Sediment fall velocity (m/s)
WCH1	Top width of channel 1 (m)
WCH2	Top width of channel 2 (m)
WCHB1	Bottom width of channel 1 (m)
WCHB2	Bottom width of channel 2 (m)
WID	Width of plain (m)

A.[illegible] Program PLAINDEP

Variable	Description
ACH	Channel flow area
AB	Coefficient for CONC(I-1,J) in transport equation
ADEN	Term in equation for transverse diffusivity
AETA	Function for calcuating transverse diffusivity in mixing zone
AL	Coefficient for CONC(I,J-1) in transport equation
AL2	Coefficient for CONC (I,J-2) in transport equation
ANUM	Term in equation for transverse diffusivity
APL	Plain flow depth
AR	Coefficient for CONC (I,J+1) in transport equation
ASSRI	Apparent shear stress ratio for channel 1
ASSR2	Apparent shear stress ratio for channel 2
AT	Coefficient for CONC (I-1,J) in transport equation
B	Constant in deposition probability calculations
BET	Fall velocity parameter
BETA	Factor relating diffusivities for sediment and momentu…
BIGD	Channel flow depth
BT	Length scale for flood plain
CA2	Reference sediment concentration for channel 2
CONC(I,J)	Sediment concentration at point I,J)
[illegible]	Length of diagonal interface between channel 1 and plain

Variable	Description
D2	Length of diagona. interfac[illegible] channel 2 and plain
DCDZ(I)	Concentration gradient [illegible]n right b[illegible]
DCDZ1(I)	Concentration gradient on left bank
DEP(J)	Concentration of deposit at poi[illegible] (J) on plain
DEV	Absolute value of difference betwe[illegible] values of CONC (I,J) at succes[illegible] iterations
DIAG1	Length of diagonal interface b[illegible] channel 1 and plain
DIAG2	Length of diagonal interface b[illegible] channel 2 and plain
DISP	Average longitudinal dispers[illegible] efficient in plain flow
DIST	Transverse distance of point from channel
DK)	Intermediate results used when cal-
DK1)	culating SOR accelerator
DK2)	
DK3)	
DMAX	Maximum value of DEV at each [illegible]- tion
DRAT	Ratio of flow depth in [illegible] flow depth on plain
DY2	Square of vertical grid spacing
DZ2	Square of horizontal grid spa[illegible]
EPSY(I,J)	Vertica. boundary at point (I,J)
EPSZ(J)	Transverse diffusivity at points
ETA	Dimensionless distance over plain
EY1	Average value of vertical diffu[illegible] ity between points (I,J) and (I+1,
EY2	Average value of vertical diffu[illegible] ity between points (I,J) and I-1,
EZ1	Average value of transverse di[illegible]- vity between points (I,J-1)

Variable	Description
EZ2	Average value of transverse diffusivity between points (I,J) and (I,J-1)
EZINF	Transverse diffusivity over plain far from channel
EZM1	Average value of transverse diffusivity in grid space adjacent to solid vertical boundary
K	Counter used in calculation of SOR accelerator
KM	M-1
KM2	KM/2
M2	M/2
MM	M-2
P	Probability of erosion from solid surface
PDEP(J)	Probability of deposition at point (J) on plain
R1	Width of interaction zone for channel 1
R2	Width of interaction zone for channel 2
RCH1	Hydraulic radius for channel 1
RCH2	Hydraulic radius for channel 2
RDEP	Concentration of deposit on plain relative to that at J=1
REP	Particle Reynolds number
RPL	Hydraulic radius for plain
RWID	Width of plain between interaction zones
SAVE	Value of CONC(I,J) for comparison with next iteration
SLOPP	Steepest gradient on plain
SLOPT	Slope on plain normal to channel
SVEL	Shear velocity on plain
TAU(J)	Boundary shear stress at point (J) on plain

Variable	Description
TB	Boundary shear stress on plain at edge of channel
TH1	Dimensionless bourdary shear stress for channel 1
TH2	Dimensionless boundary shear stress for channel 2
THETA	Dimensionless boundary shear stress on plain
THETAC	Critical value of THETA (Shields criterion)
TINF	Boundary shear stress on plain far from channel
U	Convective velocity of sediment normal to channel
VEL	Flow velocity on plain
VEL1	Flow velocity in channel 1
VEL2	Flow velocity in channel 2
VELCH	Channel flow velocity
VELDIF	Difference between dimensionless flow and sediment velocities
VELL1	Alternative estimate for flow velocity in channel 1
VELL2	Alternative estimate for flow velocity in channel 2
VELP	Flow velocity in direction of steepest gradient on plain
VELS	Velocity of sediment in direction of flow
WPCH	Wetted perimeter for channel
WPPL	Wetted perimeter for plain
Y	Height above plain surface
YY(I)	Vertical distance of point (I,J) below water surface
ZPRIM	Transverse distance over plain
ZZ	Dimensionless transverse distance over plain

A.3.3 Subroutine BCPROF

Variable	Description
A	Height of reference concentration above bed
CA	Reference concentration
D	Flow depth in channel
DM	Grain roughness in channel
SV	Shear velocity in channel
Z	Fall velocity parameter

Other variables as defined for main program

A.3.4 Subroutine SHVEL

AK	Surface roughness in equation for vertical distribution of velocity
D	Hydraulic radius
DM	Grain roughness
DR	Reduced flow depth
DR1) DR2) DR3)	Intermediate values in calculation of reduced flow depth
F3	Function relating average flow velocity and reduced flow depth

Other variables as defined for main program

A.3.5 Subroutine FLOVEL

ASSR	Apparent shear stress ratio
D	Length of diagonal interface between channel and plain
DCH	Flow depth in channel
DIAG	Length of diagonal interface between channel and plain
RCH	Hydraulic radius for channel
RM	Manning's n for channel
TAV	Apparent shear stress on vertical interface

Variable	Description
TAD	Apparent shear stress on diagonal interface
TC	Average shear stress on channel boundary
VCH	Flow velocity in channel
WCH	Top width of channel
WCHB	Bottom width of channel
WCHBS	Average width of channel

Other variables as defined for main program

A.4 Program Listing

```
C
C                              ************
C                              * PLAINDEP *
C                              ************
C
C  ***************************************************************
C  * PROGRAM TO DETERMINE THE RELATIVE TRANSVERSE DISTRIBUTION OF *
C  * FINE SEDIMENT DEPOSITS ON PLAIN AREAS ADJACENT TO CHANNELS   *
C  ***************************************************************
C
C*****  ********************************************************************
C
C  PROGRAM INPUT DATA
C  ******************
C
C  LINE    FORMAT      VARIABLES
C  ****    *******     **********
C
C   1      35A2        TITLE1:  ANY ALPHANUMERIC INFORMATION, 70 COLUMNS
C
C   2      35A2        TITLE2:  ANY ALPHANUMERIC INFORMATION, 70 COLUMNS
C
C   3      I8,F8.0     IBC    :  NUMBER OF CHANNELS (1 OR 2)
C                      DIRN   :  CHANNEL DIRECTION (DEGREES)
C
C   4      5F8.0       DATA FOR PLAIN
C                      DEPTH  :  FLOW DEPTH (M)
C                      WID    :  PLAIN WIDTH (M)
C                      SLOP   :  HYDRAULIC GRADIENT
C                      RMAN   :  MANNING'S N
C                      DM     :  GRAIN ROUGHNESS (MM)
C
C   5.A    6F8.0       DATA FOR FIRST OR ONLY CHANNEL
C                      DCH1   :  FLOW DEPTH (M)
C                      WCH1   :  TOP WIDTH (M)
C                      WCHB1  :  BOTTOM WIDTH (M)
C                      RM1    :  MANNING'S N
C                      DM1    :  GRAIN ROUGHNESS (MM)
C                      CA1    :  REFERENCE CONCENTRATION AT BED
C
C   5.B    5F8.0       DATA FOR SECOND CHANNEL: REQUIRED ONLY IF IBC=2
C                      DCH2   :  FLOW DEPTH (M)
C                      WCH2   :  TOP WIDTH (M)
C                      WCHB2  :  BOTTOM WIDTH (M)
C                      RM2    :  MANNING'S N
C                      DM2    :  GRAIN ROUGHNESS (MM)
C
C   6      3F8.0       SEDIMENT DATA
C                      DIAM   :  PARTICLE SIZE (MM)
C                      W      :  FALL VELOCITY (M/S)
C                      S      :  RELATIVE DENSITY
```

```
C
C    7      I8,F8.0,     FINITE DIFFERENCE SOLUTION PARAMETERS
C           I8,3F8.0     N      :  NUMBER OF VERTICAL GRID POINTS
C                        DELY   :  VERTICAL GRID SPACING (M)
C                        M      :  NUMBER OF HORIZONTAL GRID POINTS
C                        DELZ   :  HORIZONTAL GRID SPACING (M)
C                        TOL    :  ITERATION TOLERANCE
C                        AF     :  INITIAL ACCELERATOR VALUE
C
C    8      I8           OUTPUT REQUIREMENTS
C                        IPRINT:   1 FOR STANDARD OUTPUT
C                                  2 FOR DETAILED OUTPUT
C
C  ***************************************************************************
C
C  PROGRAM EXECUTION ON VM CMS
C  ***************************
C
C  TO EXECUTE PROGRAM, TYPE      WATFIV PLAINDEP
C  RESULTS WILL BE IN FILE   :   FILE FT08F001
C
C  ***************************************************************************
$JOB
      DIMENSION CONC(50,50),YY(50),EPSY(50,50),EPSZ(50),TAU(50),DEP(50),
     #PDEP(50),TITLE1(35),TITLE2(35),DCDZ1(50),DCDZ(50)
C
C  READ AND PRINT INPUT DATA
C  *************************
C
C  READ TITLE
C
      READ(5,126)(TITLE1(I),I=1,35)
      READ(5,126)(TITLE2(I),I=1,35)
  126 FORMAT(35A2)
      WRITE(8,127)(TITLE1(I),I=1,35)
      WRITE(8,127)(TITLE2(I),I=1,35)
  127 FORMAT(T10,35A2)
C
C  READ BOUNDARY TYPE AND CHANNEL DIRECTION
C
      READ(5,100)IBC,DIRN
  100 FORMAT(I8,F8.0)
C
C  READ DATA FOR PLAIN
C
      READ(5,101)DEPTH,WID,SLOP,RMAN,DM
  101 FORMAT(5F8.0)
      WRITE(8,102)
  102 FORMAT(/,T10,'PLAIN CHARACTERISTICS',/,T10,21('*'))
      WRITE(8,103)DEPTH,WID,SLOP,RMAN,DM
  103 FORMAT(/,T10,'FLOW DEPTH',T26,F5.3,T32,'M',/,T10,'WIDTH',T26,F5.2,
     #T32,'M',/,T10,'GRADIENT',T26,F7.5,/,T10,'MANNINGS N',T26,F5.3,/,T1
     #0,'GRAIN ROUGHNESS',T26,F6.3,T32,'MM')
C
```

```
C READ DATA FOR CHANNELS
C
      READ(5,105)DCH1,WCH1,WCHB1,RM1,DM1,CA1
  105 FORMAT(6F8.0)
      IF(IBC-1)2,2,1
    1 WRITE(8,106)
  106 FORMAT(/,/,T10,'PLAIN IS BOUNDED BY CHANNELS ON BOTH SIDES',/,/,T1
     #0,'CHARACTERISTICS OF FIR  CHANNEL',/,T10,32('*'))
      GO TO 3
    2 WRITE(8,107)
  107 FORMAT(/,/,T10,'PLAIN IS BOUNDED BY A CHANNEL ON ONE SIDE AND A SO
     #LID VERTICAL BOUNDARY',/,T10,'ON THE OTHER',/,/,T10,'CHANNEL CHARAC
     #TERISTICS',/,T10,23('*'))
    3 WRITE(8,108)DCH1,WCH1,WCHB1,SLOP,RM1,DM1
  108 FORMAT(/,T10,'FLOW DEPTH',T29,F6.3,T36,'M',/,T10,'CHANNEL TOP WIDT
     #H',T29,F6.3,T36,'M',/,T10,'CHANNEL BTM WIDTH',T29,F6.3,T36,'M',/,
     #T10,'GRADIENT',T29,F7.5,/,T10,'MANNINGS N',T29,F5.3,/,T10,'GRAIN R
     #OUGHNESS',T29,F6.3,T36,'MM')
      WRITE(8,104)CA1
  104 FORMAT(T10,'CONCENTRATION AT BED',T31,F8.3,T40,'UNITS',/)
      IF(IBC-1)5,5,4
    4 READ(5,105)DCH2,WCH2,WCHB2,RM2,DM2
      WRITE(8,109)
  109 FORMAT(/,/,T10,'CHARACTERISTICS OF SECOND CHANNEL',/,T10,33('*'))
      WRITE(8,108)DCH2,WCH2,WCHB2,SLOP,RM2,DM2
      WRITE(8,124)DIRN
  124 FORMAT(/,T10,'CHANNELS FLOW AT ',F5.2,T33,'DEGREES ACROSS PLAIN')
C
C  READ AND PRINT SEDIMENT DATA
C
    5 READ(5,110)DIAM,W,S
  110 FORMAT(3F8.0)
      WRITE(8,111)DIAM,W,S
  111 FORMAT(/,/,T10,'SEDIMENT DATA',/,T10,13('*'),/,/,T10,'PARTICLE SIZ
     #E',T26,F5.3,T32,'MM',/,T10,'FALL VELOCITY',T26,F5.3,T32,'M/S',/,T1
     #0,'REL. DENSITY',T26,F6.3,/)
C
C  READ GRID PARAMETERS
C
      READ(5,112)N,DELY,M,DELZ,TOL,AF
  112 FORMAT(I8,F8.0,I8,3F8.0)
      DY2=DELY**2.
      DZ2=DELZ**2.
C
C  READ OUTPUT REQUIREMENTS
C
      READ(5,119)IPRINT
  119 FORMAT(I8)
C
C  **********************************************************************
C
C  CALCULATE AND PRINT FLOW VELOCITIES
C  ***********************************
C
```

```
C  CALCULATE VELOCITY ON PLAIN
C
      IF(IBC.GT.1)GO TO 14
      WPPL=WID+DEPTH
      APL=WID*DEPTH+0.25*WCH1*DEPTH
      GO TO 15
   14 WPPL=WID
       APL=WID*DEPTH+0.25*WCH1*DEPTH+0.25*WCH2*DEPTH
   15 RPL=APL/WPPL
      VEL=(RPL**0.667)*SQRT(SLOP)/RMAN
C
C  CALCULATE VELOCITY IN FIRST CHANNEL
C
      DRAT=DCH1/(DCH1-DEPTH)
      IF(DRAT.LE.2.)GO TO 16
      ACH=WCH1*DEPTH+(WCHB1+0.5*(WCH1-WCHB1))*(DCH1-DEPTH)
      WPCH=WCHB1+2.*SQRT((0.5*(WCH1-WCHB1))**2.+(DCH1-DEPTH)**2.)
      RCH1=ACH/WPCH
      VEL1=(RCH1**0.667)*SQRT(SLOP)/RM1
      GO TO 26
C
C  CALCULATE VELOCITY IN FIRST CHANNEL, EXCLUDING DIAGONAL INTERFACE
C
   16 D1=SQRT(DEPTH**2.+(WCH1/2.)**2.)
      DIAG1=0.
      CALL FLOVEL(VEL,DEPTH,SLOP,WID,WCH1,WCHB1,DCH1,DIAG1,D1,RM1,VEL1,A
     #SSR1,RCH1)
      IF(ASSR1.LE.0.5)GO TO 26
C
C  RECALCULATE VELOCITY IN FIRST CHANNEL, INCLUDING INTERFACE
C
      DIAG1=D1
      CALL FLOVEL(VEL,DEPTH,SLOP,WID,WCH1,WCHB1,DCH1,DIAG1,D1,RM1,VELL1,
     #ASSR1,RR1)
      IF(ASSR1.LE.0.5)GO TO 13
      VEL1=VELL1
      GO TO 26
   13 VEL1=0.5*(VEL1+VELL1)
   26 WRITE(8,113)VE  VEL'
  113 FORMAT(/,T10, FLOW VELOCITY ON PLAIN',T40,F6.3,T48,'M/S',/,T10,'FL
     #OW VELOCITY IN 1ST CHANNEL',T40,F6.3,T48,'M/S')
C
C  CALCULATE VELOCITY IN SECOND CHANNEL
C
      IF(IBC.EQ.1)GO TO 6
      DRAT=DCH2/(DCH2-DEPTH)
      IF(DRAT.LE.2.)GO TO 17
      ACH=WCH2*DEPTH+(WCHB2+0.5*(WCH2-WCHB2))*(DCH2-DEPTH)
      WPCH=WCHB2+2.*SQRT((0.5*(WCH2-WCHB2))**2.+(DCH2-DEPTH)**2.)
      RCH2=ACH/WPCH
      VEL2=(RCH2**0.667)*SQRT(SLOP),RM2
      GO TO 25
C
C  CALCULATE VELOCITY IN SECOND CHA  L, EXCLUDING DIAGONAL INTERFACE
C
```

```
   17 D2=SQRT(DEPTH**2.+(WCH2/2.)**2.)
      DIAG2=0.
      CALL FLOVEL(VEL,DEPTH,SLOP,WID,WCH2,WCHB2,DCH2,DIAG2,D2,RM2,VEL2,A
     #SSR2,RCH2)
      IF(ASSR2.LE.0.5)GO TO 25
C
C  RECALCULATE VELOCITY IN SECOND CHANNEL, INCLUDING DIAGONAL INTERFACE
C
      DIAG2=D2
      CALL FLOVEL(VEL,DEPTH,SLOP,WID,WCH2,WCHB2,DCH2,DIAG2,D2,RM2,VELL2,
     #ASSR2,RR2)
      IF(ASSR2.LE.0.5)GO TO 18
      VEL2=VELL2
      GO TO 25
   18 VEL2=0.5*(VEL2+VELL2)
   25 WRITE(8,114)VEL2
  114 FORMAT(T10,'FLOW VELOCITY IN 2ND CHANNEL',T40,F6.3,T48,'M/S')
    6 CONTINUE
C
C  ********************************************************************
C
C  CALCULATE SHEAR VELOCITY FOR PLAIN
C  **********************************
      CALL SHVEL(DM,DEPTH,VEL,SLOP,SVEL)
C
C  ********************************************************************
C
C  GENERATE CONCENTRATIONS ON VERTICAL BOUNDARIES
C  **********************************************
C
      J=1
      CALL SHVEL(DM1,RCH1,VEL1,SLOP,SVEL1)
      WRITE(8,128)SVEL1
  128 FORMAT(/,T10,'SHEAR VELOCITY FOR 1ST CHANNEL',T41,F6.3,T49,'M/S')
      CALL BCPROF(CA1,DCH1,W,N,DELY,J,CONC,DM1,SVEL1)
      IF(IBC.EQ.1)GO TO 7
C  CALCULATE BED CONCENTRATION FOR SECOND CHANNEL
      CALL SHVEL(DM2,RCH2,VEL2,SLOP,SVEL2)
      WRITE(8,131)SVEL2
  131 FORMAT(T10,'SHEAR VELOCITY FOR 2ND CHANNEL',T41,F6.3,T49,'M/S')
      TH1=SVEL1**2./((S-1.)*9.81*DIAM)
      TH2=SVEL2**2./((S-1.)*9.81*DIAM)
      CA2=CA1*((TH2-0.047)/(TH1-0.047))**1.5
C
      J=M
      CALL BCPROF(CA2,DCH2,W,N,DELY,J,CONC,DM2,SVEL2)
    7 CONTINUE
C
C  ********************************************************************
C
C  INITIALIZE INTERIOR CONCENTRATIONS
C  **********************************
C
      MM=M-2
      KM=MM+1
```

```
      IF(IBC.EQ.1)KM=M
      DO 10 I=1,N
      DO 10 J=2,KM
      CONC(I,J)=0.0
   10 CONTINUE
C
C  ***************************************************************************
C
C  COMPUTE VERTICAL DIFFUSIVITIES
C  ******************************
C
      TINF=1000.*SVEL**2.
      DO 78 J=2,KM
      ZPRIM=(J-1)*DELZ
      KM2=KM/2
      IF(J-KM2)45,45,46
   45 BIGD=DCH1
      JJ=1
      GO TO 47
   46 IF(IBC.EQ.1)GO TO 47
      BIGD=DCH2
      ZPRIM=WID-ZPRIM
      JJ=M
   47 BT=DEPTH*0.64*(BIGD/DEPTH-1.)
      TB=TINF*(1.+0.24*(BIGD/DEPTH-1.))
      TAU(JJ)=TB
      ZZ=ZPRIM/BT
      IF(ZZ.GT.3.0)GO TO 48
      TAU(J)=TINF+(TB-TINF)*EXP(-0.693*(ZPRIM BT)**2 )
      GO TO 49
   48 TAU(J)=TINF
   49 DO 78 I=1,N
      Y=DEPTH-(I-1)*DELY
      EPSY(I,J)=0.4*SQRT(TAU(J)*0 001)*Y*(1.0-Y/DEPTH)
   78 CONTINUE
C
C  ***************************************************************************
C
C  COMPUTE TRANSVERSE DIFFUSIVITIES
C  ********************************
C
      R1=2.*DEPTH*0.64*(DCH1/DEPTH-1.)
      IF(IBC-1)8,8,9
    8 R2=0.
      GO TO 12
    9 R2=2.*DEPTH*0.64*(DCH2/DEPTH-1.)
   12 RWID=WID-R1-R2
      EZINF=0.001*SVEL*RWID*(32.77-8.03*ALOG(RWID/DEPTH))
      DO 60 J=1,M
      ZPRIM=(J-1)*DELZ
      M2=M/2
      IF(J-M2)61,61,62
   61 BIGD=DCH1
      VELCH=VEL1
      GO TO 63
```

```
      IF(IBC.EQ.1)GO TO 63
      BIGD=DCH2
      VELCH=VEL2
      ZPRIM=WID-ZPRIM
   62 BT=DEPTH*0.64*(BIGD/DEPTH-1.)
      ETA=ZPRIM/BT
      IF(ETA-0.3)64,64,65
   64 AETA=-31.5*ETA+11.45
      IF(AETA.GT.9.)AETA=9
      GO TO 66
   65 AETA=-2.37*ETA+2.71
      IF(AETA.LT.0.)AETA=0.
   66 ANUM=(VELCH-VEL)*DEPTH*0.3*(BIGD/DEPTH-1.)**3
      ADEN=((VELCH-VEL)/SVEL)**2.
      EPSZ(J)=(ANUM/ADEN)*AETA
      REP=W*DIAM*1000.
      IF(REP-5.)67,67,68
   67 BETA=1.2
      GO TO 69
   68 BETA=1.01+0.025*ALOG(REP)
      IF(BETA.GT.1.45)BETA=1.45
   69 EPSZ(J)=BETA*EPSZ(J)
      IF(EPSZ(J).LT.EZINF)EPSZ(J)=EZINF
   70 CONTINUE
```

```
COMPUTE DEPOSITION PROBABILITIES OVER PLAIN

      S=0.51
      THETAC=0.05
      DO 50 J=1,M
      THETA=TAU(J)/(S-1.)/DIAM
      IF(THETA.LE.THETAC)GO TO 51
      P=1.-(0.82*(THETA-THETAC)**(-0.25))
      GO TO 52
   51 P=0.0
   52 PDEP(J)=P
   50 CONTINUE
```

```
COMPUTE TRANSVERSE CONVECTIVE COMPONENT

      DIRN=DIRN*3.1416/180.
      SLOPP=SLOP*COS(DIRN)
      VELP=VEL*SQRT(SLOPP/SLOP)
      BET=W/(0.4*SVEL)
      VELDIF=-135.*BET**1.41
      DISP=0.4*DEPTH*SVEL/6.
      VELS=(VELDIF*DISP/DEPTH)+VELP
      SLOPT=(SIN(DIRN)/COS(DIRN))*S
      VELS=VELS*SQRT(SLOPT*SLOP)
```

```
      IF(U.LT.0.)U=0.
      WRITE(8,125)U
  125 FORMAT(/,T10,'TRANSVERSE VELOCITY [illegible]
     #T62,'M/S',/)
      WRITE(8,132)
  132 FORMAT(/,T2,70('*'),/)
C
C  ***********************************************************
C
C  COMPUTE CONCENTRATIONS BY S O R. END WHEN TOLERANCE SATISFIED
C  ***********************************************************
C
C  RE-ESTIMATE ACCELERATOR
C
      DK3=0.
      DK2=0.
      DK1=0.
      DK=0.
      K=0
   31 DMAX=0.0
      K=K+1
      DK3=DK2
      DK2=DK1
      DK1=DK
      IF(K-4)74,75,75
   75 IF(DK3-DK2)74,74,76
   76 IF(DK2-DK1)74,74,77
   77 A=ALOG10(DK2)-ALOG10(DK1)
      AF=2.0/(1.0+SQRT(1.0-10.0**(-A)))
   74 DO 70 I=1,N
      DO 70 J=2,KM
      IF(I-1)38,38,39
C
C  COEFFICIENTS FOR WATER SURFACE POINTS
C
   38 AT=0.
      EY1=(EPSY(I,J)+EPSY(I+1,J))*0.5
      AB=EY1/DY2
      EZ1=(EPSZ(J)+EPSZ(J-1))*0.5
      IF(J.EQ.M)GO TO 22
      EZ2=(EPSZ(J)+EPSZ(J+1))*0.5
      AL=EZ1/(2.*DZ2)+W/(2.*DELZ)
      AR=EZ2/(2.*DZ2)
      AM=EY1/DY2+(EZ1+EZ2)/(2.*DZ2)+W/DELY+W/(2.*DELZ)
      GO TO 29
C
C  COEFFICIENTS FOR WATER SURFACE AND SOLID VERTICAL BOUNDARY POINTS
C
   22 EZM1=(EPSZ(J-1)+EPSZ(J-2))*0.5
      AL=-(EZ1+EZM1)/DZ2
      AL2=EZM1/DZ2
      AR=0.
      AM=EY1/DY2-EZ1/DZ2+W/D LY
      GO TO 29
```

```
   39 IF(I-N)36,35,35
C
C  COEFFICIENTS FOR PLAIN BE  POINTS
C
   35 AB=0.
      EY2=(EPSY(I,J)+EPSY(J  1,J))*0.5
      AT=EY2/DY2+W/DELY
      EZ1=(EPSZ(J)+EPSZ( -1))*0.5
      IF(J.EQ.M)GO TO 23
      AL=EZ1/(2.*DZ2)+U/(2.*DELZ)
      EZ2=(EPSZ(J)+EPSZ(J+1))*0.5
      AR=EZ2/(2.*DZ2)
      AM=EY2/DY2+(EZ1+EZ2)/(2.*DZ2)+PDEP(J)*W/DELY+U/(2.*DELZ)
      GO TO 29
C
C  COEFFICIENTS FOR PLAIN BED AND SOLID VERTICAL BOUNDARY POINT
C
   23 EZM1=(EPSZ(J-1)+EPSZ(J-2))*0.5
      AL=-(EZ1+EZM1)/DZ2
      AL2=EZM1/DZ2
      AR=0.
      AM=EY2/DY2-EZ1/DZ2+PDEP(J)*W/DELY
      GO TO 29
C
C  COEFFICIENTS FOR INTERIOR POINTS
C
   36 EY1=(EPSY(I,J)+EPSY(I+1,J))*0.5
      EY2=(EPSY(I,J)+EPSY(I-1,J))*0.5
      EZ1=(EPSZ(J)+EPSZ(J-1))*0.5
      IF(J.EQ.M)GO TO 24
      AL=EZ1/DZ2+U/DELZ
      AT=EY2/DY2+W/DELY
      AB=EY1/DY2
      EZ2=(EPSZ(J)+EPSZ(J+1))*0.5
      AR=EZ2/DZ2
      AM=(EY1+EY2)/DY2+(EZ1+EZ2)/DZ2+W/DELY+U/DELZ
      GO TO 29
C
C  COEFFICIENTS FOR SOLID VERTICAL BOUNDARY POINTS
C
   24 EZM1=(EPSZ(J-1)+EPSZ(J-2))*0.5
      AT=EY2/(2.*DY2)+W/(2.*DELY)
      AB=EY1/(2.*DY2)
      AL=-(EZ1+EZM1)/DZ2
      AL2=EZM1/DZ2
      AM=(EY2+EY1)/(2.*DY2)-EZ1/DZ2+W/(2.*DELY)
C
C  CALCULATE NEW CONCENTRATIONS
C
   29 SAVE=CONC(I,J)
      IF(I.NE.1)GO TO 71
      IF(J.EQ.M)GO TO 80
      CONC(I,J)=(AF/AM)*(AL*CONC(I,J-1)+AR*CONC(I,J+1)+AB*CONC(I+1,J))-(
     *AF-1.0)*CONC(I,J)
      GO TO 72
```

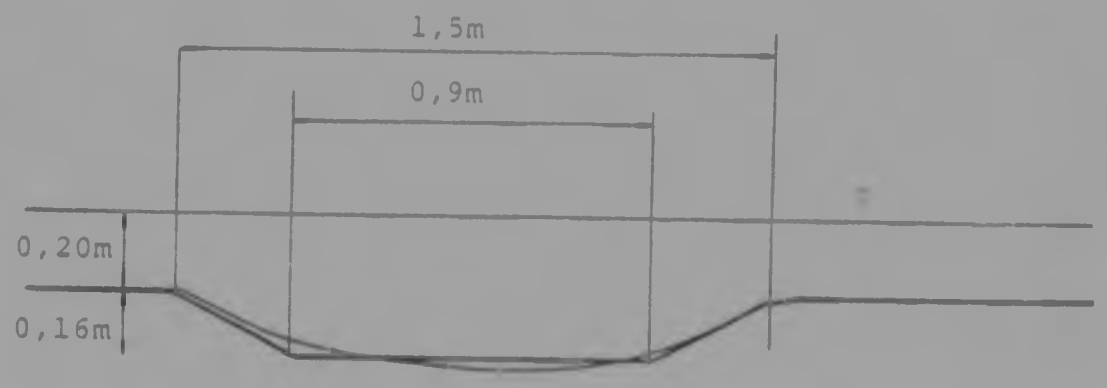
```
 80 CONC(I,J)=(AF/AM)*(AL*CONC(I,J-1)+AB*CONC(I+1,J)+AL2*CONC(I,J-2))-
   #(AF-1.0)*CONC(I,J)
      GO TO 72
 71 IF(I.NE.N)GO TO 73
      IF(J.EQ.M)GO TO 81
      CONC(I,J)=(AF/AM)*(AL*CONC(I,J-1)+AT*CONC(I-1,J)+AR*CONC(I,J+1))-(
   #AF-1.0)*CONC(I,J)
      GO TO 72
 81 CONC(I,J)=(AF/AM)*(AL*CONC(I,J-1)+AT*CONC(I-1,J)+AL2*CONC(I,J-2))-
   #(AF-1.0)*CONC(I,J)
      GO TO 72
 73 IF(J.EQ.M)GO TO 82
      CONC(I,J)=(AF/AM)*(AL*CONC(I,J-1)+AT*CONC(I-1,J)+AR*CONC(I,J+1)+AB
   #*CONC(I+1,J))-(AF-1.0)*CONC(I,J)
      GO TO 72
 82 CONC(I,J)=(AF/AM)*(AL*CONC(I,J-1)+AT*CONC(I-1,J)+AB*CONC(I+1,J)+AL
   #2*CONC(I,J-2))-(AF-1.0)*CONC(I,J)
 72 DEV=ABS(CONC(I,J)-SAVE)
      IF(DEV-DMAX)70,32,32
 32 DMAX=DEV
      DK=DMAX
 70 CONTINUE
      IF(TOL-DMAX)31,33,33
C
C  ***************************************************************************
C
C  CALCULATE DEPOSITION CONCENTRATIONS AND PRINT RESULTS
C  ****************************************************
C
 33 IF(IPRINT.EQ.1)GO TO 83
      WRITE(8,115)
115 FORMAT(1H1,T30,'CONCENTRATIONS',/)
      DO 20 I=1,N
      YY(I)=(I-1)*DELY
 20 CONTINUE
      WRITE(8,116)(YY(I),I=1,N)
116 FORMAT(T2,'Y(M)',15F7.3)
      WRITE(8,117)
117 FORMAT(T2,'Z(M)',/)
      DO 30 J=1,M
      DIST=(J-1)*DELZ
      WRITE(8,118)DIST,(CONC((N-I+1),J),I=1,N)
118 FORMAT(F5.2,15F7.4)
 30 CONTINUE
 83 WRITE(8,122)
122 FORMAT(1H1,T10,'Z(M)',T21,'BED SHEAR',T36,'EPSZ',T45,'PDEP',T54,'R
   #EL. DEPOSITION',/,T22,'(N/M**2)',T34,'(M**2/S)',/)
      DO 21 J=1,M
      DEP(J)=PDEP(J)*CONC(N,J)
      RDEP=DEP(J)/DEP(1)
      DIST=(J-1)*DELZ
      WRITE(8,123)DIST,TAU(J),EPSZ(J),PDEP(J),RDEP
123 FORMAT(T10,F5.2,T22,F7.3,T32,E11.3,T44,F6.4,T56,F7.4)
 21 CONTINUE
      WRITE(8,120)K,AF
```

```
  120 FORMAT(/,T10,'NUMBER OF ITERATIONS : ',T35,I4,/,T10,'ACCELERATOR V
     #ALUE : ',T35,F6.4)
      IF(IPRINT.EQ.1)GO TO 99
      WRITE(8,129)
  129 FORMAT(/,/,T10,'CONCENTRATION GRADIENTS :',/,T10,'Y(M)',T23,'LEFT'
     #,T33,'RIGHT',/)
      DO 84 I=1,N
      DCDZ1(I)=(CONC(I,2)-CONC(I,1))/DELZ
      DCDZ(I)=(CONC(I,M)-CONC(I,M-1))/DELZ
      WRITE(8,130)YY(N-I+1),DCDZ1(I),DCDZ(I)
  130 FORMAT(T10,F5.3,T20,F8.3,T30,F8.3)
   84 CONTINUE
   99 STOP
      END
C
C  ***************************************************************************
C
C  SUBROUTINE BCPROF
C  *****************
C
C  THIS SUBROUTINE GENERATES CONCENTRATION PROFILES ON THE VERTICAL
C  BOUNDARIES FROM BED CONCENTRATIONS IN THE CHANNELS
C
      SUBROUTINE BCPROF(CA,D,W,N,DELY,J,CONC,DM,SV)
      DIMENSION CONC(50,1)
C
      Z=W/(0.4*SV)
      A=2.*DM*0.001
      DO 11 I=1,N
      Y=D-(I-1)*DELY
      IF(I.EQ.1)Y=D-DELY/4.
      CONC(I,J)=CA*(((D-Y)*A)/(Y*(D-A)))**Z
   11 CONTINUE
      RETURN
      END
C
C  ***************************************************************************
C
C  SUBROUTINE SHVEL
C  ****************
C
C  THIS SUBROUTINE CALCULATES SHEAR VELOCITY ASSOCIATED WITH GRAIN
C  ROUGHNESS
C
      SUBROUTINE SHVEL(DM,D,VEL,SLOP,SVEL)
C
C  CALCULATE REDUCED HYDRAULIC RADIUS
C
      AK=2.5*DM/1000.
      DR1=2.0*D
      DR2=0.1*D
      DR3=0.5*(DR1+DR2)
   40 F3=6.25*2.5*ALOG(DR3/AK)-VEL/S[illegible]9.81*DR3*SLOP)
      IF(ABS(F3).LE.0.001)GO TO 44
      IF(F3)41,44,42
```

```
   41 DR2=DR3
      GO TO 43
   42 DR1=DR3
   43 DR3=0.5*(DR1+DR2)
      GO TO 40
   44 DR=DR3
      IF(DR.GT.D)DR=D
C
C  CALCULATE SHEAR VELOCITY
C
      SVEL=SQRT(9.81*DR*SLOP)
      RETURN
      END
C
C  ***************************************************************
C
C  SUBROUTINE FLOVEL
C  *****************
C
C  THIS SUBROUTINE CALCULATES FLOW VELOCITIES IN CHANNELS
C
      SUBROUTINE FLOVEL(VEL,DEPTH,SLOP,WID,WCH,WCHB,DCH,DIAG,D,RM,VCH,AS
     #SR,RCH)
      WCHBS=(WCH-WCHB)*0.5
      WPCH=WCHB+2.*SQRT(WCHBS**2.+(DCH-DEPTH)**2.)+2.*DIAG
      ACH=(WCHB+WCHBS)*(DCH-DEPTH)+0.5*WCH*DEPTH
      RCH=ACH/WPCH
      VCH=(RCH**0.667)*SQRT(SLOP)/RM
      IF(VCH.GT.VEL)GO TO 19
      WRITE(8,124)
  124 FORMAT(//,T10,'VELOCITY DIFFERENCE BETWEEN PLAIN AND CHANNEL IS INS
     #IGNIFICANT, COMPUTATION STOPPED',//)
      STOP
   19 TAV=13.84*(VCH-VEL)**0.882*(DCH/(DCH-DEPTH))**(-3.123)*(WID/WCH)**
     #(-0.727)
      TAD=(DEPTH-2.*D))*(2.*TAV-0.5*9800.*WCH*SLOP)
      TC=(9800.*ACH*SLOP)/(WCHB+2.*SQRT(WCHBS**2.+(DCH-DEPTH)**2.)+2.*D)
      ASSR=TAD/TC
      RETURN
      END
C
C  ***************************************************************
C
C  DATA
C  ****
C
SENTRY
EXAMPLE - DISTRIBUTION OF GOLD DEPOSITS
FOR CHANNEL DESCRIBED IN APPENDIX
       2     1.0
   0.200    4.00  0.0030   0.020      5.0
   0.360    1.50    0.90   0.018      2.0     100.
   0.360    1.50    0.90   0.018      5.0
   0.075   0.035   19.30
      11    .0200      41    0.10   .0010      1.0
       2
SSTOP
```

A.5 Example

The distribut'·n of gold deposits adjacent to the channel shown in Figure A.2 is computed as an example to illustrate the program input and output.



Channel direction:	2° across plain
Hydraulic gradient:	0,003
Manning's n for plain:	0,02
Manning's n for channel:	0,018
Grain roughness for plain:	5 mm
Grain roughness for channel:	5 mm
Sediment (gold) data:	
Particle size:	0,075 mm
Fall velocity:	0,035 m/s
Relative density:	19,3

Fig. A.2 Example problem

The channel cross-section is approximated by the trapezium shown.

The distribution on both sides of the channel is required. Because the channel is not parallel to the steepest gradient of the plain there will be a transverse convective component and the distribution will not be symmetrical. Therefore two identical channels will be specified at a distance apart sufficient for the two distributions to be reasonably independent, say 4,0 m.

The finite difference grid is assumed to have vertical spaces of 0,02 m and horizontal spaces of 0,10 m. The number of grid intersections is therefore 11 in the vertical direction and 41 in the horizontal direction.

The reference concentration at the bed of the channel is assumed to be 100 units and the iteration tolerance 0,001 units.

The initial SOR accelerator value is 1,0.

The data file for this problem is shown in Figure A.3 and the computer output in Figure A.4 (Detailed output is specified).

```
EXAMPLE : DISTRIBUTION OF GOLD DEPOSITS
FOR CHANNEL DESCRIBED IN APPENDIX
      2     1.0
  0.200    4.00  0.0030   0.020     5.0
  0.360    1.50    0.90   0.018     5.0    100.
  0.360    1.50    0.90   0.018     5.0
  0.075   0.035   19.30
     11   .0200      41    0.10   .0010     1.0
      2
```

Fig. A.3 Data for example problem.

The finite difference grid is assumed to have vertical spaces of 0,02 m and horizontal spaces of 0,10 m. The number of grid intersections is therefore 11 in the vertical direction and 41 in the horizontal direction.

The reference concentration at the bed of the channel is assumed to be 100 units and the iteration tolerance 0,001 units.

The initial SOR accelerator value is 1,0.

The data file for this problem is shown in Figure A.3 and the computer output in Figure A.4 (Detailed output is specified).

```
EXAMPLE : DISTRIBUTION OF GOLD DEPOSITS
FOR CHANNEL DESCRIBED IN APPENDIX
      2     1.0
  0.200    4.00  0.0030   0.020     5.0
  0.360    1.50    0.90   0.018     5.0
  0.360    1.50    0.90   0.018     5.0
  0.075   0.035   19.30
     11   .0200      41    0.10   .0010
      2
```

Fig. A.3 Data for example problem

```
EXAMPLE : DISTRIBUTION OF GOLD DEPOSITS
FOR CHANNEL DESCRIBED IN APPENDIX

PLAIN CHARACTERISTICS
*********************

FLOW DEPTH        0.200 M
WIDTH             4.00 M
GRADIENT          0.00300
MANNINGS N        0.020
GRAIN ROUGHNESS   5.000MM

PLAIN IS BOUNDED BY CHANNELS ON BOTH SIDES

CHARACTERISTICS OF FIRST CHANNEL
********************************

FLOW DEPTH            0.360 M
CHANNEL TOP WIDTH     1.500 M
CHANNEL BTM WIDTH     0.900 M
GRADIENT             0.00300
MANNINGS N           0.018
GRAIN ROUGHNESS       5.000 MM
CONCENTRATION AT BED  100.000 UNITS


CHARACTERISTICS OF SECOND CHANNEL
*********************************

FLOW DEPTH            0.360 M
CHANNEL TOP WIDTH     1.500 M
CHANNEL BTM WIDTH     0.900 M
GRADIENT             0.00300
MANNINGS N           0.018
GRAIN ROUGHNESS       5.000 MM

CHANNELS FLOW AT  1.00 DEGREES ACROSS PLAIN


SEDIMENT DATA
*************

PARTICLE SIZE   0.075 MM
FALL VELOCITY   0.035 M/S
REL. DENSITY    19.300


FLOW VELOCITY ON PLAIN          1.050  M/S
FLOW VELOCITY IN 1ST CHANNEL    1.397  M/S
FLOW VELOCITY IN 2ND CHANNEL    1.397  M/S

SHEAR VELOCITY FOR 1ST CHANNEL  0.096  M/S
SHEAR VELOCITY FOR 2ND CHANNEL  0.096  M/S

TRANSVERSE VELOCITY OF SEDIMENT PARTICLES    0.029  M/S

**********************************************************************
```

Fig. A.1 Example output

CONCENTRATIONS

Y(M) Z(M)	0.000	0.020	0.040	0.060	0.080	0.100	0.120	0.140	0.160	0.180	0.2
0.00	4.7562	3.8786	3.1630	2.5660	2.0584	1.6195	1.2342	0.8908	0.5797	0.2911	0.07
0.10	2.7998	2.1902	1.8301	1.5262	1.2560	1.0113	0.7875	0.5815	0.3915	0.2174	0.06
0.20	1.4851	1.1605	0.9826	0.8319	0.6949	0.5676	0.4483	0.3359	0.2302	0.1310	0.03
0.30	0.8010	0.6284	0.5361	0.4576	0.3853	0.3173	0.2525	0.1908	0.1318	0.0757	0.02
0.40	0.4373	0.3442	0.2949	0.2528	0.2136	0.1766	0.1411	0.1070	0.0742	0.0428	0.01
0.50	0.2403	0.1894	0.1626	0.1396	0.1181	0.0976	0.0781	0.0593	0.0411	0.0237	0.00
0.60	0.1321	0.1043	0.0895	0.0768	0.0648	0.0535	0.0427	0.0323	0.0224	0.0129	0.00
0.70	0.0724	0.0571	0.0489	0.0419	0.0351	0.0289	0.0229	0.0173	0.0120	0.0069	0.00
0.80	0.0393	0.0310	0.0265	0.0225	0.0188	0.0153	0.0121	0.0091	0.0062	0.0036	0.00
0.90	0.0211	0.0166	0.0141	0.0119	0.0098	0.0079	0.0062	0.0046	0.0031	0.0018	0.00
1.00	0.0111	0.0088	0.0074	0.0061	0.0050	0.0040	0.0031	0.0023	0.0015	0.0009	0.00
1.10	0.0057	0.0045	0.0038	0.0031	0.0025	0.0019	0.0015	0.0011	0.0007	0.0004	0.00
1.20	0.0029	0.0023	0.0019	0.0015	0.0012	0.0009	0.0007	0.0005	0.0003	0.0002	0.00
1.30	0.0014	0.0011	0.0009	0.0007	0.0005	0.0004	0.0003	0.0002	0.0001	0.0001	0.00
1.40	0.0007	0.0005	0.0004	0.0003	0.0002	0.0002	0.0001	0.0001	0.0000	0.0000	0.00
1.50	0.0003	0.0002	0.0002	0.0001	0.0001	0.0001	0.0001	0.0000	0.0000	0.0000	0.00
1.60	0.0001	0.0001	0.0001	0.0001	0.0000	0.0000	0.0000	0.0000	0.0000	0.0000	0.00
1.70	0.0001	0.0000	0.0000	0.0000	0.0000	0.0000	0.0000	0.0000	0.0000	0.0000	0.00
1.80	0.0000	0.0000	0.0000	0.0000	0.0000	0.0000	0.0000	0.0000	0.0000	0.0000	0.00
1.90	0.0000	0.0000	0.0000	0.0000	0.0000	0.0000	0.0000	0.0000	0.0000	0.0000	0.00
2.00	0.0000	0.0000	0.0000	0.0000	0.0000	0.0000	0.0000	0.0000	0.0000	0.0000	0.00
2.10	0.0000	0.0000	0.0000	0.0000	0.0000	0.0000	0.0000	0.0000	0.0000	0.0000	0.00
2.20	0.0000	0.0000	0.0000	0.0000	0.0000	0.0000	0.0000	0.0000	0.0000	0.0000	0.00
2.30	0.0000	0.0000	0.0000	0.0000	0.0000	0.0000	0.0000	0.0000	0.0000	0.0000	0.00
2.40	0.0000	0.0000	0.0000	0.0000	0.0000	0.0000	0.0000	0.0000	0.0000	0.0000	0.00
2.50	0.0000	0.0000	0.0000	0.0000	0.0000	0.0000	0.0000	0.0000	0.0000	0.0000	0.00
2.60	0.0000	0.0000	0.0000	0.0000	0.0000	0.0000	0.0000	0.0000	0.0000	0.0000	0.00
2.70	0.0000	0.0000	0.0000	0.0000	0.0000	0.0000	0.0000	0.0000	0.0000	0.0000	0.00
2.80	0.0000	0.0000	0.0000	0.0000	0.0000	0.0000	0.0000	0.0000	0.0000	0.0000	0.00
2.90	0.0000	0.0000	0.0000	0.0000	0.0000	0.0000	0.0000	0.0000	0.0000	0.0000	0.00
3.00	0.0000	0.0000	0.0000	0.0000	0.0000	0.0000	0.0000	0.0000	0.0000	0.0000	0.00
3.10	0.0000	0.0000	0.0000	0.0000	0.0000	0.0000	0.0000	0.0000	0.0000	0.0000	0.00
3.20	0.0001	0.0001	0.0001	0.0000	0.0000	0.0000	0.0000	0.0000	0.0000	0.0000	0.00
3.30	0.0004	0.0003	0.0003	0.0002	0.0002	0.0002	0.0001	0.0001	0.0001	0.0000	0.00
3.40	0.0018	0.0014	0.0012	0.0010	0.0009	0.0007	0.0005	0.0004	0.0003	0.0002	0.00
3.50	0.0072	0.0057	0.0048	0.0041	0.0035	0.0028	0.0023	0.0017	0.0012	0.0007	0.00
3.60	0.0278	0.0219	0.0184	0.0160	0.0135	0.0111	0.0089	0.0067	0.0046	0.0027	0.00
3.70	0.1072	0.0841	0.0718	0.0612	0.0515	0.0424	0.0337	0.0254	0.0176	0.0101	0.00
3.80	0.4169	0.3258	0.2759	0.2336	0.1951	0.1593	0.1258	0.0943	0.0646	0.0367	0.01
3.90	1.6469	1.2884	1.0765	0.8978	0.7389	0.5949	0.4632	0.3420	0.2303	0.1279	0.03
4.00	4.7562	3.8786	3.1630	2.5660	2.0584	1.6195	1.2342	0.8908	0.5797	0.2911	0.07

Fig. A.4 (contd) Example output

Z(M)	BED SHEAR (N/M**2)	EPSZ (M**2/S)	PDEP	REL. DEPOSITION
0.00	7.016	0.562E-02	0.7950	1.0000
0.10	6.470	0.264E-02	0.7969	0.5901
0.20	5.966	0.264E-02	0.7997	0.3141
0.30	5.889	0.264E-02	0.8002	0.1595
0.40	5.886	0.264E-02	0.8002	0.0926
0.50	5.886	0.264E-02	0.8002	0.0508
0.60	5.886	0.264E-02	0.8002	0.0280
0.70	5.886	0.264E-02	0.8002	0.0153
0.80	5.886	0.264E-02	0.8002	0.0083
0.90	5.886	0.264E-02	0.8002	0.0045
1.00	5.886	0.264E-02	0.8002	0.0024
1.10	5.886	0.264E-02	0.8002	0.0012
1.20	5.886	0.264E-02	0.8002	0.0006
1.30	5.886	0.264E-02	0.8002	0.0003
1.40	5.886	0.264E-02	0.8002	0.0001
1.50	5.886	0.264E-02	0.8002	0.0001
1.60	5.886	0.264E-02	0.8002	0.0000
1.70	5.886	0.264E-02	0.8002	0.0000
1.80	5.886	0.264E-02	0.8002	0.0000
1.90	5.886	0.264E-02	0.8002	0.0000
2.00	5.886	0.264E-02	0.8002	0.0000
2.10	5.886	0.264E-02	0.8002	0.0000
2.20	5.886	0.264E-02	0.8002	0.0000
2.30	5.886	0.264E-02	0.8002	0.0000
2.40	5.886	0.264E-02	0.8002	0.0000
2.50	5.886	0.264E-02	0.8002	0.0000
2.60	5.886	0.264E-02	0.8002	0.0000
2.70	5.886	0.264E-02	0.8002	0.0000
2.80	5.886	0.264E-02	0.8002	0.0000
2.90	5.886	0.264E-02	0.8002	0.0000
3.00	5.886	0.264E-02	0.8002	0.0000
3.10	5.886	0.264E-02	0.8002	0.0000
3.20	5.886	0.264E-02	0.8002	0.0000
3.30	5.886	0.264E-02	0.8002	0.0001
3.40	5.886	0.264E-02	0.8002	0.0004
3.50	5.886	0.264E-02	0.8002	0.0015
3.60	5.886	0.264E-02	0.8002	0.0059
3.70	5.889	0.264E-02	0.8002	0.0227
3.80	5.966	0.264E-02	0.7997	0.0882
3.90	6.470	0.264E-02	0.7969	0.3471
4.00	7.016	0.562E-02	0.7950	1.0000

NUMBER OF ITERATIONS : 23
ACCELERATOR VALUE : 1.2499

CONCENTRATION GRADIENTS :

Y(M)	LEFT	RIGHT
0.200	-0.145	0.410
0.180	-0.736	1.632
0.160	-1.882	3.494
0.140	-3.094	5.488
0.120	-4.468	7.710
0.100	-6.082	10.246
0.080	-8.024	13.105
0.060	-10.398	16.682
0.040	-13.329	20.865
0.020	-16.884	25.903
0.000	-19.564	31.093

Fig. A.4 (contd) Example output

L[illegible]AL DISTRIBUTION MODEL - LONGDIS

Description of Computer Program

The longitudinal distribution model described in the main body of this report has been coded in FORTRAN for solution by computer. Many calculations for solution of the longitudinal distribution equation are performed in program PLAINDEP. Because both models must be used to compute longitudinal distributions these calculations are not repeated in LONGDIS but the results obtained from PLAINDEP output.

Computations in LONGDIS proceed as shown in Figure B.1.

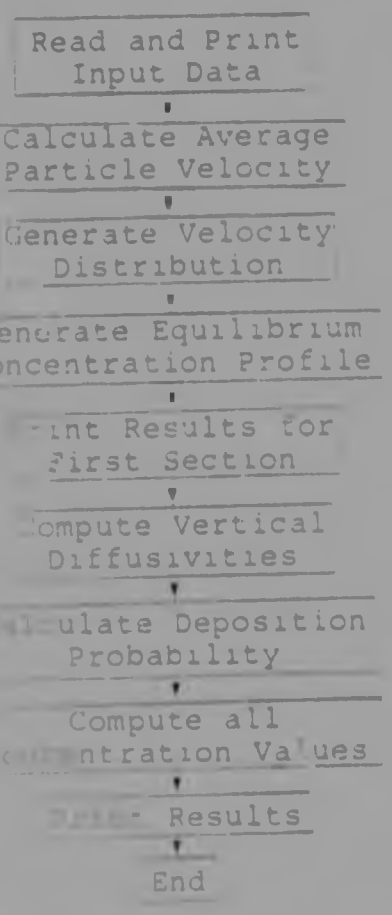


Figure B.1 Flow diagram for program LONGDIS

[illegible] file appended to the program [illegible], flow and sediment characteristics are printed immediately in the output file.

The average particle velocity is calculated from the average flow velocity and particle characteristics according to equations (4.31) to (4.34).

Particle velocity is distributed according to the logarithmic law as described in Chapter 8, or assumed to be uniformly distributed, depending on the input specification.

Results are printed for the first section, at the beginning of the reach. These include the input concentration profile and the average concentration, which is calculated from the profile by the trapezium rule.

The vertical diffusivity for sediment is calculated for each grid point on the current vertical section by equation (8.18).

The probability of deposition of particles on the channel bed is calculated using the equation of Engelund and Fredsoe (1976), equation (5.10).

Concentration values are computed for all grid points using the explicit method according to equations (8.11) to (8.14). The input concentration gradients are first modified because they depend on concentration values. The input values should correspond to the equilibrium profile as calculated from the input reference concentration at the bed. At each new vertical section the gradients are adjusted in proportion to the current concentration values. The coordinates of each grid point under consideration are checked to ensure that the appropriate finite difference equation is used and the concentration is calculated. At each grid point the rates of transfer of suspended material to the plain areas on both sides of the channel are calculated and cumulated along the vertical section. The transfer rate is equal to the sum of the diffusive and convective

rates multiplied by the area over which transfer takes place.

At each section where results are required the average concentration is calculated from the concentration profile using the trapezium rule. The deposition rate on the channel bed is calculated as the product of fall velocity, deposition probability and bed level concentration and then expressed in relative terms by dividing by the value at the beginning of the channel. The cumulated transfer rates to the left and right banks are also expressed in relative terms in the same way. The distance along the channel of the section is printed, as well as the concentration profile, the average concentration, the relative bed deposition and relative transfer rates to both banks.

Calculations proceed to the next vertical section and the process is repeated until all sections have been calculated.

B.2 Users' Guide

The input data required by program LONGDIS describe the characteristics of the channel and the sediment as well as flow characteristics and finite difference grid parameters.

Application of this program should always be preceded by a run of program PLAINDEP to obtain values for concentration gradients, average flow velocity, shear velocity and transverse diffusivity. These values will all be printed by PLAINDEP if detailed output is specified.

The data for LONGDIS are inserted immediately following the program coding. Numerical data are all entered in 8-column fields and should be right-justified.

Each input line and each data item is discussed in order of input in the following paragraphs.

Lines 1 and 2 Title

Any alphanumeric information may be entered in columns 1 to 70 in the first two lines to serve as a run identification title. This information will be printed at the beginning of the output. Two title lines must always be included and two blank lines should be inserted if no title is required.

Line 3 Channel Data

Item 1: Channel width (m). This should be a representative dimension, such as the average width. LONGDIS assumes a rectangular cross section for the channel.

Item 2: Bankfull channel depth (m). This is the depth of the channel below the surface of the plain.

Item 3: Flow depth (m). This is the total vertical distance from the water surface to the channel bed.

Item 4: Hydraulic gradient (m/m). This is the longitudinal gradient of the channel.

Item 5: Grain roughness (mm). This should be a representative size of bed particles, such as the median size, and must be the same as specified for the preceding run of program PLAINDEP from which the concentration gradients were determined.

Line 4 Finite Difference Parameters

The accuracy of the results depends on the spacing of the finite difference grid. Suitable spacing can be selected by comparing results from preliminary runs with different spacings.

Item 1: Number of grid intersections in the vertical direction. This includes the water surface and the channel bed and should be selected to give reasonable coverage to the depth above the plain surface.

Item 2: Vertical grid spacing (m). This is the distance between adjacent vertical grid intersections and is constant over the whole depth. The spacing can be calculated from the number of intersections and the total flow depth.

Item 3: Number of grid intersections in the longitudinal direction. This is determined by the length of the channel and the longitudinal grid spacing required.

Item 4: Longitudinal grid spacing (m). This is the distance between adjacent longitudinal grid intersections and is constant along the whole length of the channel. The longitudinal grid spacing must be selected to ensure stability of the finite difference calculations and the maximum spacing can be estimated from the selected vertical grid spacing using the stability criterion expressed by equation (8.13). This criterion is not exact and should be applied conservatively.

Item 5: Transverse grid spacing (m). This is the transverse grid spacing over the plains and must be the same as used in the preceding run of PLAINDEP from which the transverse concentration gradients were determined.

Line 5 Sediment Data

Item 1: Particle size (mm). This is the equivalent diameter of the particles being considered, i.e. the diameter of a sphere with the same density and fall velocity.

Item 2: Particle fall velocity (m/s). This is the termiral settling velocity of the particles and can be estimated from the particle size (Item 1) and the information provided in Chapter 2.

Item 3: Relative density of particles. This is the density of the particle material relative to that of water.

Line 6 Flow Characteristics

Item 1: Average flow velocity (m/s). This is the average velocity of flow in the channel and can best be estimated by the flow calculation method described in Chapter 4.5. The value should therefore be obtained from the output of program PLAINDEP.

Item 2: Indicator for velocity distribution. Eitner a uniform or a logarithmic velocity distribution may be specified. The logarithmic distribution is more realistic and will give more accurate results but increases the likelihood of instability of the solution. This applies particularly to small channels and mild gradients and compliance with the stability criterion can lead to excessive computation time. It is recommended that the logarithmic option be used unless instability problems arise. This item should have a value of 1 for a uniform distribution and 2 for a logarithmic distribution.

Item 3: Shear velocity (m/s). This is the shear velocity in the channel and is best calculated by the method described in Chapter 4.3. The correct value can be obtained from the output of program PLAINDEP.

Item 4: Transverse velocity component (m/s). This is the component of particle velocity normal to the channel direction. It can be estimated by the proce-

dure described in Chapter 4.4 and can be obtained from the output of program PLAINDEP.

Item 5: Transverse diffusivity (m^2/s). This is the transverse diffusivity for sediment at the interface between channel and plain flow. It can be calculated by equations (4.13) and (4.18). This value can be obtained from the output of program PLAINDEP.

Item 6: Reference concentration at bed. This is the bed concentration used to generate the equilibrium concentration profile. The value input must be the same as specified for the preceding run of PLAINDEP from which the concentration gradients were determined.

Lines 7 and 8 Concentration Gradients

Lines 7 and 8 specify the concentration gradients on the left and right sides of the channel respectively, corresponding to an equilibrium concentration profile within the channel. A value is required for each vertical grid intersection and these can be obtained from the output of program PLAINDEP.

Line 9 Initial Concentrations

These are the concentration values along a vertical section input at the beginning of the channel. A value is required at each vertical grid intersection.

Line 10 Output Requirements

Results need not be printed at every section calculated and the value inserted in line 10 specifies the distance in metres between sections at which results are required.

B.3 List of Variables

B.3.1. Input

Variable	Description
CA	Reference sediment concentration at bed of channel
CONC(N,1)	Sediment concentrations at beginning of channel
DCDZ(N)	Concentration gradients on right side of channel.
DCDZ1(N)	Concentration gradient on left side of channel.
DCH	Flow depth in channel (m).
DELX	Longitudinal grid spacing (m)
DELY	Vertical grid spacing (m).
DELZ	Transverse grid spacing (m)
DIAM	Particle size (mm)
DM	Channel bed grain roughness (mm).
EZ	Transverse sediment diffusivity At sides of channel.
IVEL	Indicator for velocity distribution.
M	Number of longitudinal grid points
N	Number of vertical grid points.
SAVEX	Distance between sections for which output is required (m).
S	Relative density of particles.
SLOP	Hydraulic gradient
SVEL	Shear velocity in channel (m/s).
TITLE1(35)	First line for title.
TITLE2(35)	Second line for title.
U	Transverse velocity component (m/s).
V	Average flow velocity in channel (m/s).

W	Particle fall velocity (m/s).
WID	Channel width (m).
YP	[illegible] channel width (m).

B.3.2 Program LONGDIS

A	Height of reference concentration above bed (m).
AVCON	Average concentration for vertical section.
B	Constant in equation for erosion probability.
BETA	Fall velocity parameter.
COFFA	Coefficient for CONC(I-1,1) in transport equation.
COFFB	Coefficient for CONC(I+1,1) in transport equation.
COFFC	Coefficient for CONC(I,1) in transport equation.
COFFD	Coefficient for DCDZ1(I) in transport equation.
COFFE	Coefficient for DCDZ(I) in transport equation.
CONC(I,J)	Concentration at grid point (I,J).
DEP	Bed deposition rate relative value at beginning of channel
DEPBED	Average bed deposition rate between adjacent sections.
DEP1	Bed deposition rate at beginning of channel.
DISP	Longitudinal dispersion coefficient (m^2/s).
DISTX	Distance of section from beginning of channel.
DY2	Square of vertical grid spacing (m^2).
ECONC(I)	Equilibrium concentration at points (I).

EPSY(I)	Vertical diffusivity for sediment at points (I).
EY1	Average vertical diffusivity for sediment between points (I) and (I+1).
EY2	Average vertical diffusivity for sediment between points (I) and (I-1).
NN	N-1
P	Probability of erosion of particle on bed.
PDEP	Probability of deposition of particle on bed.
PRINT	Distance between sections for which results are required (m).
RLONG	Length of channel (m).
RTRL	Rate of sediment transfer to left bank relative to rate of bed deposition at beginning of channel.
RTRR	Rate of sediment transfer to right bank relative to rate of bed deposition at beginning of channel.
TAU	Bed shear stress (N/m^2)
TCON	Variable in computation of average concentration.
THETA	Dimensionless bed shear stress.
THETAC	Critical dimensionless bed shear stress.
TRL	Rate of sediment transfer to left bank.
TRR	Rate of sediment transfer to right bank.
V	Average flow velocity (m/s) and average particle velocity (m/s).
VEL(I)	Particle velocity at points (I).

VELDIF	Dimensionless particle-flow velocity differential.
Y	Height above channel bed (m).
YI	Height above channel bed (m).
Z	Fall velocity parameter.

B.4 Program Listing

```
C
C                              ************
C                              * LONGDIS *
C                              ************
C
C     ********************************************************************
C     * PROGRAM TO DETERMINE THE DISTRIBUTIONS ALONG A COMPOUND *
C     * CHANNEL OF SUSPENDED AND DEPOSITED FINE SEDIMENTS       *
C     ********************************************************************
C
C  ********************************************************************
C
C  PROGRAM INPUT DATA
C  ******************
C
C  LINE     FORMAT       VARIABLES
C  ----     ******       **********
C
C   1       35A2         TITLE1:  ANY ALPHANUMERIC INFORMATION, 70 COLUMNS
C
C   2       35A2         TITLE2:  ANY ALPHANUMERIC INFORMATION, 70 COLUMNS
C
C   3       5F8.0        CHANNEL DATA
C                        WID   :  CHANNEL WIDTH (M)
C                        YP    :  BANKFULL CHANNEL DEPTH (M)
C                        DCH   :  FLOW DEPTH (M)
C                        SLOP  :  HYDRAULIC GRADIENT
C                        DM    :  GRAIN ROUGHNESS (MM)
C
C   4       I8,F8.0,     FINITE DIFFERENCE PARAMETERS
C           I8,2F8.0     N     :  NUMBER OF VERTICAL GRID POINTS
C                        DELY  :  VERTICAL GRID SPACING (M)
C                        M     :  NUMBER OF LONGITUDINAL GRID POINTS
C                        DELX  :  LONGITUDINAL GRID SPACING (M)
C                        DELZ  :  TRANSVERSE GRID SPACING (M)
C
C   5       3F8.0        SEDIMENT DATA
C                        DIAM  :  PARTICLE SIZE (MM)
C                        W     :  FALL VELOCITY (M/S)
C                        S     :  RELATIVE DENSITY
C
C   6       F6.0,I8,     FLOW CHARACTERISTICS
C           4F8.0        V     :  AVERAGE VELOCITY (M/S)
C                        IVEL  :  INDICATOR FOR VELOCITY DISTRIBUTION
C                                 1 : UNIFORM
C                                 2 : LOGARITHMIC
C                        SVEL  :  SHEAR VELOCITY (M/S)
C                        U     :  TRANSVERSE VELOCITY COMPONENT (M/S)
C                        EZ    :  TRANS DIFFUSIVITY AT INTERFACE (SQ M/S)
C                        CA    :  REFERENCE CONCENTRATION AT BED
C
C   7       9F8.0        DCDZ1 :  CONCENTRATION GRADIENTS ON LEFT SIDE
```

```
C                    CC      CONCENTRATION GRADIENTS ON RIGHT SIDE
C                    XAC     CONCENTRATIONS AT BEGINNING OF CHANNEL
C                    XLENCH  LENGTH INCREMENTS FOR OUTPUT (M)
C*****************************************************************
C
C  PROGRAM EXECUTION ON CMS(CE)
C  ----------------------------
C
C  TO EXECUTE PROGRAM, TYPE      WATFIV LONGDIS
C  RESULTS WILL BE IN FILE        FILE FT08F001
C
C*****************************************************************
C
      DIMENSION CONC1(20,2),EPSY(20),DCD21(20),DCD22(20),ECCNC(20),VEL(20)
     $,TITLE1(35),TITLE2(35)
C
C  READ AND PRINT INPUT DATA
C  -------------------------
C
C  READ TITLE
C
      READ(5,145)(TITLE1(I),I=1,35)
      READ(5,125)(TITLE2(I),I=1,35)
  125 FORMAT(35A2)
C
C  READ CHANNEL DATA
C
      READ(5,100)W,H,S2N,SLOP,DS
  100 FORMAT(5F8.0)
C
C  READ TEST PARAMETERS
C
      READ(5,101)V,DKLY,M,DELM,DELX
  101 FORMAT(5F8.0,I8,2F8.0)
C
C  READ EQUIPMENT DATA
C
      READ(5,102)DIAM,W,S
  102 FORMAT(3F8.0)
C
C  READ FLOW RATE
C
      READ(5,103)V,IVEL,SVEL,V,EZ,DA
  103 FORMAT(F 0,I8,4F8.0)
C
C  READ CONCENTRATION GRADIENTS
C
      READ(5,104)(DCD21(I),I=1,N)
      READ(5,104)(DCD22(I),I=1,N)
```

```
C READ CONCENTRATION PROFILE AT BEGINNING OF CHANNEL
C
      READ(5,104)(CONC(I,1),I=1,N)
  104 FORMAT(9F8.0)
C
C  READ OUTPUT REQUIREMENTS
C
      READ(5,117)PRINTX
  117 FORMAT(F8.0)
C
      RLONG=M*DELX
C
C  PRINT ALL INPUT DATA
C
      WRITE(8,126)(TITLE1(I),I=1,35)
      WRITE(8,126)(TITLE2(I),I=1,35)
  126 FORMAT(T10,35A2)
      WRITE(8,127)DELY
  127 FORMAT(/,T10,'CONCENTRATION PROFILES AND GRADIENTS ARE LISTED FRO
     #M WATER SURFACE',/,T10,'TO CHANNEL BED AT',F8.3,T36,' M INTERVALS'
      WRITE(8,105)
  105 FORMAT(/,T10,'REACH CHARACTERISTICS',/,T10,21('*'))
      WRITE(8,106)WID,YP,DCH,SLOP,DM
  106 FORMAT(/,T10,'CHANNEL WIDTH',T29,F5.2,T35,'M',/,T10,'CHANNEL DEPTH
     #',T29,F5.3,T35,'M',/,T10,'FLOW DEPTH',T29,F5.3,T35,'M',/,T10,'GRAD
     #IENT',T29,F7.5,/,T10,'GRAIN ROUGHNESS',T29,F5.2,T35,'MM')
      WRITE(8,107)RLONG
  107 FORMAT(T10,'REACH LENGTH',T29,F6.1,T36,'M')
      WRITE(8,130)
  130 FORMAT(/,/,T10,'FLOW CHARACTERISTICS',/,T10,20('*'))
      WRITE(8,108)V,SVEL,U,EZ
  108 FORMAT(/,T10,'FLOW VELOCITY',T29,F5.2,T35,'M/S',/,T10,'SHEAR VELOC
     #ITY',T29,F5.2,T35,'M/S',/,T10,'TRANSVERSE VEL',T29,F5.3,T35,'M/S',
     #/,T10,'TRANSVERSE DIFF',T29,F7.5,T37,'SQ M /S')
      IF(IVEL.GT.1)GO TO 25
      WRITE(8,128)
  128 FORMAT(/,T10,'VELOCITY DISTRIBUTION IS UNIFORM')
      GO TO 26
   25 WRITE(8,129)
  129 FORMAT(/,T10,'VELOCITY DISTRIBUTION IS LOGARITHMIC')
   26 WRITE(8,109)
  109 FORMAT(/,/,T10,'SEDIMENT CHARACTERISTICS',/,T10,24('*'))
      WRITE(8,110)DIAM,W,S
  110 FORMAT(/,T10,'PARTICLE SIZE',T29,F5.3,T35,'MM',/,T10,'FALL VELOCIT
     #Y',T29,F5.3,T35,'M/S',/,T10,'REL DENSITY',T29,F6.3,/)
      WRITE(8,111)
  111 FORMAT(/,T10,'TRANSVERSE CONCENTRATION GRADIENTS ON LEFT AND RIGHT
     # SIDES :')
      WRITE(8,112)(DCDZ1(I),I=1,N)
      WRITE(8,112)(DCDZ(I),I=1,N)
C
C  ********************************************************************
C
C  CALCULATE AND PRINT AVERAGE PARTICLE VELOCITY
```

```
C  ***********************************************
C
      BETA=W/(0.4*SVEL)
      VELDIF=-135.*BETA**1.41
      DISP=0.4*DCH*SVEL/6.
      V=(VELDIF*DISP/DCH)+V
      WRITE(8,124)V
  124 FORMAT(/,T10,'AVERAGE PARTICLE VELOCITY IS',T39,F5.3,T46,'M/S')
C
C  ***********************************************
C
C  GENERATE LOGARITHMIC VELOCITY DISTR BUTION
C  ******************************************
C
      DO 24 I=1,N
      Y=DCH-(I-1)*DELY
      IF(I.EQ.N)Y=0.25*DELY
      VEL(I)=(SVEL/0.4)*(ALOG(Y)+1.)+V
      IF(IVEL.LT.2)VEL(I)=V
   24 CONTINUE
C
C  ***********************************************
C
C  GENERATE EQUILIBRIUM CONCENTRATION PROFILE
C  ******************************************
C
      Z=W/(0.4*SVEL)
      A=2.*DM*0.001
      NN=N-1
      DO 23 I=1,NN
      Y=DCH-(I-1)*DELY
      IF(I.EQ.1)Y=DCH-DELY/4.
      ECONC(I)=CA*(((DCH-Y)*A)/(Y*(DCH-A)))**Z
   23 CONTINUE
      ECONC(N)=CA
      WRITE(8,122)
  122 FORMAT(/,T10,'EQUI  IUM CONCENTRATION PROFILE :')
      WRITE(8,112)(EC  .I,I=1,N)
  112 FORMAT(10F8 2)
C
C  ***********************************************
C
C  PRINT RESULTS FOR FIRST SECTION
C  *******************************
C
      WRITE(8,113)
  113 FORMAT(/,/,T10,'AT BEGINNING OF REACH',/,T10,21('*'),/,/,T10,'CONC
     #ENTRATION PROFILE IS')
      WRITE(8,120)(CONC(I,1),I=1,N)
      TCON=0.
C
C  CALCULATE AVERAGE CONCENTRATION
C
      DO 19 I=2,NN
      TCON=TCON+2.*CONC(I,1)
```

```
   19 CONTINUE
      AVCON=(TCON+CONC(1,1)+CONC(N,1))*0.5/(N-1)
      AVCON1=AVCON
      WRITE(8,114)AVCON
  114 FORMAT(/,T10,'AVERAGE CONCENTRATION IS',T36,F7.2)
C
C  ***************************************************************
C
C
C  COMPUTE VERTICAL DIFFUSIVITIES
C  ******************************
      DO 15 I=1,N
      Y=DCH-(I-1)*DELY
      EPSY(I)=0.4*SVEL*Y*(1.0-Y/DCH)
   15 CONTINUE
C
C  ***************************************************************
C
C
C  CALCULATE DEPOSITION PROBABILITY
C  ********************************
C
      TAU=1000.*SVEL**2.
      B=0.51
      THETAC=0.05
      THETA=TAU/((S-1.)*9.81*DIAM)
      IF(THETA.LT.THETAC)GO TO 16
      P=(1.+(0.52*B/(THETA-THETAC))**4.)**(-0.25)
      GO TO 17
   16 P=0.
   17 PDEP=1.-P
      DEP1=W*PDEP*CONC(N,1)*WID
      DEP=1.
      WRITE(8,118)DEP
      WRITE(8,123)PDEP
  123 FORMAT(/,T10,'DEPOSITION PROBABILITY IS',T36,F6.4)
C
C  ***************************************************************
C
C
C  COMPUTE CONCENTRATIONS AT ALL GRID POINTS AND PRINT RESULTS
C  ***********************************************************
C
      DY2=DELY**2.
C
C  CALCULATE CONCENTRATION GRADIENTS
C
      DO 22 I=1,N
      DCDZ1(I)=DCDZ1(I)*(CONC(I,1)/ECONC(I))
      DCDZ(I)=DCDZ(I)*(CONC(I,1)/ECONC(I))
   22 CONTINUE
C
      PRINT=PRINTX
C
      DO 14 J=2,M
      DISTX=J*DELX
      TRL=0.
      TRR=0.
```

```
      DO 10 I=1,N
      IF(I.NE.1)GO TO 11
C
C  CALCULATIONS FOR WATER SURFACE POINTS
C
      EY1=(EPSY(I)+EPSY(I+1))*0.5
      COFFB=EY1/DY2
      COFFC=COFFB+W/DELY-VEL(I)/(2.*DELX)
      COFFD=EZ/(2.*(DELZ+WID))
      COFFE=COFFD+U*DELZ/(2.*(DELZ+WID))
      CONC(I,2)=(2.*DELX/VEL(I))*(COFFB*CONC(I+1,1)-COFFC*CONC(I,1)+COFF
     #D*DCDZ1(I)-COFFE*DCDZ(I))
      TRL=TRL+(-EZ*DCDZ1(I)+U*CONC(I,2))*DELY/2.
      TRR=TRR+(EZ*DCDZ(I)-U*(CONC(I,2)-DCDZ(I)*DELZ))*DELY/2.
      GO TO 10
   11 IF(I.EQ.N)GO TO 12
C
C  CALCULATIONS FOR INTERIOR POINTS
C
      EY1=(EPSY(I)+EPSY(I+1))*0.5
      EY2=(EPSY(I-1)+EPSY(I))*0.5
      COFFA=EY2/DY2+W/DELY
      COFFB=EY1/DY2
      COFFC=COFFA+COFFB-VEL(I)/DELX
      YI=(N-I)*DELY
      IF(YI.GT.YP)GO TO 13
      CONC(I,2)=(DELX/VEL(I))*(COFFA*CONC(I-1,1)+COFFB*CONC(I+1,1)-COFFC
     #*CONC(I,1))
      IF(ABS(YI-YP).GT.0.001)GO TO 10
      TRL=TRL+(-EZ*DCDZ1(I)+U*CONC(I,2))*DELY/2.
      TRR=TRR+(EZ*DCDZ(I)-U*(CONC(I,2)-DCDZ(I)*DELZ))*DELY/2.
      GO TO 10
   13 COFFD=EZ/(DELZ+WID)
      COFFE=COFFD+U*DELZ/(DELZ+WID)
      CONC(I,2)=(DELX/VEL(I))*(COFFA*CONC(I-1,1)+COFFB*CONC(I+1,1)-COFFC
     #*CONC(I,1)+COFFD*DCDZ1(I)-COFFE*DCDZ(I))
      TRL=TRL+(-EZ*DCDZ1(I)+U*CONC(I,2))*DELY
      TRR=TRR+(EZ*DCDZ(I)-U*(CONC(I,2)-DCDZ(I)*DELZ))*DELY
      GO TO 10
C
C  CALCULATIONS FOR POINTS ON BED
C
   12 EY2=(EPSY(I-1)+EPSY(I))*0.5
      COFFA=EY2/DY2+W/DELY
      COFFC=EY2/DY2+PDEP*W/DELY-VEL(I)/(2.*DELX)
      CONC(I,2)=(2.*DELX/VEL(I))*(COFFA*CONC(I-1,1)-COFFC*CONC(I,1))
   10 CONTINUE
C
C  PRINT RESULTS
C
      IF(ABS(DISTX-PRINT).GT.0.0001)GO TO 20
      WRITE(8,115)DISTX
  115 FORMAT(/,T10,'AT X =',T17,F6.1,T24,'M',/,T10,15('*'),/,/,T10,'CONC
     #ENTRATION PROFILE IS')
      WRITE(8,120)(CONC(I,2),I=1,N)
```

```
  120 FORMAT(T2,8F8.2)
      TCON=0.
      DO 21 I=2,NN
      TCON=TCON+2.*CONC(I,2)
   21 CONTINUE
      AVCON=(TCON+CONC(1,2)+CONC(N,2))*0.5/(N-1)
      WRITE(8,116)AVCON
  116 FORMAT(/,T10,'AVERAGE CONCENTRATION IS',T36,F7.2,T44,'UNITS')
      DEPBED=W*PDEP*(CONC(N,1)+CONC(N,2))*0.5*WID
      DEP=DEPBED/DEP1
      WRITE(8,118)DEP
  118 FORMAT(T10,'RELATIVE DEPOSITION IN CHANNEL IS',T45,F7.3)
      RTRL=TRL/DEP1
      RTRR=TRR/DEP1
      WRITE(8,119)RTRL
  119 FORMAT(T10,'RELATIVE TRANSFER TO LEFT BANK IS',T50,E10.3)
      WRITE(8,121)RTRR
  121 FORMAT(T10,'RELATIVE TRANSFER TO RIGHT BANK IS',T50,E10.3,/)
      PRINT=PRINT+PRINTX
C
   20 DO 18 I=1,N
      DCDZ1(I)=DCDZ1(I)*(CONC(I,2)/CONC(I,1))
      DCDZ(I)=DCDZ(I)*(CONC(I,2)/CONC(I,1))
      CONC(I,1)=CONC(I,2)
      AVCON1=AVCON
   18 CONTINUE
C
   14 CONTINUE
      STOP
      END
C  ***************************************************************
C
C  DATA
C  ****
C
$ENTRY                                          EXAMPLE
     2.000   0.500    1.00    .0050    5.0
        11   0.100    1000    0.100    0.2
    0.075   0.035   19.30
    2.353       2   0.153    .0000   0.0470  100.00
   -0.918  -1.776  -3.457   -5.105   -7.018  -8.301   0.000      0.      0.
      0.      0.
    0.918   1.776   3.457    5.105    7.018   8.301   0.000      0.      0.
      0.      0.
     100.    100.    100.     100.     100.    100.    100.     100.    100.
     100.    100.
     50.0
$STOP
```

B.5 Example

The longitudinal distribution of sediment in the standard channel used as a basis for the sensitivity analyses in Chapter 10.2 is analysed as an example to illustrate the use of program LONGDIS.

The channel is 2,0 m wide and has a bankfull depth of 0,5 m. The gradient is 0,005, the grain roughness is 5 mm and the total flow depth is 1,0 m. Gold particles with a representative diameter of 0,075 mm, fall velocity of 0,035 m/s and relative density of 19,3 are input at the beginning of the channel at a uniformly distributed concentration of 100 units. The velocity distribution is to be logarithmically distributed. The finite difference grid spacing is 0,10 m vertically and longitudinally with 11 intersections in the vertical direction and 1000 in the longitudinal direction, giving a channel length of 100 m. Results are to be printed at 50 m intervals.

Program PLAINDEP is run first to obtain values for average flow velocity, shear velocity, transverse diffusivity and concentration gradients. For this run it is assumed that the channel has a trapezoidal section with a top width of 2,4 m and a bottom width of 1,2 m and a Manning's n of 0,020. The plain is assumed to be 4,0 m wide with a solid vertical boundary on one side. The grain roughness for the plain is 5 mm and the Manning's n is 0,025. the reference gold concentration at the channel bed is 100 units. The data file for PLAINDEP is shown in Figure B.2 and the results in Figure B.3.

Because only 1 channel is considered in this case concentration gradients are given for the left bank only. For the right bank the values are the same but the signs are different.

The data file for LONGDIS is shown in Figure B.4 and the final longitudinal distribution results in Figure B. 5.

```
                    EXAMPLE
                    ********
    1      0.0
0.500      4.00   0.0050    0.025      5.0
1.000      2.40     1.20    0.020      5.0      100.
0.075     0.035    19.30
    6      0.100      21     0.20     .0010      1.0
    2
```

Fig. B.2 Data file for PLAINDEP

```
                              EXAMPLE
                              *******

PLAIN CHARACTERISTICS
*********************

FLOW DEPTH          0.500 M
WIDTH               4.00 M
GRADIENT            0.00500
MANNINGS N          0.025
GRAIN ROUGHNESS     5.000MM

PLAIN IS BOUNDED BY A CHANNEL ON ONE SIDE AND A SOLID VERTICAL BOUNDARY
ON THE OTHER

CHANNEL CHARACTERISTICS
***********************

FLOW DEPTH             .000 M
CHANNEL TOP WIDTH      .400 M
CHANNEL BTM WIDTH     1.200 M
GRADIENT              0.00500
MANNINGS N            0.020
GRAIN ROUGHNESS       5.000 MM
CONCENTRATION AT BED  100.000 UNITS


SEDIMENT DATA
*************

PARTICLE SIZE   0.075 MM
FALL VELOCITY   0.035 M/S
REL. DENSITY    19.300

FLOW VELOCITY ON PLAIN          1.808  M/S
FLOW VELOCITY IN 1ST CHANNEL    2.353  M/S

SHEAR VELOCITY FOR 1ST CHANNEL  0.153  M/S

TRANSVERSE VELOCITY OF SEDIMENT PARTICLES    0.000  M/S

*****************************************************************************
```

Fig. B.3 PLAINDEP output

CONCENTRATIONS

Y(M) / Z(M)	0.000	0.100	0.200	0.300	0.400	0.500
0.00	7.2433	5.7456	4.4639	3.2809	2.0644	0.8933
0.20	5.5831	4.3420	3.4429	2.5895	1.7092	0.7097
0.40	2.6755	2.0718	1.6729	1.2870	0.8728	0.3550
0.60	1.2959	1.0045	0.8167	0.6332	0.4319	0.1739
0.80	0.6308	0.4895	0.3989	0.3099	0.2117	0.0848
1.00	0.3076	0.2387	0.1946	0.1512	0.1033	0.0413
1.20	0.1499	0.1163	0.0947	0.0736	0.0502	0.0201
1.40	0.0730	0.0566	0.0460	0.0357	0.0243	0.0097
1.60	0.0355	0.0274	0.0222	0.0172	0.0117	0.0047
1.80	0.0172	0.0133	0.0107	0.0083	0.0056	0.0022
2.00	0.0083	0.0064	0.0051	0.0039	0.0027	0.0011
2.20	0.0040	0.0030	0.0024	0.0019	0.0012	0.0005
2.40	0.0019	0.0014	0.0011	0.0009	0.0006	0.0002
2.60	0.0009	0.0007	0.0005	0.0004	0.0003	0.0001
2.80	0.0004	0.0003	0.0002	0.0002	0.0001	0.0000
3.00	0.0002	0.0001	0.0001	0.0001	0.0001	0.0000
3.20	0.0001	0.0001	0.0000	0.0000	0.0000	0.0000
3.40	0.0000	0.0000	0.0000	0.0000	0.0000	0.0000
3.60	0.0000	0.0000	0.0000	0.0000	0.0000	0.0000
3.80	0.0000	0.0000	0.0000	0.0000	0.0000	0.0000
4.00	0.0001	0.0001	0.0001	0.0000	0.0000	0.0000

Z(M)	BED SHEAR (N/M**2)	EPSZ (M**2/S)	PDEP	REL. DEPOSITION
0.00	19.609	0.470E-01	0.7901	1.0000
0.20	18.709	0.738E-02	0.7901	0.7708
0.40	17.099	0.738E-02	0.7901	0.3694
0.60	16.146	0.738E-02	0.7901	0.1789
0.80	15.864	0.738E-02	0.7902	0.0871
1.00	15.814	0.738E-02	0.7902	0.0425
1.20	15.814	0.738E-02	0.7902	0.0207
1.40	15.814	0.738E-02	0.7902	0.0101
1.60	15.814	0.738E-02	0.7902	0.0049
1.80	15.814	0.738E-02	0.7902	0.0024
2.00	15.814	0.738E-02	0.7902	0.0011
2.20	15.814	0.738E-02	0.7902	0.0005
2.40	15.814	0.738E-02	0.7902	0.0003
2.60	15.814	0.738E-02	0.7902	0.0001
2.80	15.814	0.738E-02	0.7902	0.0001
3.00	15.814	0.738E-02	0.7902	0.0000
3.20	15.814	0.738E-02	0.7902	0.0000
3.40	15.814	0.738E-02	0.7902	0.0000
3.60	15.814	0.738E-02	0.7902	0.0000
3.80	15.814	0.738E-02	0.7902	0.0000
4.00	15.814	0.738E-02	0.7902	0.0000

NUMBER OF ITERATIONS 18
ACCELERATOR VALUE : 1.4275

CONCENTRATION GRADIENTS :

Y(M)	LEFT	RIGHT
0.500	-0.918	0.000
0.400	-1.776	0.000
0.300	-3.457	0.000
0.200	-5.105	0.000
0.100	-7.018	0.000
0.000	-8.301	0.000

Fig. B.3 (contd) PLAINDEP output

```
                                        EXAMPLE
                                        *******
 2.000    0.500     1.00     .0050      5.0
    11    0.100     1000     0.100      0.2
 0.075    0.035    19.30
 2.353        2    0.153     .0000    0.0470   100.00
-0.918   -1.776   -3.457   -5.105    -7.018   -8.301    0.000      0.       0
    0.       0.
 0.918    1.776    3.457    5.105     7.018    8.301    0.000      0.       0
    0.       0.
  100.     100.     100.     100.      100.     100.     100.      100.     100
  100.     100.
  50.0
```

Fig. B.4 Data file for LONGDIS

```
                                        EXAMPLE
                                        *******

CONCENTRATION PROFILES AND GRADIENTS ARE LISTED FROM WATER SURFACE
TO CHANNEL BED AT   0.100 M INTERVALS

REACH CHARACTERISTICS
*********************

CHANNEL WIDTH          2.00 M
CHANNEL DEPTH         0.500 M
FLOW DEPTH            1.000 M
GRADIENT            0.00500
GRAIN ROUGHNESS      5.00 MM
REACH LENGTH         100.0 M


FLOW CHARACTERISTICS
********************

FLOW VELOCITY          1.15 M/S
SHEAR VELOCITY        0.15 M/S
TRANSVERSE VEL      0.000 M/S
TRANSVERSE DIFF     0.04700 SQ M /S

VELOCITY DISTRIBUTION IS LOGARITHMIC


SEDIMENT CHARACTERISTICS
************************

PARTICLE SIZE         0.075 MM
FALL VELOCITY        0.035 M/S
REL DENSITY           19.300

      TRANSVERSE CONCENTRATION GRADIENTS ON LEFT AND RIGHT SIDES :
-0.92   -1.78   -3.46   -5.10   -7.02   -8.30    0.00    0.00    0.00    0.00
 0.00
 0.92    1.78    3.45    5.10    7.02    8.30    0.00    0.00    0.00    0.00
 0.00

      AVERAGE PARTICLE VELOCITY IS 1.727  M/S

      EQUILIBRIUM CONCENTRATION PROFILE :
 0.69    2.06    3.27    4.45    5.[illegible]    7.22    [illegible]    11.73    15.96    25.38
100.00
```

Fig. B.5 LONGDIS output

```
      AT BEGINNING OF REACH
      ********** *******

      CONCENTRATION PROFILE IS
100.00  100.00  100.00  100.00  100.00  100.00  100.00  100.00
100.00  100.00  100.00

      AVERAGE CONCENTRATION IS   100.00
      RELATIVE DEPOSITION IN CHANNEL IS    1.000

      DEPOSITION PROBABILITY IS 0.0002

      AT X =   50.0 M
      ***************

      CONCENTRATION PROFILE IS
  6.67   15.45   22.99   31.00   40.35   52.14   67.92   88.48
118.96  176.45  403.96

      AVERAGE CONCENTRATION IS    81.91 UNITS
      RELATIVE DEPOSITION IN CHANNEL IS    4.041
      RELATIVE TRANSFER TO LEFT BANK IS        0.823E 03
      RELATIVE TRANSFER TO RIGHT BANK IS       0.823E 03


      AT X =  100.0 M
      ***************

      CONCENTRATION PROFILE IS
  4.58   10.65   15.92   21.55   28.16   36.50   47.66   62.22
 83.80  124.45  285.09

      AVERAGE CONCENTRATION IS    57.57 UNITS
      RE  ,IVE DEPOSITION IN CHANNEL IS    2.852
      RELATIVE TRANSFER TO LEFT BANK IS        0.573E 03
      RELATIVE TRANSFER TO RIGHT BANK IS       0.573E 03
```

Fig. B.5 (cont'd) LONGDIS output

REFERENCES

...: Numerical Methods for Partial Differential ...ons, Second Edition, Academic Press, New York, 1977.

Apelt, C.J. and Isaacs, L.T.: On the Estimation of the Optimum Accelerator for SOR applied to Finite Element Methods, Computer Methods in Applied Mechanics and Engineering, 12(1977), pp383-391.

Bagnold, R.A.: Experiments on a Gravity-free Dispersion of Large Solid Spheres in a Newtonian Fluid Under Shear, Proc. Roy. Soc. London (A) 225, 49, 1954.

Bagnold, R.A.: An Approach to the Sediment Transport Problem from General Physics, Prof. Paper U.S. Geol. Surv. 422-I, 1966).

Brady, L.L. and Jobson, H.E.: An Experimental Study of Heavy Mineral Segregation under Alluvial Flow Conditions, Prof. Paper U.S. Geol. Surv. 562-K, 1973.

Chen , Y.H.: ter and Sediment Routing in Rivers, in Modeling of Rivers, ed. Hsieh Wen Shen, John Wiley and Sons, New York 1979.

...: Turbulence Phenomena, Academic Press, New York, 1972.

...egaard, P.: Longitudinal and Transverse Sorting of Grain ... Alluvial Rivers, Series paper No. 26, ...te of Hydrodynamics and Hydraulic Engineering, ... University of Denmark, Lyngby, 1980.

...W., Toebes, G.H. and Udeozo, B.C. : Uniform ... Idealized Channel Geometries, 12th International ...nference of International Association for ..., Fort Collins, Colo. U.S.A., 1967.

..., S.A. : The Bed-Load Function for Sediment Transport ... Open Channel Flows, Technical Bulletin ..., United States Department of Agriculture, ...ice, Washington, D.C., Sept.

Einstein, H.A.: Deposition of Suspended Particles [illegible] Gravel Bed, Journal of the Hydraulics Division, ASCE, Vol. 94, No. HY5, Proc. Paper 6102, Sept. 1968, pp 1197-1205.

Engelund, F. : Steady Transport of Moderately Graded Sediment, Lyngby, Tech. Univ. Denmark, Inst. Hydrodynamics and Hydraulic Engineering, Prog. Report No. 29, 1973, pp [illegible].

Engelund, F. and Fredsoe, J. : A Sediment Transport Model for Straight Alluvial Channels, Nordic Hydrology, [illegible], 1976.

Engelund, F. and Hansen, E. : A Monograph on Sediment Transport in Alluvial Streams, Teknisk Forlag, Copenhagen, 1967.

Fernandez Luque, R. and van Beek, [illegible]: Erosion and Transport of Bed-Load Sediment, Journal of Hydraulic Research, Vol. 14, No. 2, 1976.

Francis, J.R.D. : Experiments [illegible] the Motion of Solitary Grains along the Bed of a [illegible]ater Stream, Proc. Roy. Soc. London, Ser. A, V.332, 1973, pp 443-471.

Gerald, Curtis F. : Applied Numerical Analysis, Addison Wesley Publishing Company, 197[illegible].

Ghosh, S. and Jena, S.B. : Boundary Shear Distribution in Open Channel Compound, Proc. Instn. Civil Engrs., Vol. 49, August 1971.

Graf, Walter H. : Hydraulics of Sediment Transport, McGraw-Hill Book Company, 1971.

Jobson, H.E. and Sayre, W.W. : Vertical Transfer in Open Channel Flow, Journal of the Hydraulics Division, ASCE, Vol. 96, No. HY3, Proc. Paper 7148, March 1970, pp 703-724.

Krishnappan, B.G.: Programming Manual for MOBED - An Unsteady, Nonuniform, Mobile Boundary Flow Model, Hydraulics Division, National Water Research Institute, Burlington, Ontario, Canada, 1981.

Krishnappan, B.G. and Lau, Y.L. : Transverse Mixing in Meandering Channels with Varying Bottom Topogr , Journal of Hydraulic Research, 15, No. 4, 1977.

Lane, E.W. and Kalinske, A.A. : The Relation of Suspended to Bed Material in Rivers, Am. Geophys. Union Trans., 1939, pp 637-641.

Lau, Y.L. and Krishnappan, B.G. : Transverse Dispersion in Rectangular Channels, Journal of the Hydraulics Division, ASCE, Vol. 103, No. HY10, Proc. Paper 13294, Oct. 1977, pp 1173-1189.

Lau, Y.L. and Krishnappan, B.G. : Modelling Transverse Mixing in Natural Streams, Journal of the Hydraulics Division, ASCE, Vol. 107, No. HY2, Proc. Paper 16048, Feb. 1981. pp 209-225.

Leeder, M.R.: On the Interactions Between Turbulent Flow, Sediment Transport and Bedform Mechanics in Channelized Flows, Spec. Publs. Int. Ass. Sediment, 6, 1983.

Middleton, G.V. : Hydraulic Interpretation of Sand Size Distributions, Journal of Geology, Vol. 84, 1976, pp 405-426.

Miller, A.C. and Richardson, E.V. : Diffusion and Dispersion in Open Channel Flow, Journal of the Hydraulics Division, ASCE, Vol. 100, No. HY1, Proc. Paper 10298, Jan. 1974, pp 159-171.

Msutwana, S.B. : An Investigation into the Fall Velocity of Sold Grains, Undergraduate Investigational Project Report, Dept. of Civil Engineering, University of the Witwatersrand, 1982.

Myers, W.R.C. : Momentum Transfer in a Compound Channel, Journal of Hydraulic Research, Vol. 16, No. 2, 1978, pp 139-150.

Myers, R.C. and Elsawy, E.M. : Boundary Shear in Channel with Flood Plain, Journal of the Hydraulics Division, ASCE, Vol. 101, No. HY7, Proc. Paper 11452, July 1975, pp 933-946.

Nami, M. : Small Scale Gold Distribution Patterns on Carbon Leader Placer at Blyvooruitzicht Gold Mines, Part 1: Sedimentological Investigation, Chamber of Mines Research Report No. 39/82, 1982.

Nami, M. : Gold Distribution in Relation to Depositional Processes in the Proterozoic Carbon Leader Placer, Witwatersrand, South Africa, Spec. Pubis. Int. Ass. Sediment, 6, 1983.

Nordin, C.F. and McQuivey, R.S. : Suspended Load, in River Mechanics, Vol. 1, ed. Shen, 1971.

Posey, C.J. : Computation of Discharge Including Overbank Flow, Civil Engineering, ASCE, Apr. 1967, pp 62-63.

Querner, E.P. and Doyle, W.S. : Velocity Distribution in Open Channels - Analysis by the Finite Element Method, The Civil Engineer in South Africa, Vol. 22, No. 11, November 1980.

Rajaratnam, N. and Ahmadi, R.M. : Interaction Between Main Channel and Flood Plain Flows, Journal of the Hydraulics Division, ASCE, Vol. 105, No. HY5, Proc. Paper 14591, May 1979, pp 573-588.

Rajaratnam, N. and Ahmadi, R.M. : Hydraulics of Channels with Flood Plains, Journal of Hydraulic Research, Vol. 19, No. 1, 1981, pp 43-60.

Rana, S.A., Simons, P.B. and Mahmood, K.: Analysis of Sediment Sorting in Alluvial Channels, Journal of the Hydraulics Division, ASCE, Vol. 99, No. HY7, Proc. Paper 10168, November 1973.

Raudkivi, A.J.: Loose Boundary Hydraulics, Second Edition, Pergamon Press, 1976.

Sarikaya, H.Z. : Numerical Model for Discrete Settling, Journal of the Hydraulics Division, ASCE, Vol. 103, No. HY8, Proc. Paper 13150, Aug. 1977, pp 865-876.

Schumm, S.A.: The Fluvial System and Associated Processes

of Mineralization, Course Notes, ER652, Colorado State University, 1975.

Sellin, R.H.J. : A Laboratory Investigation into the Interaction Between the Flow in the Channel of a River and that over its Flood Plain, La Houille Blanche, No. 7, 1964, pp 793-802.

Singamsetti, S.R. : Di fusion of Sediment in a Submerged Jet, Journal of the Hydraulics Division, ASCE, Vol. 92, No. HY2, Proc. Paper 4726, Mar. 1966, pp 133-168.

Smith, G.D. : Numerical Solution of Partial Differential Equations, Second Edition, Oxford University Press, 1978.

Sumer, B.M. : Mean Velocity and Longitudinal Dispersion of Heavy Particles in Turbulent Open-Channel Flow, Journal of Fluid Mechanics, Vol. 65, Part 1, 1974.

Townsend, A.A. : An Investigation of Turbulence Characteristics in a River Model of Complex Cross-section, Proc. Instn. Civ. Engrs, Vol. 40, June 1968.

Vanoni, V.A. : Transport of Suspended Sediment by Water, Transactions, ASCE, Vol. 111, Paper No. 2267, 1946, p 67.

Weiss, E.W. : An Integrated Approach to Mathematical Flood Plain Modelling, PhD Thesis, University of the Witwatersrand, Johannesburg, 1976.

Wormleaton, P.R., Allen, J. and Hadjipanos, P. : Discharge Assessment in Compound Channel Flow, Journal of the Hydraulics Division, ASCE, Vol. 108, No. HY9, Proc. Paper 17310, Sept. 1982, pp 975-994.

Wright, R.R. and Carstens, M.R. : Linear Momentum Flux in Overbank Sections, Journal of the Hydraulics Division, ASCE, Vol. 96, No. HY9, Proc. Paper 7517, Sept. 1970, pp 1781-1793.

Yalin, M.S.: Mechanics of Sediment Transport, Second Edition, Pergamon Press, 1977.

Yen, C. and Overton, D.E. : Shape Effects on Resistance in Flood-Plain Channels, Journal of the Hydraulics Division, ASCE, Vol. 99, No. HY1, Proc. Paper 9506, Jan. 1973, pp 219-238.

Zheleznyakov, G. V. : Interaction of Channel and Flood Plain Streams, Proc. Int. Ass. Hydr. Res., Vol. 5/71, 1971, pp 141-148.

Author James C S
Name of thesis Numerical modelling of Gold Transport and Deposition 1984

PUBLISHER:
University of the Witwatersrand, Johannesburg
©2013

LEGAL NOTICES:

Copyright Notice: All materials on the University of the Witwatersrand, Johannesburg Library website are protected by South African copyright law and may not be distributed, transmitted, displayed, or otherwise published in any format, without the prior written permission of the copyright owner.

Disclaimer and Terms of Use: Provided that you maintain all copyright and other notices contained therein, you may download material (one machine readable copy and one print copy per page) for your personal and/or educational non-commercial use only.

The University of the Witwatersrand, Johannesburg, is not responsible for any errors or omissions and excludes any and all liability for any errors in or omissions from the information on the Library website.